Dissertation zur Erlangung des Doktorgrades
der Fakultät für Chemie und Pharmazie
der Ludwig-Maximilians-Universität München

Synthetic biology approaches for cell engineering of CHO biofactories producing heterodimeric bispecific IgG-like antibodies

Niels Bauer

aus

Erlangen, Deutschland

2024

Erklärung

Diese Dissertation wurde im Sinne von §7 der Promotionsordnung vom 28. November 2011 von Herrn Prof. Dr. Julian Stingele betreut.

Eidesstattliche Versicherung

Diese Dissertation wurde eigenständig und ohne unerlaubte Hilfe erarbeitet.

München, 05.08.2024

_____

Niels Bauer

Dissertation eingereicht am 05.08.2024

1. Gutachter: Prof. Dr. Julian Stingele

2. Gutachter: PD Dr. Christian Klein

Mündliche Prüfung am 25.10.2024

“For things to reveal themselves to us,
we need to be ready to abandon our views about them.”

- Thích Nhất Hạnh

This thesis has been prepared from October 2019 to June 2024 in the laboratories of Roche Diagnostics GmbH, Penzberg, Germany under supervision of Dr. Simon Ausländer and Professor Dr. Julian Stingele (Gene Center of the Ludwig-Maximilians-University München).

This is a cumulative thesis based on the following publications:

Niels Bauer*, Marco Boettger*, Stella Papadaki, Tanja A. Leitner, Stefan Klostermann, Hubert Kettenberger, Guy Georges, Vincent Larraillet, Dino Gluhacevic von Kruechten, Lars Hillringhaus, Annette Vogt, Simon Ausländer & Oliver Popp, Procollagen-Lysine 2-Oxoglutarate 5-Dioxygenases are Responsible for 5R-Hydroxylysine Modification of Therapeutic T-Cell Bispecific Monoclonal Antibodies Produced by Chinese Hamster Ovary Cells, *Frontiers in Bioengineering and Biotechnology,* Volume 12, 2024, 12:1414408, https://doi.org/10.3389/fbioe.2024.1414408, * *These authors contributed equally.*

Niels Bauer, Benedikt Oswald, Maximilian Eiche, Lisa Schiller, Emma Langguth, Christian Schantz, Andrea Osterlehner, Amy Shen, Shahram Misaghi, Julian Stingele & Simon Ausländer, An arrayed CRISPR screen reveals Myc depletion to increase productivity of difficult-to-express complex antibodies in CHO cells, *Synthetic Biology*, Volume 7, Issue 1, 2022, ysac026, https://doi.org/10.1093/synbio/ysac026

Niels Bauer, Christoph Oberist, Michaela Poth, Julian Stingele, Oliver Popp & Simon Ausländer, Genomic barcoding for clonal diversity monitoring and control in cell-based complex antibody production. *Scientific Reports*, Volume 14, Issue 1, 2024, Pages 14587, https://doi.org/10.1038/s41598-024-65323-7

Table of content

Abstract

Recombinant therapeutic antibodies mimic and upgrade common functions of natural IgG antibodies, mediating novel modes of action and therapeutic effects beyond their natural counterpart. Complex heterodimeric bispecific antibodies attach to multiple extracellular target specific epitopes sequentially or simultaneously, conveying functionalities which would not exist in mixtures of the parental binders. The extended target space is, however, chained to difficulties in manufacturing: their asymmetric nature requires two distinct heavy and light chains to pair with strict stoichiometry to prevent formation of non-functional or monospecific molecules. State-of-the-art CHO biofactories therefore need to assure optimal production of heterodimeric bispecific antibodies by control over the relative level at which each chain is constitutively expressed. This is enabled by targeted integration into pre-defined genetic hot spots, obviating intra-clonal heterogeneity by generation of isogenic clones. Additionally, static cell engineering efforts generate CHO biofactories with disruptive step-change in cellular competence. As of now, the field can therefore generate isogenic targeted integration CHO cell lines with improved functionality. Still, within clonally-derived cellular populations distinct sub-lineages emerge rapidly and substantial phenotypic variance with regard to production-relevant parameters remains. As the underlying reasons are incompletely understood, establishing new CHO producer cell lines relies on laborious empirical screenings with limited *a priori* knowledge to identify phenotypes feasible for large-scale manufacturing.

This thesis applies insights from the interdisciplinary field of synthetic biology, i.e. rational genetic engineering using standardized biological parts and forward genetic screens, to improve the manufacturing capabilities of CHO biofactories. In the first part of this thesis, rational design-build-test-learn cycles are employed to investigate and eliminate the formation of 5R-hydroxylysine in T cell bispecific antibodies (TCB). These undesired post-translational modifications were found in multiple sites within each TCB molecule, with a conspicuous hotspot motif located at the crossed C_H1-VL domain of each T cell bispecific antibody. As only 2OG-dependent hydroxylases can catalyze the formation of 5R-hydroxylysine in mammalian cells, procollagen-lysine 2-oxoglutarate 5-dioxygenases (PLODs) were conclusively identified as the catalyzing enzymes accountable. Depletion of all three PLOD isoenzymes is demonstrated to be required and sufficient for complete inhibition of Hyl formation.

In the second part of this thesis, an arrayed CRISPR screening is utilized to characterize genotype-phenotype relationships in two high producer clones to uncover previously unknown genes determining CHO productivity. The screening comprised 187 rationally chosen target genes in two CHO high producer clones expressing two different complex antibody formats in a production-mimicking set-up. Notably, Myc depletion was revealed to drastically increased product expression (>40%) by enhancing cell-specific productivity. Myc-depleted cells demonstrated retarded proliferation rates associated with substantially higher product titers in industrially-relevant bioprocesses employing scale-down bioreactors. To prove reliability, the effects of Myc depletion were validated across multiple different clones, each expressing a distinct heterodimeric antibody format. Our findings reinforce the mutually exclusive relationship between growth and production phenotypes and provide a targeted cell engineering approach to impact productivity without impairing product quality.

In the third part of this thesis, the underlying factors contributing to phenotypic diversity in CHO cells are characterized using genomic barcodes for lineage tracing. Genomic barcoding of CHO biofactories provided novel insights about clone diversity during stable cell line selection on pool level, enabled an imaging-independent monoclonality assessment after single cell cloning, and eventually improved hit-picking of antibody producer clones by monitoring of cellular lineages during the cell line development (CLD) process. Strikingly, clonal cell lines from one individual TI event demonstrated a significantly lower variance regarding production-relevant and phenotypic parameters as compared to cell lines from distinct TI events. This implies that the observed cellular diversity lies within pre-existing cell-intrinsic factors and that the majority of clonal variation did not develop during the CLD process, especially during single cell cloning. Enriching cellular diversity improved CLD screening workflows and reduced the screening burden by propelling phenotypic variance. Overall, these results revisit and update CHO cell engineering options in the context of isogenic targeted integration cell line development.

1 General introduction

1.1 Drug development of recombinant antibodies

1.1.1 Recombinant antibodies as therapeutic agents

Recombinant therapeutic antibodies are designed molecules which mimic and potentially extend common functions of antibodies found in the immune system (Posner et al., 2019) (Figure 1). These proteins recognize and target specific epitopes on an antigen, typically cell bound or secreted molecules, resulting in constant affinity to a single antigenic domain (Hafeez et al., 2018). The feasibility to use cells as expression systems for recombinant therapeutic proteins has first been demonstrated with the peptide Somatostatin in 1977 (Itakura et al., 1977). This discovery essentially repurposed cellular systems to biofactories, with the first FDA-approved therapeutic protein (Humulin®, Insulin) for human application in 1982 produced with *Escherichia coli*. As of now, recombinant therapeutic proteins provide indispensable treatment options for broad indications including cancer, inflammation-related conditions, neutropenia, and diabetes. Notably, the World Health Organization (WHO) list of essential medicines contains insulin, vaccines, human growth hormones, erythropoietin, monoclonal antibodies, interferons and coagulation factors which are all produced using cellular expression systems (WHO, 2023). This trend continues currently with more than 7800 recombinant therapeutic molecules in clinical development globally and over 1000 in clinical phase 3 studies (Walsh & Walsh, 2022). These copious demands require potent cellular expression systems which allow industrial scale production. Among the recombinant therapeutic proteins, monoclonal antibodies (mAbs) have become the predominant treatment modality for various diseases (Lu et al., 2020). Using IgG-like mAbs as a basis, the field has since created novel heterodimeric bispecific antibody (bsAb) formats extending the therapeutic target space by, e.g. neutralization, cytolytic activity, and membrane receptor targeting (Figure 1). Utilizing recombinant expression systems circumvents the restrictions faced by previous use of canonically occurring antibodies (i.e. full-length monospecific antibodies), and extend the possible mode-of-action substantially. This is exemplified by over 60 bispecific formats, which vary in binding valency for each antigen, spatial geometry of antigen-binding sites, pharmacokinetic half-life, and in some cases effector functions. (Spiess et al., 2015). As of now, mammalian expression systems continue to be the most frequently used expression system for recombinant antibody production, dictated by the need of human-like glycosylation (Walsh & Walsh, 2022).

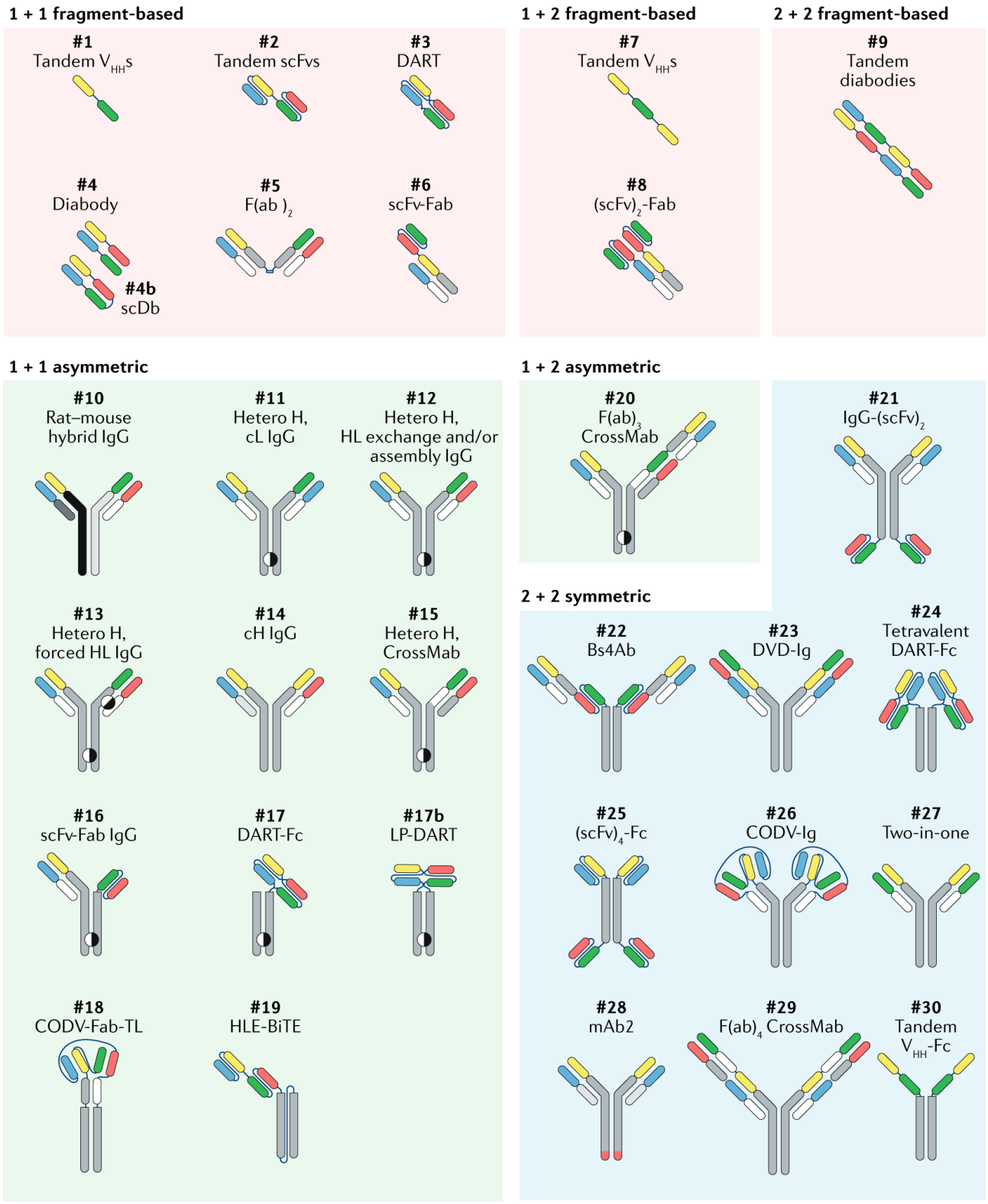

Figure 1. Systematic overview of bispecific antibody formats (increasing valency from left to right). Formats are divided into fragment-based (lacking an Fc domain), asymmetric-, and symmetric Fc-bearing molecules. Molecules of all formats increasingly contain mutations which positively influence pharmacokinetics/dynamics, or manufacturability parameters, e.g. Fc-mediated effector functions, half-life, or chain pairing. Reprinted from Labrijn et al. (2019)

The main host organisms for recombinant protein production are bacteria (*Escherichia coli*), yeast (*Saccharomyces cerevisiae*, *Pichia pastoris*), and mammalian cells (CHO, BHK, HEK, and NS0 cells (C. J. Huang et al., 2012)). Mammalian cells are used for the majority of approved recombinant proteins, because of their capability to produce human-like N-glycosylation. Protein glycosylation substantially influences efficacy, serum half-life, and antigenicity of therapeutic proteins (Egrie & Browne, 2001; Elliott et al., 2003; Wolf et al., 2022). Accordingly, non-glycosylated therapeutic proteins are mostly produced in bacterial and yeast expression systems due the overall lower costs in contrast to mammalian expression systems (Demain & Vaishnav, 2009). The importance of glycosylation as a critical quality attribute is highlighted by guidelines from the US Food and Drug Administration (FDA, 2012a, 2012b) and the European Medicines Agency (EMEA, 2014a, 2014b).

The choice of the most appropriate expression host depends on the specific therapeutic protein to be expressed. In case of non-glycosylated therapeutic proteins, bacterial and yeast expression systems are preferred as they have low media requirements, display rapid cell growth and return high protein yields. However, bacterial systems lack the intracellular compartmentalization and the enzymatic components necessary for complex human-like glycosylation (Ghaderi et al., 2012; Graumann & Premstaller, 2006). Therapeutic proteins expressed in bacterial expression systems often aggregate and form inclusion bodies because of low intracellular solubility and absence of appropriate protein chaperone systems. In contrast, yeast cells can display glycosylation with a human-like N-glycan core structure (Ghaderi et al., 2012). However, the hyper-mannosylated N-glycans are highly immunogenic for humans, result in short *in vivo* half-life, and reduced efficacy (Gerngross, 2004).

1.1.2 Eukaryotic hosts used for recombinant antibody production

Recombinant antibody production requires mammalian cells, which are competent in expressing large and complex recombinant proteins with human-like PTMs (i.e. glycosylation, disulfide bond formation, phosphorylation, or proteolytic processing). The specific selection of an appropriate mammalian host species is mainly driven around safety concerns, as recombinant proteins possibly transmit disease-causing agents during human application. Until today, three cellular components are commonly agreed as potential risk factors if they were found to be contaminants in biological products: (retro-) viruses, (potentially) oncogenic cellular DNA, and transforming proteins (prions). The selection of an appropriate mammalian host thus requires a balanced risk versus benefits decision for each biological product. For production of recombinant proteins in general, three types of mammalian cells – classified by their growth characteristics - have been used until today: i) primary cells explanted from normal tissues, ii) diploid cells with finite amount of cell divisions, and iii) continuous cell lines. Primary cells, i.e. primary monkey kidney cells for production of attenuated live poliovirus vaccine, were first accepted for commercial production of recombinant proteins. This was based on the early assumptions that cells derived from “normal” tissues bear the lowest risk in terms of an (at that time) unspecific oncogenic potential (Hilleman, 1968). Notably, during the first decades of bioproduction, several human pathogenic viruses, in contrast to a latent unknown oncogenic potential, were identified as a clear risk in primary cells and tissues: e.g. polio vaccines contamination with SV-40 (Sweet & Hilleman, 1960), hepatitis B viruses in plasma derivatives (Gerety & Aronson, 1982), and transmission of rabies by corneal grafts (Baer et al., 1982). Gradual acceptance of diploid cells was therefore achieved, as diploid cells have the advantage of greater assurance of virus-free material, being independent of fresh tissue supply, storing certified cell seed stocks, more economic cell production, and the possibility for cultivation in chemically defined media (Vaccines, 1963). In the 1970s, little was known about the basis for human cancer, emphasis was placed on karyotype as a major criterion for “normality” and diploid cells were accepted as equivalent to normal cells as long as the karyotype was stable (Moorhead et al., 1974). WI-38 (human fetal lung cells) represents the first defined mammalian expression system and characterized production host with a stable chromosomal pattern. (Swim & Parker, 1957).

While production of recombinant proteins in diploid cells is feasible for vaccines and other low demand products, manufacturing of pharmaceutical drugs, at that time especially interferon, was economically unviable in freshly collected human leukocytes. Additionally,

diploid fibroblast cells yielded a molecule which was chemically and biologically different from human interferon (WHO, 1978). Production in lymphoblastoid cell lines (Namalwa) however, was proven to be a reliable and economically acceptable source of human-like interferon (Zoon et al., 1978). Namalwa cells originated from a Burkitt tumor patient, are “transformed”, and contained the Epstein-Barr virus genome integrated into the cellular DNA. This bares the risk of transmitting whole virus or DNA with viral elements together with interferon products. Based on an advanced purification process (Hughes et al., 1974), potential contamination with virus and cellular DNA was mitigated by affinity chromatography, low pH of the eluate, and TCA/ethanol treatment (Beale, 1979). The final interferon product was free of Epstein-Barr virus and cellular DNA, which were both undetectable after purification. The FDA therefore allowed human clinical studies with material generated in Namalwa cells, by the end of the 1970s (Petricciani & Sheets, 2008).

Continuous cell lines, i.e. cancer cell lines, were subsequently the host of choice because of their rapid growth in suspension, high protein expression levels, and less stringent media requirements. After numerous conferences in the US and Europe, a broad consensus emerged from conclusions of the WHO Study Group on Biologicals in 1986 (WHO, 1987). While transforming proteins and cellular DNA (limited to 100 pg per dose) were essentially dismissed as an area of concern, major focus was placed on viral contamination. Cellular DNA can contain up to 0.01% of integrated retroviral sequences (Benveniste et al., 1977). Transmissible retroviruses have consecutively been detected, albeit only under laboratory conditions with extensive co-cultivation of *Macaca arctoides* cells using heterologous indicator cells (George J. Todaro et al., 1978). Notably, in a more extensive study transmissible retroviruses could not be isolated from other species of Old World monkeys, higher apes, or from human normal or tumor tissues (G. J. Todaro et al., 1976). In murine and avian systems transmissible virus transformation with retroviruses requires combinatorial events. However, transformation events have been extremely rare with less than one in one hundred million (Rapp & Todaro, 1978). The risk of retroviral contaminants in biological products therefore lacks evidence for demonstrable clinical significance and importantly evidence that infectious nucleic acid sequences are more common in immortalized cell lines than primary cell cultures. As a major conclusion of the WHO Study group, the host cells for production may simply be chosen based on efficiency of production as long as the manufacturing process can eliminate potential viruses and host DNA to acceptable levels.

More continuous cell lines were gradually accepted by regulatory authorities, with Chinese Hamster Ovary (CHO) cells being used for the first recombinant therapeutic protein (recombinant tissues plasminogen activator, Activase®) in 1987. For biotherapeutic antibody production, murine myeloma cell lines (NS0 and Sp2/0) and CHO cells were dominantly chosen.

CHO cells showed several major advantages in contrast to other continuous cell lines: i) suspension growth with serum-free chemically defined media (Ishida et al., 1990) ii) compatibility with gene amplification systems for stable transfection, such as dihydrofolate reductase (DHFR)-mediated (Scahill et al., 1983) or glutamine synthetase (GS)-mediated gene amplification (Nunberg et al., 1978). iii) human-like post-translational modifications (PTMs), with bioactive and human compatible glycosylation patterns iv) high tolerance to changes in process parameters, such as pH, oxygen level, pressure or temperature (Lai et al., 2013), and v) species barrier protection for many viral agents, with less expression of many viral entry genes as compared to other mammalian cell lines (Berting et al., 2010).
Most importantly, CHO cells are preferred as they produce proteins with human-like complex bioactive PTMs (Figure 2). Specifically, CHO-derived proteins are decorated with glycosylation patterns closely mimicking material produced in human cells with only minor deviations. Rodent cell lines (CHO, NS0, and Sp2/0) can produce glycans not expressed in humans, i.e. galactose-α1,3-galactose (α-gal) and N-glycolylneuraminic acid (NGNA). Humans are genetically deficient in biosynthesizing terminal α-gal on N-glycans which consequently can lead to immune response (Galili, 2004). NGNA is synthesized by the CMAH gene, which is irreversibly mutated in all humans in contrast to non-human mammalian cells (Varki, 2007). Because of these potential immunogenic PTMs non-human cell lines are typically screened to identify clones with acceptable glycan profiles (Ghaderi et al., 2010). While NS0 and Sp2/0 cells are equipped with the cellular machinery to secrete antibodies, as they originate from immunoglobulin-producing tumors, antibodies produced in these cell lines have a greater tendency to confer immunogenic α1,3-linked galactose and NGNA residues (K. N. Baker et al., 2001). Driven by the overall efficiency of antibody production, CHO cells are currently dominantly chosen for 89% of mAb products (95 out of 107 mAb products with modest interest in developing alternative hosts (Walsh & Walsh, 2022)).

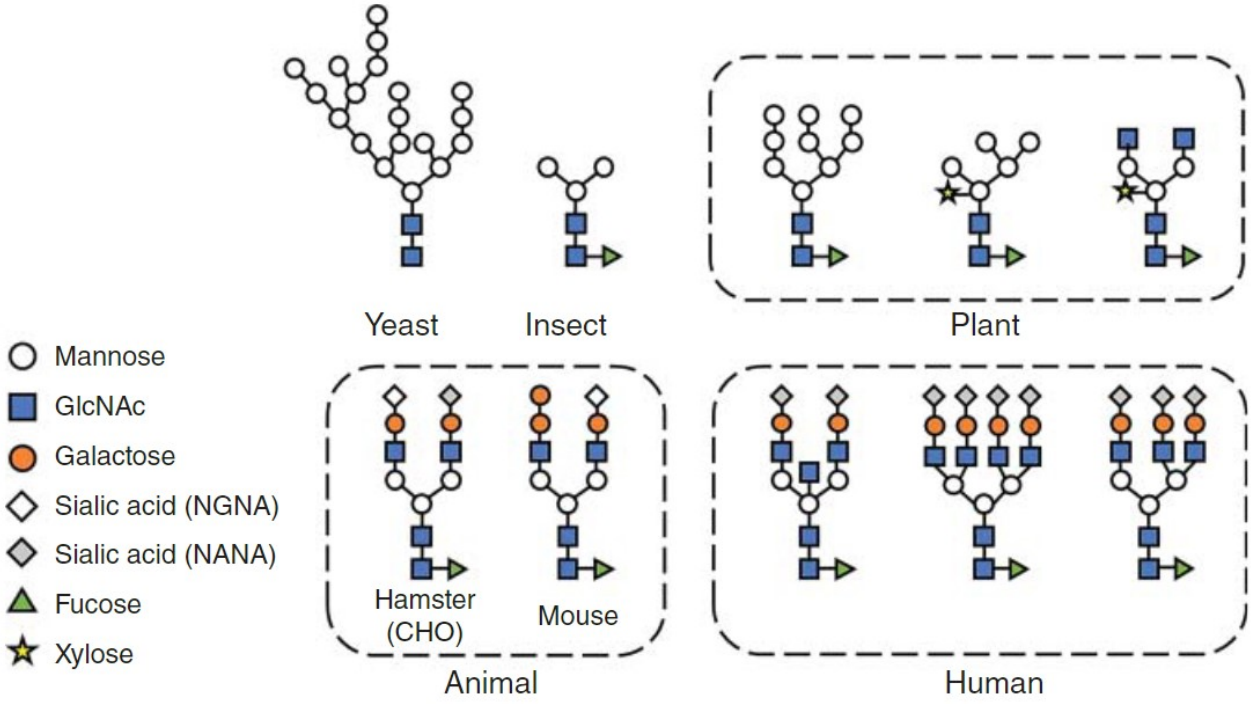

Figure 2 N-linked glycosylation patterns vary across different organisms. Recombinant proteins expressed from yeast, insect, or plant cells are deficient in synthesizing complex oligosaccharides such as galactose and terminal sialic acid (upper panel). Notably, yeast cells additionally show high-mannose type oligosaccharides. In contrast, murine and hamster cells are capable of synthesizing human-like glycosylation patterns, which are bi-antennary, contain fucose and galactose and additionally terminal sialic acid. Reprinted from Soo Min Noh et al. (2019)

1.1.3 The CHO expression platform for stable recombinant antibody expression

Historically, different CHO sub lineages were generated from the original CHO ori cell line, which was isolated from Chinese Hamster ovaries in 1956 (Puck et al., 1958). Initially, these cells were fundamental for research in molecular cell genetics. CHO cells have large chromosomes which enabled convenient studies on association of chromosomal rearrangements with gene functions (Siciliano et al., 1985; Thompson & Baker, 1973). However, CHO cells quickly gained popularity because of their resilience and rapid adaptation to *in vitro* cultures with fast generation times. Recombinant proteins are produced by two main approaches: transient gene expression, where recombinant plasmid DNA is solely delivered into the host cell, and stable gene expression with stably integrated foreign DNA into the host cell genome. Transient gene expression is an established method for small-scale and rapid production during pre-clinical development of recombinant antibodies (Pham et al., 2006). Stable transfection is the method of choice for large-scale production of recombinant antibodies with consistent product quality, as transiently transfected cells inevitably lose the plasmid DNA after several cell divisions. CHO cells, undergoing extensive undirected mutagenesis in early research, enabled the isolation of auxotrophic cell lines, facilitating their use for convenient stable transfection (Puck & Kao, 1967). Early stable transfection was achieved using such auxotrophic cell lines and random (no pre-defined integration site) selection systems, namely the dihydrofolate reductase-mediated (DHFR) methotrexate (MTX)-based and the glutamine synthetase-mediated (GS) methionine sulfoximine (MSX)-based selection systems. Two CHO cell lines have been routinely used for DHFR-based selection: DUXB11 and DG44, which originate from an early sub clone of CHO ori: CHO-K1 (Urlaub & Chasin, 1980). These cells are engineered to be deficient in dihydrofolate reductase activity and require exogenous nucleotide precursors for survival. By combining the recombinant gene of interest with a DHFR gene, only cells with rare stable integration of the plasmid DNA survive in the absence of nucleotide precursors. This method results in reliable and simple stable gene expression, with additional gene amplification by MTX (a competitive DHFR inhibitor). Increasing supplementation of MTX in the cultivation media results in selection of cells with multiple copies of DHFR integration which frequently correlates with increased transgene copy number and high product yields (Lai et al., 2013). The ability to transfect, select, amplify and stably express recombinant biotherapeutic proteins using the DHFR system was fundamental for large-scale production (Jayapal et al., 2007).

Stably transfected cell populations remain heterogeneous, consisting of cell lineages with various integration sites and copy numbers (placement effects) which impact specific productivity. To ensure high productivity and product quality, individual cell colonies (cell clones) are isolated to receive a more uniform cell population. The chosen clones are expanded and subsequently tested in scale-down model systems mimicking large-scale production facilities. Random integration results in substantial productivity variations due to copy number and placement effects, requiring extensive clone screening programs. As an alternative, site-specific integration of the transgene at a pre-defined “genetic hotspot” with high and stable long-term expression levels has emerged (Crawford et al., 2013; J. Y. Kim et al., 2012). Here, recombinase-mediates cassette exchange (RMCE) systems (e.g. Cre/loxP, Flp/FRT, PhiC31) enable targeted integration of transgenes flanked by recombinase-recognition sequences using site-specific recombinases. The Cre/loxP systems, consisting of the Cre recombinase and loxP recognition sequences, was first used to achieve high-producing clones by site-specific integration (Inao et al., 2015; Kito et al., 2002). Alternatively endonuclease-mediated targeted integration technologies have been used for site-specific integration, i.e. zinc-finger nuclease, transcription activator-like effector nuclease, and clustered regularly interspaced short palindromic repeats (CRISPR) /CRISPR-associated protein RNA-guided nuclease (Carroll, 2014). As a compromise between site-specific integration and random integration, DNA transposons, such as Sleeping Beauty, Tol2, Mos1, and PiggyBac have been demonstrated to integrate transgenes into specific regions of the genome (X. Huang et al., 2010; Wu et al., 2006).

For bioproduction, cells have initially been grown in batch cultivation over 3-4 days to allow synthesis and product secretion. Accumulation of end-products of cellular metabolism (lactic acid and ammonia), depletion of nutrients (mostly glucose and glutamine), changes of pH, and osmolality then quickly limit cell growth and productivity. Thus, volumetric productivity has substantially improved with a shift from batch mode production towards fed batch cultures with feeding of concentrated nutrients (L. Z. Xie & Wang, 1997). Of note, proliferating cells tend to ingest more nutrients than bioenergetically needed (DeBerardinis et al., 2008; Heiden et al., 2009). Nutrient overfeeding consequently can shift cells to a less efficient energy metabolism leading to higher lactate productivities (Reinhart et al., 2015). Most successful strategies therefore maintain a balanced low target concentration of the major carbon substrates to limit excessive ammonia and lactate production (Butler, 2005).
Fed batch typically follow an initial proliferation phase followed by arrested cell division, e.g. by using a decrease in culture temperature (Fox et al., 2004) to optimize volumetric

productivity. Substantial work has been done in optimizing the chemical environment, e.g. media optimizations (Gronemeyer et al., 2014), and adapted feeding strategies (Reinhart et al., 2015). The chemical environment combined with controlled physical environment parameters such as temperature, pH, pO2, and agitation rate together form the production process. Manufacturer invest extensive resources on the production process which is individually performed for each cell line (F. M. Wurm, 2004). Fed batch cultivation remains the dominantly chosen production mode, due to batch traceability, short operation period, and high volumetric titers (Pollock et al., 2013).

Most recently the constantly changing environment in fed batch processes (depletion of nutrition, accumulation of metabolic by-products and the target protein) can be circumvented in perfusion processes with constant media exchange. Notably, this changing environment influences product quality attributes (PTMs) resulting in product heterogeneity in fed batch processes (Figure 3b-d) (Pacis et al., 2011; W. C. Yang et al., 2014). The final product in fed batch processes is consequently the average collection of heterogeneous molecules across the process time. In contrast, perfusion processes allow a steady state environment by exchanging media, extracellular material, and excessive cells (cell “bleed”) with more constant product quality attributes (Ivarsson et al., 2014; W. C. Yang et al., 2014) (Figure 3).

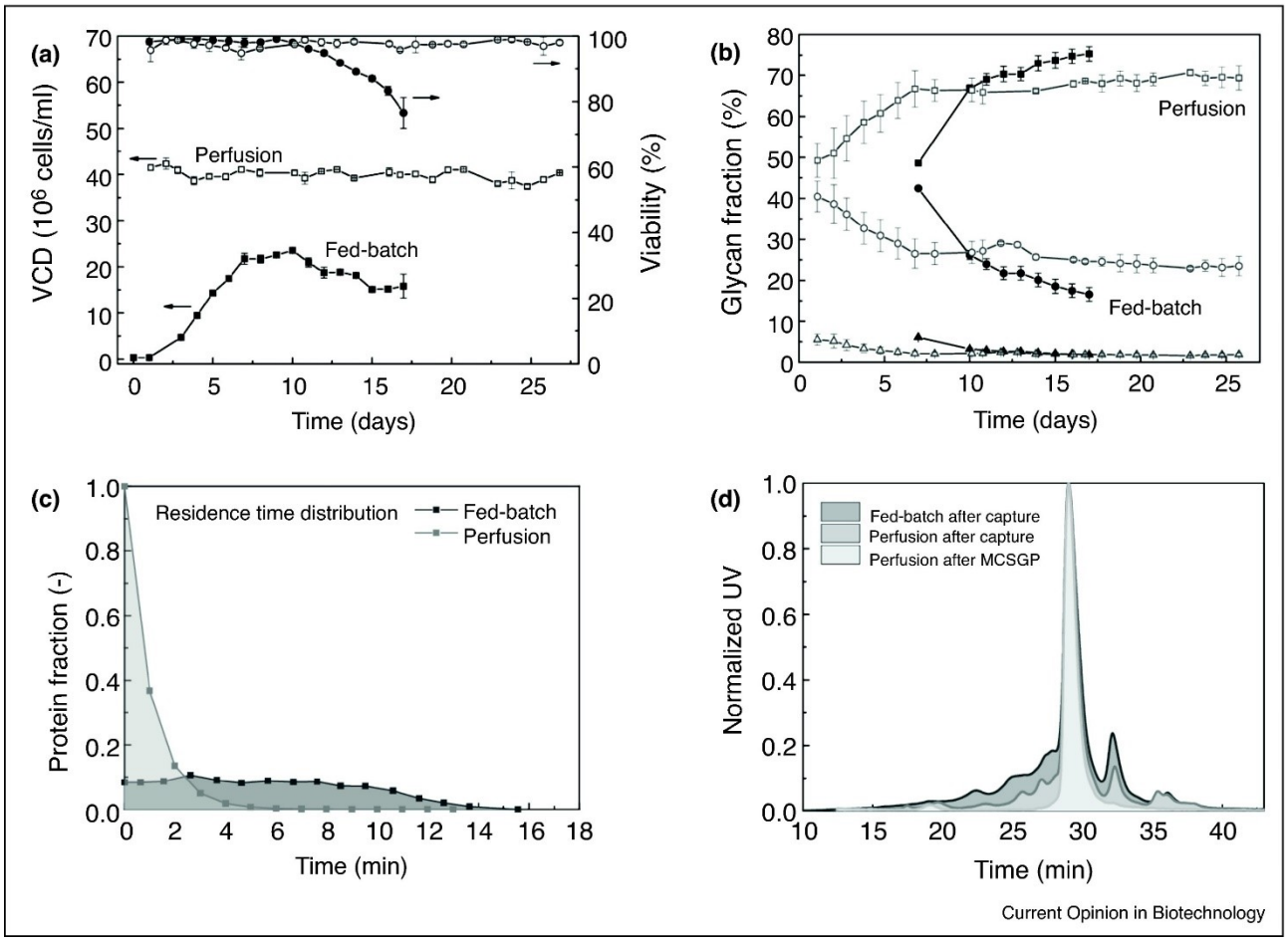

Figure 3 Comparison of production-relevant parameters comparing fed-batch production mode with perfusion mode. Comparison of a) cellular viable cell density and viability profiles, b) product glycan fractions including FA2G0 (■), FA2G1 (●), FA2G2(▲) c) residence time distribution, i.e the variation in the time that different molecules or cells spend within the reactor, and d) and product charge isoform distributions (after full downstream purification) Reprinted from Karst et al. (2018)

1.1.4 Scale-down model systems to mimic large-scale bioreactors

Small scale model systems (i.e. plates, shake flasks, bench top bioreactors) aim to mimic large-scale industrial bioreactors to accurately translate processes from laboratory to industrial scale (Manahan et al., 2019). Cellular physiology strongly depends on environmental conditions with consequences for product yield and quality if the culture milieu cannot be maintained (Lara et al., 2006). Scale-independent parameters which are stable across scales include, e.g. pH, temperature, dissolved oxygen, seeding density, cell age. In contrast, scale-dependent parameters such as agitation and gas transfer rates require special scaling strategies (Flickinger, 2010). Expression host and culture milieu form a complex relationship requiring extensive multifactorial statistical experimentation. Reliable testing systems demonstrate monitoring and control of scale-independent parameters, with laboratory-scale stirred tank bioreactors (STB, 1-100 l) as the cultivation vessel of choice (Doig et al., 2006). STB demonstrate a defined environment with extensive analytical options because of the large volumes utilized. As STB are geometrically identical to industrial scale vessels, all output information is applicable for scale-up (Xing et al., 2009). However, the number of experiments is restricted by the labor intensive setup which involved cleaning, sterilization, calibration, and inoculation in large volumes.

For high throughput experiments, especially during early stages of cell line cultivation, microtiter plates and *Erlenmeyer* shake flasks are extensively used, despite a low amount of parameter control in these uncontrolled systems (Figure 4) (Buchs, 2001). Both systems use orbital shaking for mixing, rely on surface aeration for oxygen mass transfer, and have very limited oxygen and pH control options. Because of their substantial higher throughput options they still remain valuable screening tools during early stages of cell line development. Driven by the need for high throughput cell line cultivation in controlled systems, miniaturized small-scale bioreactors are now dominantly used during cell line and bioprocess development (Bareither et al., 2013).

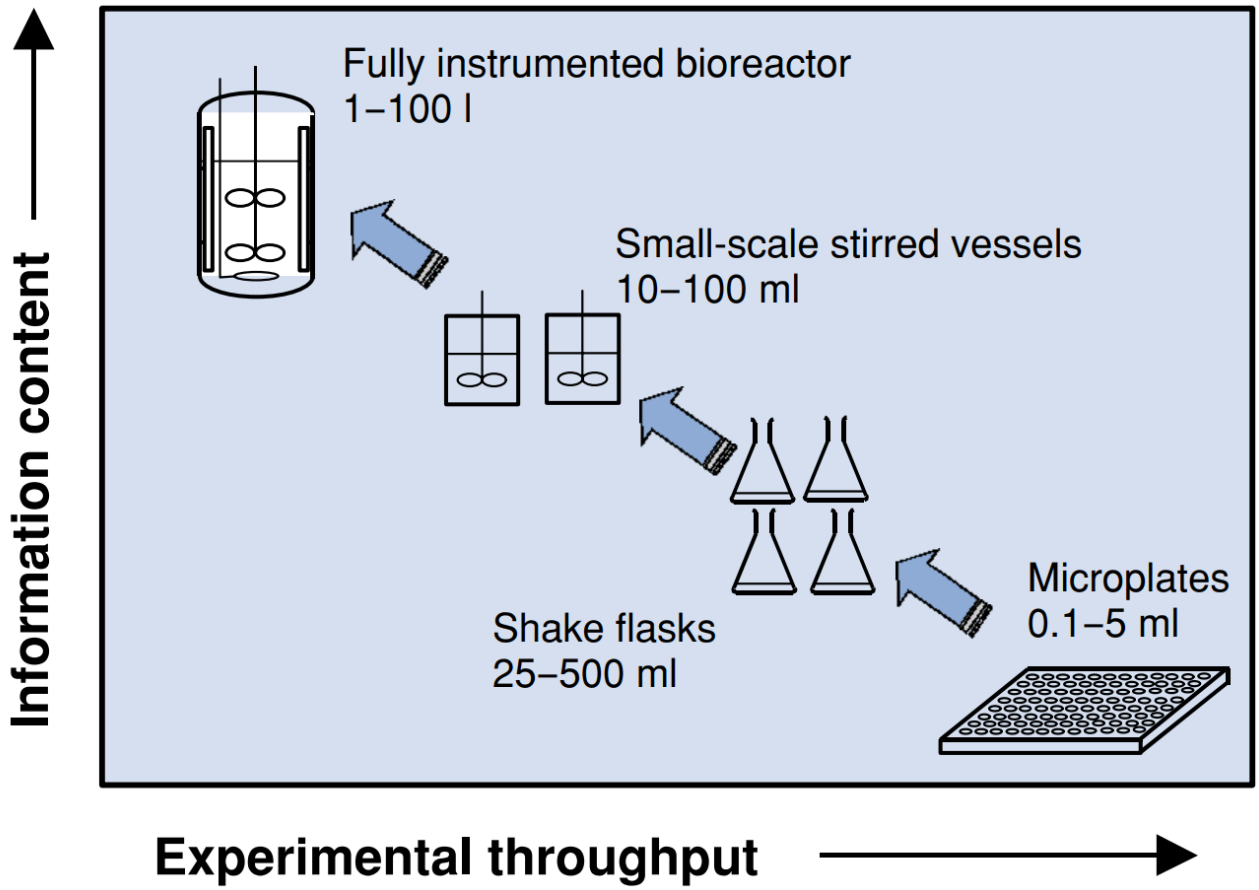

Figure 4. Inverse relationship between experimental throughput and information content observed during CHO cell line development. While microplates are uncontrolled systems with low information content, they offer high-throughput and *vice versa* for stirred-tank bioreactors. Reprinted from Doig et al. (2006).

1.2 CHO cell line development for recombinant antibodies

Development of stable recombinant CHO cell lines is essential for manufacturing of large-scale therapeutic proteins with consistent batch-to-batch quality (Shin & Lee, 2020). Historically, expression vectors (plasmid DNA) encoding the gene of interest (GOI) and a selection marker were transfected into CHO host cells for random integration. To enrich the stochastic random integration events, cells are cultivated in media containing selection pressure. Cells with stable integration retain the ability to express the GOI and the selection marker, thereby allowing these cells to survive. In contrast, cells without stable integration quickly dilute the expression vectors with subsequent cell division events and cannot survive after loss of plasmid DNA. Simple monoclonal antibodies (humanized IgG) could be produced with volumetric productivities using random integration technology. However, fundamental problems of random integration remain, such as placement effects of the integration site, loss of copy numbers, and transgene/chromosomal rearrangement (J. S. Lee et al., 2019). With increasingly complex heterodimeric antibody formats, e.g. artificial fusion proteins and bsAb, high volumetric productivities are additionally challenged by post-translational bottlenecks such as improper single chain folding, light chain aggregates, or incorrect chain association (Kaneyoshi et al., 2019; Klein et al., 2012; Mathias et al., 2020). In contrast to cell populations achieved by random integration, site-specific integration into pre-validated genomic hot spots show substantially reduce placement effects and copy number variations (J. S. Lee et al., 2015). However, CHO cells remain heterogeneous after stable integration due to inherent genomic and epigenetic plasticity (Dahodwala & Lee, 2019; Lewis et al., 2013). To mitigate cell line heterogeneity, cell lines with single cell origin are generated, as clonal lineages are generally considered to offer a more stable and consistent product quality profile (Welch & Arden, 2019). To obtain the highest specific productivity from clonal cell lines, typically hundreds of cell clones are empirically screened (Borth et al., 2002). Thus, recent cell line development protocols aim to further reduce the observed variability and the amount of blind-screening of genetic heterogeneity by data-driven rational engineering efforts (Srirangan et al., 2020).

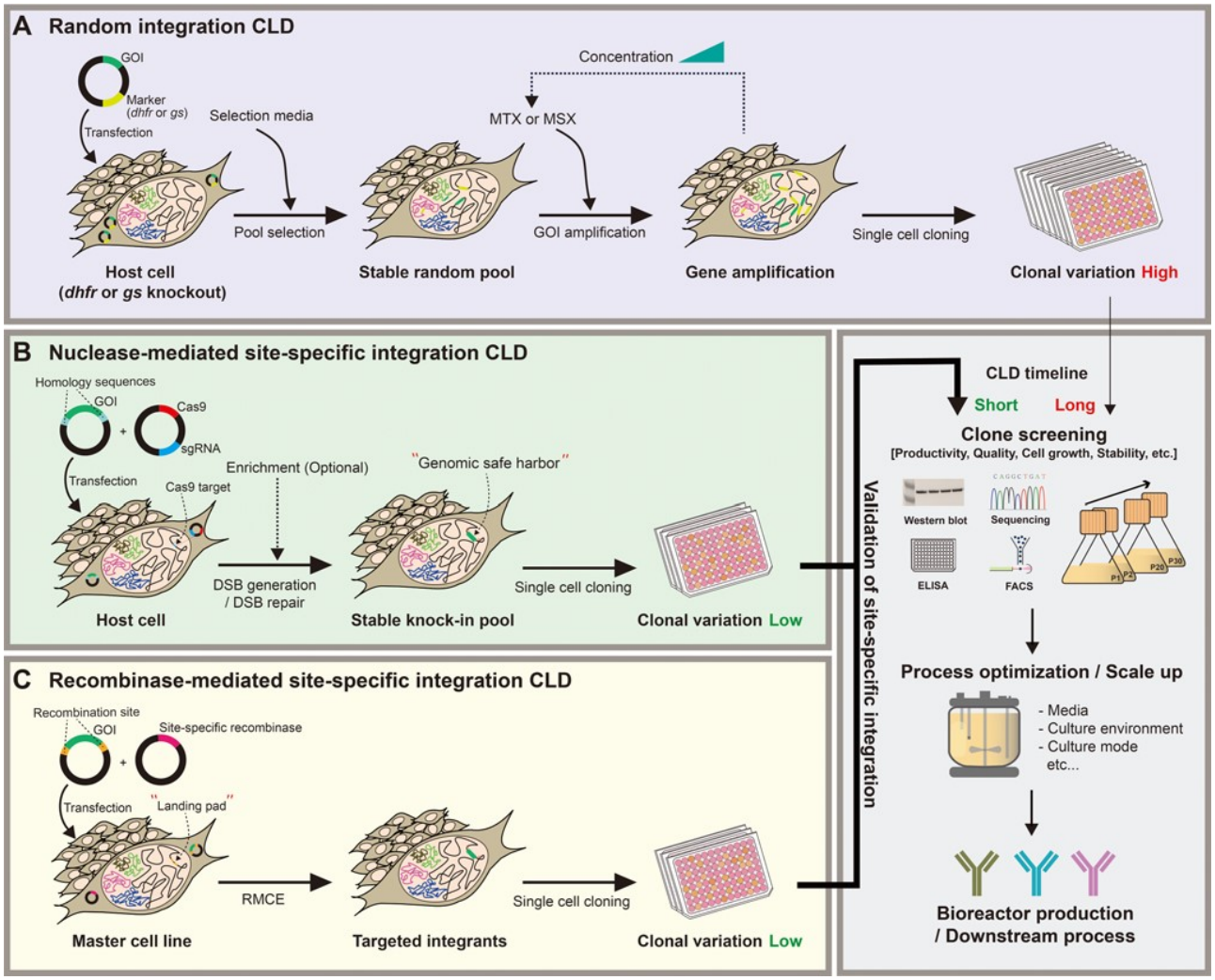

Figure 5. Schematic comparison random and site-specific cell line development methods. a) Random integration methods relies on transgene amplification using DHFR (MTX) or GS (MSX) inhibitors to boost copy numbers and consequently cell productivity. Resulting clonal variability is high due to copy number variations and placement effects. In contrast, site-specific integration methods rely on either b) nucleases and HDR or c) recombinase-mediated-cassette-exchange, which consequently results in less phenotypic variation of producer clones. All methods subsequently undergo clone screening, process optimization, and scale up validation. Notably, clones generated via random integration require more intensive clone screening. CLD, cell line development, GOI, gene of interest, MTX; methotrexate, MSX, methionine sulphoximine, DSB, double strand break. Reprinted from Shin and Lee (2020)

1.2.1 Transgene subunit dosage in CLD

Recombinant cell lines generated by random integration of expression vectors display substantial heterogeneity with regard to expression properties, cell growth, and transgene expression stability (Gödecke et al., 2021). Synthetic gene expression cassettes perturbate the endogenous chromatin structure at the integration site, leading to unpredictable consequences for the endogenous neighboring genes and the transgene itself. These placement and copy number effects in combination with the intrinsic genomic epi-/genetic plasticity of the cells itself results in remarkable phenotypic variance. Notably, recombinant cell lines concurrently need to express 3-4 distinct polypeptides in case of heterodimeric bsAbs, in contrast to only 2 different polypeptides when expressing an homodimeric mAb molecule (Klein et al., 2012). Consequently, cell line development for heterodimeric bispecific antibodies is complicated by the need to optimize expression level stoichiometry of 3-4 distinct polypeptide chain to obtain acceptable levels of correctly associated antibody – the so-called chain association issue (Z. Lee et al., 2024).

To come up with a commercially acceptable clone, two main cell line development strategies are followed: i) high throughput screening after random integration of transgenes to identify rare phenotypic variants out of heterogeneous populations and ii) site-specific integration of expression cassettes into pre-characterized genomic hot spots. For homodimeric antibodies with two different polypeptides: heavy chain (HC) and light chain (LC), random integration in combination with high throughput screening remains a reliable strategy. Studies from murine pre-B cells reveal that HCs form homodimers which are retained in the ER until initiation of LC expression allow completion of the correct quaternary structure (HC_2LC_2) (Leitzgen et al., 1997). While free LC dimers can compete with HC secretion, LC excess generally supports antibody folding by minimizing accumulation of unfolded HC and reducing ER stress (Bertolotti et al., 2000; Y. K. Lee et al., 1999; Schlatter et al., 2005). High productivity cell lines therefore frequently display excess free LCs as the only undesired by-product in the cell culture media. Subsequently, affinity chromatography using protein A (isolated from *Staphylococcus aureus*) shows negligible binding to the Fab region and can therefore reliably produce material with >99% purity in a single capture step (Shukla et al., 2007). This results in a broad spectrum of possible subunit gene dosages with copy number variations and placement effects which are compatible with high productivity and quality.

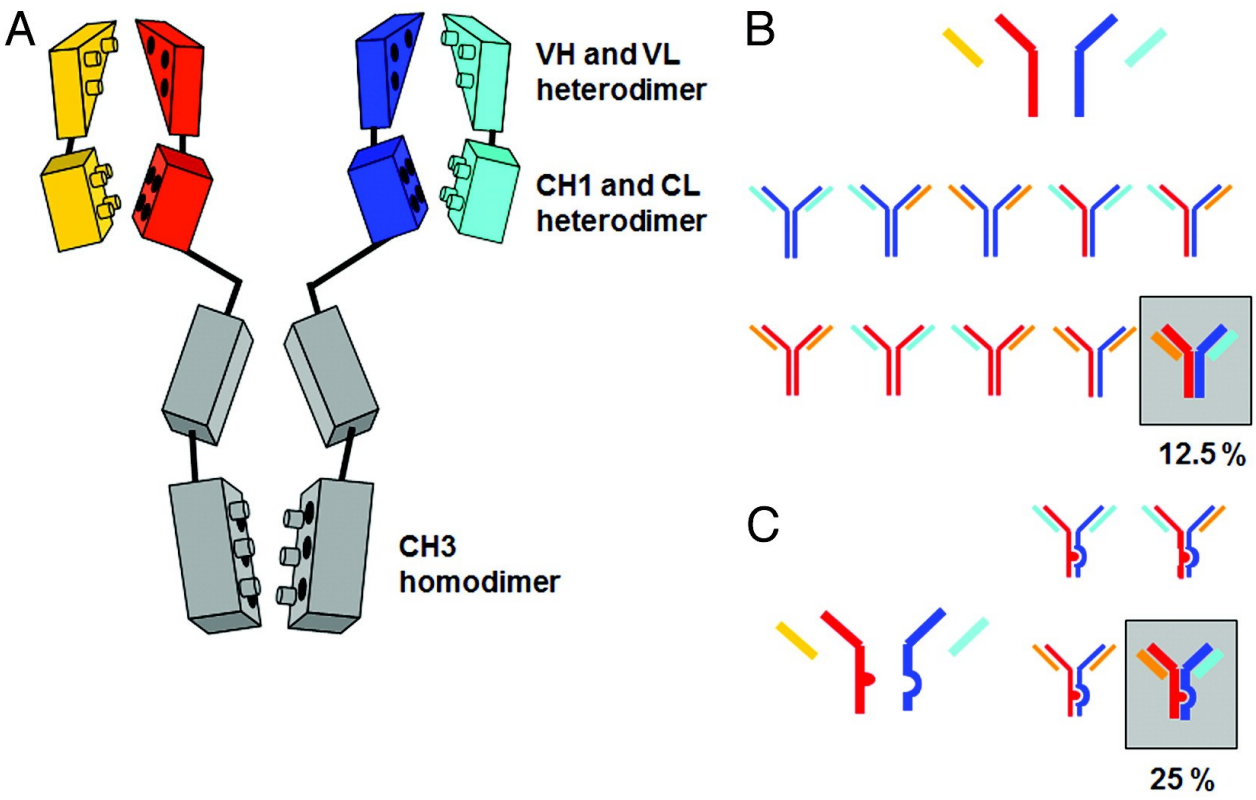

Figure 6. Schematic illustration of a) all possible homo- and heterodimerization interfaces between light- and heavy-chain domains for heterodimeric bispecific antibodies, b) combinatorial options for random chain association if chains have no preferential binding site. The desired heterodimeric and fully functional antibody is formed in 12.5% of cases. c) improved light chain association issue when enforcing heavy chain heterodimerization leading to correctly formed bispecific antibodies in 25% of cases. Reprinted from Klein et al. (2012)

In stark contrast, random assembly of heterodimeric bispecific antibodies results in 16 combinations, with only 2 (12.5%) representing the desired main product (Figure 6a and b). (Brinkmann & Kontermann, 2017). Alternative chain assemblies can result in either non-functional or monospecific molecules with possibly severe adverse effects, such as immunogenicity, anaphylaxis or neutralization of the antibody (Y. F. Li, 2019; van Beers & Bardor, 2012). This is of particular concern for T cell bispecific antibodies due to the possible formation of hyperactive CD3-binding homodimers resulting in off-target T cell activation through T-cell receptor dimerization (H. Y. Lee et al., 2019). Much progress has been achieved in enhancing heavy and light chain hetero dimerization by modifications of the respective structural interface between the chains. For heavy chains, a bulky “knob” residue is introduced in one chain (achieved by specific mutations in the CH3 domain: S354C, T366W) whereas the other “hole” HC is equipped with an appropriate pocket (achieved by the mutations: Y349C, T366S, L368A, Y407V, Figure 6c) (Ridgway et al., 1996). This “knobs-into-holes” approach mitigates homo dimerization effectively as long as both chains are expressed with equal levels (Klein et al., 2012). Similarly, light chain hetero dimerization

is supported by Fab domain cross-over introduced in one arm of the bispecific antibody, the so called “CrossMab” approach (Schaefer et al., 2011). Either the VH-VL or the CH1-CL domains are exchanged between heavy and light chain, resulting in strong preference of hetero dimerization without specific connectors or mutations. Of note, although potentially side-products are substantially reduced, a titration of the expression levels between the two different light chains remains necessary (Schaefer et al., 2011).

For optimal expression of heterodimeric bsAbs, it remains inevitable to achieve control of the relative level at which each chain is constitutively expressed. This multigene co-expression at different stoichiometry is inherently context-specific and changes substantially depending on the respective transgene and vector design features (Patel et al., 2021). Site-specific integration into pre-defined genetic hot spots obviates intra-clonal heterogeneity by generating genetically uniform, i.e. isogenic, clones (Gödecke et al., 2021). This single copy site-specific integration enables iterative testing of various expression vector designs which can be optimized in a uniform genomic context (Beal et al., 2023; Nehlsen et al., 2009). The emergence of genome engineering tools has facilitated wide-spread use of site-specific integration, notably: homology directed repair (HDR) using programmable nucleases, such as clustered regularly interspaced short palindromic repeats (CRISPR) / CRISPR-associated protein 9 (Cas9), and recombinase-mediates cassette exchange (RMCE), utilizing serine (*e.g.* Bxb1/attB, PhiC31) and threonine recombinases (e.g. Cre/loxP, Flp/FRT). Initial site-specific integration was mostly achieved using RMCE and paved the way for rational and controllable expression cassette design (Crawford et al., 2013; Nov et al., 2007). RMCE requires the generation of host cell lines containing a “landing pad” harboring recombination sites. These host cell lines are typically established using semi-/random landing pad integration followed by subsequent empirical screening and locus characterization (Crawford et al., 2013; L. Zhang et al., 2015). Empirical identification of hot spots with intrinsic stability and enhanced transcriptional activity remains the gold standard in CHO cells, as the underlying molecular mechanism are incompletely understood (Gaidukov et al., 2018). This is further exemplified by the predicted hot spot activity of *ROSA26* and *GRIK1* loci integration based on locus properties in human and murine cells (Cheng et al., 2016; Zambrowicz et al., 1997). While integration into the *ROSA26* locus supported robust expression in CHO cells, *GRIK1* integration was comparable to random loci (Gaidukov et al., 2018; Zhao et al., 2018). Importantly, site-specific integration supports reduced copy numbers, usually restricted to less than nine copies (Altamura et al., 2022), as compared to random integration, with up to 1000 copies after gene amplification

(Kaufman & Sharp, 1982). However, cells with optimized expression vector arrangements and genomic positions have been shown to match or exceed productivity of random integration clones, suggesting a limited benefit of integrating excessive transgene copies (Z. Lee et al., 2024; Ng et al., 2021; S. M. Noh et al., 2018). While the generation of host cell lines is labor-intensive due to the limited knowledge about favorable integration sites and the necessary clone screening process, the host cell line can subsequently be re-used for reproducible generation of many high-producing cell lines (Carver et al., 2020).

In contrast, *de novo* site-specific integration utilizes HDR triggered by introduction of a double-strand break (DSB) in mammalian cells (Cong et al., 2013; J. S. Lee et al., 2015). Introducing DSBs via CRISPR/Cas9 to trigger HDR has emerged as the predominant methodology for de novo site-specific integration in CHO cells. The CRISPR/Cas9 method enables facile introduction of DSBs as compared to zinc finger nucleases or transcription factor-like effector nucleases which require extensive protein design, synthesis, and validation (Doudna & Charpentier, 2014). However, HDR efficiency is inherently limited in CHO cells with simultaneous high rates of random integrations, due to high activity of non-homologous end-joining (NHEJ) pathway (Bosshard et al., 2019; Cristea et al., 2013; Vasquez et al., 2001). Notable attempts to overcome low HDR rates include i) fluorescent enrichment of genome-edited cells (J. S. Lee et al., 2016), ii) modifying culture conditions around transfection (Guo et al., 2018), iii) donor template modifications (O. Baker et al., 2017) (J. P. Zhang et al., 2017) v) and chemical inhibition/promotion of NHEJ and HDR, respectively. While site-specific integration by programmable nuclease has successfully been used for integration of transgenes, the aberrant risk of recombination events and off-target integration in combination with low integration rates hampers broad utilization (Phan et al., 2017).

1.2.2 Expression vector design in CLD

Mammalian cells can adjust gene expression levels on various levels by adaptations during i) transcription (conversion of information encoded in DNA to transient mRNA), ii) post-transcription (mRNA abundance and stability), iii) translational efficiency (conversion of mRNA to amino acid polymers) and iv) post-translation (protein stability). Therefore, to optimize abundance of correctly assembled heterodimeric bsAbs, the rate and timing of each level of gene expression require thorough arrangement. The expression system is required to express multiple transgenes at precise relative stoichiometry while maintaining high productivity and growth rates (Brown & James, 2016). Accordingly, synthetic expression vectors that harbor multiple genetic components are required, which drive stable high levels of transgene expression at optimal, designed stoichiometry (Barnes et al., 2003; Mariati et al., 2014). Stable expression levels are required for the time frame necessary to expand the cells for master cell bank generation, seed train cultures and subsequent production phases which typically requires over 60 generations (F. M. Wurm & Wurm, 2017). Substantial loss of productivity (less than 70% of the initial expression) compromises regulatory approval of the product by impairing product yield and quality (Barnes et al., 2003). The prevalent entry point to expression level control is transcriptional regulation, as the first step in protein expression. Transcriptional levels are relatively easy to manipulate and offer a wide dynamic range of expression control. Transcription control is typically achieved by engineering of promotors, terminators, untranslated regions (UTRs), or coding sequences (Brown & James, 2016; Ferreira et al., 2013; Quax et al., 2015). Promotor engineering displays the most common and effective method, due to their key role in high and consistent transgene transcription (O'Callaghan et al., 2010). Two discrete structural components can be engineered: the proximal promoter containing transcription factor regulatory elements (*i.e*. binding site for regulatory transcription factors which function as activators or repressors) and the core promoter with binding sites for general transcription factors (*i.e.* the pre-initiation complex) (Lenhard et al., 2012).

Given that specifically engineered and built-for-purpose synthetic promotors are not broadly applicable yet, naturally occurring promotors are prevalently used and modified for use in synthetic gene expression cassettes. Natural promotors can be classified as either endogenous or of viral origin. In the context of CHO cells, mostly strong viral promoter/enhancer elements based on human cytomegalovirus immediate early 1 (hCMV-IE1) and simian virus 40 (SV40) are utilized and effectively redistribute cellular resources towards the transgene and selection marker genes, respectively (Figure 7a) (Xia

et al., 2006). These viral sequences accept several ubiquitously expressed transcription factors and have evolved to recruit host cell transcription factors using highly efficient and concise recognition elements (Stinski & Isomura, 2008; X. Y. Wang et al., 2016). Notably, the strongest promotors in mammalian cell lines are of viral origin (Foecking & Hofstetter, 1986; Ho & Yang, 2014; X. Y. Wang et al., 2016). While hCMV-IE1 shows generally strong transcription achieved with only 650 bp full-length size, the expression is restricted to S phase and can be epigenetically silenced by enzymatic DNA methylation within CpG dinucleotides (Brightwell et al., 1997; Osterlehner et al., 2011). In contrast, heterologous eukaryotic promotors, such as Chinese hamster elongation factor-1 alpha (CEF1α) promoter, potentially preserve high transcription strength with reduced risk of silencing due to their endogenous nature (Deer & Allison, 2004). Because endogenous promoters are comparably large (in case of CEF1 α, a minimum size of 8.3 kbp), their use in multigene expression cassettes is limited.

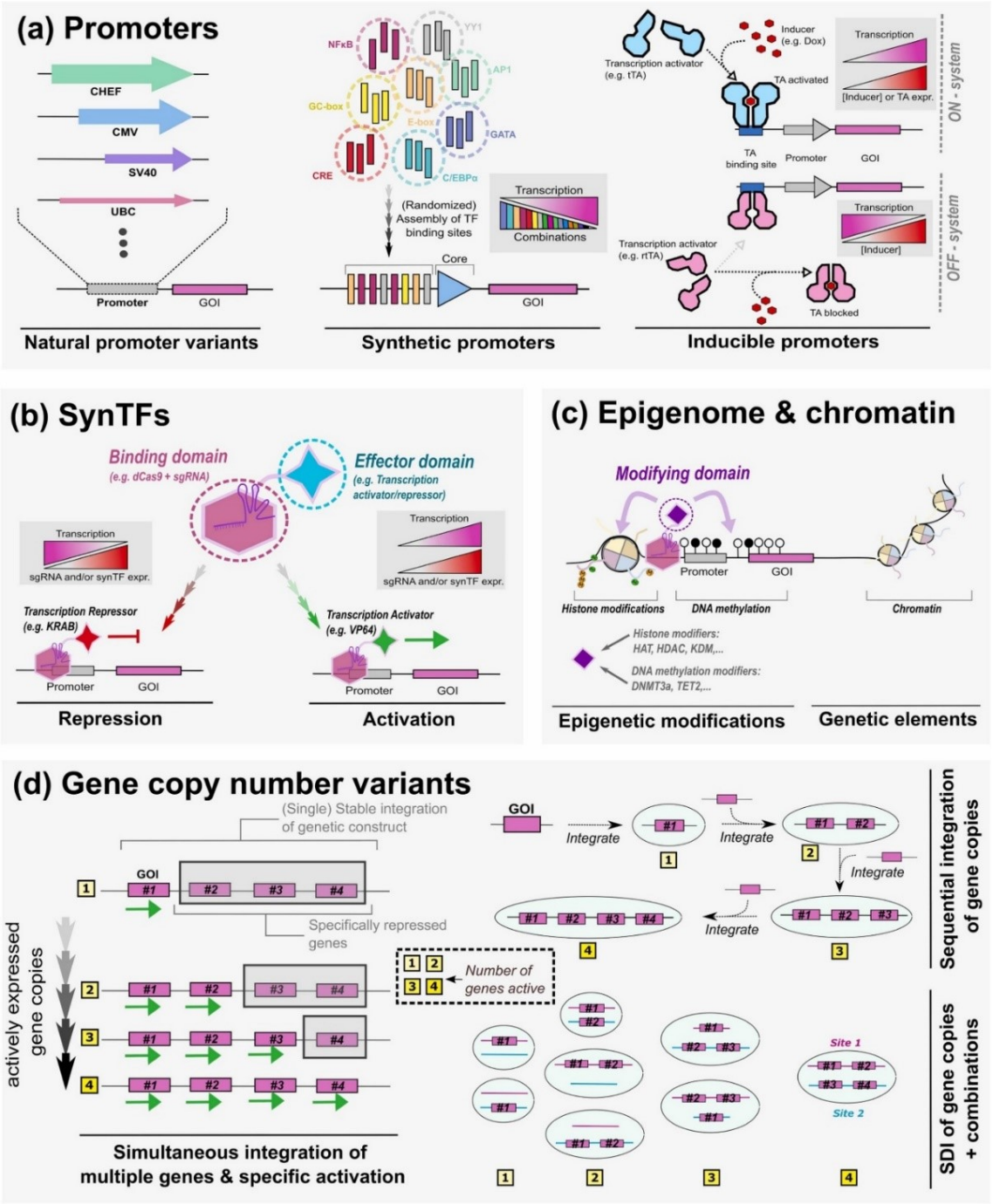

Figure 7. Genetic engineering options to achieve transcriptional control. a) Natural promoters (endogenous or viral) are constitutively active and show a wide range of expression strength. Synthetic promoters are assembled by rational combination of transcription factor binding sites. Inducible promoters utilize natural molecule-responsive transcription factors or b) synthetic build-for purpose transcription factors. c) Epigenetic modifier domains influence spatially close histone structure and DNA methylation levels. d) Gene dosage control by rationally choosing number of gene expression cassettes. GOI; gene of interest. Reprinted from Eisenhut et al. (2024)

While viral promotors demonstrate strong and robust constitute expression, they lack regulatory levers to fine tune expression ratios within multiple transgenes. To correlate transcription rates between multiple transgenes in a targeted integration setup, studies have suggested programmed transgene dosage increase, gene rank shuffling, and varying transcriptional activity (Figure 7d) (Carver et al., 2020; Z. Lee et al., 2024; Patel et al., 2021). Incremental elevated copy numbers frequently improve mRNA levels and productivity, while the additional benefit plateaus with increased copy number (Altamura et al., 2022; Z. Lee et al., 2024; Sergeeva et al., 2020). Typically the amount of HC transcript is rate limiting and thus increased HC copy numbers result in higher antibody expression (Schlatter et al., 2005). However, LC excess as compared to HC remains necessary for optimal expression (O'Callaghan et al., 2010). To support increased transgene gene dosage, multiple genes are typically placed in close proximity on a multigene expression vector, as plasmid vectors are limited in cargo space (frequently below 25 kbp). Multiple expression cassettes in close proximity can be prone to deviations in targeted expression levels by RNA-polymerase and ribosome competition, occlusion-mediated transcriptional interference and promoter competition (Bateman & Paule, 1988; Conte et al., 2002; Proudfoot, 1986; Qian et al., 2017). Transcriptional decisions at individual promoters depend on the local regulatory network, especially when sharing identical transcription factor binding sites (Brewster et al., 2014; Rydenfelt et al., 2014). The vast majority of CMV promoter activity is driven by only two transcription factor regulatory elements: NF-κB and CRE, which consequently compete for available free transcription factors (Brown et al., 2015). In addition, transcriptional interference is most severe for exceptionally strong promoters arranged in tandem orientation, where both transcriptional units elongate in the same direction (Tian & Andreadis, 2009). Shielding of transcriptional units is difficult due to inefficient transcription termination or transcription run-through observed in higher eukaryotes (Figure 7c) (Shearwin et al., 2005). Thus, the first position within a multigene expression vector commonly shows the strongest expression, as downstream promoters can be occluded by inefficient transcription termination of upstream transcriptional units (Eszterhas et al., 2002). Disruption of transcriptional interference may be reached by combination of chromatin-modifying elements (e.g. insulators, matrix attachment regions, ubiquitously acting chromatin opening elements) or alternatively by combining multiple genes in one expression cassette (Eszterhas et al., 2002; Tian & Andreadis, 2009).

Apart from engineering host cell dependent elements, control of multigene expression stoichiometry can be achieved using completely synthetic systems via inducible systems,

synthetic promoters, and complex gene switches with minimal dependencies on host transcription factors (Figure 7a and b) (Ausländer et al., 2012; Nissim & Bar-Ziv, 2010; Ye & Fussenegger, 2014). Synthetic systems can achieve orthogonality, i.e. decoupling of transgene expression from the host cell transcription machinery and *vice versa*, while offering additional trigger-response options resulting in inducible expression systems (Bacchus et al., 2013). In contrast to constitutive promoters, inducible expression enables aligning expression levels in response to internal and external cues such as cellular state and environmental conditions (Ma et al., 2022). Such features are highly desirable, however, their widespread use is hampered by dependency on small chemical compounds (e.g. tetracycline, cumate, vanilic acid) which are incompatible with downstream processing regulations or process economics and their inferior expression strength as compared to constitutive viral promoters (Weber & Fussenegger, 2007). Rather constitutive promoters with varying potency used in a modular fashion allow installation of programmed and predictable multigene expression (Figure 7a) (Pristovsek et al., 2019). Specific and rational composition of individual genetic elements created synthetic promoters which can be employed to mediate expression at predictable relative stoichiometry (Patel et al., 2021). While such elements frequently remain inferior in expression strength as compared to the CMV promoter, a library of synthetic promoters allowed rational expression control over two orders of magnitude in CHO cells (Figure 7b) (Brown et al., 2015). Additionally, deliberate choice of diverse TFREs and consequently dependence on distinct transcription factors effectively minimizes promoter competition (Patel et al., 2021). Supplementing the multigene expression vector with independent transcriptional and mRNA capping machineries have been proposed (Jones et al., 2020). These approaches require substantially less space to achieve transcriptional shielding. Alternative solutions include achieving more efficient transcription terminator via terminator, polyA or epigenome/chromatin modifying elements, such as the beta-globulain cotranscriptional cleavage terminator, or the chicken hypersensitivitiy site 4 insulator (Uchida et al., 2013; White et al., 2013).

Albeit to a much lesser extent, post-transcriptional steps in protein expression have been engineered by control of mRNA levels using specific RNA secondary structures (Riboswitches) in the untranslated regions (Ausländer & Fussenegger, 2017; Ausländer et al., 2014). While Riboswitches are minute compared to modules used in transcriptional regulation, there are usually inferior in basal expression performance and dynamic range. However, in case large sequences are unfeasible, e.g. due to limited cargo size in adeno-associated viral vectors, riboswitches can be attractive tools for transgene control (Ketzer et

al., 2014). Similarly, altering translation of mRNA sequences by 5'/3'UTR customizations offer small-sized regulation of transgene expression (Eisenhut et al., 2020). Tuning expression by post-transcriptional and translational modifications efficiently reduce expression as compared to the WT variants rather than boosting it.

In summary a strict balance between strong multigene expression strength, stoichiometry, and plasmid size for efficient integration is required for stable and high level expression of recombinant antibodies in CHO biofactories (Hornstein et al., 2016). Multigene co-expression remains inherently context and molecule specific. Plasmid vector composition effectively influences the expression of recombinant antibodies (Chin et al., 2015; T. Y. Wang & Guo, 2020).

1.2.3 Generation and screening of producer cell clones in CLD

Cell line development starts with introduction of expression vectors into cells and subsequent selection pressure to generate stable transfected pools. Various transfection methods exist, which can be broadly classified into: i) biological methods utilizing viral methods, i.e. transduction, ii) chemical methods, based on cationic polymers / lipids or calcium phosphate, iii) physical methods, e.g. electroporation, micro-needle injection, which transiently disrupt the cell membrane to allow plasmid intake. Non-viral transfection methods are usually preferred, as they have been approved by regulatory agencies for production of proteins for human administration. Following selection, the transfected population is considered to be a pool of distinct cell lineages, i.e. a heterologous mixture of cells with varied epi-/ genetic and phenotypic characteristics. This cellular heterogeneity hampers large-scale production, which relies on stable and consistent product attributes (critical quality attributes, CQA) across manufacturing batches (Du et al., 2013; Eon-Duval et al., 2012). Historically, this diversity of phenotypes has been attributed to genetic variance due to gene dosage and placement effects which are inevitable when using random transgene integration. To generate isogenic clonally-derived cell lines, cell pools are consequently subcloned under the assumption that clones are phenotypically more homogenous as compared to the parental pool (Welch & Arden, 2019). However, cellular phenotypes remain diverse despite site-specific integration of transgenes or upon subcloning of already isogenic cell lines (Ko et al., 2018; J. S. Lee et al., 2018; Tharmalingam et al., 2018). Moreover, genome homogeneity, as assessed by karyotype stability and homogeneity, between cell pools and clones does not significantly differ (Vcelar et al., 2018b). While the underlying mechanisms are still incompletely understood, it is broadly accepted that phenotypic clonal homogeneity is transient in nature and phenotypic drift is an inherent feature of immortalized cells (Bandyopadhyay et al., 2019; Feichtinger et al., 2016). While accumulation of genetic variants appears to be a continuous process with less impact on phenotype (Kuhn et al., 2020), recent studies revealed epigenetic regulation as a large driver of phenotypic diversity (Weinguny et al., 2020; Weinguny et al., 2021). During subcloning each clone shows a new and distinct DNA methylation pattern, possibly resulting in individual expression patterns and cellular phenotypes despite their common clonal origin (Weinguny et al., 2020). This epigenetic profile is homogenous as long as the environment is kept stable. This epigenetic response may support cells in overcoming the problematic situation of subcloning itself and equip the cells with an suitable cellular milieu supportive for producing recombinant antibodies (Chang et al., 2022). Clonal homogeneous cell line hence represent an ideal but unrealistic concept (Barnes et al., 2001). Rather, clonally-derived cell lines constitute the

best effort so far to - at least transiently - reduce phenotypic heterogeneity and obtain a cell line with advantageous growth, productivity and stability (Barnes et al., 2006).

1.3 Synthetic biology tools for improved CHO bioproduction capabilities

From a simplified perspective, CHO biofactories for recombinant antibody production need to fulfill four key requirements: i) high productivity phenotype, ii) stable product expression over many generations, iii) consistent product quality, and iv) rapid cellular biomass accumulation. Fundamental developments in molecular biology and genetic engineering increasingly enable more sophisticated cell engineering options towards knowledge-based control of biofactory manufacturing performance. Especially synthetic biology tools allow increasingly sophisticated removal of cellular reactions or co-expression of processing enzymes in addition to recombinant gene expression for incremental improvement of CHO biofactories (Figure 8a) (Borth et al., 2005; Dreesen & Fussenegger, 2011; Z. Yang et al., 2015). These improvements rely on permanent cellular changes by knocking out or knocking down endogenous genes that negatively impact production features or constitutive co-expression of genes with positive impact (Fischer et al., 2015b). Such static engineering options are effective for general cellular characteristics, such as removal of α1,6-fucosyltransferase (Yamane-Ohnuki et al., 2004) or constitutive co-expression of β1-4-N-acetylglucosaminyltransferase III (J. Davies et al., 2001). However, cellular features which are most beneficial during individual bioprocess time points, e.g. biomass accumulation during cell cultivation and high expression during production phase, require dynamic engineering with synthetic sense-and-respond programs (Figure 8b). Historically, bioindustrial CHO cell line development relied on extensive blind screening of functional heterogeneity in CHO cell populations to identify a suitable production cell clone (Brown & James, 2016; W. W. Yang et al., 2022). Synthetic biology aims to extend the cell engineering options beyond the cell intrinsic heterogeneity created by epi-/genetic instability and reliably provide difficult-to-express complex antibodies with sophisticated requirements to their host cell (Brinkmann & Kontermann, 2017). This is achieved by repurposing naturally occurring molecular tools from various organisms and implementing them in the target expression system (Eisenhut et al., 2024). Cell engineering of CHO biofactories has dramatically increased since the first CHO genome has been published in 2011 enabling rational design of genetic manipulations and promises to steadily improve production of biotherapeutics to meet increasing demands (X. Xu et al., 2011).

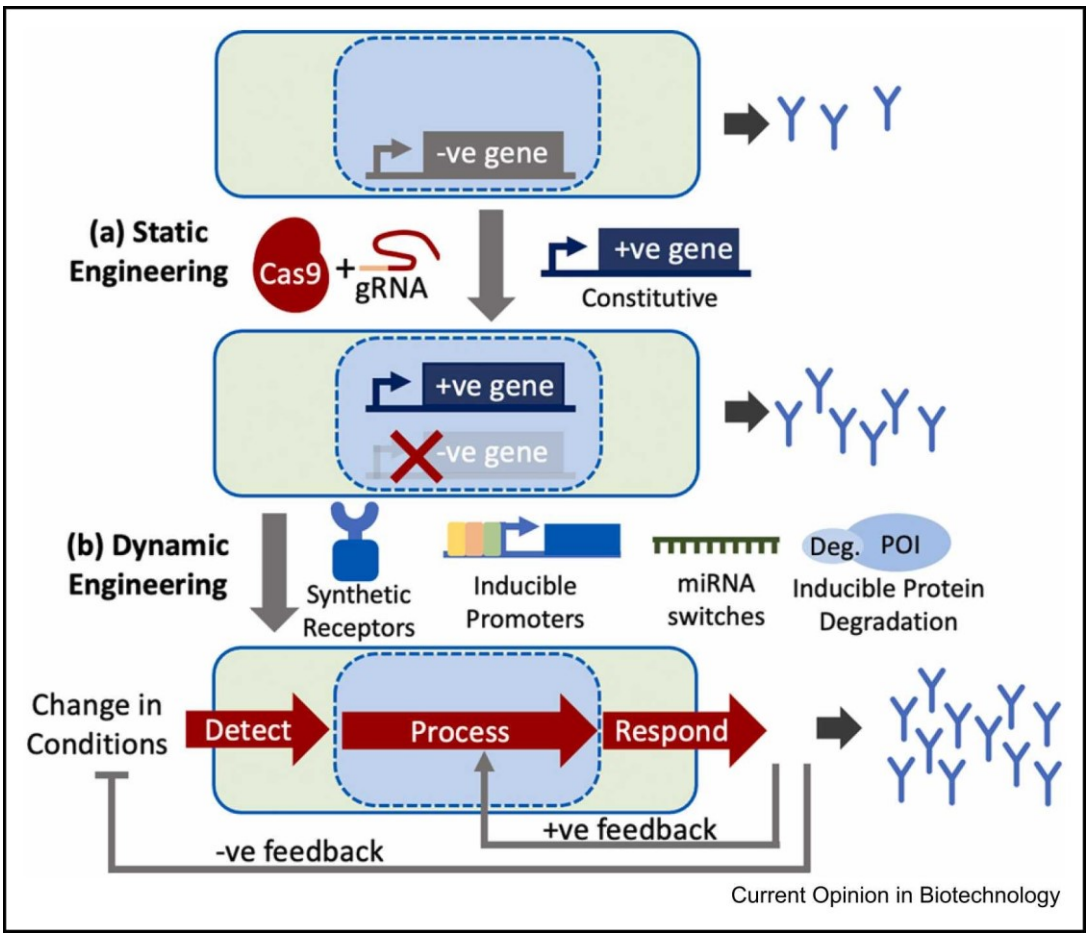

Figure 8. Static and dynamic CHO cell engineering approaches. a) Static cell engineering encompass ablation of endogeneous genes or constitutive overexpression of beneficial genes. b) Dynamic cell engineering with sense-and-respond capabilities may further improve productivity of CHO biofactories. Characterized genetic parts such as synthetic receptors, inducible promoters, and gene switches can create genetic circuits to achieve feedback circuits. Reprinted from Donaldson et al. (2022)

1.3.1 Static CHO cell engineering tools

Improved manufacturing performance of CHO biofactories beyond carefully considered transgene design and integration are classically achieved by rational genome modifications: gene deletions / knockouts (KOs), knockdowns (KDs), overexpression, or pathway deregulation. Desired functional improvements generally fall into: i) improved cell specific / volumetric productivity, by targeting secretory pathways or mitigate cell proliferation ii) beneficial product quality attributes, mainly glycosylation patterns iii) enhanced cell growth and biomass accumulation and iv) prolonged cell viability, by preventing autophagy, apoptosis or undesired metabolic byproducts (Figure 9).

The earliest described engineering approaches using overexpression for enhanced bioprocess productivity were described for *E. coli* bacteria (Khosla et al., 1990), which showed markedly improved protein synthesis upon overexpression of *Vitreoscilla* hemoglobin. Transgene overexpression is the oldest and most traditional way for cell engineering, with a broad spectrum of methods readily available.

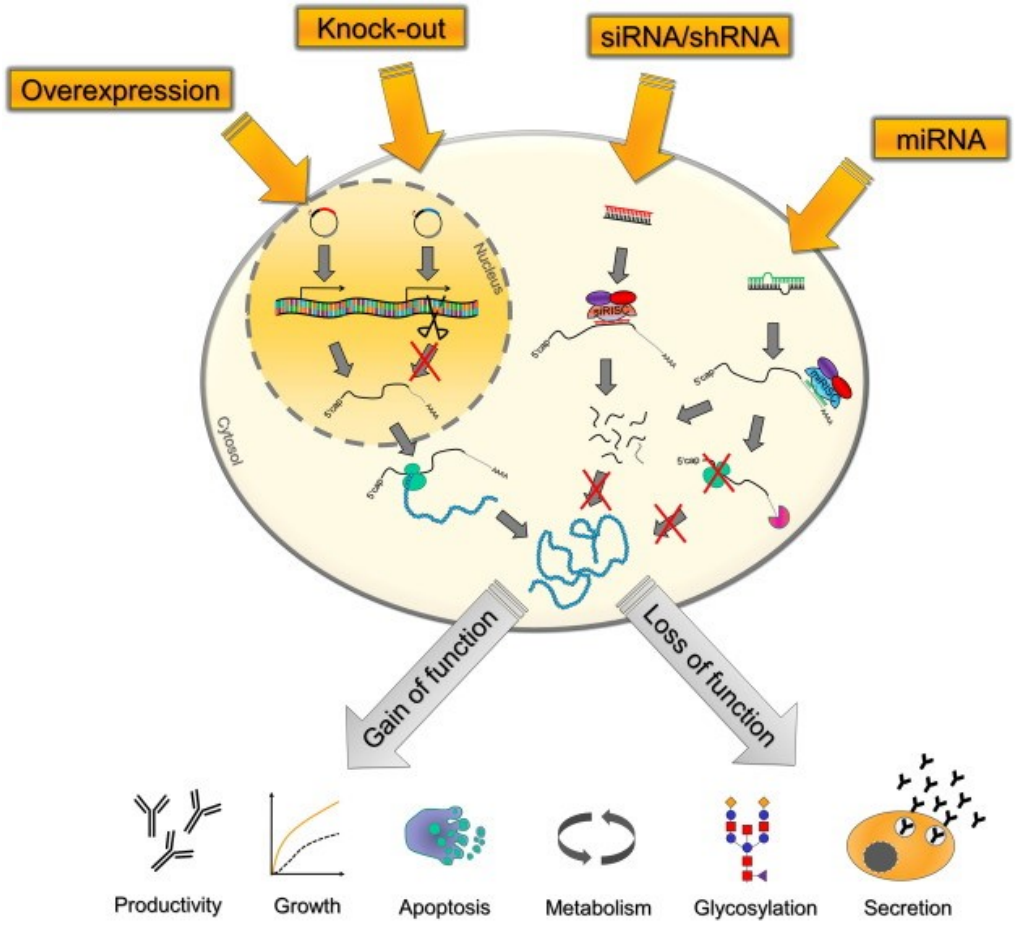

Figure 9. Static cell engineering options for improved functionality of CHO biofactories. Overexpression of beneficial genes, endogenous gene knockout (KO), and modulation of siRNA and miRNA represent molecular tools for gain of loss of a specific cellular function. Reprinted from Fischer et al. (2015b)

In CHO biofactories, early studies showed that mimicking cytostatic production phases by overexpression of tumor suppressor genes p21 and p27 resulted in higher reporter gene expression (Fussenegger et al., 1997; Fussenegger et al., 1998). Attenuating proliferation, i.e. cell cycle pathways, has since been linked to higher productivity, possibly by enabling cells to divert more resources to production processes (Weisse et al., 2015). Notably, enhanced productivity has been achieved by higher cell specific productivity (pg/cell/day) which is linked to attenuated cell division and by higher biomass accumulation (increased cell division) resulting in increased volumetric productivity (g/l). Overexpression resulting in improved cell specific productivity include i) $p21^{CIP1}$ and C/EBP- α (Fussenegger et al., 1998), supplemented by BCL-xL (Astley et al., 2007), ii) $p27^{KIP1}$ (Mazur et al., 1998), iii) GADD45 (W. Kim et al., 2014), iv) BLIMP1 (Torres & Dickson, 2021), v) MPC1/2 (Bulté et al., 2020), and vi) SERPINB1 (N. Lin et al., 2015). Inversely, improved biomass accumulation by higher proliferation rates frequently reduce cell specific productivity. However, the benefit from increased biomass can overcome the reduced cell specific productivity rates and result in improved volumetric titers. Cell engineering targets for increased cell division rates include i) Myc and Bcl-2 (Ifandi & Al-Rubeai, 2005), ii) eIF3i/c (Roobol et al., 2020), iii) VCP (Doolan et al., 2010), iv) GADD34 (Otsuka et al., 2016), and v) PTEN (Q. Zhou et al., 2021). Higher proliferation and biomass in turn results in increased nutrient and oxygen transport demand to prevent metabolic by-products and elevated osmolarity (Rish et al., 2022). Thus, increased cell division rates synergistically benefit from evasion of autophagy and apoptotic programmed cell death to prolong cultivation times and consequently volumetric productivity (Arden & Betenbaugh, 2004). Three main molecular pathways trigger apoptosis by recruiting downstream caspase effectors: i) death receptor pathway: FasL. TRAIL and TNF ligation, ii) mitochondrial pathway, activated by mitochondrial or genotoxic stress, and iii) the endoplasmic reticulum induced stress pathway, induced by misfolded and aggregated proteins. Autophagy, mainly observed following nutrient depletion, can contribute to cell death especially if apoptosis is inhibited (Shimizu et al., 2004). Hence, many attempts to increase cellular robustness and delay apoptosis have been reported by overexpressing genes in apoptotic and autophagy pathways: i) death receptor pathway inhibition, using HSP27/70 (Y. Y. Lee et al., 2009; Tan et al., 2015) or FAIM (D. C. F. Wong et al., 2006), ii) resistance to mitochondrial pathway activation, by overexpressing BCL2 (Jeon et al., 2011) eventually combined with BCL-xL (Meents et al., 2002), iii) caspase inhibitors, such as XIAP (Sauerwald et al., 2002) and Aven (Figueroa et al., 2004), and iv) autophagy engineering using Beclin-1 (J. S. Lee et al., 2013). Beside maintenance of viable cells which continue to

express transgene, restriction of programmed cell death suppresses release of intracellular proteases (Kaneko et al., 2010).

In addition to indirect beneficial effects which support productivity by sustained cellular health, targeting protein folding and secretory pathways directly improves cell specific and volumetric productivity. XBP-1S, the transcriptionally active isoform of XBP1, improves protein secretion when celsl exhibit secretory bottlenecks (Ku et al., 2008). As a results of XBP-1S expression, a plethora of secretion supportive processes are triggered including ER, Golgi, and mitochondria content increase (A. H. Lee et al., 2003). In line with the model that assembly and folding in the ER are rate-limiting in CHO biofactories (Bibila & Flickinger, 1992), overexpression of ER folding factors increase productivity, such as i) protein disulfide isomerase (Borth et al., 2005), ii) BiP and ATF6c (Pybus et al., 2014), or iii) ERO1-L (Cain et al., 2013). More broadly, studies have targeted multiple secretory processes along their intracellular secretion path all pointing towards potential bottlenecks. This includes, i) ER and cis-Golgi interface engineering by overexpression of KDEL receptor 1 (Samy et al., 2020), ATF4 (Haredy et al., 2013), ii) transport from the Golgi to the plasma membrane by overexpression of CERT (Florin et al., 2009), and iii) fusion of synaptic vesicles with the plasma membrane by overexpression of exocytic SNARE proteins (Peng et al., 2011). More holistically, mTOR overexpression increases not only specific productivity, but also cell growth, viability and apoptosis resistance moving towards a general enhanced productivity phenotype (Dreesen & Fussenegger, 2011).

Despite the ability of CHO cells to form human-like glycosylation, some minor differences remain with the risk of severe immunological reactions (Ghaderi et al., 2012). Importantly, CHO cells lack expression of α-2,6-sialyltransferase (ST6GAL) but instead express α-2,3-sialyltransferase (ST3GAL) (Jenkins et al., 1996). To more closely resemble native human N-glycans, engineering efforts aim to prevent immunogenic α-1,3-galactose (α-gal) and N-glycolylneuraminic acid (NGNA). Consequently, the earliest approaches successfully enabled α-2,6-sialylated N-glycans by overexpression of ST6GAL (E. U. Lee et al., 1989; Minch et al., 1995). To further refine the N-glycan profile, further efforts involved overexpression of various enzymes within the N-glycosylation pathway, especially i) GalT (Jeong et al., 2008), ii) CMP-SAT (N. S. C. Wong et al., 2006) combined with GNE (Son et al., 2011), iii) GnT-III (J. Davies et al., 2001) and GnT-IV/V (Fukuta et al., 2000), and iv) RMD (von Horsten et al., 2010). Overexpression of genes therefore represents the first and well

described area of static cell engineering, given that tools for overexpression were early accessible and straightforward to implement.

In contrast, tools for gene KO were not easily accessible until the advent of programmable nucleases, especially CRISPR/Cas9, which hampered widespread targeted gene knockouts in mammalian cells until 2013 (Doudna & Charpentier, 2014; Hsu et al., 2014). In the absence of targeted approaches, researchers relied on random mutagenesis and excessive clone screening to identify cell clones with desired edits. Earliest efforts for targeted gene knockouts were achieved using HDR, which occurs only in less than one per 10^5 cells, unless stimulated by a double-strand break (DSB) (Vasquez et al., 2001). Undesired off-target random integration occurs much more frequently in up to one in 10^2 cells, which results in a cumbersome search for successfully edited cells (Vasquez et al., 2001). As CHO cells show even lower HDR rates, the first described CHO targeted gene KO in 2004 required screening of 120 000 cell clones for identification of three homozygous KO cell clones (Yamane-Ohnuki et al., 2004). In comparison, programmable nucleases (zinc-finger nucleases, TALENs, and Cas9) allow the introduction of DSBs with editing efficiencies mostly between 6-89% (Castro et al., 2021). This revolution paved the way for promising engineering options by removal of disadvantageous endogenous genes.

Researchers have since aimed mostly at retardation of programmed cell death and modulation of product quality attributes with clear genotype-phenotype relationships using gene KOs. Driven by the discovery that interaction of FcγRIIIa to defucosylated IgG1 was substantially increased as compared to fucosylated IgG1, disruption of the FUT8 gene enabled the production of defucosylated antibodies using CHO biofactories (Yamane-Ohnuki et al., 2004). Similar results were achieved by removal of FX, with the additional option to generate primarily fucosylated material by titration of fucose (Louie et al., 2017). Further improvement was achieved by combined removal of SLC35C1 and SLC35A1, resulting in cells which produce asialylated and afucosylated antibodies dramatically improving antibody-dependent cellular cytotoxicity (ADCC) (Haryadi et al., 2013). To aid improved immunogenicity profiles, CMAH KO results in abolished NGNA levels (Chai et al., 2020). Likewise, host cell proteins (HCP), which accumulate during mammalian cell culture, can contaminate the final drug product, potentially impairing product quality and pose an immunogenicity risk (X. Wang et al., 2009). Once responsible proteins have been identified, removal by KO abolished HCP content, *e.g.* ST14 (Laux et al., 2018), Lpl (Chiu et al., 2017), and Anxa2/Ctsd (Fukuda et al., 2019).

Comparable to overexpression of anti-apoptotic genes, double KO of pro-apoptotic proteins Bax and Bak resulted in higher cell viability which in turn enabled higher productivity (Cost et al., 2010; Macaraeg et al., 2013; Tang et al., 2022). Cells lacking both Bax and Bak, fail to activate any downstream caspase within the mitochondrial apoptotic pathway, rendering these cells resistant to DNA damage and ER stress (Ruiz-Vela et al., 2005). Notably, the benefit of hampered apoptotic cell death enabled synergistic increase in specific productivity by KO of PERK (Castellano et al., 2023). KO of PERK alone improved productivity at the cost of increased apoptotic cell death.

In case full gene KO is lethal or undesired, siRNA mediated gene knockdown (KD) can effectively reduce expression levels (Fire et al., 1998). To achieve stable expression, siRNA are expressed from small hairpin RNA containing vectors and processed by the host RNA pol III, in contrast to directly transfected siRNA which is inherently instable after transfection (Moore et al., 2010). They largely utilize the same target genes as compared to gene KO with multiple studies describing beneficial effects when knocking down: i) Caspases, FADD/FAIM, Bax/Bak to inhibit apoptosis (N. S. Kim & Lee, 2002; Lim et al., 2006; Sung et al., 2007; D. C. F. Wong et al., 2006; Yun et al., 2007), or ii) FUT8, GMD, and NEU1-3 for improving N-glycosylation (Beuger et al., 2009; Kanda et al., 2007; Ngantung et al., 2006; M. Zhang et al., 2010). Interestingly, only few studies have utilized the unique feature of KD and targeted genes where KO is potentially detrimental for CHO cell fitness. Although only effective in an adherent cell culture context, CFL1 KD did result in destabilized actin cytoskeleton and enhances SEAP reporter protein production (Hammond & Lee, 2012). Further potentially sensitive target genes only include only cell cycle checkpoint kinases ATR/ATM (K. H. Lee et al., 2013) and lactate metabolism: LDHa together with PDHKs (M. X. Zhou et al., 2011).

Instead, miRNA engineering has been investigated in greater detail due to their unique ability to control entire pathways while avoiding translational burdening (Hackl et al., 2012; Müller et al., 2008). Remarkably, many miRNA species (*e.g*. let-7 and lin-4) show prominent conservation across animal phylogeny (Pasquinelli et al., 2000). Due to their unspecific binding activity, largely determined by the short (8 bp) core or seed region in animals, individual miRNA can translationally repress or degrade mRNA of hundreds of different target genes by binding to the 3’-untranslated region of gene transcripts (Pasquinelli, 2012). miRNAs quickly emerged as promising targets for engineering CHO biofactories as they control a broad spectrum of cellular control processes such as cell cycle, cell growth, and

programmed cell death (B. H. Zhang et al., 2007). Consequently, this enabled researchers to synergistically engineer expression of multiple target genes without increased metabolic load in CHO biofactories. However, the unspecific nature of miRNAs impede to predict target effects reliably which frequently results in unexpected phenotypes during CHO miRNA engineering (Jadhav et al., 2013). Further, individual mRNAs are targeted by a multiplicity of miRNAs redundantly and cooperatively, to buffer transcriptomic balance upon individual miRNA dropout (Fischer et al., 2015a). Despite this complexity, researchers have successfully engineered miRNA expression to achieve more desired phenotypes in CHO biofactories.

Mimicking the effects of proliferation control by temperature shift, miR-7 overexpression resulted in ceased cell proliferation and increased cell specific productivity (Barron et al., 2011). Similar effects result from miR-107 overexpression (Jari et al., 2024), as well as from miR-17, -19b, 20a, and -92a (Jadhav et al., 2012; Loh et al., 2014), accompanied by upregulation of previously described engineering targets such as MYC and mTOR.
Further miRNAs which positively influence productivity include, i) miR-574-3p, accompanied by anti-apoptotic effects and increased proliferation (Svab et al., 2021), ii) miR-2861 (Fischer et al., 2015c), iii) miR-200a (Bryan et al., 2021), iv) miR-30a-e, additionally targeting ubiqutinilation (Fischer et al., 2014), v) miR-557 and miR-1287 (Strotbek et al., 2013) vi) miR-483 (Emmerling et al., 2016) vii) miR-31 (Martinez-Lopez et al., 2021), and viii) miR-136/miR-3074 (Weis et al., 2018).

1.3.2 Dynamic CHO cell engineering tools

Influencing gene expression by static engineering methods is immune to environmental cues, i.e. the engineered effect is permanent without sense-and-respond options depending on the intra- and extracellular context (Ausländer et al., 2012; M. Q. Xie & Fussenegger, 2018). This incompletely reflects the cellular environment during bioprocessing as conditions, such as nutrient availability and metabolite concentration, continually change. Instead, it is desired that cells respond to such cues by exhibiting high growth rates during initial scale up phases with no need for transgene expression and *vice versa* during main fed batch cultivation (Donaldson et al., 2022). Consequently, optimization beyond methods used in static cell engineering require gene circuits allowing initiation, interruption and termination of target gene expression. Ideally, CHO cells must detect environmental cues (e.g. accumulation of lactate metabolites) and in turn respond with an actuation program (e.g. expression of transgene, or growth inhibitors). Dynamic cell engineering promises fine-tuned cellular behavior and enables optimal resource utilization tailored to the stage specific needs of the production process.

Traditional dynamic transcriptional expression-control systems rely on external input signals, mostly small-molecules, e.g. tetracycline, phloretin, vanillic acid, or cumate (Gitzinger et al., 2009; Gitzinger et al., 2012; Gossen et al., 1995; Poulain et al., 2017) or physical inducers, e.g. heat-, light-, -gas, or electrical stimulation (Figure 10a) (Krawczyk et al., 2020; Miller et al., 2018; Weber et al., 2004; Ye et al., 2011). Optimally, such stimulus-dependent inducible systems demonstrate minimal background expression (in absence of a trigger signal) and high dynamic range upon induction (maximal expression once triggered), with a wide array of inducible systems described so far (Ausländer & Fussenegger, 2013). Each system is based on synthetic transcription factors (containing a DNA binding domain, DBD, e.g. Gal4, ZFP, TALE, gRNA) fused to an actuator domain (AD, with trans-activator or trans-silencing domains e.g. VP16, p65, E2F4, KRAB, YY1) (M. Q. Xie & Fussenegger, 2018). In absence of a trigger signal, the DBD remains inactive. Once activated the DBD-AD fusion protein can bind to their cognate DNA sequence where the AD facilitates or represses expression, respectively. Of note, most inducible systems show low level expression in the absence of inducers. The only described non-leaky inducible system has been achieved by combining three distinct expression control systems: LacI-TetR-RNAi (Figure 10b) (Deans et al., 2007). Utilizing the tetracycline inducible expression system, the first proliferation control strategy for improved productivity in CHO biofactories was already published in 1998 by control of

$p27^{Kip1}$ and $p21^{Cip1}$ (Fussenegger et al., 1998). Multiple studies showed similar results with different expression-control systems and gene combinations (Bi et al., 2004; Carvalhal et al., 2003; Mazur et al., 1998). However, cyclin-dependent kinase overexpression remains inferior in effect size as compared to temperature shift, hampering widespread application (Kaufmann et al., 2001).

Likewise, expression of the product itself can be placed under control of inducible expression systems allowing scale up phases in absence of transgene expression (Lam et al., 2017; Misaghi et al., 2014; Poulain et al., 2017). This has been particularly beneficial for expression of difficult-to-express bispecific antibodies (Maltais et al., 2023; Q. Wang et al., 2019). Alternatively, CHO cells have been engineered to constantly emit the stimulus (acetaldehyde) independently of user-intervention, while simultaneously placing a transgene under control of an acetaldehyde-responsive expression system enabling cell density-controlled gene expression (Weber et al., 2007). To preserve baseline expression, inducible and constitutive expression systems may also be combined in hybrid systems to compensate the lower peak expression observed in inducible systems alone (Lam et al., 2023). Repressing the expression during selection of stable pools was linked with a higher frequency of high-expressing cells, likely by limiting the metabolic burden of high-level transgene expression during selection (Maltais et al., 2023; Ong et al., 2019; Poulain et al., 2019). In line with this hypothesis, clonal instability – when triggered by toxic antibody expression itself – can be circumvented by induced antibody expression (Misaghi et al., 2014). Still, overall applicability of placing the transgene under direct control of inducible systems remains low, dictated by the dominant requirement of bioprocessing, especially i) maximum expression strength comparable to those reached with constitutive systems and ii) use of an physiologically inert trigger molecule (Weber & Fussenegger, 2007). Of note, complex co-expressed genetic components compete for cellular resources, with strong promoters claiming a larger resource footprint (Frei et al., 2020). This limits implementation of genetic circuits for CHO biofactories, as they are less suitable for applications which aim at maximum expression.

Nevertheless, the field of synthetic biology has created a plethora of valuable tools for designing higher-order genetic circuits in mammalian cells (Figure 10). To boost CHO bioproduction capacities, these tools can fine-tune the expression machinery and the cellular physiological status towards a build-for-purpose biofactory (Gibson et al., 2008). Each newly

created circuit can be designed for specific trigger events, the type of signal processing, and the final cellular response. Whereas traditional stimulus-responsive gene expression systems are dependent on user-intervention and slow (transcriptional responses require hours in eukaryotes), cell surface receptors (e.g. GPCRs, RTKs, CARs) (M. Q. Xie & Fussenegger, 2018) respond automatically and fast (milliseconds to minutes) to extracellular cues. Cell surface receptors thus mimic sensors which specifically detect and respond to target ligands (Dixon et al., 2021). Upon ligand detection, receptors frequently undergo conformational change and relay the extracellular cue via second messengers into the cytosol and nucleus. In semi-synthetic approaches, such receptors still cascade to endogenous signaling pathways, such as CARs (chimeric antigen receptors) which trigger the native T cell response upon binding of tumor antigens (Figure 10c_a) (Altenschmidt et al., 1996; Eshhar et al., 1993). In case additional transgene expression is desired, synthetic promotors containing identical endogenous response elements are placed upstream of the transgene (M. Q. Xie & Fussenegger, 2018). The cross-talk between endogenous pathways and activated components, however, impedes independent functions within cells. In contrast, synthetic or orthogonal approaches replaces endogenous signaling pathways by fully synthetic transcription factors (Figure 10c_b) (McClune et al., 2019). Such systems are commonly based on synthetic Notch variants with replaced extracellular sensor module (e.g. scFv, nanobodies, myc-tags) and intracellular transcriptional module (DBD fused to AD, e.g. Gal4-KRAB, dCas9-VP64) (Morsut et al., 2016).

To further expand design opportunities, post-transcriptional control systems provide another layer for higher-order gene circuit design by direct control of RNA-levels. Similar to their transcription control counterpart, they combine an RNA effector part (e.g. hammerhead ribozymes, toehold switches, riboregulators, siRNA, gRNA) with an RNA sensor part (e.g. aptamers, X^{on}). Notably, aptamers itself may mediate control of gene expression by stabilizing RNA secondary structures, e.g. block translation initiation, activate antisense-domains, or inhibit dicer processing (Wieland & Fussenegger, 2010). The most common RNA-based gene switches combine self-cleaving hammerhead ribozymes with ligand-responsive aptamers embedded in the transcript or other functional RNAs (Ausländer et al., 2010; Ausländer et al., 2014). Aptamers, small and highly folded RNA structures, undergo considerable conformational change upon specific ligand binding. Consequently, combined with hammerhead ribozymes, which induce efficient self-cleaving, ribozymes offer ligand-responsive control of RNA-levels (Figure 10d_b).

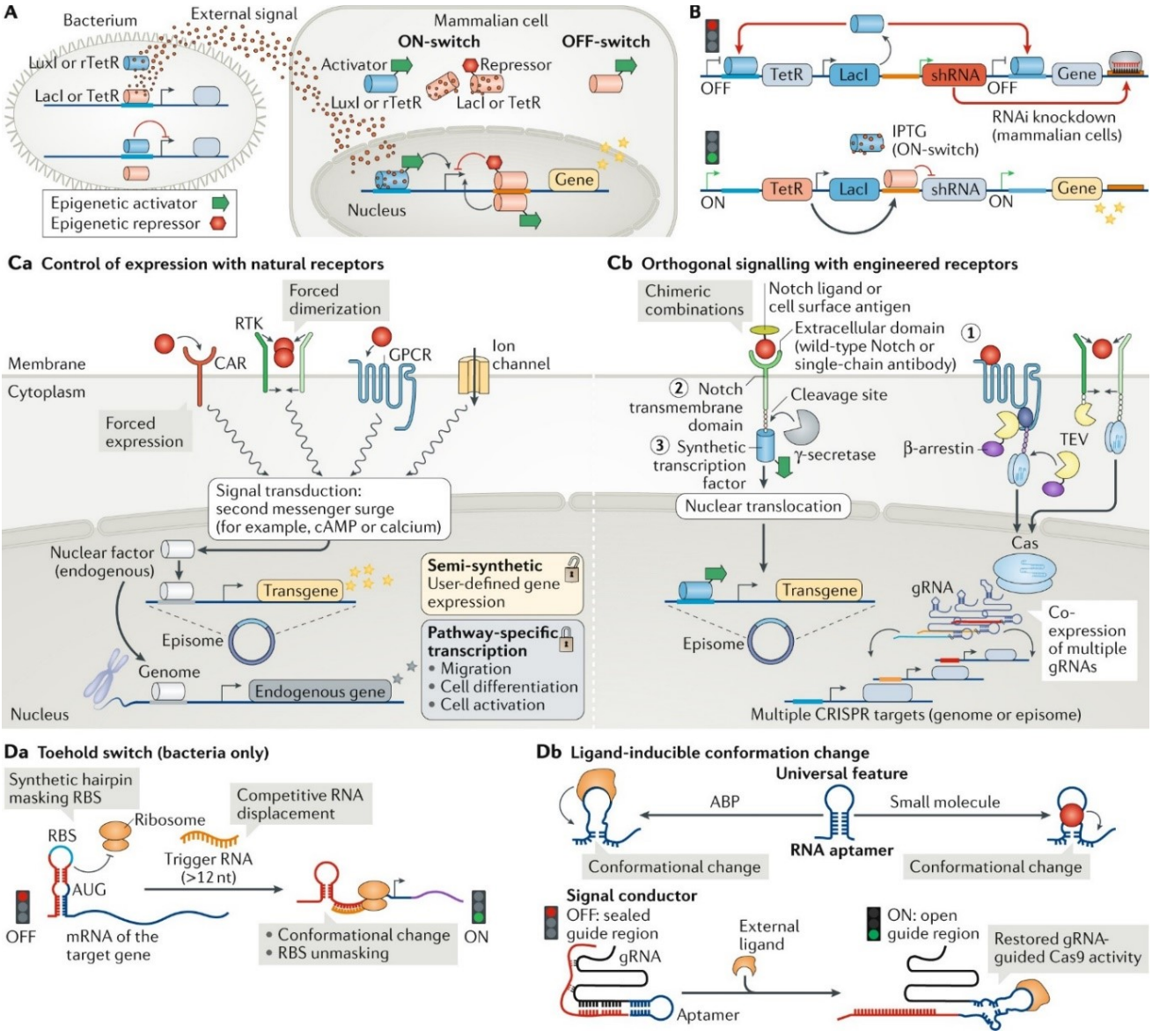

Figure 10 Schematic illustrations of dynamic cell engineering options in CHO biofactories. a) inducible expression systems based on prokaryotic transcription factors. b) LacI-TetR-RNAi switch for tight gene expression control. c) Surface receptors as molecular sensors initiate downstream receptor-mediated signaling. Downstream signaling can utilize either endogenous or semi-synthetic pathways. Orthogonal signaling are based on synthetic transcription factors and interfere less with host signaling. d) RNA switches regulate mRNA levels by RNA displacement or using aptamers for ligand-responsive ribozyme activity. ABP, aptamer-binding protein; CAR, chimeric antigen receptor; gRNA, guide RNA; nt, nucleotide; TetR, tetracycline-dependent repressor, rTetR, reversed TetR, lacI, lactose operon repressor, GPCR, G protein-coupled receptor, TRK, receptor tyrosine kinases, TEV, tobacco etch virus protease. Reprinted from M. Q. Xie and Fussenegger (2018)

Over the years, regulated gene expression has been extended by spatiotemporal control and achieved unprecedented complex and novel functionalities, notably i) therapeutic bacteria, which either collect diagnostic information (Riglar et al., 2017) or directly treat colorectal disease (Din et al., 2016), ii) multiplex drug-gated CAR circuits, regulating timing and magnitude of anti-cancer CAR T cell activity (H. S. Li et al., 2022), and iii) therapeutic biocomputer implants, treating e.g. diabetes, arthritis, hypertension (Kemmer et al., 2010; Rossger et al., 2013; M. Xie et al., 2016). While this clearly indicates the enormous potential of dynamic cell engineering tools for optimization of CHO biofactories, only few basic gene regulatory circuits have demonstrated benefit for bioprocessing so far.

1.3.3 Next-generation cell engineering efforts

Despite the general success of static and dynamic cell engineering approaches, the sheer complexity observed in biological networks hampers the establishment of simplified genotype-phenotype relationships which guide such approaches. Especially in the context of CHO biofactories, describing the function of genes remains challenging as CHO cells have escaped genetic control mechanisms (M. J. Wurm & Wurm, 2021). Genetic drift and chromosomal instability are constant features among immortalized cell lines, such as CHO cells, resulting in rapid accumulation of mutations and variance within clonal populations (Frye et al., 2016; Lewis et al., 2013; Tharmalingam et al., 2018; Vcelar et al., 2018a). Notably, these mutations mostly accumulate in pathways associated with cell survival and fitness, such as WNT and mTOR (Lewis et al., 2013). While this genomic plasticity may explain the capacity of CHO cells to adapt to any given environment quickly, accurate predictions of genotype-phenotype relationships are mostly cell strain specific or differ depending on the expressed transgene (Figure 11a) (Gutierrez et al., 2020; Hefzi et al., 2016). During development of a CHO cell line, even isogenic cell clones display a wide range of production-relevant phenotypes (i.e. transgene expression, growth or stability characteristics), corresponding to their individual adaptation pathway and the interaction between transgene and host cell (Grav et al., 2018). Importantly, the process of subcloning itself induces random DNA methylation patterns which contributes to phenotypic clone-to-clone diversity (Weinguny et al., 2021). It is therefore generally established that clonally-derived cell lines show equal genomic and phenotypic diversity as their parents (Bandyopadhyay et al., 2019; Derouazi et al., 2006; Feichtinger et al., 2016), and repeated subcloning does not reduce this phenomena (Ko et al., 2018; Pilbrough et al., 2009; Scarcelli et al., 2018; Tharmalingam et al., 2018). Instead, keeping the cellular environmental uniform and stable across cell line development improves clonal homogeneity (Borsi et al., 2023; Feichtinger et al., 2016; Grav et al., 2018).

Cell engineering efforts generally depends on cytotoxic delivery of biological cargo into cells with high efficiencies, such as by integration of multiple transgenes, gene circuits, or gene knockouts (V. Marx, 2016). Consequently, environmental conditions inevitable change during enrichment of cells carrying desired edits, i.e. selection procedures and generation of clonal cell lines, resulting in substantial variability of phenotypes. Identical engineering efforts in CHO cells hence vary dramatically in their outcome, depending on cellular and experimental factors (Hansen et al., 2017). Application of such conditional results is

consequently limited and instead requires discrimination between general genotype-phenotype relationships (i.e. engineering results which are consistent across CHO cell strains, cell clones, environmental conditions, and the expressed transgene) and context-dependent relationships (Hansen et al., 2017). Given the intractable nature of establishing general genotype-phenotype relationships empirically, more systematic insights into the numerous dynamic cellular processes are a prerequisite for future rational engineering strategies. Data available from high-content omic-technologies result in increasingly refined mathematical models of CHO biofactories which may enable accurate predictions on productivity bottlenecks as engineering targets. Additionally, high-throughput gene perturbation screenings, enabled by CRISPR/Cas9 technology, aid in the search for general beneficial genotype-phenotype relationships. As an interesting alternative, comparison of plasma cells - which can secrete 10-20 fold higher antibody rates as compared to CHO cells, i.e. 200-400 pg/cell/day (Randall et al., 1992) - with CHO cells using omic-technology, may additionally provide rational for engineering. (Raab et al., 2024; Raab et al., 2022).

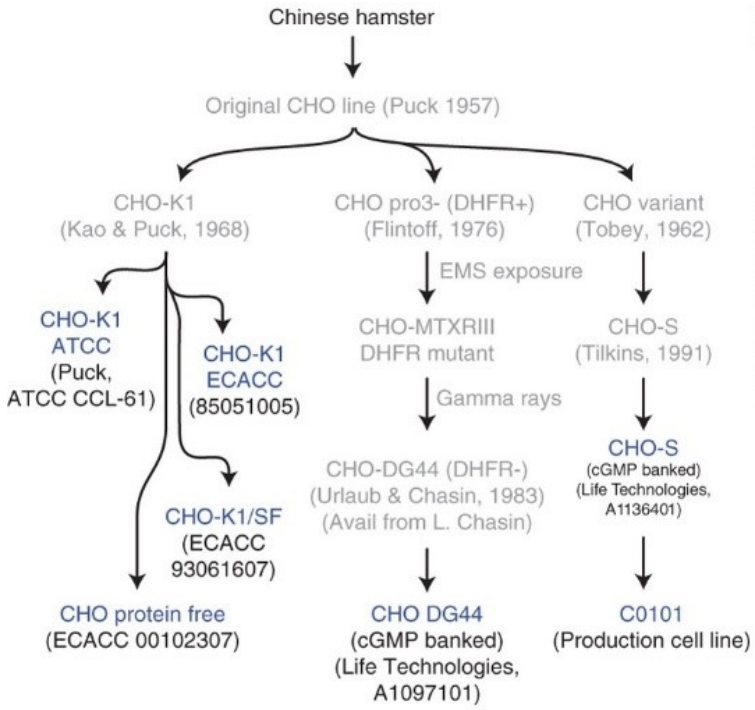

Figure 11. Divergence of CHO cell lines over time by accumulation of mutations, selection, and isolation of CHO clones. Modified from Lewis et al. (2013)

In contrast to rather simple prokaryotic cell factories, CHO biofactories show substantially higher complexity with multicellular compartments and diverse post-transcriptional and post-translational processing of proteins (Kildegaard et al., 2013). Following the publication of the CHO cell genome in 2011 (F. M. Wurm & Hacker, 2011), genome-scale metabolic models (GEMs) based on flux balance analysis (FBA) provided a basis for mathematically linking genotype with phenotype (Figure 12) (S. Y. Park et al., 2024). Published in 2016, the iCHO1766 model represents the first attempt to predict growth and production phenotypes (Hefzi et al., 2016). More specifically, the applied FBA model i) collected all known biochemical relationships between genes, proteins, and reactions, based on CHO homologs to humans (King et al., 2016) ii) applied known physicochemical constraints, e.g. mass balance and thermodynamics using constraint-based reconstruction and analysis (COBRA) (King et al., 2015), iii) used an objective function, i.e. a particular flux which should be optimized, in this case biomass (Feist & Palsson, 2010) and production of erythropoietin and IgG (Figure 12). As a result, iCHO1766 could predict growth phenotypes and auxotrophy of CHO cells, implying the enormous potential of GEMs (Hefzi et al., 2016).

This model has since been incrementally refined by including i) kinetome parameters of enzymes, such as turnover numbers and molecular weights in the enzyme capacity constrained FBA (iCHO2296) (Yeo et al., 2020), ii) integrating product-specific energetic cost and secretory machinery demand (iCHO2048s) (Gutierrez et al., 2020), iii) general gap-fillip and removal of dead-end reactions (iCHO2291) (Yeo et al., 2020), and iv) a combination of updated reactions from iCHO2291 with the secretory machinery in iCHO2048 (iCHO2441) (Strain et al., 2023). Nonetheless, GEMs are still in their infancy and dominantly used in a descriptive fashion (Kol et al., 2020), as they still poorly predict pathway flux (average Pearson correlation below 0.5) and engineering targets (Richelle et al., 2020; Strain et al., 2023). This is further reflected by their low sensitivity to detect essential genes (below 30%), when compared to a list of empirically validated essential genes for CHO or human cell lines (Robinson et al., 2020; Xiong et al., 2021a). Their dependency on FBA insufficiently emulates overall cellular reality and may be improved by i) including fluxes which are not in steady-state or conditionally inactive, such as condition-specific cellular regulations (Richelle et al., 2020) ii) continue to integrate mechanistic details (similar to improvements in iCHO2291, which included the secretory machinery) for well-described cellular processes, e.g. protein synthesis, folding, trafficking, iii) hybrid frameworks including frequent metabolite

measurements to calibrate cellular flux and objectives, instead of defining them *a priori* (Gopalakrishnan et al., 2024).

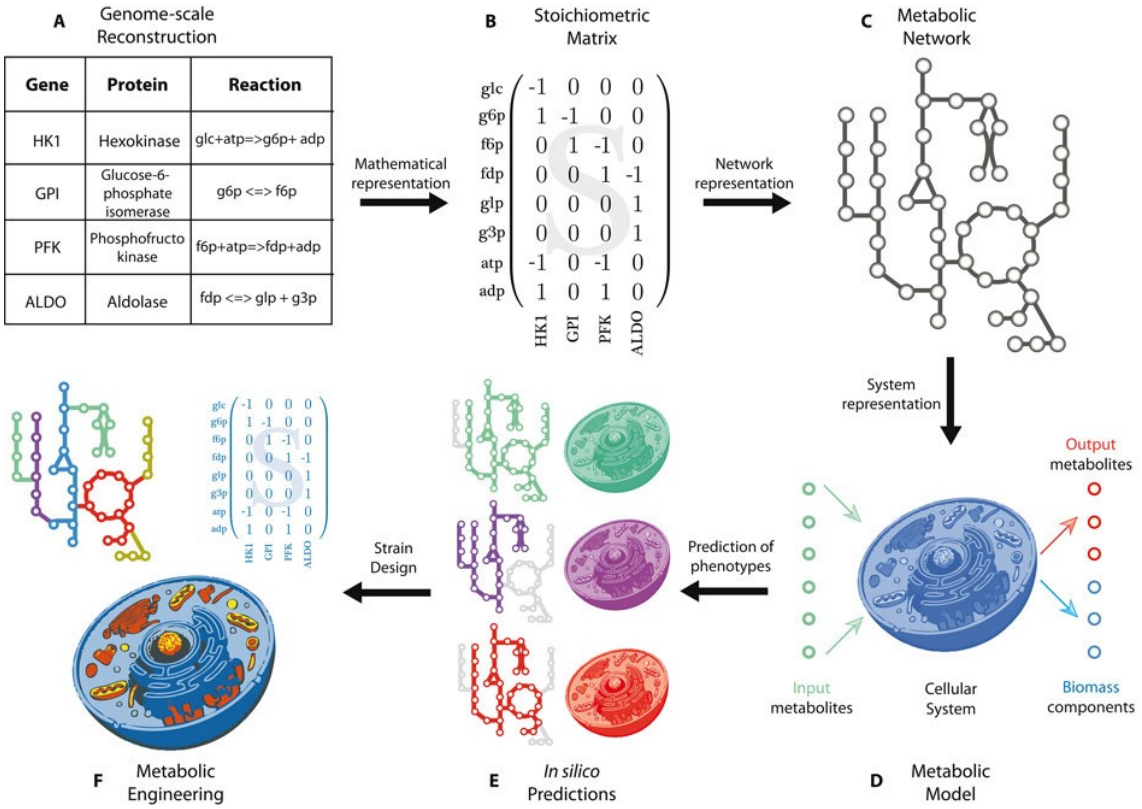

Figure 12 Schematic illustration of a general workflow in genome-scale reconstructions. a) Consolidation of all known gene-protein-reactions within the cellular context. b) Mathematical description of all known reactions in a stoichiometric matrix. c) Representation of a network based on the stoichiometric matrix. d) System representation based on the network, including inputs (metabolites consumed by the cell) and outputs (biomass components required for cell growth, secreted metabolites). e) Adding constraint-based analysis, the phenotypic response of gene knockouts or metabolite changes can be predicted. f) Predicted results are used for rational cell engineering. Reprinted from (Gutierrez & Lewis, 2015)

In absence of predictive models and in-depth mechanistic understanding of molecular processes at play, gene perturbation screenings represent an appealing option for identification of genes, pathways, and mechanisms responsible for a given phenotype or biological process (Bock et al., 2022).

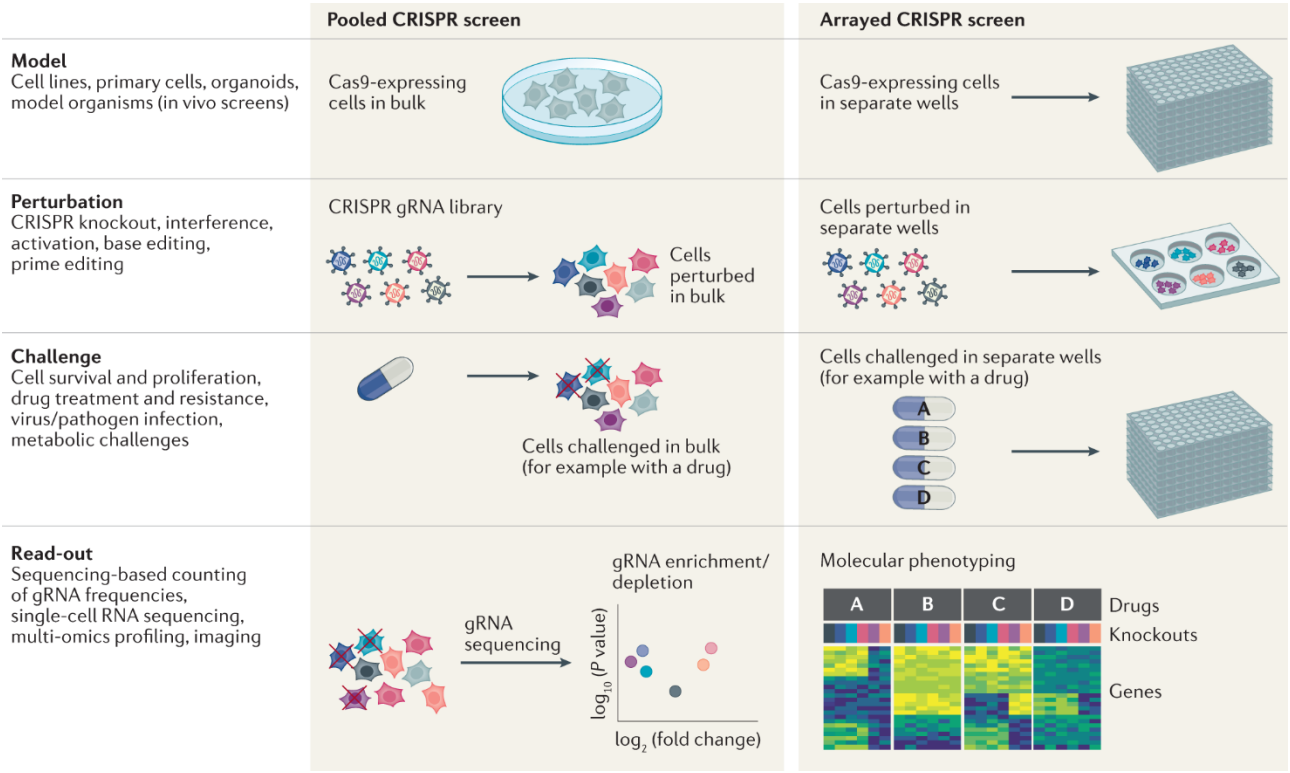

Figure 13 CRISPR screens in forward genetics. Pooled screens rely on bulk perturbation and enrichment of variants based on a biological challenge. gRNA depletion (negative screen) or enrichment (positive screen) indicates that the respective target gene is associated with the biological challenge. In arrayed screens different perturbations are kept in individual containers, allowing complex readouts beyond enrichment and depletion in response to a biological challenge. gRNA, guide RNA, CRISPR, clustered-regulatory-interspaced-short-palindromic-repeats. Reprinted from Bock et al. (2022)

CRISPR technology, due to its simplicity, efficiency, and flexibility, propelled the field of forward genetics and allow genome-scale interrogation in quasi every context (Jinek et al., 2012). The CRISPR/Cas9 system consists of the Cas9 nuclease, programmed to induce DSBs at pre-defined genomic loci, using synthetic single-guide RNA for target direction (Cong et al., 2013). Pooled CRISPR screens typically introduce a library of perturbations (i.e. sgRNAs) via lentiviral vectors into cells expressing Cas9 in bulk (Figure 13). Consecutively, the pool of perturbed cells compete for representation when facing a biological challenge (e.g. drug treatment), or undergo physical separation by flow cytometry. sgRNA frequency of surviving or enriched cells (enrichment or depletion as compared to the original frequency) indicate genotype-phenotype relationships. In contrast, arrayed CRISPR screens separate each perturbation in an individual compartment or well, which is preferred for complex readouts that cannot be easily sequenced. Beyond classical loss-of-function perturbations using Cas9, fusion of functionally inactivate Cas9 (dCas9) to trans-repressor

or trans-activator domains enabling another dimension of screenings, CRISPR interference and CRISPR activation, respectively (Alerasool et al., 2020; Konermann et al., 2015).

In general, pooled CRISPR screens with genome-wide interrogation capacity are favored and very recently, first studies describe applications for CHO biofactories. The first CHO-specific sgRNA library was designed in 2021 (Xiong et al., 2021b). Following tunicamycine treatment to simulate ER-stress, the authors identified Zfx and Bag6 as engineering targets which substantially increased cell survival in presence of tunicamycine (Xiong et al., 2021b). In a similar study, Cas9-expressing CHO cells underwent 6-thioguanine (6-TG) treatment after lentiviral sgRNA transduction, recapitulating that the HPRT1 gene is essential for 6-TH resistance (Kretzmer et al., 2022). However, to mitigate off-target Cas9 activity and phenotype variation by random transgene integrations (Morgens et al., 2017; Tycko et al., 2019), site-specific RMCE integration of sgRNAs with transient Cas9 expression is strongly preferred over lentiviral transduction methods (S. H. Kim et al., 2023). Hyperosmotic treatment (460 mOsm/kg) enriched genes associated with tRNA wobble uridine modification, regulation of mRNA stability, and small molecule catabolic processes (S. H. Kim et al., 2023). Interestingly, upon verification of the top hits ZFR and PNP mAb- and bsAb-expressing cells, revealed significantly higher biomass accumulation but unchanged specific productivity rates (S. H. Kim et al., 2023). While the ZFRgene has no described function as of now, emphasizing the value of CRISPR screens for detection of unknown gene-function relationships, PNP is known to convert inosine to hypoxanthine in the purine degradation pathway (Krenitsky et al., 1986). Inosine levels in turn have been associated with increased cell proliferation (Yin et al., 2018).

However, while negative and positive selection screens based on context-dependent cell survival have resulted in substantial insights in cancer biology (Tsherniak et al., 2017; Tzelepis et al., 2016; T. Wang et al., 2017), they are artificial for use as a biological challenge in a bioprocessing context and commonly do not reveal targets relevant for bioproduction (S. H. Kim et al., 2024; P. C. Lin et al., 2021). Instead, cell survival and proliferation inversely correlate with productivity in CHO biofactories (Maltais et al., 2023; Ong et al., 2019; Zou et al., 2018). To prevent enrichment of low producer cells, CRISPR screens consequently require more sophisticated selection pressure. In a recent example, KOs associated with increased productivity of bsAb were enriched based on surface labeling of secreted proteins transiently associated with the cell surface, i.e. the cold-capture approach (Brezinsky et al.,

2003; S. H. Kim et al., 2024). The study revealed consistent higher specific productivities upon KO of MCAF and SETDB1, which are binding partners for depositing H3K9me3 (Fujita et al., 2003; H. Wang et al., 2003). Further, the KO of MCAF and SETDB1 resulted in markedly improved bsAb/mAb transgene mRNA and specific productivity levels in batch cultivation.

1.4 Aim of this Study

This study aims at addressing the challenges in bioproduction of heterodimeric bispecific antibodies, which offer unique therapeutic applications unmatched by using conventional IgG-based antibodies. Despite increasingly sophisticated advancements in genetic engineering, such as targeted integration which attenuates the clonal fraction of non-producers and effectively decreases exacerbated production-relevant phenotypic diversity, the development of CHO biofactories still requires extensive empirical testing due to limited predictive knowledge about the biological mechanisms or early biomarkers to identify phenotypes feasible for large-scale manufacturing.

This thesis aims to leverage the principles of synthetic biology, i.e. rational genetic engineering using standardized biological parts and forward genetic screens, to improve the manufacturing capabilities of CHO biofactories. First, rational design-build-test-learn cycles are employed to investigate and eliminate the formation of specific micro-heterogeneities in T cell bispecific antibodies. These rational engineering efforts are based on *a priori* knowledge by prediction of orthologous gene functions between human and CHO cells. Second, to uncover previously unknown genes determining CHO productivity, an arrayed CRISPR screening is used to characterize genotype-phenotype relationships in two high producer clones. Results are validated across clones, produced antibody formats, and after bioprocess scale-up, indicating the reliability of the employed screening method. Last, the underlying factors contributing to phenotypic diversity in CHO cells are characterized using genomic barcodes for lineage tracing, a concept widely employed in hematopoiesis, development, and cancer research. This attempts to reveal whether the majority of clone-to-clone phenotypic diversity in CHO biofactories is a constant feature or subject to disruptive bottleneck and founder effects. Overall, these results revisit and update CHO cell engineering options in the context of isogenic targeted integration cell line development.

2 Publications

2.1 Procollagen-Lysine 2-Oxoglutarate 5-Dioxygenases are Responsible for 5R-Hydroxylysine Modification of Therapeutic T-Cell Bispecific Monoclonal Antibodies Produced by Chinese Hamster Ovary Cells

Niels Bauer*, Marco Boettger*, Stella Papadaki, Tanja A. Leitner, Stefan Klostermann, Hubert Kettenberger, Guy Georges, Vincent Larraillet, Dino Gluhacevic von Kruechten, Lars Hillringhaus, Annette Vogt, Simon Ausländer & Oliver Popp, Procollagen-Lysine 2-Oxoglutarate 5-Dioxygenases are Responsible for 5R-Hydroxylysine Modification of Therapeutic T-Cell Bispecific Monoclonal Antibodies Produced by Chinese Hamster Ovary Cells, *Frontiers in Bioengineering and Biotechnology,* Volume 12, 2024, 12:1414408, https://doi.org/10.3389/fbioe.2024.1414408, * *These authors contributed equally.*

Author contribution:
I designed, performed, and analyzed all experiment associated with CRISPR gene knockout of PLOD1/2/3 and JMJD4/6/7. Further I employed and analyzed all experiments regarding iron availability. I was involved in discussing and interpreting all results in the study. I was involved in writing the manuscript.

frontiers | Frontiers in Bioengineering and Biotechnology

TYPE Original Research
PUBLISHED 28 October 2024
DOI 10.3389/fbioe.2024.1414408

OPEN ACCESS

EDITED BY
Simon Fischer,
Boehringer Ingelheim Pharma GmbH and Co. KG, Germany

REVIEWED BY
Katharina Koether,
Boehringer Ingelheim, Germany
Fabian Higel,
Boehringer Ingelheim Pharma GmbH and Co. KG, Germany
Saurabh Sen,
Sanofi Pasteur, United States

*CORRESPONDENCE
Oliver Popp,
oliver.popp@roche.com

†These authors have contributed equally to this work

RECEIVED 08 April 2024
ACCEPTED 08 October 2024
PUBLISHED 28 October 2024

CITATION
Bauer N, Boettger M, Papadaki S, Leitner T, Klostermann S, Kettenberger H, Georges G, Larraillet V, Gluhacevic von Kruechten D, Hillringhaus L, Vogt A, Ausländer S and Popp O (2024) Procollagen-lysine 2-oxoglutarate 5-dioxygenases are responsible for 5R-hydroxylysine modification of therapeutic T-cell bispecific monoclonal antibodies produced by Chinese hamster ovary cells.
Front. Bioeng. Biotechnol. 12:1414408.
doi: 10.3389/fbioe.2024.1414408

Procollagen-lysine 2-oxoglutarate 5-dioxygenases are responsible for 5R-hydroxylysine modification of therapeutic T-cell bispecific monoclonal antibodies produced by Chinese hamster ovary cells

Niels Bauer[1,2†], Marco Boettger[1†], Styliani Papadaki[1], Tanja Leitner[1], Stefan Klostermann[3], Hubert Kettenberger[1], Guy Georges[1], Vincent Larraillet[1], Dino Gluhacevic von Kruechten[4], Lars Hillringhaus[4], Annette Vogt[1], Simon Ausländer[1] and Oliver Popp[1*]

[1]Large Molecule Research, Roche Pharma Research and Early Development (pRED), Roche Innovation Center Munich, Penzberg, Germany, [2]Gene Center and Department of Biochemistry, Ludwig-Maximilians-Universität München, Munich, Germany, [3]Data and Analytics, Roche Pharma Research and Early Development (pRED), Roche Innovation Center Munich, Penzberg, Germany, [4]Special Chemistry, Roche Diagnostics, Roche Innovation Center Munich, Penzberg, Germany

We present a detailed mass spectrometric analysis of three 2 + 1 T-cell bispecific monoclonal antibodies (TCB mAbs), where an unexpected +15.9950 Da mass shift in tryptic peptides was observed. This modification was attributed to the occurrence of 5R-hydroxylysine (Hyl) using a hybrid LC–MS/MS molecular characterization and CRISPR/Cas9 gene deletion approach. The modification was found at various sites within TCB mAbs, with a conspicuous hot spot motif mirroring a prior observation where Hyl was mapped to the C_H1–VH Fab domain interface of IgGs. In contrast to the preceding report, our structural modeling analysis on TCB mAbs unveiled substantial differences in the orientation and flexibility of motifs in immediate proximity and across the artificial C_H1–VL cross Fab interface and upstream elbow segment. Utilizing a hybrid database search, RNAseq, and a CRISPR/Cas9 knockout methodology in Chinese hamster ovary (CHO) production cell lines, procollagen-lysine, 2-oxoglutarate 5-dioxygenases (PLODs) were conclusively identified as the catalyzing enzymes accountable for the 5R-Hyl modification in TCB mAbs. To quantitatively inhibit Hyl formation in TCB mAbs, the activity of all three Chinese hamster PLOD isoenzymes needs to be depleted via CRISPR/Cas9 gene knockout. Moreover, our investigation identified cell culture iron availability, process duration, and clonal variability in CHO cells as elements influencing the levels of Hyl formation in TCB mAbs. This research offers a solution for circumventing Hyl formation in therapeutic

complex mAb formats, such as TCB mAbs, produced in CHO cell culture processes, thereby addressing potential technical and biological challenges associated with unintended Hyl modification.

KEYWORDS

T-cell bispecific monoclonal antibodies, Chinese hamster ovary cells, hydroxylysine, CRISPR/Cas9, post-translational modification, mass spectrometry, metal cofactor

Introduction

Most recombinant generic monoclonal antibodies (mAbs) and novel, complex mAb-derived formats approved or under clinical investigation for the treatment of diverse therapeutic purposes are produced by mammalian Chinese hamster ovary (CHO) cells (Wurm, 2004). Innovative, complex mAb derivatives, such as T-cell bispecific (TCB) mAbs, exhibit potential therapeutic efficacies by orchestrating T-cell cytotoxicity toward pathogenic cells (Figure 1A) (Augsberger et al., 2021; Iurlaro et al., 2022). CHO cells, as the most prominent representative of mammalian expression systems, are preferred over other hosts due to their ability to grow in suspension at large scales in serum-free and chemically defined media and their capacity to produce high quantities of recombinant biotherapeutic proteins required to meet clinical demands. Importantly, CHO cells have demonstrated the ability to produce recombinant proteins with correct protein folding and human-tolerant post-translational modifications (PTMs), which are essential for clinical applications (Kunert and Reinhart, 2016). Significant investments in developing robust production strategies and metabolically balanced media formulations have enabled processes with high yields and product quality, as well as substantially improved batch-to-batch reproducibility (Birch and Racher, 2006). Despite the implementation of rigorous control strategies in the production of biologics, these proteins still exhibit minor variations that arise from both enzymatic functions and non-enzymatic chemical reactions during the production process. These micro heterogeneities include N- and O-types of glycosylation, cysteine modifications, carbonylations, oxidations, glycation, isomerizations of aspartate, and variations at the C-terminal lysine (Geist et al., 2013; Luo et al., 2012; Raju and Jordan, 2012; Gramer, 2014). In recent studies, an unanticipated modification of lysine hydroxylation was detected in various recombinant proteins produced by CHO cells, including tissue plasminogen activator (rtPA), soluble and chimeric CD4 receptor variants, the De13a toxin from a marine cone snail, somatostatin, and IgG1 monoclonal antibodies, all of which are present in significant quantities (Table 1) (Molony et al., 1995; Aguilar et al., 2005; Andrews et al., 1984; Xie et al., 2016). The hydroxylation in the recombinant IgG1 mAb has been identified by a +16 Da mass shift and is comparable to the other hydroxylated proteins in a Xaa-Lys-Gly (XKG) consensus sequence via a tryptic fragmentation and liquid chromatography–mass spectrometry approach (Xie et al., 2016).

In nature, enzymatic hydroxylysine (Hyl) formation by lysyl hydroxylases is a vital upstream key element in extracellular matrix reconstitution by crosslinking pro-collagen and collagen-like structures by O-glycosylation (Pornprasertsuk et al., 2004; Schegg et al., 2009). Pro-collagen protein Hyl formation in humans is facilitated by procollagen-lysine, 2-oxoglutarate 5-dioxygenases (PLOD) in the endoplasmatic reticulum (ER), which belong to the enzymatic class of 2-oxoglutarate (2OG) oxygenases (Markolovic et al., 2015). In humans, three genes, namely, *PLOD1*, *PLOD2*, and *PLOD3*, encode for protein lysyl hydroxylases, which catalyze the 5R-Hyl formation in pro-collagen and collagen-like proteins. For PLOD2, two splice variants, namely, LH2a (PLOD2A) and LH2b (PLOD2B) exist, where LH2b differs from LH2a by incorporating the small exon 13A (Valtavaara et al., 1997). The variety of PLOD gene products and splice variants suggest different layers of regulation in (patho)physiological processes; however, the role of the diverse gene products and splice variants is not fully understood yet (Qi and Xu, 2018). In mammalian systems, for example, a multiprotein complex containing the lysyl hydroxylase *PLOD1* and the proline hydroxylases P3H3 and P3H4 is responsible for the hydroxylation of C5 of lysyl and the C4 prolyl residues in pro-collagen α-chains, respectively, which subsequently triggers the accurate assembly and crosslinking of collagen fibrils (Heard et al., 2016).

Facilitating the enzymatic oxygenase activity, PLOD enzymes require Fe^{2+} as a cofactor and 2OG. In a sequential binding mechanism of the first 2OG, the substrate, and then oxygen, an active ferryl intermediate is formed by oxidative decarboxylation of 2OG. The ferryl intermediate finally reacts with the substrate, leading to hydroxylation. The proteinogenic substrates represent a generic XKG consensus sequence that targets the activity of oxygenases to specific protein surface features. PLODs differ from the other mammalian lysyl 2OGs of the Jumonji domain-containing (JmjC) protein family, like JMJD4, JMJD6, and JMJD7, due to differences in their subcellular spatial localization, respective downstream control mechanisms, and in generating isobar yet structurally different Hyl products: 5R-Hyl (PLODs), 5S-Hyl (JMJD6), 4RS-Hyl (JMJD4), and 3S-Hyl (JMJD7) (Markolovic et al., 2015; Markolovic et al., 2018).

The presence of the Hyl moiety in proteins alters their physicochemical properties since the additional hydroxyl group can cause local changes in hydrophobicity and charge and can act as an accessible active group for subsequent modifications like glycosylation [reviewed by De Giorgi et al. (2021)]. Such alterations have the potential to act as intended or unintended signaling modulators in biological systems and may induce undesirable complexity in the technical development and production of therapeutic proteins. Since Hyl residues are utilized for crosslinking in collagens, the accidental aggregation and/or neoepitope formation of Hyl in modified therapeutic proteins poses a risk to protein stability and functionality. For example, this may modulate target protein binding efficacy, increase the efforts required for analytical characterization and purification process development, and, ultimately, trigger immunogenicity in patients. In addition, Hyl can be targeted by lysyl oxidases to form hydroxyallysine through oxidative deamination, releasing ammonia and the strong oxidizing reagent

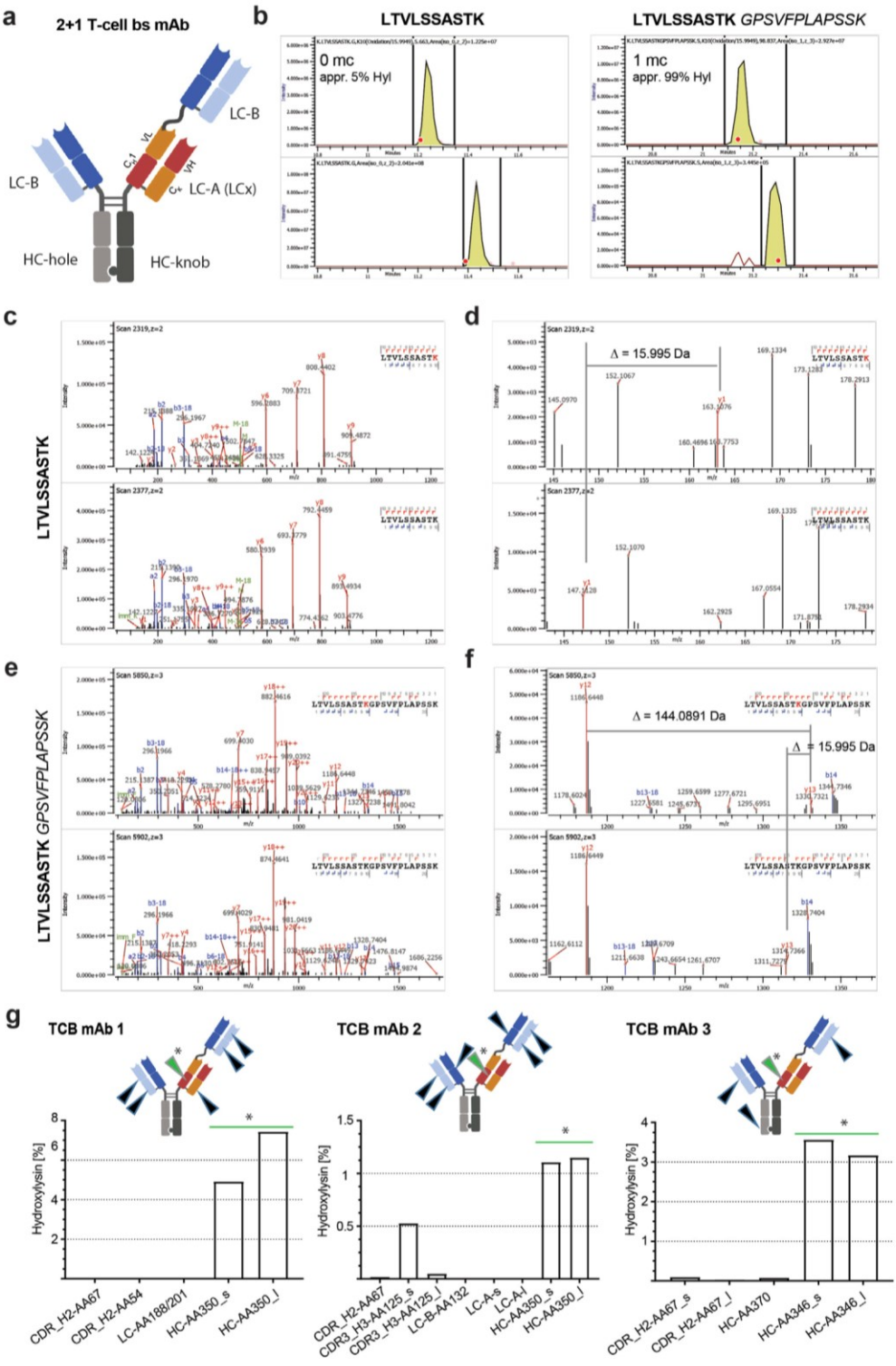

FIGURE 1
Conformation of hydroxylysine modification and relevance for tryptic digestion. **(A)** Schematic model of a 2 + 1 T-cell bispecific (TCB) mAb (dotted lines: disulfide bridge). **(B)** Example XIC of modified (upper panel) and unmodified (bottom panel) tryptic peptide HC-AA350 of TCB mAb 3 with zero missed cleavage LTVLSSASTK and the tryptic peptide with one missed cleavage LTVLSSASTKGPSVFLAPSSK. The bold red dots indicate the timepoints when the MS/MS fragmentations of the precursors have been triggered, which represent the main species of the respective XIC signals. Note the difference in the intensity scale of both unmodified peptides compared to the respective modified peptides. **(C)** Overview of HCD fragment spectra of the modified (upper panel) and unmodified peptide (bottom panel) HC-AA350 of TCB mAb 3. **(D)** Zoomed view of modified (upper panel) and unmodified peptides (lower panel). The shift of 15.9950 Da of the y1-ion confirms the modification on lysine. **(E)** Example overview of HCD fragment spectra of the modified (upper panel) and unmodified peptides (bottom panel) with one missed cleavage. **(F)** Zoomed view of the same MS/MS scans with a focus on the fragment ions y12 and y13 that belong to the KG motif. The distance between both fragments is equivalent to the mass of a Hyl residue with −5.6 ppm
(*Continued*)

FIGURE 1 (Continued)
deviation (theoretical mass of Hyl = 144.0899). **(G)** Identified sites and levels of cleaved and missed cleaved tryptic peptides of three different TCB mAb molecules (arrowheads indicate the Hyl modification site in respective TCB molecule: green arrowhead and star represent hot spot positions and black arrowhead represents alternative positions).

TABLE 1 Hyl-containing therapeutic peptides and proteins reported.

Peptide/protein	Sequence	Level of Hyl	Reference
Recombinant human plasminogen activator (rtPA)	I**K**GGLFADIASHPWQAAIFAK	Up to 20%	Molony et al. (1995)
Recombinant antibody CD4/rCD4IgG	ILGNEGSFLT**K**GFSK	Up to 10%	Molony et al. (1995)
De13a, a toxin of marine cone snail	DCPTSCPTTCANGWECC**K**GYPCVN**K**ACSGCTH	Up to 100%	Aguilar et al. (2005)
Somatostatin-28, a peptide hormone from anglerfish	RSVDSTNNLPPRERKAGCKNFYW**K**GFTSC	Up to 40%	Andrews et al. (1984)
IgG1 mAb	XXXXXXXXXWGQGTLVTVSSAST**K**	Not assessed	Xie et al. (2016)
TCB mAb 1	XXXXXXXXXXXX**K**GR XXXXXXXXXXXX**K** DSTYSLSSTLTLS**K** LTVLSSAST**K**GPSVFPLAPSSK	12.4%	This work
TCB mAb 2	XXXXXXXXXXXX**K**GR XXXXXXWGQGVLVTVSSAST**K**GPSVFPLAPSSK L**K**SGTASVVCLLNNFYPR DSTYSLSSTLTLS**K**ADYEK LTVLSSAST**K**GPSVFPLAPSSK	2.9%	This work
TCB mAb 3	XXXXXXXXXXX**K**GR NQVSLSCAV**K** LTVLSSAST**K**GPSVFPLAPSSK	7.0%	This work

The red lysine represents the position of Hyl modification. Please note that "X" represents amino acids of the identified peptides from the mAb CDR regions.

H_2O_2 or serve as a motive for downstream O-glycosylation events (Abbasov et al., 2021). Therefore, once identified, detailed molecular and functional characterization of this PTM in biotherapeutics is required, as well as ways to control it. In an optimal situation, measures should be developed to avoid the *de novo* formation of Hyl modifications.

In this work, we report the identification of 5R-Hyl as a PTM in three different TCB mAbs produced by CHO cell culture processes via LC–MS/MS peptide mapping. In recent studies, CHO endogenous lysyl hydroxylase enzymes were postulated to mediate the formation of Hyl in mAbs. Using CRISPR/Cas9 knockout approaches, we demonstrate for the first time that all existing host-derived *Cricetulus griseus* PLOD isozymes, namely, PLOD1, PLOD2, and PLOD3, are responsible for the formation of the 5-Hyl modification of three recombinant TCB mAbs in CHO-based expression systems. Unexpectedly, the deletion of the PLOD genes in the respective recombinant CHO production cell lines correlated with significant benefits in cell culture performance and an increase in the product quality of the TCB mAbs in the harvested cell culture fluids.

Results

Identification of hydroxylysine modification in TCB mAbs

Using a spectrometric tryptic peptide mapping approach, we identified several +15.9950 Da mass shifts in three different recombinant TCB mAbs, namely, TCB mAb 1, TCB mAb 2, and TCB mAb 3, each expressed by three different recombinant CHO cell lines (Figures 1A, B). The levels of the peptide modifications varied based on the positions in the TCB mAb molecule (Table 2). The mass shifts were observed in the respective CDRs at low levels (<1%) and high levels in the C_H1 heavy-chain knob (HC-K) backbone (up to 12.4%) downstream of the intramolecular crossed Fab CDR (Table 2; Figure 1G). The detected motif with the +15.9950 Da modification in the prominent C_H1 mAb element is similar to the position described earlier by Xie et al. (2016) at a lysine residue in HC101–HC124 (XXXXXXXXXWGQGTLVTVSSASTK), yet differs in the present study by the crossed HC organization in TCB mAbs by introducing an artificial C_H1–VL interface (Figure 1A). Xie et al. (2016) attributed the +15.9950 Da modification to the hydroxylation of the lysine residue in the identified peptide. Based on this previous observation, we aimed to identify the cause of observed mass shifts and evaluate the possibility of the Hyl modification in the three analyzed TCB mAbs. For this, the exact amino acid positions of the modifications were determined by the analysis of the higher-energy collisional dissociation (HCD) fragmentation data (Table 2). The location of the +15.9950 Da modification in the prominent LTVLSSASTK peptide (amino acids 341–350 according to HC position numbering–amino acid 350 corresponds to 117 according to Kabat numbering) of HC-K was attributed to oxidation and confirmed at lysine K350 in the analyzed peptide using extracted ion chromatograms of the modified and the unmodified peptide LTVLSSASTK350 for both cases with and

10.3389/fbioe.2024.1414408

TABLE 2 Hyl levels of TCBs produced by wild-type (wt) and PLOD KO production cell lines.

TCB mAb 1											
TCB mAb domain	Cleaved	Sequence	Protein annotation	Start AA	End AA	Mod. AAs	Mod. names	Var. Pos. Protein	TCB mAb 1 wt [%]	TCB mAb 1 KO [%]	Hyl reduction [%]
LC-B	nd	XXXXXXXXXXXXX**K**GR	CDR-H2	55	69	K	Oxidation/ 15.9949	67	<0.1	<0.1	79*
LC-B	nd	XXXXXXXXXXXX**K**	CDR-H2	53	67	K	Oxidation/ 15.9949	54	<0.1	<0.1	84*
LC-A & B	nd	DSTYSLSSTLTLS**K**		175/188	188/201	K	Oxidation/ 15.9949	188/201	<0.1	<0.1	91*
HC-K	s	LTVLSSAST**K**		341	350	K	Oxidation/ 15.9949	350	4.9	0.2	93
HC-K	l	LTVLSSAST**K**GPSVFPLAPSSK		341	362	K	Oxidation/ 15.9949	350	7.4	0.7	
								Sum	12.3	0.9	
TCB mAb 2											
TCB mAb domain		Sequence	Protein annotation	Start AA	End AA	Mod. AAs	Mod. names	Var. Pos. Protein	TCB mAb 2 wt [%]	TCB mAb 2 KO [%]	Hyl reduction [%]
LC-A	nd	XXXXXXXXXXXXX**K**GR	CDR-H2	55	69	K	Oxidation/ 15.9949	67	<0.1	<0.1	65*
HC-K	s	XXXXXXWGQGVLVTVSSAST**K**	CDR-H3	104	125	K	Oxidation/ 15.9949	125	0.5	<0.1	92
HC-K	l	XXXXXXWGQGVLVTVSSAST**K** GPSVFPLAPSSK	CDR-H3	104	137	K	Oxidation/ 15.9949	125	<0.1	<0.1	
								Sum	0.6	<0.1	
LC-B	nd	L**K**SGTASVVCLLNNFYPR		131	148	K	Oxidation/ 15.9949	132	<0.1	<0.1	96*
LC-A & B	s	DSTYSLSSTLTLS**K**		188/176	201/189	K	Oxidation/ 15.9949	201/189	<0.1	<0.1	98*
LC-A & B	l	DSTYSLSSTLTLS**K**ADYEK		188/176	206/198	K	Oxidation/ 15.9949	201/198	<0.1	<0.1	
								Sum	<0.1	<0.1	

(Continued on following page)

TABLE 2 (*Continued*) Hyl levels of TCBs produced by wild-type (wt) and PLOD KO production cell lines.

TCB mAb 2											
TCB mAb domain		Sequence	Protein annotation	Start AA	End AA	Mod. AAs	Mod. names	Var. Pos. Protein	TCB mAb 2 wt [%]	TCB mAb 2 KO [%]	Hyl reduction [%]
HC-K	s	LTVLSSAST**K**		341	350	K	Oxidation/ 15.9949	350	1.1	<0.1	98
HC-K	l	LTVLSSAST**K**GPSVFPLAPSSK		341	362	K	Oxidation/ 15.9949	350	1.2	<0.1	
								Sum	2.3	<0.1	
TCB mAb 3											
TCB mAb domain		Sequence	Protein annotation	Start AA	End AA	Mod. AAs	Mod. names	Var. Pos. Protein	TCB mAb 3 wt [%]	TCB mAb 3 KO [%]	Hyl reduction [%]
LC-A	s	XXXXXXXXXXXX**K**	CDR-H2	55	67	K	Oxidation/ 15.9949	67	0.1	<0.1	99*
LC-A	l	XXXXXXXXXXXX**K**GR	CDR-H2	55	69	K	Oxidation/ 15.9949	67	<0.1	<0.1	
								Sum	0.1	<0.1	
HC-H	nd	NQVSLSCAV**K**		361	370	K	Oxidation/ 15.9949	370	0.1	<0.1	97*
HC-K	s	LTVLSSAST**K**		337	346	K	Oxidation/ 15.9949	346	3.6	0.1	98
HC-K	l	LTVLSSAST**K**GPSVFPLAPSSK		337	358	K	Oxidation/ 15.9949	346	3.2	<0.1	
								Sum	6.8	0.1	

Comparison of Hyl levels between wild-type and KO clones of three different TCB mAbs (TCB mAb 1–3) together with the relative reduction in Hyl after PLOD-KO. The modified K is highlighted in bold. If different cleavage versions are quantified together, the single quantities are summed to build a total for the respective locus. The cleaved peptide is marked with an "s" (short) and the non-cleaved version with a "l" (long). Note that not for every locus a peptide with missed cleavage was detected and highlighted in the table with "nd" (not detected); "<0.1" means confirmed detection of modification; yet, no valid concentrations can be generated. * semi quantitative

10.3389/fbioe.2024.1414408

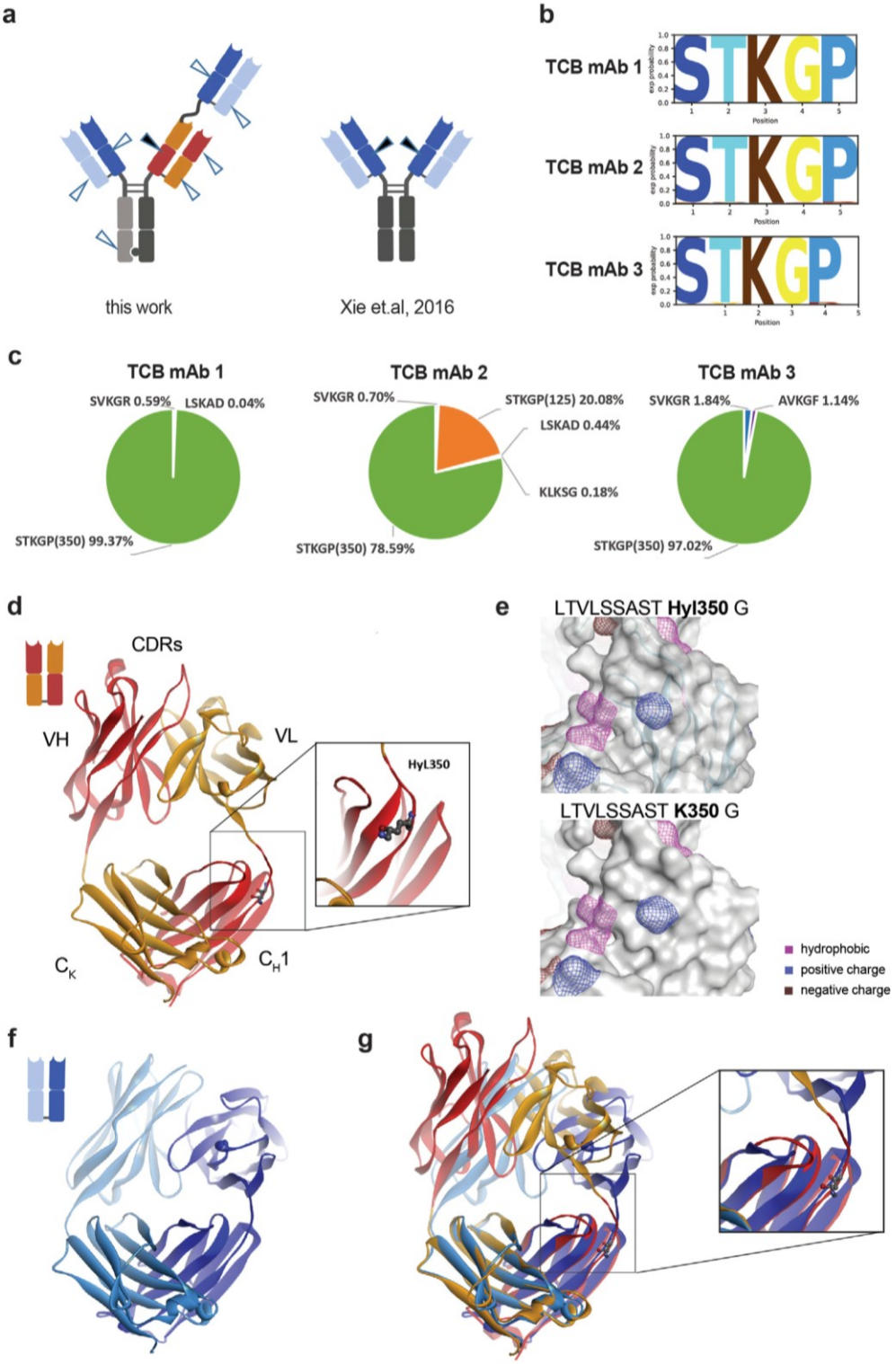

FIGURE 2
Localization of Hyl modification hot spot and structural consequence in TCB mAbs. **(A)** Several exposed lysine residues were detected by hydroxylation in TCB mAbs (arrowheads). The hot spot (dark arrowhead) with the highest Hyl modification levels is similar to previous observations by Xie et al. (2016) (dark arrowhead). **(B)** Probability analysis of amino acids from positions −2 to +2 identified in hydroxylated peptides identified by LC–MS. **(C)** The percentage distribution of detected Hyl-modified peptides differ for the three analyzed TCB mAbs. TCB mAb 2 is the only molecule where the identical hot spot motif LTVLSSASTK and modified at K125, located in the N-terminal Fab binder. **(D)** Structure of the crossed Fab as represented in red/orange ribbons with Hyl350 (balls and sticks) and the respective domain annotations. The identified hot spot Hyl350 TCB mAbs is located right after the interface of VL to C_H1 in the HC knob polypeptide chain. **(E)** Predicted influence of hydroxylysine modification on hydrophobicity and positively and negatively charged patches. The prediction is based on *in silico* protonation, energy minimization and protein patch calculation in MOE 2022. **(F)**
(*Continued*)

FIGURE 2 (Continued)
Structure of trastuzumab Fab domain (pdb code 1n8z), as an exemplary example for a generic IgG Fab, is represented in dark blue and light blue colors for HC and LC, respectively. **(G)** Overlap of a crossed Fab and a generic Fab using the two constant regions C_H1 and C_K. The overlap of the structures reveals a difference in the elbow segment and the orientation of the neighbored loop.

without missed cleavage (Figure 1C). The hydroxylation of lysine results in a decreased hydrophobicity of the tryptic peptide with an expected earlier retention time compared to the unmodified peptide, which is confirmed by the XIC comparison of both and is in line with data, as previously reported by Xie et al. (2016) (Figure 1B).

In a previous publication, the influence of the Hyl residue on the selectivity of trypsin was reported (Molony et al., 1995; Molony et al., 1998). To consider a possible selectivity loss due to Hyl, the tryptic peptide with one missed cleavage, LTVLSSASTKGPSVFPLAPSSK350, was also evaluated for the presence of a modification. By comparing the XIC intensity scales and calculating the ratios separately for both cleavage species, it was observed that the Hyl ratio is significantly higher (ca. 99%) for the peptides with missed cleavage than the ratio obtained by quantifying the correct cleaved peptides only (ca. 5%) (Figure 1B). The majority of the peptide with missed cleavage is present in the modified form. In contrast to the reported observation by Xie et al. (2016), this result implies that lysine hydroxylation influences the cleavage efficiency of trypsin. For some samples, the unmodified peptide with missed cleavage could not be detected based on MS2 because the precursor intensity was below the MS2 trigger limit. The tryptic peptide with one missed cleavage was only found in its modified form. A comparison of modified and unmodified peptides based on XIC and retention time was not possible. Yet, the MS/MS fragment spectrum of the modified peptide also shows nearly 100% coverage and confirms the modification position for the same lysine K350 located in the HC-K C_H1 domain (Figures 1C–F).

Hot spot modification of lysine 350 in crossed C_H1–VL domain of the knob heavy chain in TCB mAbs

Based on the molecular design of TCB mAbs, one arm contains an N-terminal fused additional Fab binder with similar structural characteristics as the other binder domains (see Figure 1A). By this, the hydroxylation hot spot peptide LTVLSSASTK is present in all three Fab binding domains. As reported earlier by Xie et al. (2016), the hydroxylation modification of the C_H1 lysine in an analyzed IgG was attributed to an existing XKG consensus sequence, which is a prominent site of modification in several endogenous hydroxylated polypeptides (Xie et al., 2016). Remarkably, only the lysine in the XKG motif located in the C_H1 heavy chain was detected as the only hydroxylation site although several further XKG motifs exist in the sequence (Xie et al., 2016).

Interestingly, the LTVLSSASTK350 peptide located in the crossed HC C_H1 Fab domain seems to be favored for Hyl modification. Although the hot spot motif is present in all three C_H1 Fab domains of the three tested TCB mAb molecules, only for TCB mAb 2 a Hyl modification were detected in the further HC-knob LTVLSSASTK125 peptide that did not originate from the crossed HC knob C_H1 Fab (Figures 1G, 2C). The level of modification is five times lower than the LTVLSSASTK350 peptide located in the crossed C_H1–VL domain of the knob heavy chain, indicating additional structural requirements for Hyl modification efficiency than solely amino acid sequence identity. For TCB mAb 1 and TCB mAb 3, no Hyl modification of the LTVLSSASTK125 peptide was detected, comprising the same consensus sequence STKGP at lysine125. In contrast to the findings of previous report by Xie et al. (2016), minor yet measurable hydroxylation was detected not only in TCB mAbs within alternative, similar XKG-containing positions but also in different sequence motifs representing XKA and XKS (Figure 2A). The overall propensity of modification in comparison to all hydroxylated peptide sequences detected, however, is dominated by the STKGP sequence motif (Figure 2B).

The prominent hot spot at K350 in the crossed C_H1–VL domain of the knob heavy chain is near the transition to the chimeric–VL domain, downstream of the intramolecular CDR (Figure 2D). K350 is located within the unstructured C_H1–VL interface, close to an exposed loop in the C_H1 domain. We wondered whether the introduction of a hydroxyl group at this position alters the close spatial structure of the C_H1 domain and physicochemical parameters. Using a molecular prediction approach using artificial lysine protonation, energy minimization, and subsequent protein patch calculation, no substantial differences were observed for surface hydrophobicity, as well as for positive and negative charge patches, indicating either no or only minor effects on overall molecular properties (Figure 2E).

Using a structural model comparison approach, we aimed to decipher the potential structural differences between both LTVLSSASTK motifs, located in the generic N-terminal C_H1–VH and in the crossed C_H1–VL domain of the knob heavy chain, respectively, and we also sought to determine whether this analysis could provide an explanation for the observed preferential hydroxylation of K350. For that, the trastuzumab Fab domain (Figure 2F), as an exemplary example of a generic IgG Fab, was overlapped with a crossed Fab domain using the two constant regions C_H1 and C_K for orientation alignment. Structural analysis of the crossed Fab domain by comparing the structural organization of the Fab domain of trastuzumab revealed indeed significant differences in the upstream elbow segment and for a neighboring exposed loop (Figure 2G). The exposition of the elbow segment looks higher in the cross Fab compared to the "regular" Fab, which may be caused by the one amino acid longer elbow sequence for the crossed Fab. In addition, a K350-neighbored loop in C_H1 adopts a different conformation, which indicates some structural flexibility that may influence eventually the rate of the hydroxylation of lysine 350 by providing favored steric accessibility for potential modifying enzymes.

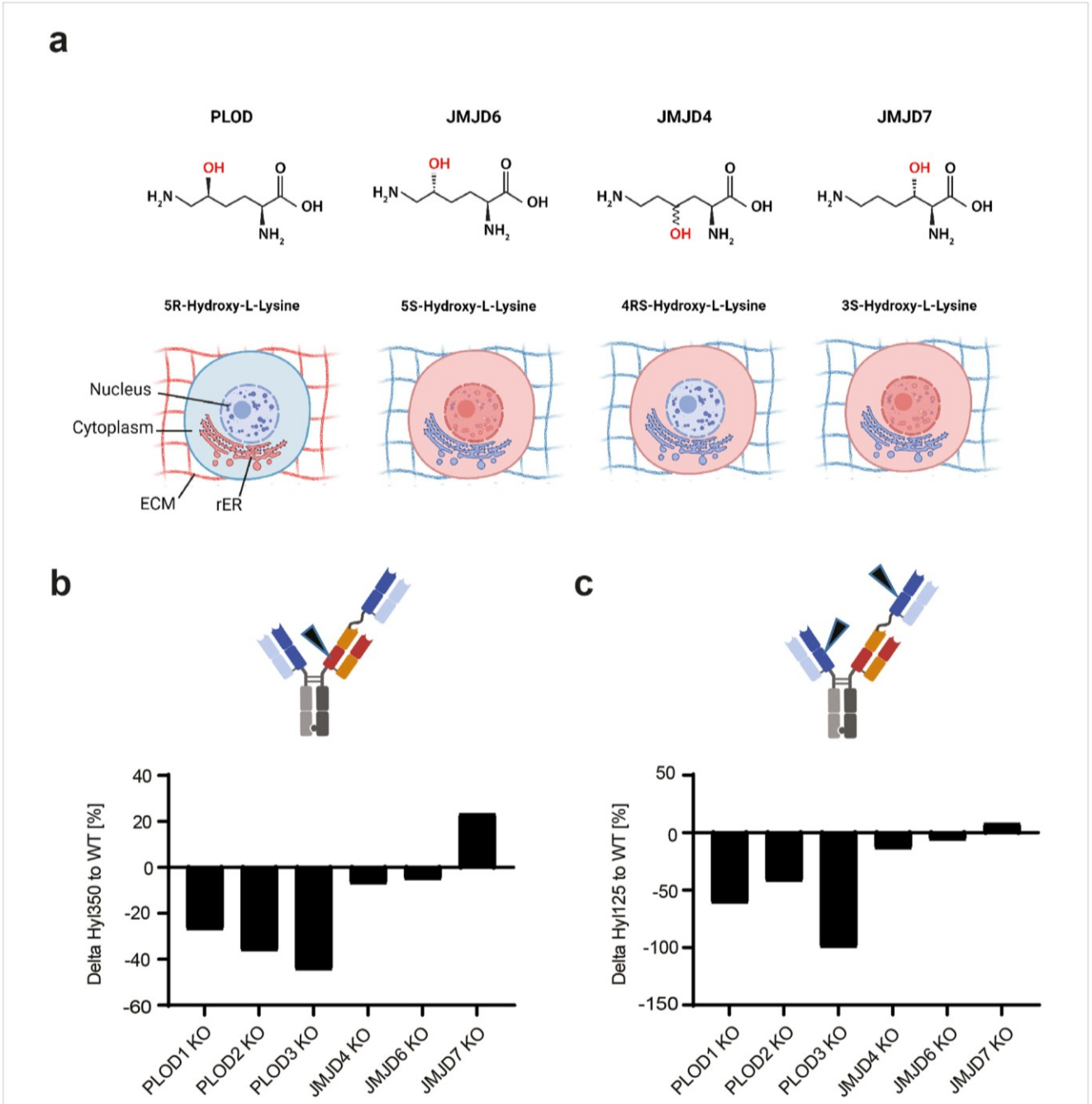

FIGURE 3
PLODs and not JMDJ hydroxylases are responsible for Hyl modification in TCB mAbs. **(A)** Lysine hydroxylation modification as catalyzed by PLODs, JMJD4, JMJD6, and JMJD7, with respective C-positions in lysine stereospecificity. Different 2OG-dependent hydroxylases, PLOD, JMJD4, JMJD6, and JMJD7 create isobaric yet conformationally different Hyl variants. The enzymatically generated hydroxyl groups are highlighted in red. The cellular localization of the respective lysine hydroxylase, as annotated in UniProt, is shown by red emphasized structures in a mammalian cell (ECM, extracellular matrix; rER, rough endoplasmic reticulum). CRISPR/Cas9 screen of mammalian Lys hydroxylases in TCB mAb 1 expressing production CHO cell line indicate that PLODs are responsible for Hyl modification of TCB mAb 1, as shown by observed peptide Hyl350 **(B)** and Hyl125 **(C)** levels normalized to wild-type controls.

PLODs are responsible for lysine hydroxylation in TCB mAbs produced by CHO cell lines

In general, protein hydroxylation can be catalyzed by several 2OG-dependent hydroxylases (Markolovic et al., 2015). In mammalian cells, two enzyme family classes catalyze the post-translational formation of Hyl in proteins: procollagen-lysine, 2-oxoglutarate 5-dioxygenases, comprising PLOD1, PLOD2a (LH2a), PLOD2b (LH2b), and PLOD3 and the Jumonji domain-containing protein family, like JMJD4 and JMJD6 (Markolovic et al., 2015). As reported earlier, the single Hyl modification of an IgG C_H1 peptide identified by Xie et al. (2016) contains an XKG consensus sequence, which is known to be the site of modification in other hydroxylated

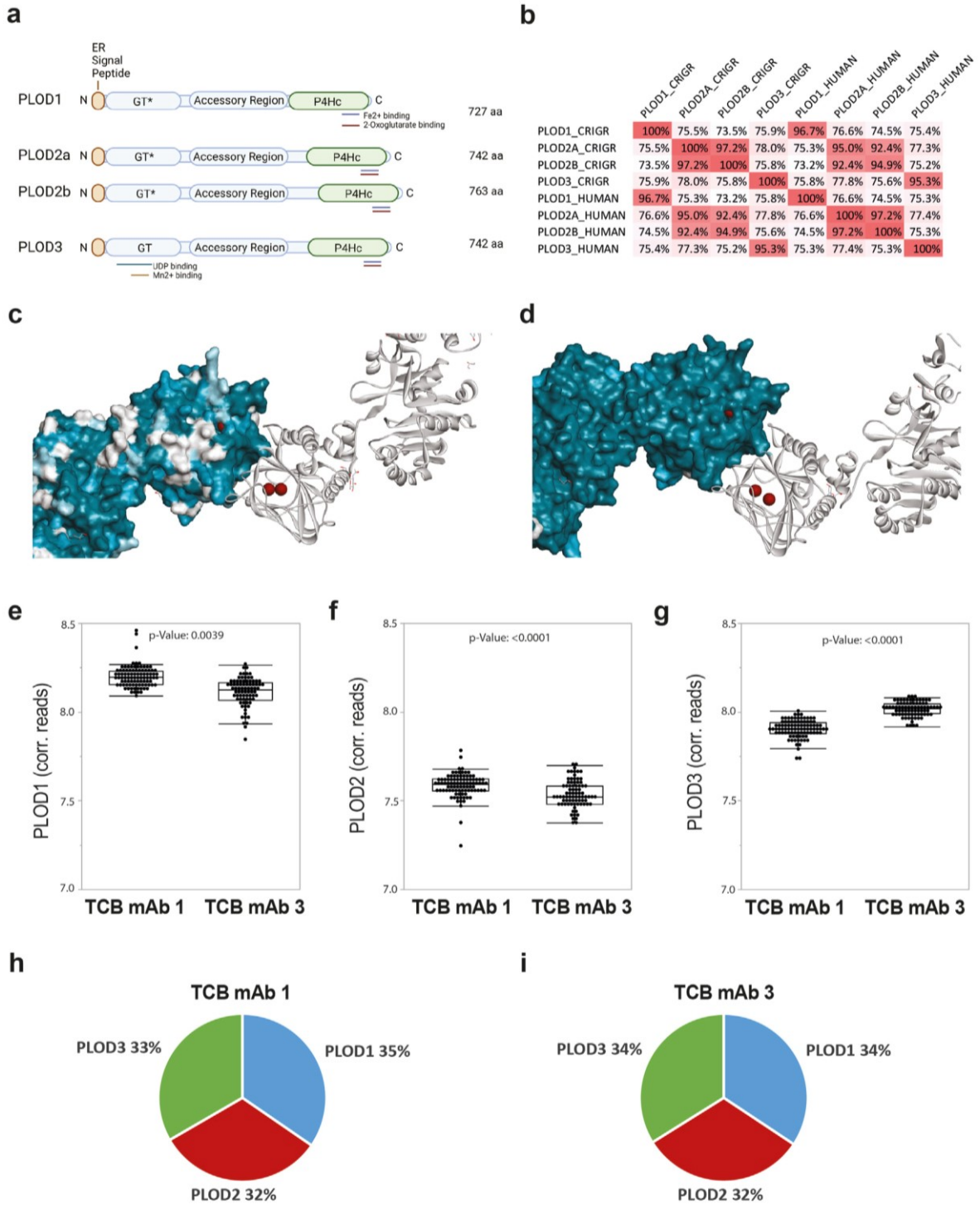

FIGURE 4
PLODs are expressed by CHO cells and show high homology to human orthologs. **(A)** Schematic representation of Chinese hamster PLOD sequence fishing and the knockout domain organization of Chinese hamster PLOD isoenzymes 1, 2a, 2b, and 3 with the glycotransferase domain (GT, note GT* represents defect activity in PLOD1, PLOD2a, and PLOD2b), accessory domain, and hydroxylase domain (P4Hc), respectively. The respective metal cofactor and substrate binding sites for Mn^{2+}, Fe^{2+}, UDP, and 2-oxoglutarate, necessary for respective enzymatic activity, are highlighted by colored bars. **(B)** Sequence homology analysis matrix comparing Chinese hamster (CHRGR) to human PLOD isoenzymes. **(C)** Low surface conservation between human PLODs. Structure conservation analysis by mapping PLOD1, PLOD2a, and PLOD2b onto PLOD3 (PDB 6fxt) structure with a focus on the P4Hc subunit domain as the surface. The catalytic Fe^{2+} metal ions are presented in brown. **(D)** High surface conservation between human and Chinese hamster PLOD3. Structure conservation analysis by mapping Chinese hamster PLOD3 onto human PLOD3 (PDB 6fxt) structure with a focus on the P4Hc subunit domain as the surface. The catalytic Fe^{2+} metal ions are presented in brown. Chinese hamster PLOD1 **(E)**, PLOD2 **(F)**, and PLOD3 **(G)** transcript expression levels analyzed by RNAseq analysis in TCB mAb 1 (n = 73) and TCB mAb 3 (n = 84) CHO production clones shown as single events and box plot. The *p*-value was calculated using the Kruskal–Wallis test. Median transcript expression proportion in CHO production clones for TCB mAb 1 **(H)** and TCB mAb3 **(I)**.

proteins such as collagen. Consequently, the authors speculated that the CHO cell-derived homologs of the lysyl hydroxylase complex cause lysine modification (Xie et al., 2016). So far, and to our knowledge, the mechanism and involved enzymatic factors responsible for the Hyl formation of recombinant proteins produced in CHO cells have not been identified. The cellular localization and compartments of enzymatic activity of PLODs and JMJDs are believed to differ by the ER/extracellular matrix and cytoplasm/nucleus/nucleolus, respectively, which suggests that PLODs function as recombinant TCB mAb modifying enzymes (Figure 3A). However, a contribution of JMJDs on TCB mAb hydroxylation by cell lysis induced by stressful bioreactor cultivations and/or cytoplasmic enzyme shedding events cannot be ruled out. In addition, several reports have described the presence of unexpected "classical" cytosolic proteins such as thioredoxin, glutathione S-transferase, and L-lactate dehydrogenase in CHO cell culture extracellular space, which suggested a deeper analysis of potential lysine modulation enzymes (Koterba et al., 2012; Jones et al., 2021). Based on this, we intended to identify specific involved CHO enzymes that cause the detected Hyl modification in TCB mAbs and develop methods to avoid the Hyl presence in the target product proteins.

For this purpose, we employed CRISPR/Cas9 knockout (KO) screen targeting 2OG-dependent lysyl hydroxylases PLOD1, PLOD2, PLOD3, JMJD4, JMJD6, and JMJD7. All these enzymes catalyze lysine hydroxylation, but they differ in the position and/or stereochemistry of the hydroxyl group (Figure 3A). The screen was performed in the CHO genetic background using the TCB mAb 1-expressing CHO production cell line and the CHO reference genome, GCA_003668045.2_CriGri-PICR_genomic. The sgRNAs were designed according to Doench et al. (2016). For each target, three distinct sgRNAs were designed and used for transfection into the TCB mAb 1-expressing CHO production cell line (Supplementary Table S1). Post-recovery, the cells were cultivated for 4 days in batch cultivation, the supernatant was harvested, and the produced TCB mAb 1 was purified and analyzed for Hyl abundance. Unexpectedly, lysine hydroxylation was identified not only in the known hot spot tracer peptide LTVLSSASTK350 but also in the alternative Fab peptide K125. The observed lack of hydroxylation at the K125 position in the initial experiment could potentially be attributed to variations in the cell culture procedures employed (10 day bioreactor fed-batch vs. 4 day shaker batch cell culture process) or inherent discrepancies within the analytical methods utilized. For both analyzed hydroxylated peptides, CRISPR/Cas9 knockout of Chinese hamster PLOD enzymes reduced the lysine hydroxylation level by 27%–99%, with PLOD3 showing the highest effect. For JMJD4 and JMJD6 enzymes, either a small decrease (up to 7%) or even an elevated level of Hyl of 23% by JMJD7 was observed (Figures 3B, C). This approach demonstrated the relevance of PLODs, rather than JMJD enzymes, for TCB mAb lysine hydroxylation. Interestingly, the knockout of JMJD4, JMJD6, or JMJD7 did not have an effect on general cell viability, indicating its essential role in CHO cellular homeostasis (data not shown).

For a more detailed analysis of putative further CHO-derived PLOD enzyme homologs to human PLOD enzymes PLOD1, PLOD2A, PLOD2B, and PLOD3, we identified the predicted orthologs of all PLOD genes in the Chinese hamster (s. M&M, Figures 4A, B; Supplementary Figures S6–S9). By this, for all known human PLOD isoenzymes, Chinese hamster homologs could be established. The nucleotide sequence comparison between human and Chinese hamster transcripts and protein sequences shows very high similarity for PLOD1 (96.7%), PLOD2A (95.0%), PLOD2B (94.9%), and PLOD3 (95.3%) (Figure 4B; Supplementary Figures S2A), confirming a high degree of conservation among species and also among other vertebrates (data not shown). Similar to human homologs, PLOD isoenzyme sequence similarity between PLOD1, PLOD2 and PLOD3 is only moderate (for human PLODs: 73.5%–75.9% and for Chinese hamster PLODs: 74.5%–76.6%) and results in significant sequence variations (Figure 4C), while the functional domains are present in all isoforms (Figure 4A). In addition, iron and 2-oxoglutarate cofactors and substrate-binding sites are conserved in Chinese hamster PLOD enzymes, suggesting the same enzymatic activity as in human orthologues (Supplementary Figures S2B, C). An exemplarily additional structural similarity analysis of human and Chinese hamster PLOD3 shows a high degree of molecular similarity, which strongly indicates the same functional activity of PLODs in CHO cell cultures as in humans (Figure 4D).

In a subsequent step, we evaluated the existence and putative differences of Chinese hamster PLOD transcript expression in CHO cells. For this, we first checked the presence of PLOD1, PLOD2, and PLOD3 mRNA transcripts as annotated in an internal RNAseq transcript database containing expression profiles form 157 different CHO production cell lines expressing TCB mAb 1 or TCB mAb 3. Intriguingly, when corrected for gene length, the transcript levels of PLODs in the tested monoclonal CHO production cell lines expressing either TCB mAb 1 or TCB mAb 3 exhibited a significant disparity between the expressed products, with PLOD1 and PLOD3 having an increased transcript expression level compared to PLOD2 (Figures 4E–G). However, each of the PLOD enzymes was transcribed at approximately equivalent yet statistically significant different levels for both tested TCB mAbs, with a slight increase in the abundance of PLOD1 and PLOD2 in TCB mAb 1 and a higher level of PLOD3 in TCB mAb 3-expressing cell lines. However, in the aggregate, each of the PLOD enzymes was transcribed at approximately equivalent levels in CHO cell lines for both tested TCB mAbs, albeit with a slight inclination toward elevated levels of PLOD1 and PLOD3 (Figures 4H, I).

Gene transcript expression of PLOD isoenzymes is dynamic in CHO cells expressing a TCB mAb, is dependent on the cell culture process, and correlates with the Hyl modification level

Given the significant variation in PLOD isoenzyme transcript levels among individual monoclonal Chinese hamster ovary (CHO) cell lines, we wanted to assess their presence and expression behavior through a 14-day fed-batch fermentation process using Ambr 250 bioreactors, representative for TCB mAb production. We utilized TCB mAb 2 and tested three monoclonal CHO production cell lines stably producing the respective TCB mAb. Additionally, two different process variants, Process A and Process B, were applied, which differ in nutrient concentrations in the feed and the feeding regimen applied.

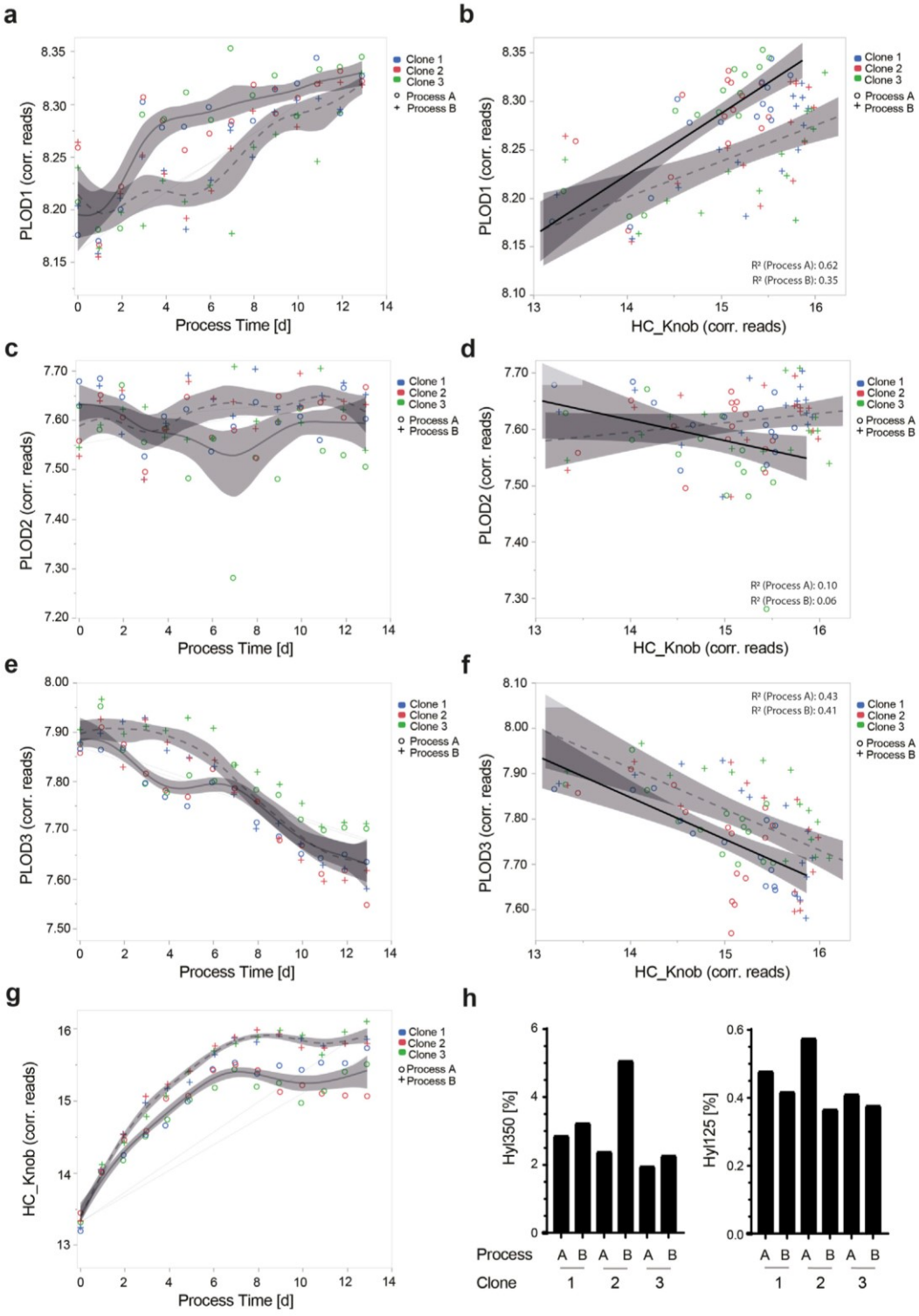

FIGURE 5
Transcript expression kinetics for PLOD1, PLOD2, and PLOD3 is dynamic in CHO cell culture processes. Gene length-corrected Chinese hamster PLOD1 **(A)**, PLOD2 **(C)**, and PLOD3 **(E)** and HC_knob target protein **(G)** transcript expression kinetics of three different monoclonal production clones, all expressing TCB mAb 2. All clones were cultivated in two different fed-batch fermentation processes (circles: Process A and crosses: Process B). Using linear correlation analysis for PLOD isoenzymes with the HC_knob target protein, the respective endogenous PLODs and ectopic HC_knob gene transcript levels were analyzed **(B, D, F)**. Correlation R^2 for each process variant is shown in the graphs. The impact of different cell culture process variants A and B using three different CHO expression clones for TCB mAb 2, namely, clone 1, clone 2, and clone 3 on the lysine hydroxylation abundance for Hyl350 and Hyl125 is shown **(H)**.

As previously observed for TCB mAb 1- and TCB mAb 3-expressing clones, the initial transcript expression levels at day 0 of PLOD1, PLOD2, and PLOD3 in TCB mAb 2 clones once again exhibited the same difference in expression levels, with PLOD1 > PLOD3 > PLOD2 (Figures 5A, C, E). Interestingly, the expression kinetics of different PLOD isoenzymes' transcript levels varied between PLODs and were sensitive to cell culture process variations. While the transcript level for PLOD1 increased over process duration, PLOD2 remained constant, and PLOD3 even decreased (Figures 5A, C, E). The PLOD transcript levels differed between the applied process variants, particularly from days 2 to 6/8 for PLOD1 and PLOD3, correlating with different feeding regime timings of process variants. Interestingly, the initial and final transcript levels were quite similar between process variants A and B (Figures 5A, C, E).

In a subsequent step, we analyzed the ectopic transgene transcript expression level for the HC_knob chain, where the Hyl hotspot motif is encoded, and its expression over the process duration. Remarkably, the transcript level increased until day 8 quite similarly for all three tested CHO production clones, albeit with a clearly increased expression level for Process A. From day 8 to the end of the process, the transcript levels stagnated for both process variants, with a slight difference between the clones (Figure 5G). Overall, the transcript expression levels of the HC_knob chain were approximately twice as high as those of the endogenous Chinese hamster PLOD isoenzymes.

Assuming an approximate transferable expression level from transcript to protein, we analyzed the correlation between the HC_Knob chain and the respective PLOD isoenzymes in CHO production clones. Only PLOD1 and PLOD3 showed a reasonable correlation to HC_knob (PLOD1 for Process A: R^2 = 0.62 and Process B: R^2 = 0.35; PLOD3 for Process A: R^2 = 0.43 and Process B: R^2 = 0.41), with the process variant being favorable for PLOD1 transcript expression and worse for PLOD3 and *vice versa* (Figures 5B, D, F). Knowing that the Chinese hamster PLOD isoenzymes and HC_Knob transcript levels can be affected by the cell culture process variant, we aimed to analyze the level of TCB mAb 2 Hyl levels. Here, clear, yet opposite, differences in lysine hydroxylation abundances were observed for the hot spot motif at K350 (Hyl abundance for Process B > A) and the motif at K125 (Hyl abundance for Process A > B), with the highest levels detected for clone 2, underscoring the relevance of PLOD enzyme expression level and the importance of testing for cell culture process variants and production clones (Figure 5H).

Deletion of all three Chinese hamster PLOD enzymes by CRISPR/Cas9 gene knockout is needed to avoid 5R-Hyl formation in TCB mAbs

The CRISPR/Cas9 KO screen of 2OG-dependent lysyl hydroxylases, the presence of a highly conserved Chinese hamster PLOD homolog, and the TCB mAb modification dominantly observed in the known lysyl hydroxylase consensus sequence XKG strongly suggest that this class of hydroxylases is responsible for the observed lysine hydroxylation modification. We applied a CRISPR/Cas9 gene deletion approach aiming to analyze the Chinese hamster PLOD KO relevance in a production culture and the level of TCB mAbs Hyl modification. In addition, we intended to elucidate which of the three known PLODs, PLOD1, PLOD2, and PLOD3, contributes to the modification and to what extent using two parallel cell culture studies (Figure 6A). Each TCB mAb 1-, TCB mAb 2-, and TCB mAb 3-expressing CHO production cell line was transfected with preselected sgRNAs, targeting PLOD1, PLOD2, and PLOD3 each, as well as the respective Cas9 ribonuclease. Three sgRNAs per target *PLOD* gene were used to ensure most efficient KO effects (Figure 6B, Supplementary Table S2) in the first "Phenotype Study." The pools were cultivated for 4 weeks after transfection to allow for recovery and expansion of cell biomass needed for subsequent production fermentation evaluation. For this purpose, the wild-type (WT) and KO pools were used in a fed-batch cultivation experiment using a fully controlled Ambr 250 fermentation system. The cell cultures were harvested after 10 days, and purified TCB mAbs were analytically characterized via LC-Ms for Hyl abundance, as described before. The PLOD knockout relevance on Hyl modification formation was evaluated by analyzing the prominent K350 in the tryptic peptides, as described before. A strong reduction in Hyl modification was observed in all noticeable peptides generated form TCB mAbs in PLOD KO compared to WT CHO cell lines (Figure 6F; Table 2). Remarkably, the combined Hyl reduction for the dominant LTVLSSASTK350 peptide that is present in the crossed knob heavy-chain C_H1 backbone in all three antibodies reached 93% for TCB mAb 1, 98% for TCB mAb 2, and 98% for TCB mAb 3 (Figure 6G).

The knockout of specific target genes may induce pleiotropic effects within the cellular system (Sonnichsen et al., 2005; Liu et al., 2020). In severe instances, these effects could result in undesirable alterations in cellular performance, which may not be compatible with certain cellular protein production cell systems. Analyzing the entire cell culture growth performance, we recognized an integral of viable cell density (IVCD) over time, which is a measure of overall generated cell biomass in a fermentation process (Figure 6E). The expressed TCB mAb titers, however, showed either a slight (for TCB mAb 1 PLOD1–3 KO and TCB mAb 3 PLOD1–3 KO) or substantial increase (for TCB mAb 2 PLOD1–3 KO) compared to WT cell lines (Figure 6F). By this, the overall specific productivity of KO CHO cell lines was slightly lower (for TCB mAb 1 PLOD1–3 KO) or similar (for TCB mAb 1 PLOD1–3 KO and TCB mAb 3 PLOD1–3 KO) to WT cell lines (data not shown). Further in-depth analysis of cell culture key performance indicators, such as cell viability kinetics and nutrient and metabolic byproduct consumption/formation rates, did not show any significant variance in overall metabolic behavior (data not shown). Interestingly, the product quality of the respective TCB mAbs originating from PLOD1–3 KO cell lines assessed by CE-SDS and SEC demonstrated that all three PLOD1–3 KO cell lines had a higher content of the intended TCB mAb main product (Supplementary Figure S4). The HMW1 species, which are annotated as knob-knob homodimer species, showed a lower level in all PLOD1-3 KO cell lines expressing either TCB mAb 1, TCB mAb 2, or TCB mAb 3 compared to wild-type cell lines (Supplementary Figure S4C). In addition, TCB mAb 1, derived from both PLOD1–3 KO and wild-type cell lines, was subjected to molecular charge species analysis using CIEF. A minor but significant reduction in a specific acidic charge species peak was

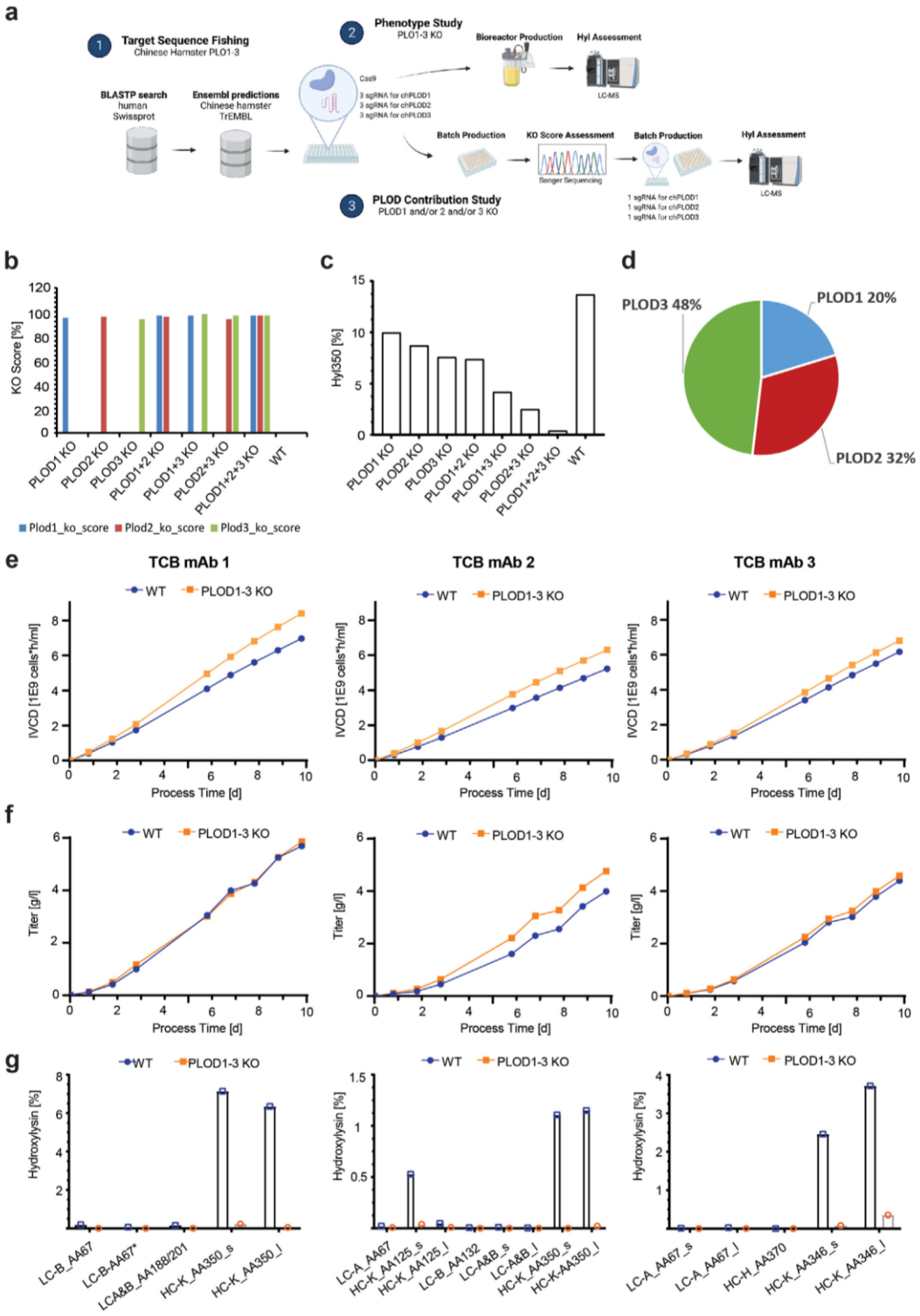

FIGURE 6
Synergistically gene knockout of Chinese hamster PLOD1, PLOD2, and PLOD3 eliminates Hyl modifications in TCB mAbs. **(A)** Schematic representation of Chinese hamster PLOD sequence fishing and knockout studies. 1) Chinese hamster PLOD gene product orthologs were extracted and predicted by BlastP and Ensembl. sgRNAs were designed for PLOD1, PLOD2, and PLOD3 and used in a subsequent bioreactor "phenotype study" 2), where all chPLODs are deleted using three guide RNAs per *PLOD* gene, and a "PLOD contribution study" and 3), where the most efficient guide RNAs per *PLOD* gene were used. **(B)** The KO score for the most efficient guide RNA per *PLOD* gene used in the "PLOD contribution study" on Hyl modification levels in TCB mAbs. **(C)** Hyl350 levels after CRISPR KO of various combinations of PLOD1–3 in a 4-day batch process using TCB mAb 1-expressing CHO production cell line. **(D)** Contribution of single PLOD on Hyl350 modification based on multi-regression model with "PLOD contribution study" results (see Supplementary Tables for multi regression model results). **(E)** Influence of PLOD1–3 KO on cells in a "phenotype study" during a 10-day fed-batch bioreactor cultivation with TCB mAb 3-expressing CHO production cell line on the integral of viable cell density (IVCD), **(F)** volumetric productivity, and **(G)** hydroxylysine levels across all identified hydroxylysine motives.

observed in the material from PLOD1–3 KO cell lines compared to wild-type CHO cells (Supplementary Figures S10A).

Modulation of 5R-Hyl formation in TCB mAbs is dynamic and dependent on iron availability in CHO cell cultures

Upon examining the Hyl levels of TCB mAb 1 over the process duration, we observed a trend of decreasing Hyl level in the produced TCB mAb, particularly at the prominent K350 residue located in the intersecting C_H1–VL domain during the later process phases, beginning from day 6 and continued until harvest on day 10 (Figure 7A). The process productivity at various timepoints was determined by calculating the daily formation of new products, which contributed to the cumulative final product concentration at the time of harvest. A consistent augmentation in the levels of newly formed product was observed until the initiation of the shift phase on day 6, followed by a subsequent decline (Figure 7B). Intriguingly, through the simulation of the time-resolved levels of the newly modified Hyl350 peptide between the sampling days using a sigmoid interpolation function (Figure 7C), we discerned a specific temporal decrease in the levels at the day corresponding to the onset of the global Hyl350 shift on day 6, followed by subsequent growth again (Figure 7B).

As identified in the tested knockout panel, we confirmed that the Hyl modification of TCB mAbs originates from enzymatic PLOD activity. Given that PLODs necessitate Fe^{2+} ions as a cofactor for catalytic activity (Figure 7D), we sought to analyze the available cell culture iron level during the process duration. We observed a clear decrease over time, which became more pronounced when examining the iron availability per cell, where iron levels stagnated at a low level from day 6 onward (Figures 7E, F). This low iron level was also accompanied by a very low steady-state level of cell-specific iron consumption rate qS_{Iron} from day 6 until the end of the process on day 10 (Figure 7G). Both reduced iron availability and lower cellular iron uptake occur contemporaneously with the shift phase of decreased Hyl350 formation.

In a subsequent experiment, we investigated whether the initial levels of iron in the cell culture media influenced the Hyl modification of TCB mAb motifs. For this, the TCB mAb 1-expressing CHO cell line was cultivated with ferrous ion levels ranging from 0 to 200 µM, and samples of the produced product were subsequently analyzed for Hyl350 abundance. The analysis of the Hyl modification levels of the hot spot motif K350 and the less abundant K67 location, situated near the CDR region of the N-terminal Fab domain, revealed a dose-dependent increase in Hyl modification, reaching saturation with 80 µM iron in the culture (Figures 7H, I). The low level of Hyl modification at 0 µM iron supplementation is likely induced by the residual iron transferred from the precursor culture, which is used to inoculate the experiment. This experiment suggests that levels below 40 µM iron are a rate-limiting factor for Hyl modification in CHO cultures producing TCB mAbs. Furthermore, our objective was to evaluate the concentration of ferrous ions required to achieve the half-maximal effect, as reflected by the observed normalized levels of Hyl350 and Hyl67 in the CHO cell culture experiment. The fitting models suggest that concentrations less than 10 µM Fe^{2+} are already adequate to cause the half-maximum activation of the hydroxylation reactions in the employed CHO cell culture system (Figure 7J).

More in-depth analyses were conducted to examine the iron dependency related to TCB mAbs and different lysine-hydroxylated peptides at iron concentrations below 60 µM. To this end, three distinct CHO cell lines, each expressing one of three different TCB mAbs (TCB mAb 1, TCB mAb 2, or TCB mAb 3), were cultured within a cell culture model representative of production conditions, with Fe^{2+} ion concentrations varying from 0 to 60 µM. For each TCB mAb, three peptides were investigated, encompassing the hydroxylation-sensitive residues K67, K125/121, and K350/K346. The observed levels of hydroxylation were normalized, and the data from the Fe^{2+} ion titration were modeled using a non-linear least squares fitting approach. The half-maximum effective concentration (EC50) for all three TCB mAbs and peptides was determined to be less than 10 µM with a 95% confidence interval (Figures 7K–M). Notably, the hydroxylation of the light-chain residue K67, a motif newly characterized for lysine hydroxylation in this study, exhibited a general trend for a slightly increased requirement for Fe^{2+} ions for hydroxylation, as evidenced by a higher EC50 value. This suggests that a higher concentration of iron is requisite to attain an equivalent level of hydroxylation.

Discussion

Lysine is one of the most chemically reactive amino acids in biology, and specialized cellular enzymes ensure spatial and temporal regulation of lysine modifications (Abbasov et al., 2021). Lysine hydroxylation is a well-known molecular modification of endogenous proteins, which is often needed for essential downstream regulatory events and structural organizations (Markolovic et al., 2018; Zurlo et al., 2016; Cockman et al., 2022). However, several therapeutic proteins reported in the past contain hydroxylysine instead of lysine in their structure (Molony et al., 1995; Aguilar et al., 2005; Andrews et al., 1984; Xie et al., 2016). In this study, we report for the first time that Chinese hamster PLODs are responsible for 5R-Hyl modification of TCB mAbs produced by CHO production cell lines. For the identification of PLODs as Hyl-forming enzymes in TCB mAbs, a combination of mass spectrometry peptide map analysis and CRISPR/Cas9 KO approach was applied.

The Hyl modification was dominantly located at the C-terminal K350 of the LTVLSSASTK peptide, which is located within the unstructured, crossed C_H1–VL interface of the heavy knob chain. It was found to a much lesser content at K125 in a similar peptide, LTVLSSASTK, which is located in the N-terminal Fab domain. The hot spot position is similar, but not identical, to the upstream sequence and structural vicinity of the previously described HC101–HC124 motif (XXXXXXXXXWGQGTLVTVSSASTK) (Aguilar et al., 2005) identified in generic IgGs. The reason for the differences observed in TCB mAbs may originate from a unique crossed C_H1–VL interface that allows for efficient pairing of the intended light chains, which differ for the two identical N-terminal binders and the intra-chain Fab binder (Figure 1A). The structural analysis of the crossed Fab domain revealed favorable accessibility of PLOD enzymes at the K350 position compared to the generic Fab domain in IgGs. These results suggest potential

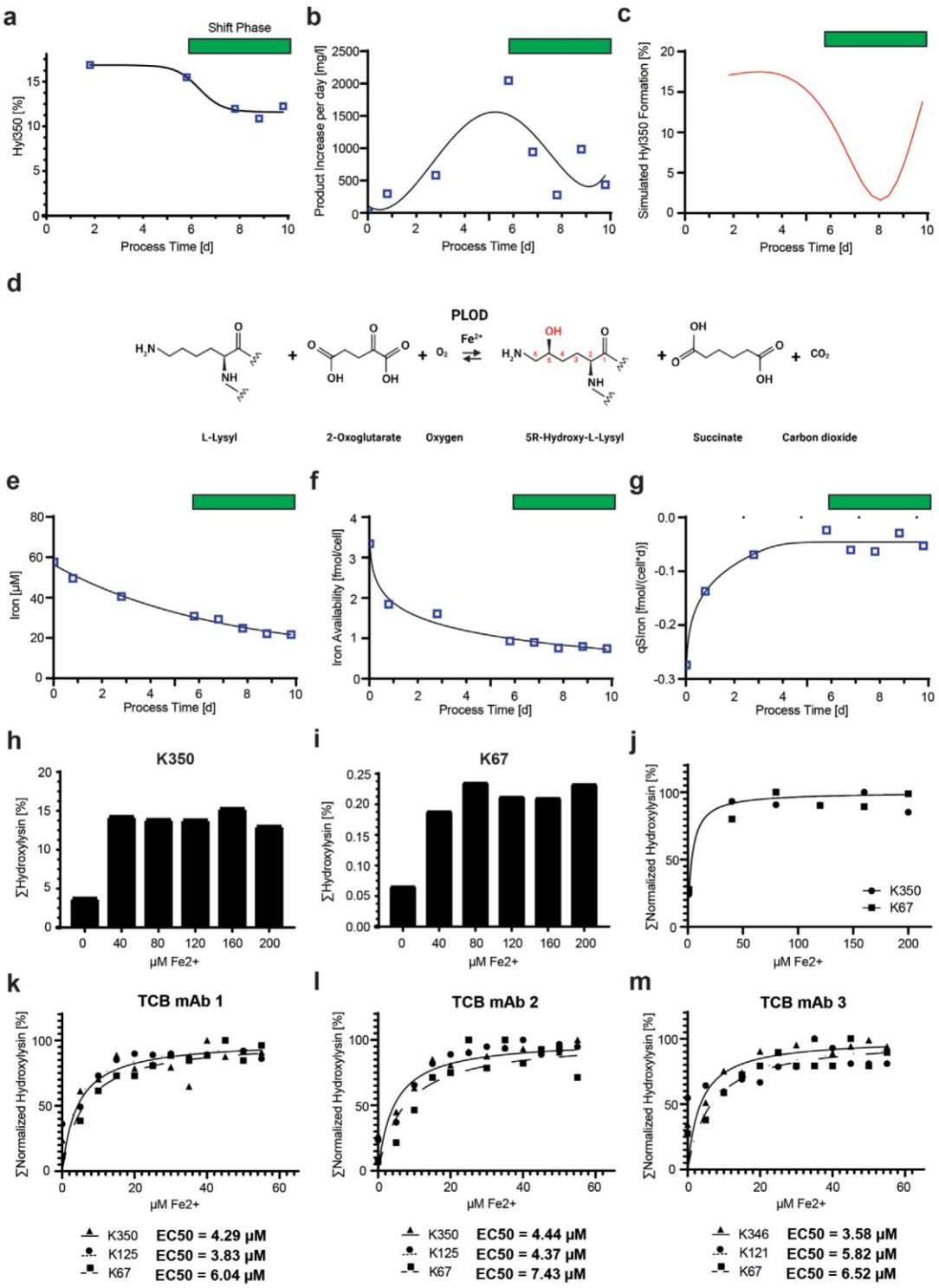

FIGURE 7
Variability of Hyl modification during cell culture is dependent on iron availability. **(A)** Time course of Hyl350 levels of TCB mAb 1 during a representative fed-batch fermentation process show a decrease in the late process phase. The green bar represents the period of time where the Hyl modification level shifted. **(B)** Kinetic of the delta TCB mAb 1 product increase per day during the fermentation cultivation peaks in the middle of the process. **(C)** Simulated kinetic of %Hyl350 levels newly produced to describe the observed kinetic of product Hyl30 modification in **(A)**. **(D)** Mechanistic description of the enzymatic reactions of PLODs. In proteins, an L-lysyl residue, predominantly located in a Xaa-Lys-Gly consensus sequence, is recognized by the PLOD enzymes and hydroxylated using 2-oxoglutarate and oxygen and the cofactor Fe^{2+} to a 5R-hydroxy-L-lysyl residue, succinate, and carbon dioxide. **(E)** Free iron (Fe^{2+}) concentrations measured in the cell-free cell culture supernatant during the fed batch cultivation process. The iron cell density concentrations at a specific process timepoint were used to calculate the iron availability per cell **(F)** and the cell-specific iron uptake rate **(G)**. Both indicate stagnation in trends in the late process phase and suggest a switch in iron metabolism, which is not observed in global iron concentration measurements. Analysis of iron concentration effect on TCB mAb 1 hydroxylation for K350 hot spot motif **(H)** and the lower abundant
(*Continued*)

FIGURE 7 (Continued)
K67 motif **(I)**. The iron ion activity response curve for Hyl modification stimulation was created by fitting the normalized K350 and K67 hydroxylation levels for the tested iron concentrations using a representative cultivation model **(J)**. Iron ion levels ranging from 0 to 60 μM were tested for all three TCB mAbs in representative cell culture models, and activity response curves for Hyl modification were fitted for three different Hyl-containing peptides using normalized cumulative Hyl levels for each peptide **(K–M)**. EC50 values needed for half-maximum Hyl modification for each peptide were calculated using non-linear least squares fits.

opportunities for further sequence optimization around the LTVLSSASTK350 neighborhood to reduce the observed flexibility as an alternative approach to PLOD enzyme depletion in order to avoid Hyl formation. Interestingly, different PLOD enzymes seem to target favored structural characteristics although the modifying consensus sequence XKG is the same. In procollagens, for example, PLOD2 hydroxylates lysine residues in the telopeptide, and PLOD1 targets lysine residues in the central or α-helical domain (Gilkes et al., 2013a). In contrast, the substrate specificity and favored target motif characteristics for PLOD3 are still unidentified (van der Slot et al., 2003; Takaluoma et al., 2007). Our current example of hot spot-specific Hyl formation in TCB mAbs with multiple XKG motifs supportively suggests that higher-order structural characteristics are important for enzyme target recognition rather than simplified, short consensus sequence definitions.

The modification of lysine residues by 2OG-dependent PLOD hydroxylases is attributed to an XKG consensus sequence (Yamauchi and Sricholpech, 2012). As previously reported by Xie et al. (2016), the generic IgG sequence comprises multiple alternative XKG motifs where a Hyl modification was not detected (Aguilar et al., 2005). TCB mAbs share this characteristic of multiple XKG motifs within their molecule framework; yet small but significant levels of Hyl were detected at alternative XKG sites in the present study. In addition, we detected Hyl at so far unknown XKA and XKS motifs in antibodies. Both motifs are recognized in collagen (Yamauchi and Sricholpech, 2012), suggesting a certain level of flexibility in consensus sequence acceptance of PLOD enzymes in cellular production systems.

The presence of the Hyl moiety in a peptide can abolish tryptic digestion (Markolovic et al., 2018). In contrast to the previous reports by Xie et al. (2016) and Aguilar et al. (2005), the peptide mapping analyses on TCB mAbs showed a clear effect of Hyl on digestion efficiency (Table 2). Approximately half of the prominent, high-abundant peptides with Hyl modification showed a tryptic miscleavage event. Although cleavage levels may be optimized by the applied trypsin activity using higher quantities and/or improved reaction conditions, biological effects, such as Hyl modification influence on trypsin digestion efficiency, may be overlooked via LC–MS. In general, the reason for the additional Hyl spot observations compared to the report by Xie et al. (2016) can be diverse and may be due to a different analytical setup and available detection sensitivity, as well as differences in the structure of the analyzed molecule.

Comparable to humans, we showed for the first time that Chinese hamster ovary cells express all PLOD major isoforms, PLOD1, PLOD2, and PLOD3. The enzyme orthologs are highly conserved between species and own the respective substrate and cofactor-binding sites needed for enzymatic activity. Using a combinatorial CRISPR KO and factor modeling approach, the relevance of different PLOD isoenzymes for TCB mAb lysine hydroxylation was analyzed. Therefore, a dominant role for PLOD3 could be identified, explaining almost half of the observed K350 hydroxylation of the hotspot motif. The reason for the dominant relevance of PLOD3 may be triggered by the PLOD's unique feature of multiple cellular localization characteristics in the ER and the extracellular environment, where PLOD3 is an important factor in facilitating ECM remodeling (Salo et al., 2006). In our study, we did not analyze the contribution of conditioned cell culture media on TCB mAb Hyl formation by secreted hydroxylases, such as PLOD3, by inhibiting extracellular activity or supplementation with recombinant active enzymes. Consequently, we cannot rule out that the Hyl modification of TCB mAbs in CHO cell cultures also happened as a post-secretion process. Further studies have to be conducted to elucidate this option in CHO cell cultures in detail.

In general, PLODs have been described to play a key role in fibrotic diseases and cancer progression (van der Slot et al., 2003; Mia and Bank, 2015). However, several recent studies on PLODs in cancer suggest that PLOD3 plays an important role in a variety of cancer types, such as in lung and gastric cancer, glioma, and sarcoma (Baek et al., 2018; Deng et al., 2021; Gong et al., 2022). For example, in a most recent study on ovarian cancer, specifically higher PLOD3 expression has been associated with poor prognosis (Li et al., 2020) although all PLOD enzymes are overexpressed in ovarian cancer tissue and cell lines (Guo et al., 2021). Using an RNAi approach, PLOD3 was attributed to specifically regulate gap junction's functionality by connexin 43 gene expression. Therefore, the authors concluded that the different PLOD isoenzymes possess non-overlapping functionality in ovarian cancer with unexpected impact on gene regulation networks in addition to their direct enzymatic roles in hydroxylation and glycosylation of target proteins (Guo et al., 2021).

In comparison to the distinct roles of PLODs in cancer, our data showed that all three PLOD enzymes must be depleted from the cellular system to quantitatively avoid lysine hydroxylation for TCB mAbs, as suggested by the "PLOD contribution" study on TCB mAb 1 (Figures 6C, D). Interestingly, no unintended cell culture performance decrease was detected by a concomitant loss of all Chinese hamster PLOD isoenzymes, chPLOD1, chPLOD2, and chPLOD3, using a triple knockout CRISPR/Cas9 approach. In contrast, the three different production cell lines modified by PLOD1–3 KO showed a significantly increased cell growth performance as well as a minor but obvious improvement in final product concentration and intended main product levels. These results were not expected, especially not for observed larger biomass formation since PLODs have been attributed to cancer progression, metastasis, and cancer cell proliferation (Baek et al., 2018; Song et al., 2017). For example, decreasing PLOD1 expression impairs the proliferation and colony-

TABLE 3 Lysine hydroxylase enzymes.

Enzyme *Splice variant*	EC numbering	Lysine modification	Domain	Enzymatic activity	Cofactor	Consensus sequence	Organization	Localization	Interaction partners (Heard et al., 2016; Scietti et al., 2018; Duran et al., 2017; Gjaltema et al., 2016; and Liefhebber et al., 2010)
PLOD1	1.14.11.4	(5R)-5-hydroxy-L-lysine	GT_LH P4Hc	Lysyl hydroxylase (LH) (N-terminal)	Fe^{2-} and ascorbate	-Xaa-Lys-Gly-	Homodimer[a]	rER	SC65, P3H3, P3H4[b], and CYPB
PLOD2 2a/b	1.14.11.4	(5R)-5-hydroxy-L-lysine	GT_LH P4Hc	Lysyl hydroxylase (LH)	Fe^{2-} and ascorbate	-Xaa-Lys-Gly-	Homodimer	rER ECM	HSP47, FKBP65, and BiP
PLOD3	1.14.11.4 2.4.1.50	(5R)-5-hydroxy-L-lysine	GT_LH Glyco_tranf_2_3 P4Hc	Lysyl hydroxylase (LH) Galactosyltransferase (GT)	Fe^{2-} and ascorbate Mn^{2+}	-Xaa-Lys-Gly- -Xaa-Hyl-Gly-	Homodimer	rER ECM	GLT25D1/2
JMJD4 2 splice variants	1.14.11.-	(4RS)-5-hydroxy-L-lysine	JmjC	Lysyl hydroxylase (LH)	Fe^{2-}	Not known	Homodimer	Cytoplasm	DRG1 and DRG2
JMJD6	1.14.11.4	(5S)-5-hydroxy-L-lysine	JmjC	Lysyl hydroxylase (LH)	Fe^{2-}	Not known	Homo oligomerizes	Cytoplasm Nucleus Nucleolus	LUC7L2, LUC7L3, U2AF2/U2AF65, CDK9, CCNT1, and BRD4
JMJD7	1.14.11.63	(3S)-5-hydroxy-L-lysine	JmjC NLS	Lysyl hydroxylase (LH)	Fe^{2-}	Not known	Homo oligomerizes	Cytoplasm Nucleus	LUC7L2, LUC7L3, U2AF2/U2AF65, CDK9, CCNT1, and BRD4

[a]By similarity; P4Hc, prolyl 4-hydroxylase alpha subunit homologs; GT_LH, catalytic glycosyltransferase (GT) domain found in the lysyl hydroxylase (LH) family–including UDP and Mn binding sites; Glyco_tranf_2_3, glycosyltransferase-like family 2; JMJD, Jumonji domain-containing protein.

[b]NLS, nuclear localization signal motifs. Interaction partners are extracted from the literature and UniProt database (https://www.uniprot.org/).

10.3389/fbioe.2024.1414408

formation capacity of A549 lung cancer cells by the activation of E2F transcription factor 1 (E2F1) (Li et al., 2021). Although immortalized CHO cells also share common hallmarks of cancer cells [see review by Wurm and Wurm (2021)], the biological relevance of PLODs may be different from reported cancer cell observations due to extensive evolution as highly adopted production cell lines for growing in suspension cultures (Wurm, 2004). Our study cannot exclude the unlikely event that the observed differences in cell culture performance between wild-type and PLOD1–3 knockout cell lines may, in addition, be influenced by indirect effects. PLOD enzymes are known to interact with various factors, leading to multifunctional biological effects, as provided in Table 3. Past research has identified distinct interaction partners for PLOD1, PLOD2, and PLOD3, suggesting that they have unique biological roles (Heard et al., 2016; Scietti et al., 2018; Duran et al., 2017; Gjaltema et al., 2016; Liefhebber et al., 2010). However, the regulatory networks involving PLOD enzymes are not fully understood, particularly in the context of cellular biologics production systems like CHO cells. For the analysis of regulatory mechanisms that differentially influence recombinant protein expression in wild-type and PLOD knockout CHO cells, further comprehensive comparative studies on the system level are needed. These studies should include transcriptomic, proteomic, and metabolomic profiling to provide a holistic understanding of cellular changes and their impact on biological production.

Mammalian cells harbor two primary classes of 2OG-dependent lysyl hydroxylases: PLODs and JMJDs. These mammalian lysyl hydroxylases exhibit differences in their cellular localization, chiral activity, and the formation of structurally distinct enantiomer Hyl products, specifically 5R-Hyl (catalyzed by PLODs), 5S-Hyl (catalyzed by JMJD6), 4RS-Hyl (catalyzed by JMJD4), or 3S-Hyl (catalyzed by JMJD7). Despite the fact that these hydroxylases have been reported to localize in different compartments, the possibility of unexpected dysregulated intracellular trafficking (Targa et al., 2023), enzyme mislocalization (Wang and Li, 2014), and/or enzyme shedding from disrupted cells (Koterba et al., 2012) contributing to or causing the observed Hyl modification in TCB mAbs cannot be excluded. Our initial CRISPR/Cas9 screen strongly suggested that PLODs, not JMJD lysine hydroxylases, are responsible for TCB mAb modification. Although knockout screens using CRISPR/Cas9 are an established methodology for identifying enzymatic factors relevant to a specific phenotype, the effect can also be indirect, as the deleted target gene product can act upstream of the actual modifier (Bock et al., 2022). Orthogonal methods such as gene overexpression (Bauer et al., 2022) or analytical approaches (Markolovic et al., 2018) are essential tools to validate the genes identified by CRISPR/KO screens. Given that JMJDs generate Hyl enantiomers, identifying the respective Hyl enantiomer would further substantiate that a specific hydroxylase class is responsible for the observed Hyl modification in CHO-produced TCB mAbs. For this approach, Hyl-containing TCB mAb 3 would need to be digested by trypsin, and a tracer peptide like LTVLSSASTK/Hyl would need to be selectively collected. Subsequent digestion of the isolated peptide with carboxypeptidase Y and derivatization of the isolated amino acids by 6-aminoquinolyl-N-hydroxysuccinimidyl carbamate (AQC) would allow for chiral characterization of the respective Hyl stereoisometry and variant (Markolovic et al., 2018). Utilizing this methodology, the approximate +16 Da modification at the identified lysine residues in CHO-produced TCB mAbs could be definitively characterized as 5R-Hyl (Supplementary Figure S5). This strongly substantiates that PLODs, rather than any other 2OG-dependent lysyl hydroxylase, are accountable for the observed hydroxylation of lysine residues.

Process-induced variability of Hyl modification

All three analyzed TCB mAbs in this study exhibited Hyl modification at different levels, especially at the hot spot motif LTVLSSASTK350. Interestingly, the levels were different although the production cell cultivation process was apparently similar for all three TCB mAbs. Furthermore, the rate of Hyl modification at the K350 residue for TCB mAbs diminishes over the duration of the cell culture process, as exemplified by TCB mAb 3.

Most therapeutic proteins, such as TCB mAbs and generic IgGs, use dynamic cell cultivation processes and high-performance CHO production cell lines [see review by Kim et al. (2012)]. Although these CHO production cell lines originate from the same CHO ancestor cell line and related CHO host cell sublineages, each final production clone demonstrates a more or less unique metabolic profile (Popp et al., 2016). As a consequence, the availability of specific substrates and cofactors needed for biocatalytic processes is tightly linked to cell-specific consumption rates of small molecules present in cell culture. In the conducted research, we demonstrated that iron, acting as a cofactor for enzymatic hydroxylation activity in PLODs, was empirically validated to modulate the formation level of Hyl in TCB mAbs produced by CHO cells *in vitro*. Our study observed a dynamic alteration in the per-cell iron availability and consumption rate, which diminished during the later stages of the cell cultivation process. This fluctuating iron availability for cells could be attributed to various factors, such as different cell culture process phases, variations in cell culture media compound concentrations, impurities from other media and process components, and/or the overall cellular iron metabolism. The observed reduction in cofactor bioavailability further substantiates this hypothesis. Similar to iron, the availability of other requisite factors in cell culture for PLOD activity, such as 2OG, may also have a significant influence. Additional investigations are imperative to decode the presence and temporal regulation of 2OG in CHO cell culture processes.

The transcriptomic analysis of Chinese hamster PLOD1, PLOD2, and PLOD3 unveiled a significant disparity in expression levels among PLOD isoenzymes, with the hierarchy being PLOD1 and PLOD3 surpassing PLOD2 (Figures 4E–G). Fluctuations in PLOD transcript expression levels, originated by external triggers, have also been documented in other cellular models and primary tissues, suggesting varying biological roles and importance (Qi et al., 2021). In addition, transcript expression levels vary among different monoclonal CHO clones, despite all expressing the identical TCB mAb molecule. This suggests that the translation of transcript levels into enzymatic activity may explain the observed variations in Hyl modification across TCB mAb 1, TCB mAb 2, and TCB mAb 3. The observed variation could potentially be amplified as the expressions of the

PLOD1 and *PLOD2* genes have been demonstrated to be regulated by hypoxic conditions (Gilkes et al., 2013a; Gilkes et al., 2013b; Wang et al., 2021). Hypoxic scenarios can occur in bioprocesses due to transitions into different scales and alterations in system aeration configurations (Fu et al., 2014).

The application of various production process variants, which include different media and feeding strategies, and/or physicochemical parameters such as cell culture pH and temperature set points, has been documented to influence the quality of the therapeutic product molecule (Ehret et al., 2019; Lee et al., 2021; Reinhart et al., 2015). Specifically, the use of an optimized pH and temperature process regime leads to a reduction in the level of a therapeutic interleukin-2 variant (IL2v) cytokine–mAb fusion protein (Schneider et al., 2019). In our study, we evaluated the effects of using different production processes and cell lines on the production of TCB mAb 2. We found that both the production processes and the cell lines may influence the regulation of PLOD transcript levels. Intriguingly, the variation in transcript levels appears to be cell line-dependent, underscoring the significance of representative cell line screening procedures and appropriate readouts. This is particularly critical in the context of product quality evaluation, which should also encompass early, comprehensive, and extended characterization studies utilizing mass spectrometry. In addition, the analysis of ectopic product transcript expression is also recommended since it aids in predicting the performance of cell line production (Dorai et al., 2006; Bhoskar et al., 2013). Beyond productivity prediction, the expression of the heavy-chain (HC) knob gene transcript, encompassing the hotspot motif LTVLSSASTK350, was observed to increase in a pattern similar to the *PLOD1* gene transcript in our investigation.

Consequence of Hyl modification for biotherapeutic TCB mAbs

Therapeutic pharmaceuticals often display microheterogeneity, which necessitates an in-depth characterization to determine their impact on drug efficacy and safety and the establishment of analytical control strategies to maintain consistent product quality (Scietti et al., 2018). The examination of Hyl modification sites and levels calls for intricate and time-consuming mass spectrometric methodologies. Multiple Hyl modifications were identified in TCB mAbs in this study, but apart from the hot spot motif LTVLSSASTK350, the levels in other motifs are remarkably low, less than 1%. Given the extremely low levels, especially in the CDRs, the probability that Hyl modifications in TCB mAbs affect binding efficacy to intended targets or functionality is quite low; yet, additional investigations need to be undertaken to substantiate this hypothesis. Since both clonal variations and process conditions can influence the level of Hyl modification, it is recommended to incorporate Hyl analysis early in the process to avoid selecting clones with significant Hyl modifications. Generally, Hyl modification is a common biological phenomenon, and unexpected reactions, such as immunogenicity, are not typically anticipated.

The hotspot motif LTVLSSASTK350 is situated within the chimeric C_H1–VL domain. Structural analysis conducted in our study indicated a conformational divergence in the elbow segment and the neighboring loop when compared to the generic IgG Fab domain, as found in the N-terminal binders. Beyond the conventional methodologies for the capture and purification of mAbs that target the Fc region using agents like protein A, (Hober et al., 2007), there are alternative binders that target the C_H1 domain (Nesspor et al., 2020). These commercially available C_H1 binders can be utilized for affinity capture in both analytical and preparative chromatography. There is a potential risk that Hyl modification of the exposed C_H1 binding site could influence this binding although its overall contribution might be limited, considering that TCB mAbs contain one chimeric C_H1-VL cross-Fab segment and two generic C_H1 domains.

The analysis of PLOD1–3 KO cell lines expressing TCB mAb 1 revealed a diminished peak of a specific acidic molecular charge species compared to wild-type CHO cells. Hydroxylysine exhibits distinct dissociation constants relative to lysine (Klemperer et al., 1942). Klemperer et al. (1942) suggested that the presence of a hydroxyl group in hydroxylysine reduces its basicity compared to lysine, which could partly explain the observed decrease in acidic species in a material containing >12% hydroxylysine versus less than 1% in TCB mAb 1 (Supplementary Figures S10B, C). However, the unlikely case that additional minor other differences in the product quality profile may contribute to the observed differences in the charge pattern, or if both effects act synergistically to modulate the molecular charge pattern, yet in a small amount, cannot be excluded.

The crosslinking and stabilization of collagen fibrils in the extracellular space have been shown to be influenced by both enzymatic and non-enzymatic processes. Enzymatic processes are mediated by PLODs and lysyl oxidases, which trigger lysine modifications, whereas non-enzymatic processes are facilitated by advanced glycation end products (AGEs) and riboflavin/UV-mediated reactions (Gelse et al., 2003; McKay et al., 2019). PLOD3 is of particular importance due to its additional glycotransferase activity, which produces specific glucosyl-galactosyl-hydroxylysine (Glc-Gal-Hyl) AGE modifications necessary for the non-enzymatic crosslinking of collagen fibrils. Despite not detecting any further AGEs in the respective Hyl-modified motifs in our studies, we cannot rule out the possibility that minor amounts of the intended TCB mAb may be modified. This could lead to the product being cross-linked by a process originating from Hyl, as indicated by the observed increase in TCB mAb monomer content and decreasing trends in high molecular weight (HMW) fractions. Moreover, forced stability testing of TCB mAb 1 and TCB mAb 2 in phosphate-buffered saline (PBS) at 40°C for 4 weeks revealed a minor increase in HMW species although the overall Hyl content remained constant (Supplementary Figure S1). This suggests that non-enzymatic product crosslinking, potentially originating from micro heterogeneities such as hydroxylation modifications, could occur. These observations warrant further investigation in subsequent studies.

Conclusion

In this study, we document for the first time the occurrence of Hyl modification in TCB mAbs produced by Chinese hamster ovary (CHO) production cell lines. The modification transpires at several XKG positions and, to a lesser extent, in alternative positions, underscoring the importance of comprehensive mass spectrometric characterization efforts to identify post-translational microheterogeneities. The

prominent Hyl350 modification is situated in the artificial C_H1–VL cross Fab interface. The crossing of the chains induces an altered structural situation and a more flexible, exposed hot spot motif LTVLSSASTK350 compared to generic C_H1–VH interfaces in IgG Fab domains. This may account for the increased Hyl modification compared to the generic LTVLSSASTK125 motif. Chinese hamster PLOD enzymes are forcefully suggested as mediators of the Hyl modification in TCB mAbs. A synergistic knockout of all three isoenzymes, PLOD1, PLOD2, and PLOD3, is necessary to prevent Hyl formation in TCB mAbs compared to single knockouts. Interestingly, the cell culture and productivity performance remain unaffected or even improved compared to the WT control. Overall, Hyl modification does not induce functional or safety issues and has been classified as a monitoring post-translational modification. Further research is required to definitively understand the role of PLOD enzymes in influencing other quality attributes besides lysine hydroxylation of TCB mAbs. Acquiring knowledge on the role of PLOD enzymes may contribute to enhancing the robustness and consistency of biologics production processes through the development and integration of targeted control strategies.

We propose an approach to circumvent Hyl modification in TCB mAbs by eliminating the respective enzymatic factors and/or activity through alternative strategies. This strategy can likely be applied to other products produced by CHO cell lines to avoid labor-intensive characterization activities in the development of protein-based therapeutics.

Materials and methods

Cell culture

All cell lines were created using a previously generated CHO host cell line (International patent publication number WO 2019/126634 A2). CHO cells were cultured in a chemically, protein-free medium in 125–500 mL shake flask vessels at 150 rpm, 37°C, 80% rH, and 5% CO_2. Cells were passaged at a seeding density of 3–6 × 10^5 cells/mL every 3–4 days. Pools of cells that stably express TCB mAb molecules were generated as described by Carver et al. (2020). In brief, expression plasmids were transfected into CHO cells via MaxCyte STx electroporation (MaxCyte Inc., Rockville, Maryland, United States). Transfected cells were then selected, and the expression of TCB mAb was confirmed by flow cytometry via human IgG staining using a BD FACSCanto II Flow Cytometer (BD, Eysins, Switzerland). CHO clones were selected after single-cell cloning by limited dilution, titer and binder validation by ELISA, and the evaluation of cell growth and productivity performance in fed-batch production assays using Ambr 250 bioreactors (Sartorius AG, Göttingen, Germany).

Fed-batch production assay

Fed-batch production cultures were performed in 24-deep well plates, shake flasks, or Ambr 250 bioreactors (Sartorius AG, Göttingen, Germany) using proprietary chemically defined production media. Cells were seeded as indicated between 2 and 15 × 10^6 cells/mL on day 0 of the production stage after adaptation to production media during two passages. Cultures received daily proprietary feed medium after day 3 and additional feed bolus on days 3 and 7, with an optional bolus on day 10. Cells were cultivated for 14 days. Production in the Ambr 250 system was operated at set points of 35°C, DO 30%, pH 7.0, and an agitation rate of 1,300 rpm, with a shift to 1,600 rpm on day 3.5.

Off-line sample analysis

Process parameters were analyzed using Osmomat Auto (Gonotec GmbH, Berlin, Germany) for the measurement of osmolality and a Cedex Bio HT Analyzer (Roche Diagnostics GmbH, Mannheim, Germany) for the measurement of product and selected metabolite concentrations, including iron. Total cell count, viable cell concentration, and average cell diameter were measured using the Cedex HiRes Analyzer (Roche Diagnostics GmbH, Mannheim, Germany). Integrated viable cell density (IVCD) and specific productivity rates for each condition are calculated as indicated in Equation 1 and Equations 2–4, respectively

$$IVCD_n = IVCD_{n-1} + \frac{VCD_n + VCD_{n-1}}{2} * (t_n - t_{n-1}). \quad (1)$$

The cell-specific productivity qP and iron consumption rate qS_{Iron} are calculated as follows:

$$(dS \text{ or } dP)/dt = (qS \text{ or } qP) * X \quad (2)$$

$$qP = \frac{1}{X} * \frac{P_i - P_{i-1}}{t_i - t_{i-1}}, \quad (3)$$

$$qS_{Iron} = \frac{1}{X} * \frac{S_i - S_{i-1}}{t_i - t_{i-1}}. \quad (4)$$

Negative and positive values for qS and qP represent consumption and production of a compound, respectively.

Chinese hamster PLOD sequence database extraction

The ortholog PLOD protein sequences from Chinese hamsters were identified by BlastP searches of the human Swiss-Prot PLOD entries (PLOD1_HUMAN, PLOD2_HUMAN isoform1 "A" and 2 "B," and PLOD3_HUMAN) against UniProt and RefSeq. The identified PLOD entries reflect the top hits in TrEMBL for Chinese Hamster and are all based on predictions from Ensembl (PLOD1: A0A8C2QN41, PLOD2A: A0A8C2MXC8, and PLOD2B: A0A8C2N5H0, PLOD3: manually assembled based on A0A8C2MCH2 and A0A3L7HLU9). All these hits are confirmed by RefSeq (except PLOD3 AAs #1-41, which is solely based on TrEMBL).

Analysis of PLOD transcript expression levels in CHO cells by RNAseq

The library prep needed for RNAseq sample measurements was done using a proprietary rRNA depletion protocol. RNA sequencing was performed on a NovaSeq 6000 System (Illumina Inc.) using read mode SE100 for TCB mAb 3 and PE100 for TCB mAb 1 and TCB mAb 2.

For RNAseq data preprocessing, the quality of the raw FASTQ files was evaluated using FastQC software (version 0.11.9). For the adapter's removal (ILLUMINACLIP: TruSeq3-PE.fa:2:30:10), Trimmomatic software (version 0.39) was used. Sequences for the transgene and the reference genome were mapped and further analyzed separately. Reads were aligned to the CDS sequences of *PLOD1*, *PLOD2*, and *PLOD3* genes using HISAT2 software (version 2.2.1). Feature quantification was performed using HTSeq (version 0.13.5). The final reads were normalized to the library size and library composition using edgeR's (version 3.38) (Robinson et al., 2010) trimmed mean of M-value method (TMM).

Structural modeling analysis

A homology model of the cross Fab was constructed utilizing MoFvAb/IgNORANT, with the incorporation of Hyl achieved through MOE 2022. Structures were protonated at pH 7.4, and energy was minimized using MOE 2022. The trastuzumab Fab domain (PDB code 1n8z) served as a representative example of a generic IgG Fab.

For the evaluation of physicochemical parameters, such as hydrophobicity and the presence of positively or negatively charged patches, both the non-modified and Hyl-modified SSASTK360 motifs of C_H1–VL were analyzed using MOE 2022.

Surface conservation analysis was conducted for PLODs, as revealed by structure conservation analysis. This involved homology model building of PLOD1, PLOD2a, and PLOD2b using AlphaFold 2, according to Jumper et al. (2021), onto the PLOD3 structure (PDB code 6fxt).

Generation of pooled single-gene KOs and KO confirmation

Targets were rationally chosen, and guides were designed using Geneious Prime software (version 2020.2.4., off-target library: CHO Reference Genome GCA_003668045.1_CriGri-PICR_genomic). All sgRNA sequences and verification primers are listed in Supplementary Table S1. For knockout (KO) introduction, three recombinant CHO production clones producing TCB mAb 1, 2, and 3 were transfected using ribonucleoprotein complexes comprising gene-targeting sgRNA and Cas9 protein using the MaxCyte STx Electroporation System (MaxCyte, Inc.) or the Lonza 96-well Shuttle System (Lonza Group Ltd.). Guide RNA–Cas9 ribonucleoprotein (RNP) complexes were prepared by mixing 1–3 sgRNA (40 pmol per sgRNA) with an equimolar amount of Cas9 protein (TrueCut Cas9 Protein v2, Thermo Fisher Scientific Inc.), followed by incubation at room temperature (RT) for 20 min. Cells were washed in PBS (300g, 5 min) and resuspended in the respective electroporation buffer (SF Cell Line 4D-Nucleofector™ X Kit, Lonza Group Ltd. or MaxCyte EP buffer, MaxCyte Inc.).

Genomic DNA was extracted using QuickExtract™ DNA Extraction Solution (Lucigen) according to the manufacturer's instructions after cells had recovered from transfection (6–8 days post-transfection). PCR (98°C for 30 s; 35 times: 98°C for 5 s, 60°C for 20 s, 72°C for 90 s, and 72°C for 90 s) was performed with the Q5 Polymerase 2x Master Mix (New England Biolabs, Inc.). Amplicons were purified using the QIAquick® 96 PCR Purification Kit (QIAGEN). Sanger sequencing was performed by Microsynth AG (Balgach, Switzerland). The PCR products produced were analyzed via electrophoresis on 2% agarose.

KO scores were assessed by the offline version of ICE software for analyzing Sanger sequencing data (available at https://github.com/synthego-open/ice).

TCB mAb aggregate, fragment, and charge variant analytics

Supernatants were clarified (1,000 g, 30 min, 4°C centrifugation, and 1.2 µm filtration; AcroPrep 96-well Filter Plates, Pall Corporation). Chromatography of analytical protein A was performed via UHPLC with UV detection (Dionex UltiMate 3000 UHPLC fitted with POROS™ A 20 µm Column, Thermo Fisher Scientific Inc.).

Antibody integrity was analyzed after protein A affinity chromatography (PreDictor RoboColumn MabSelect SuRe, Cytiva) and normalization with protein quantitation using UV measurement (NanoQuant Infinite M200, Tecan). The percentage of correctly assembled antibodies (Main-Peak) was assessed by CE-SDS (HT Antibody Analysis 200 assay on the LabChip GXII system, PerkinElmer) under non-reducing conditions by relative quantification of the expected protein size to total protein content.

Size exclusion chromatography (SEC) for the determination of the aggregation and oligomeric state of recombinant immunoglobulins was performed via HPLC chromatography. In brief, protein A purified product was applied to a TSKgel QC-PAK GFC 300 Column (Tosoh Bioscience) or a Tosoh TSKgel UP-SW3000 Column in 250 mM of KCl and 200 mM of K_2HPO_4/KH_2PO_4 buffer (pH 6.2) on a Dionex UltiMate® HPLC System (Thermo Fischer Scientific, Waltham, Massachusetts, United States). The eluted antibody was quantified via UV absorbance and integration of peak areas. Bio-Rad's Gel Filtration Standard #151–1901 served as a gel filtration calibration standard.

Charge variants of TCB mAb 1 were analyzed via capillary isoelectric focusing (CIEF) according to the manufacturer's protocol (Bio-Techne, Minneapolis, MN, United States).

LC–MS peptide map procedure for Hyl analytic

Expressed and purified (ProtA) antibodies were denatured and reduced with 6 M of guanidine and 16 mM of DTT at pH 7 and 37°C for 1 h. The denatured reduced protein was then carboxymethylated using 73 mM of IAA-C12 (Fluka) and then buffer-exchanged on a NAP-5 column (GE Healthcare Life Sciences) into 50 mM TRIS and 2 mM $CaCl_2$ at a pH of 7.5 and digested by trypsin (Promega) at 37°C for 1 h. The digested samples were then analyzed via LC–MS/MS. Liquid chromatography was performed on a Waters ACQUITY UPLC (Waters) using a reversed-phase ACQUITY CSH C18 column, 1.7 µm, 130 A, 2.1 × 150 mm (Waters). The aqueous mobile phase (mobile phase A) contained 0.1% (v/v) formic acid (FA) in HPLC-grade water. The organic mobile phase (mobile phase B) contained 0.1% (v/v) FA in acetonitrile. The gradient that was utilized in this experiment used a two-step

linear gradient of 1%–30% of mobile phase B from 2 min to 33 min and to 60% until 42 min, followed by an increase to 90% between 42.5 and 44.5 min and a decrease back to 50% between 44.6 min and 50 min, followed by a re-equilibration at 1% eluent B from 50 min to 56 min. The column temperature was set to 65°C.

UPLC was coupled to an Orbitrap Fusion™ Mass Spectrometer (Thermo Scientific). MS1 spectra were acquired using the Orbitrap mass analyzer with a resolution of 120,000, while MS/MS data were acquired in the Orbitrap analyzer with a resolution of 50,000. The MS/MS event on the Orbitrap was repeated for the TopN precursor ions with a dynamic exclusion window of 4.5 s enabled. The resulting MS data were processed using Byos™ and Byonic™ software (Protein Metrics Inc.). Manual data interpretation was performed using Byologic™ software (Protein Metrics Inc.). The MS/MS Byos™ search settings include a precursor mass tolerance of 5 ppm and a fragment mass tolerance of 20 ppm. Enzyme specificity was set to fully specific, allowing for one missed cleavage. The quantification of relative Hyl ("Kox," lysine oxidized)-modified tryptic peptides, considering missed cleavage products (0 mc and 1 mc), compared to unmodified peptides ("K") was calculated as indicated in Equation 5:

$$rel.\,area\,Hyl\,modified = \frac{[area\,Kox\ (0\,mc) + area\,Kox\ (1\,mc)]}{[area\,K\ (0\,mc) + area\,K\ (1\,mc)] + [area\,Kox\ (0\,mc) + area\,Kox\ (1\,mc)]}. \quad (5)$$

Data availability statement

The original contributions presented in the study are included in the article/Supplementary Material, further inquiries can be directed to the corresponding author.

Ethics statement

Ethical approval was not required for the studies on animals in accordance with the local legislation and institutional requirements because only commercially available established cell lines were used.

Author contributions

NB: conceptualization, data curation, formal analysis, investigation, methodology, resources, visualization, writing–original draft, and writing–review and editing. MB: conceptualization, formal analysis, investigation, methodology, software, visualization, writing–original draft, and writing–review and editing. SP: data curation, formal analysis, investigation, methodology, visualization, and writing–review and editing. TL: data curation, formal analysis, investigation, and writing–review and editing. SK: conceptualization, data curation, formal analysis, investigation, methodology, software, visualization, and writing–review and editing. HK: data curation, formal analysis, investigation, methodology, software, visualization, and writing–review and editing. GG: formal analysis, investigation, methodology, software, visualization, and writing–review and editing. VL: conceptualization, formal analysis, investigation, methodology, and writing–review and editing. DG: conceptualization, formal analysis, methodology, and writing–review and editing. LH: conceptualization, methodology, and writing–review and editing. AV: conceptualization, funding acquisition, methodology, project administration, resources, supervision, and writing–review and editing. SA: conceptualization, funding acquisition, methodology, project administration, resources, supervision, and writing–review and editing. OP: conceptualization, data curation, formal analysis, funding acquisition, methodology, project administration, resources, supervision, visualization, writing–original draft, and writing–review and editing.

Funding

The author(s) declare that financial support was received for the research, authorship, and/or publication of this article. The authors declare that this study received funding from Roche Diagnostics GmbH. The funder was not involved in the study design, collection, analysis, interpretation of data, the writing of this article, or the decision to submit it for publication.

Acknowledgments

The authors are grateful to Harald Duerr, Bianca Nussbaum, Korbinian Kneidl, Uta Werner, and Stephanie Kappelsberger for TCB mAb purification and product quality analytics. The support of Viktoria Kroenauer in cell culture experiments is highly appreciated. Parts of the figures are created using BioRender.com. Parts of the language were polished by using an internal large language model.

Conflict of interest

A patent based on this work has been filed with authors NB, MB, AV, TL, SA, and OP as inventors. NB, MB, TL, AV, HK, SA, and OP were employees of Roche Diagnostics GmbH, which develops and sells pharmaceuticals during the time when this research was carried out.

The remaining authors declare that the research was conducted in the absence of any commercial or financial relationships that could be construed as a potential conflict of interest.

Publisher's note

Supplementary material

The Supplementary Material for this article can be found online at: https://www.frontiersin.org/articles/10.3389/fbioe.2024.1414408/full#supplementary-material

References

Abbasov, M. E., Kavanagh, M. E., Ichu, T. A., Lazear, M. R., Tao, Y., Crowley, V. M., et al. (2021). A proteome-wide atlas of lysine-reactive chemistry. *Nat. Chem.* 13 (11), 1081–1092. doi:10.1038/s41557-021-00765-4

Aguilar, M. B., Lopez-Vera, E., Ortiz, E., Becerril, B., Possani, L. D., Olivera, B. M., et al. (2005). A novel conotoxin from conus delessertii with posttranslationally modified lysine residues. *Biochemistry-Us* 44 (33), 11130–11136. doi:10.1021/bi050518l

Andrews, P. C., Hawke, D., Shively, J. E., and Dixon, J. E. (1984). Anglerfish preprosomatostatin-ii is processed to somatostatin-28 and contains hydroxylysine at residue-23. *J. Biol. Chem.* 259 (24), 15021–15024. doi:10.1016/s0021-9258(17)42507-5

Augsberger, C., Hanel, G., Xu, W., Pulko, V., Hanisch, L. J., Augustin, A., et al. (2021). Targeting intracellular wt1 in aml with a novel rmf-peptide-mhc-specific t-cell bispecific antibody. *Blood* 138 (25), 2655–2669. doi:10.1182/blood.2020010477

Baek, J. H., Yun, H. S., Kwon, G. T., Kim, J. Y., Lee, C. W., Song, J. Y., et al. (2018). Plod3 promotes lung metastasis via regulation of stat3. *Cell Death Dis.* 9 (12), 1138. doi:10.1038/s41419-018-1186-5

Bauer, N., Oswald, B., Eiche, M., Schiller, L., Langguth, E., Schantz, C., et al. (2022). An arrayed crispr screen reveals myc depletion to increase productivity of difficult-to-express complex antibodies in cho cells. *Synth. Biol. (Oxf).* 7 (1), ysac026. doi:10.1093/synbio/ysac026

Bhoskar, P., Belongia, B., Smith, R., Yoon, S., Carter, T., and Xu, J. (2013). Free light chain content in culture media reflects recombinant monoclonal antibody productivity and quality. *Biotechnol. Prog.* 29 (5), 1131–1139. doi:10.1002/btpr.1767

Birch, J. R., and Racher, A. J. (2006). Antibody production. *Adv. Drug Deliv. Rev.* 58 (5-6), 671–685. doi:10.1016/j.addr.2005.12.006

Bock, C., Datlinger, P., Chardon, F., Coelho, M. A., Dong, M. B., Lawson, K. A., et al. (2022). High-content crispr screening. *Nat. Rev. Methods Prim.* 2 (1), 8. doi:10.1038/s43586-021-00093-4

Carver, J., Ng, D., Zhou, M., Ko, P., Zhan, D., Yim, M., et al. (2020). Maximizing antibody production in a targeted integration host by optimization of subunit gene dosage and position. *Biotechnol. Prog.* 36 (4), e2967. doi:10.1002/btpr.2967

Cockman, M. E., Sugimoto, Y., Pegg, H. B., Masson, N., Salah, E., Tumber, A., et al. (2022). Widespread hydroxylation of unstructured lysine-rich protein domains by jmjd6. *Proc. Natl. Acad. Sci. U. S. A.* 119 (32), e2201483119. doi:10.1073/pnas.2201483119

De Giorgi, F., Fumagalli, M., Scietti, L., and Forneris, F. (2021). Collagen hydroxylysine glycosylation: non-conventional substrates for atypical glycosyltransferase enzymes. *Biochem. Soc. Trans.* 49 (2), 855–866. doi:10.1042/bst20200767

Deng, X., Pan, Y., Yang, M., Liu, Y., and Li, J. (2021). Plod3 is associated with immune cell infiltration and genomic instability in colon adenocarcinoma. *Biomed. Res. Int.* 2021, 1–10. doi:10.1155/2021/4714526

Doench, J. G., Fusi, N., Sullender, M., Hegde, M., Vaimberg, E. W., Donovan, K. F., et al. (2016). Optimized sgrna design to maximize activity and minimize off-target effects of crispr-cas9. *Nat. Biotechnol.* 34 (2), 184–191. doi:10.1038/nbt.3437

Dorai, H., Csirke, B., Scallon, B., and Ganguly, S. (2006). Correlation of heavy and light chain mrna copy numbers to antibody productivity in mouse myeloma production cell lines. *Hybrid. (Larchmt).* 25 (1), 1–9. doi:10.1089/hyb.2006.25.1

Duran, I., Martin, J. H., Weis, M. A., Krejci, P., Konik, P., Li, B., et al. (2017). A chaperone complex formed by HSP47, FKBP65, and BiP modulates telopeptide lysyl hydroxylation of type I procollagen. *J. Bone Min. Res.* 32 (6), 1309–1319. doi:10.1002/jbmr.3095

Ehret, J., Zimmermann, M., Eichhorn, T., and Zimmer, A. (2019). Impact of cell culture media additives on igg glycosylation produced in Chinese hamster ovary cells. *Biotechnol. Bioeng.* 116 (4), 816–830. doi:10.1002/bit.26904

Fu, Z., Verderame, T. D., Leighton, J. M., Sampey, B. P., Appelbaum, E. R., Patel, P. S., et al. (2014). Exometabolome analysis reveals hypoxia at the up-scaling of a saccharomyces cerevisiae high-cell density fed-batch biopharmaceutical process. *Microb. Cell Fact.* 13 (1), 32. doi:10.1186/1475-2859-13-32

Geist, B. J., Davis, D., McIntosh, T., Yang, T. Y., Goldberg, K., Han, C., et al. (2013). A novel approach for the simultaneous quantification of a therapeutic monoclonal antibody in serum produced from two distinct host cell lines. *mAbs-Austin* 5 (1), 150–161. doi:10.4161/mabs.22773

Gelse, K., Poschl, E., and Aigner, T. (2003). Collagens--structure, function, and biosynthesis. *Adv. Drug Deliv. Rev.* 55 (12), 1531–1546. doi:10.1016/j.addr.2003.08.002

Gilkes, D. M., Bajpai, S., Chaturvedi, P., Wirtz, D., and Semenza, G. L. (2013b). Hypoxia-inducible factor 1 (hif-1) promotes extracellular matrix remodeling under hypoxic conditions by inducing p4ha1, p4ha2, and plod2 expression in fibroblasts. *J. Biol. Chem.* 288 (15), 10819–10829. doi:10.1074/jbc.m112.442939

Gilkes, D. M., Bajpai, S., Wong, C. C., Chaturvedi, P., Hubbi, M. E., Wirtz, D., et al. (2013a). Procollagen lysyl hydroxylase 2 is essential for hypoxia-induced breast cancer metastasis. *Mol. Cancer Res.* 11 (5), 456–466. doi:10.1158/1541-7786.mcr-12-0629

Gjaltema, R. A., van der Stoel, M. M., Boersema, M., and Bank, R. A. (2016). Disentangling mechanisms involved in collagen pyridinoline cross-linking: the immunophilin FKBP65 is critical for dimerization of lysyl hydroxylase 2. *Proc. Natl. Acad. Sci. U. S. A.* 113 (26), 7142–7147. doi:10.1073/pnas.1600074113

Gong, S., Schopow, N., Duan, Y., Wu, C., Kallendrusch, S., and Osterhoff, G. (2022). Plod family: a novel biomarker for prognosis and personalized treatment in soft tissue sarcoma. *Genes (Basel)* 13 (5), 787. doi:10.3390/genes13050787

Gramer, M. J. (2014). Product quality considerations for mammalian cell culture process development and manufacturing. *Adv. Biochem. Eng. Biot.* 139, 123–166. doi:10.1007/10_2013_214

Guo, T., Gu, C., Li, B., and Xu, C. (2021). Plods are overexpressed in ovarian cancer and are associated with gap junctions via connexin 43. *Lab. Invest* 101 (5), 564–569. doi:10.1038/s41374-021-00533-5

Heard, M. E., Besio, R., Weis, M., Rai, J., Hudson, D. M., Dimori, M., et al. (2016). Sc65-null mice provide evidence for a novel endoplasmic reticulum complex regulating collagen lysyl hydroxylation. *PLoS Genet.* 12 (4), e1006002. doi:10.1371/journal.pgen.1006002

Hober, S., Nord, K., and Linhult, M. (2007). Protein a chromatography for antibody purification. *J. Chromatogr. B Anal. Technol. Biomed. Life Sci.* 848 (1), 40–47. doi:10.1016/j.jchromb.2006.09.030

Iurlaro, R., Waldhauer, I., Planas-Rigol, E., Bonfill-Teixidor, E., Arias, A., Nicolini, V., et al. (2022). A novel egfrviii t-cell bispecific antibody for the treatment of glioblastoma. *Mol. Cancer Ther.* 21 (10), 1499–1509. doi:10.1158/1535-7163.mct-22-0201

Jones, M., Palackal, N., Wang, F., Gaza-Bulseco, G., Hurkmans, K., Zhao, Y., et al. (2021). High-risk host cell proteins (hcps): a multi-company collaborative view. *Biotechnol. Bioeng.* 118 (8), 2870–2885. doi:10.1002/bit.27808

Jumper, J., Evans, R., Pritzel, A., Green, T., Figurnov, M., Ronneberger, O., et al. (2021). Highly accurate protein structure prediction with alphafold. *Nature* 596 (7873), 583–589. doi:10.1038/s41586-021-03819-2

Kim, J. Y., Kim, Y. G., and Lee, G. M. (2012). Cho cells in biotechnology for production of recombinant proteins: current state and further potential. *Appl. Microbiol. Biotechnol.* 93 (3), 917–930. doi:10.1007/s00253-011-3758-5

Klemperer, F. W., Hastings, A. B., and Van Slyke, D. D. (1942). The dissociation constants of hydroxylysine. *J. Biol. Chem.* 143 (2), 433–437. doi:10.1016/s0021-9258(18)72632-x

Koterba, K. L., Borgschulte, T., and Laird, M. W. (2012). Thioredoxin 1 is responsible for antibody disulfide reduction in cho cell culture. *J. Biotechnol.* 157 (1), 261–267. doi:10.1016/j.jbiotec.2011.11.009

Kunert, R., and Reinhart, D. (2016). Advances in recombinant antibody manufacturing. *Appl. Microbiol. Biot.* 100 (8), 3451–3461. doi:10.1007/s00253-016-7388-9

Lee, A. P., Kok, Y. J., Lakshmanan, M., Leong, D., Zheng, L., Lim, H. L., et al. (2021). Multi-omics profiling of a cho cell culture system unravels the effect of culture ph on cell growth, antibody titer, and product quality. *Biotechnol. Bioeng.* 118 (11), 4305–4316. doi:10.1002/bit.27899

Li, B., Yang, H., Shen, B., Huang, J., and Qin, Z. (2021). Procollagen-lysine, 2-oxoglutarate 5-dioxygenase 1 increases cellular proliferation and colony formation capacity in lung cancer via activation of e2f transcription factor 1. *Oncol. Lett.* 22 (6), 851. doi:10.3892/ol.2021.13112

Li, S. S., Lian, Y. F., Huang, Y. L., Huang, Y. H., and Xiao, J. (2020). Overexpressing plod family genes predict poor prognosis in gastric cancer. *J. Cancer* 11 (1), 121–131. doi:10.7150/jca.35763

Liefhebber, J. M., Punt, S., Spaan, W. J., and van Leeuwen, H. C. (2010). The human collagen beta(1-O)galactosyltransferase, GLT25D1, is a soluble endoplasmic reticulum localized protein. *BMC Cell Biol.* 11, 33. doi:10.1186/1471-2121-11-33

Liu, L., Liu, M., Zhang, D., Deng, S., Chen, P., Yang, J., et al. (2020). Decoupling gene functions from knockout effects by evolutionary analyses. *Natl. Sci. Rev.* 7 (7), 1169–1180. doi:10.1093/nsr/nwaa079

Luo, J., Zhang, J., Ren, D. Y., Tsai, W. L., Li, F., Amanullah, A., et al. (2012). Probing of c-terminal lysine variation in a recombinant monoclonal antibody production using Chinese hamster ovary cells with chemically defined media. *Biotechnol. Bioeng.* 109 (9), 2306–2315. doi:10.1002/bit.24510

Markolovic, S., Wilkins, S. E., and Schofield, C. J. (2015). Protein hydroxylation catalyzed by 2-oxoglutarate-dependent oxygenases. *J. Biol. Chem.* 290 (34), 20712–20722. doi:10.1074/jbc.r115.662627

Markolovic, S., Zhuang, Q., Wilkins, S. E., Eaton, C. D., Abboud, M. I., Katz, M. J., et al. (2018). The jumonji-c oxygenase jmjd7 catalyzes (3s)-lysyl hydroxylation of trafac gtpases. *Nat. Chem. Biol.* 14 (7), 688–695. doi:10.1038/s41589-018-0071-y

McKay, T. B., Priyadarsini, S., and Karamichos, D. (2019). Mechanisms of collagen crosslinking in diabetes and keratoconus. *Cells* 8 (10), 1239. doi:10.3390/cells8101239

Mia, M. M., and Bank, R. A. (2015). The IκB kinase inhibitor ACHP strongly attenuates TGFβ1-induced myofibroblast formation and collagen synthesis. *J. Cell Mol. Med.* 19 (12), 2780–2792. doi:10.1111/jcmm.12661

Molony, M. S., Quan, C., Mulkerrin, M. G., and Harris, R. J. (1998). Hydroxylation of lys residues reduces their susceptibility to digestion by trypsin and lysyl endopeptidase. *Anal. Biochem.* 258 (1), 136–137. doi:10.1006/abio.1997.2513

Molony, M. S., Wu, S. L., Keyt, L. K., and Harris, R. J. (1995). The unexpected presence of hydroxylysine in non-collagenous proteins. *Tech. Prot. Chem.* 6, 91–98. doi:10.1016/s1080-8914(06)80014-1

Nesspor, T. C., Kinealy, K., Mazzanti, N., Diem, M. D., Boye, K., Hoffman, H., et al. (2020). High-throughput generation of bipod (Fab × scFv) bispecific antibodies exploits differential chain expression and affinity capture. *Sci. Rep.* 10 (1), 7557. doi:10.1038/s41598-020-64536-w

Popp, O., Muller, D., Didzus, K., Paul, W., Lipsmeier, F., Kirchner, F., et al. (2016). A hybrid approach identifies metabolic signatures of high-producers for Chinese hamster ovary clone selection and process optimization. *Biotechnol. Bioeng.* 113 (9), 2005–2019. doi:10.1002/bit.25958

Pornprasertsuk, S., Duarte, W. R., Mochida, Y., and Yamauchi, M. (2004). Lysyl hydroxylase-2b directs collagen cross-linking pathways in mc3t3-e1 cells. *J. Bone Min. Res.* 19 (8), 1349–1355. doi:10.1359/jbmr.040323

Qi, Q., Huang, W., Zhang, H., Zhang, B., Sun, X., Ma, J., et al. (2021). Bioinformatic analysis of plod family member expression and prognostic value in non-small cell lung cancer. *Transl. Cancer Res.* 10 (6), 2707–2724. doi:10.21037/tcr-21-73

Qi, Y., and Xu, R. (2018). Roles of plods in collagen synthesis and cancer progression. *Front. Cell Dev. Biol.* 6, 66. doi:10.3389/fcell.2018.00066

Raju, T. S., and Jordan, R. E. (2012). Galactosylation variations in marketed therapeutic antibodies. *mAbs-Austin* 4 (3), 385–391. doi:10.4161/mabs.19868

Reinhart, D., Damjanovic, L., Kaisermayer, C., and Kunert, R. (2015). Benchmarking of commercially available cho cell culture media for antibody production. *Appl. Microbiol. Biotechnol.* 99 (11), 4645–4657. doi:10.1007/s00253-015-6514-4

Robinson, M. D., McCarthy, D. J., and Smyth, G. K. (2010). Edger: a bioconductor package for differential expression analysis of digital gene expression data. *Bioinformatics* 26 (1), 139–140. doi:10.1093/bioinformatics/btp616

Salo, A. M., Wang, C., Sipila, L., Sormunen, R., Vapola, M., Kervinen, P., et al. (2006). Lysyl hydroxylase 3 (lh3) modifies proteins in the extracellular space, a novel mechanism for matrix remodeling. *J. Cell Physiol.* 207 (3), 644–653. doi:10.1002/jcp.20596

Schegg, B., Hulsmeier, A. J., Rutschmann, C., Maag, C., and Hennet, T. (2009). Core glycosylation of collagen is initiated by two β(1-*O*)galactosyltransferases. *Mol. Cell Biol.* 29 (4), 943–952. doi:10.1128/mcb.02085-07

Schneider, A., Gorr, I. H., Larraillet, V., Frensing, T., and Popp, O. (2019). Reduction of il-2 fragmentation during manufacturing of a novel immunocytokine by doe process optimization. *Biotechnol. Bioeng.* 116 (10), 2503–2513. doi:10.1002/bit.27090

Scietti, L., Chiapparino, A., De Giorgi, F., Fumagalli, M., Khoriauli, L., Nergadze, S., et al. (2018). Molecular architecture of the multifunctional collagen lysyl hydroxylase and glycosyltransferase lh3. *Nat. Commun.* 9 (1), 3163. doi:10.1038/s41467-018-05631-5

Song, Y., Zheng, S., Wang, J., Long, H., Fang, L., Wang, G., et al. (2017). Hypoxia-induced plod2 promotes proliferation, migration and invasion via pi3k/akt signaling in glioma. *Oncotarget* 8 (26), 41947–41962. doi:10.18632/oncotarget.16710

Sonnichsen, B., Koski, L. B., Walsh, A., Marschall, P., Neumann, B., Brehm, M., et al. (2005). Full-genome rnai profiling of early embryogenesis in caenorhabditis elegans. *Nature* 434 (7032), 462–469. doi:10.1038/nature03353

Takaluoma, K., Lantto, J., and Myllyharju, J. (2007). Lysyl hydroxylase 2 is a specific telopeptide hydroxylase, while all three isoenzymes hydroxylate collagenous sequences. *Matrix Biol.* 26 (5), 396–403. doi:10.1016/j.matbio.2007.01.002

Targa, G., Mottarlini, F., Rizzi, B., Leo, D., Caffino, L., and Fumagalli, F. (2023). Dysregulation of ampa receptor trafficking and intracellular vesicular sorting in the prefrontal cortex of dopamine transporter knock-out rats. *Biomolecules* 13 (3), 516. doi:10.3390/biom13030516

Valtavaara, M., Papponen, H., Pirttila, A. M., Hiltunen, K., Helander, H., and Myllyla, R. (1997). Cloning and characterization of a novel human lysyl hydroxylase isoform highly expressed in pancreas and muscle. *J. Biol. Chem.* 272 (11), 6831–6834. doi:10.1074/jbc.272.11.6831

van der Slot, A. J., Zuurmond, A. M., Bardoel, A. F., Wijmenga, C., Pruijs, H. E., Sillence, D. O., et al. (2003). Identification of plod2 as telopeptide lysyl hydroxylase, an important enzyme in fibrosis. *J. Biol. Chem.* 278 (42), 40967–40972. doi:10.1074/jbc.m307380200

Wang, X., and Li, S. (2014). Protein mislocalization: mechanisms, functions and clinical applications in cancer. *Biochim. Biophys. Acta* 1846 (1), 13–25. doi:10.1016/j.bbcan.2014.03.006

Wang, Z., Shi, Y., Ying, C., Jiang, Y., and Hu, J. (2021). Hypoxia-induced PLOD1 overexpression contributes to the malignant phenotype of glioblastoma via NF-κB signaling. *Oncogene* 40 (8), 1458–1475. doi:10.1038/s41388-020-01635-y

Wurm, F. M. (2004). Production of recombinant protein therapeutics in cultivated mammalian cells. *Nat. Biotechnol.* 22 (11), 1393–1398. doi:10.1038/nbt1026

Wurm, M. J., and Wurm, F. M. (2021). Naming cho cells for bio-manufacturing: genome plasticity and variant phenotypes of cell populations in bioreactors question the relevance of old names. *Biotechnol. J.* 16 (7), e2100165. doi:10.1002/biot.202100165

Xie, Q., Moore, B., and Beardsley, R. L. (2016). Discovery and characterization of hydroxylysine in recombinant monoclonal antibodies. *mAbs-Austin* 8 (2), 371–378. doi:10.1080/19420862.2015.1122148

Yamauchi, M., and Sricholpech, M. (2012). Lysine post-translational modifications of collagen. *Essays Biochem.* 52, 113–133. doi:10.1042/bse0520113

Zurlo, G., Guo, J., Takada, M., Wei, W., and Zhang, Q. (2016). New insights into protein hydroxylation and its important role in human diseases. *Biochim. Biophys. Acta* 1866 (2), 208–220. doi:10.1016/j.bbcan.2016.09.004

Supplementary Information

Procollagen-Lysine 2-Oxoglutarate 5-Dioxygenases are Responsible for 5R-Hydroxylysine Modification of Therapeutic T-Cell Bispecific Monoclonal Antibodies Produced by Chinese Hamster Ovary Cells

Niels Bauer[1,2*], Marco Boettger[1*], Stella Papadaki[1], Tanja A. Leitner[1], Stefan Klostermann[3], Hubert Kettenberger[1], Guy Georges[1], Vincent Larraillet[1], Dino Gluhacevic von Kruechten[4], Lars Hillringhaus[4], Annette Vogt[1], Simon Auslaender[1] & Oliver Popp[1,#]

[1]Large Molecule Research, Roche Pharma Research and Early Development (pRED), Roche Innovation Center Munich, Penzberg, Germany; [2]Gene Center and Department of Biochemistry, Ludwig-Maximilians-Universität München, 81377, Munich, Germany; [3]Data and Analytics, Roche Pharma Research and Early Development (pRED), Roche Innovation Center Munich, Penzberg, Germany; [4]Special Chemistry, Roche Diagnostics, Roche Innovation Center Munich, Penzberg, Germany

**These authors contributed equally*

[#]corresponding author, Dr. Oliver Popp, oliver.popp@roche.com, Phone: +49 8856 60 18420

Table S1 sgRNA sequences and verification primers used in this study. sgRNA with highest knock-out score is highlighted in bold. (ch: Chinese hamster); na: not available

Target	sgRNA Name	sgRNA Sequence	Knock-out score
chPLOD1	**PLOD1_1**	**5' - TAAGAGTTCCCGGGGCCCCG - 3'**	**98**
	PLOD1_2	5' - AACTCATCTACCCCGACCGG - 3'	96
	PLOD1_3	5' - CGCTTGCCATCAGACACCGT - 3'	13
chPLOD2	**PLOD2_1**	**5' - GTGGCCGGATAAGCGACTCG - 3'**	**97**
	PLOD2_2	5' - GTTTACCAATGTGCACTACA - 3'	86
	PLOD2_3	5' - AAACGCTACCTGAATTCTGG - 3'	na
chPLOD3	PLOD3_1	5' - GATGTTGCTCGAACAGTTGG - 3'	na
	PLOD3_2	**5' - GGAGAAATATGCAAACCGGG - 3'**	**94**
	PLOD3_3	5' - CAAATTGCTGGTGATCACCG - 3'	na
chJMJD4	JMJD4_1	5' - TGGGCCCCGCATAGACAAAG - 3'	83
	JMJD4_2	**5' - CTGTAGGTCTCCCTTCCATG - 3'**	**95**
	JMJD4_3	5' - GCCTCCTGTATGACTTCAAG - 3'	69
chJMJD6	JMJD6_1	5' - TGAATCCCGGTTCCAGAACG - 3'	91
	JMJD6_2	**5' - TCCAGGCACTCGTTCCCAGA - 3'**	**96**
	JMJD6_3	5' - AAGGTGACCCGAGAAGAAGG - 3'	50
chJMJD7	**JMJD7_1**	**5' - GCACAGCACGAGGTACACTG - 3'**	**97**
	JMJD7_2	5' - CAATCCCGGTAGAAGCAGAG - 3'	83
	JMJD7_3	5' - AGCCATAGTGGGCTCCACGG - 3'	87

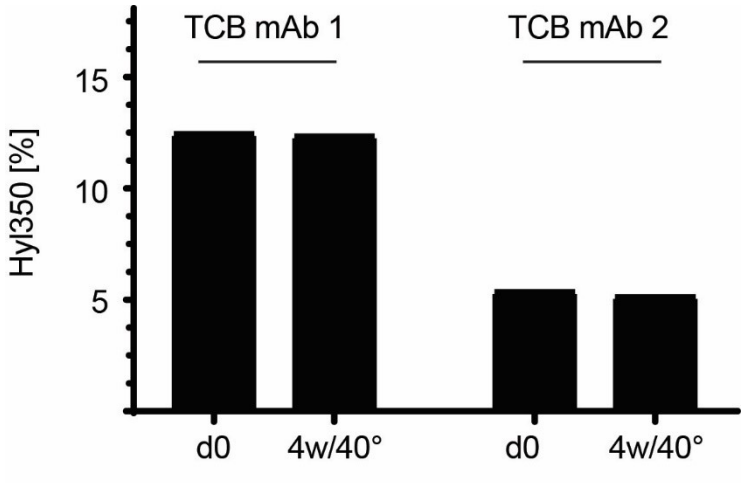

Supplementary Figure S1 Hyl modification level is stable under stress conditions. TCB mAb 1 and TCB mAb 2 Hyl levels at the start (d0) and after 4 weeks at 40°C in PBS buffer show no difference.

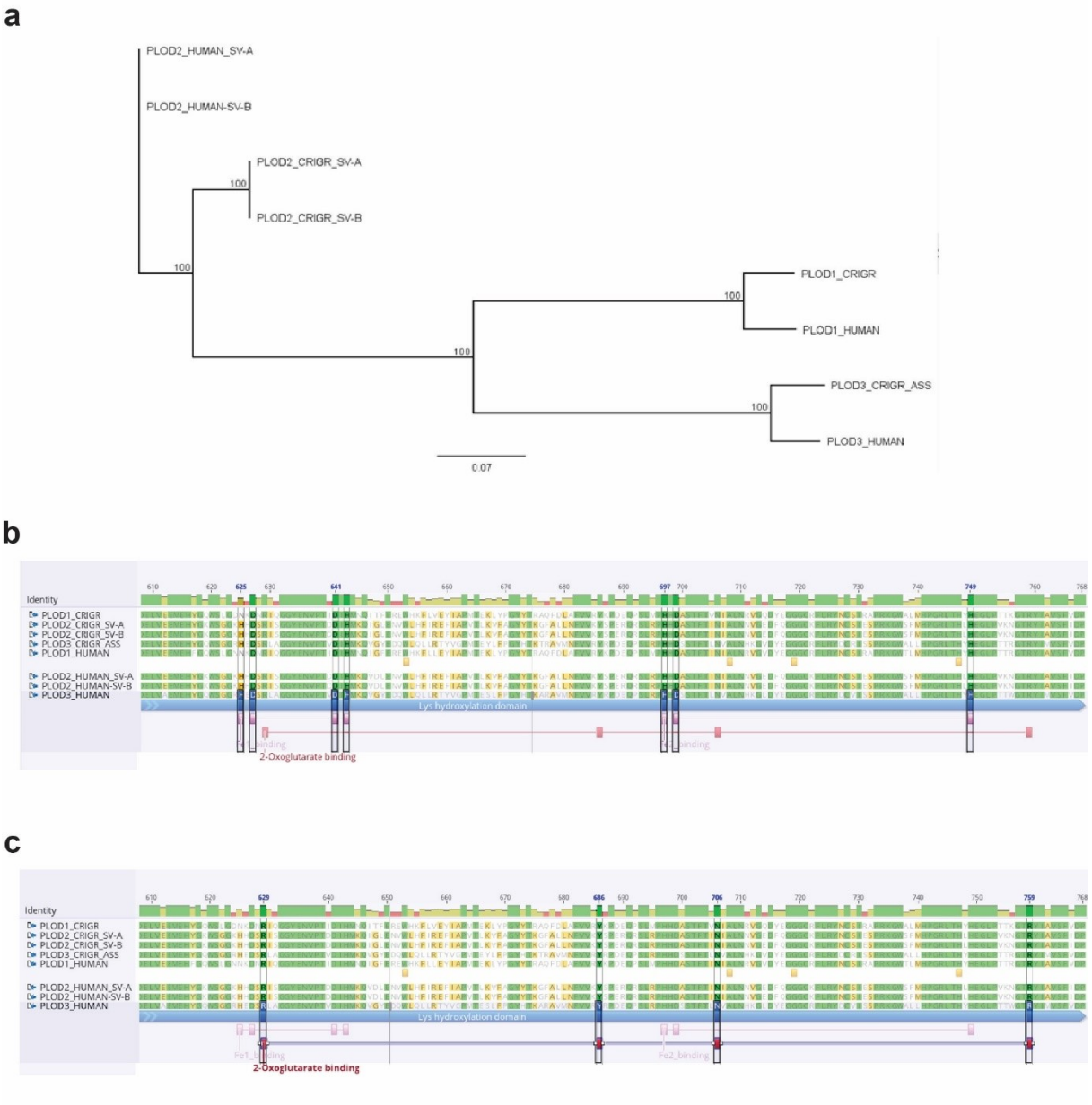

Supplementary Figure S2 Chinese Hamster PLODs are highly conserved to human orthologues. a) Hierarchical clustering analysis of Chinese hamster and human PLOD protein sequence suggest that PLODs of both species are highly conserved. b) Fe^{2+} and c) 2OG binding sites of Chinese hamster

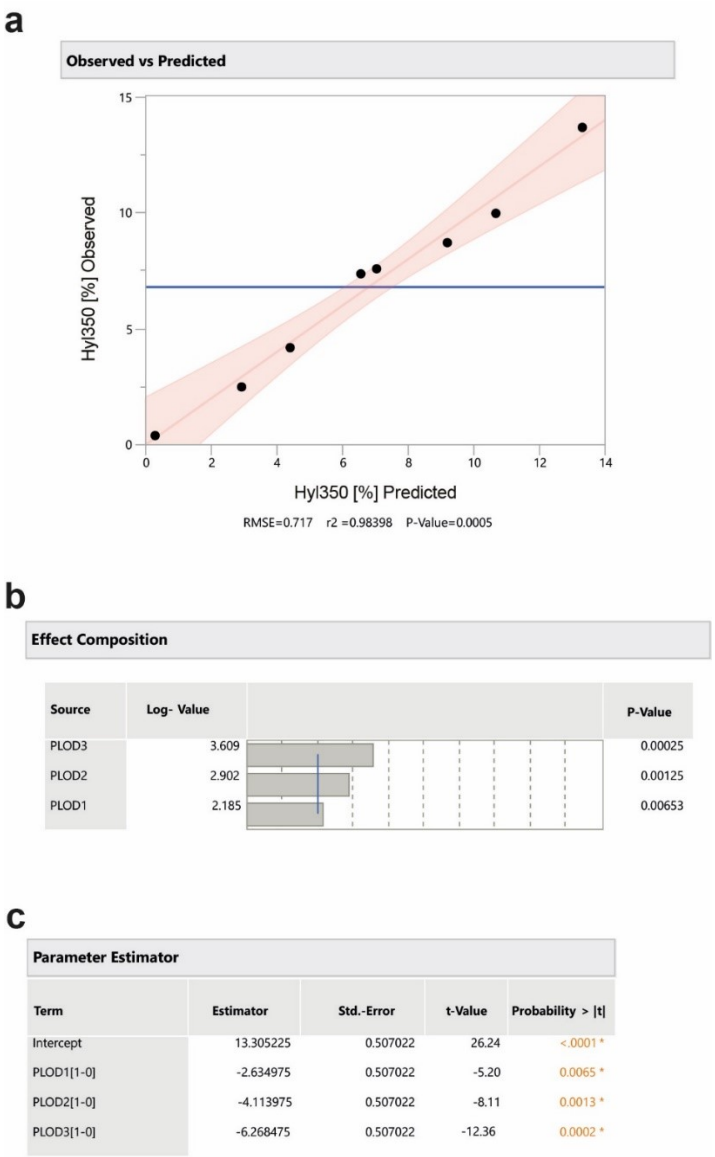

Supplementary Figure S3 PLOD3 is main contributor to Hyl modification in TCB mAbs. a) Multiregression model on observed “PLOD Contribution Study” Hyl modification values. The respective RMSE, r2 and P-Value indicating that the data can be described by a valid, statistically significant model. b) The effect composition analysis revealed the importance of PLOD3 over PLOD2 over PLOD1. c) The parameter estimator analysis show the respective estimator contribution and statistical probability. The analysis were conducted using JMP analysis tool.

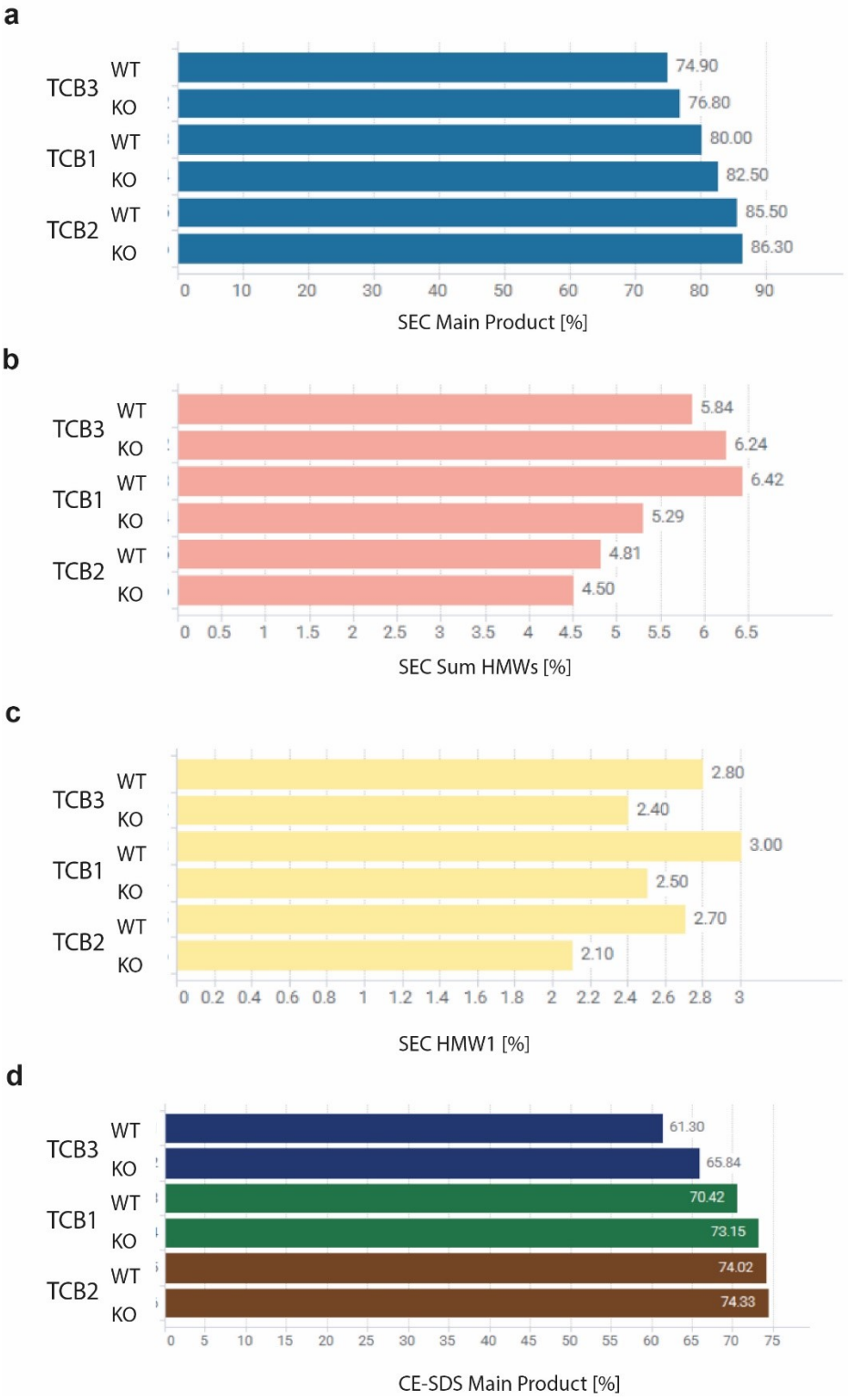

Supplementary Figure S4 PLOD KO improves product quality of TCB mAb expression cultures. Cell culture supernatants of wild-type (wt) and CRISPR/Cas9 KO cultures for PLOD1-3 were purified by ProtA and subsequently assessed by SEC and CE-SDS. a) Main product, b) sum HMWs, and c) HMW1 suggest an improved product quality by CHO cell PLOD depletion. Same ProtA purified materials were analyzed by non-reducing CE-SDS (d) which supported the observation of improved product quality by SEC.

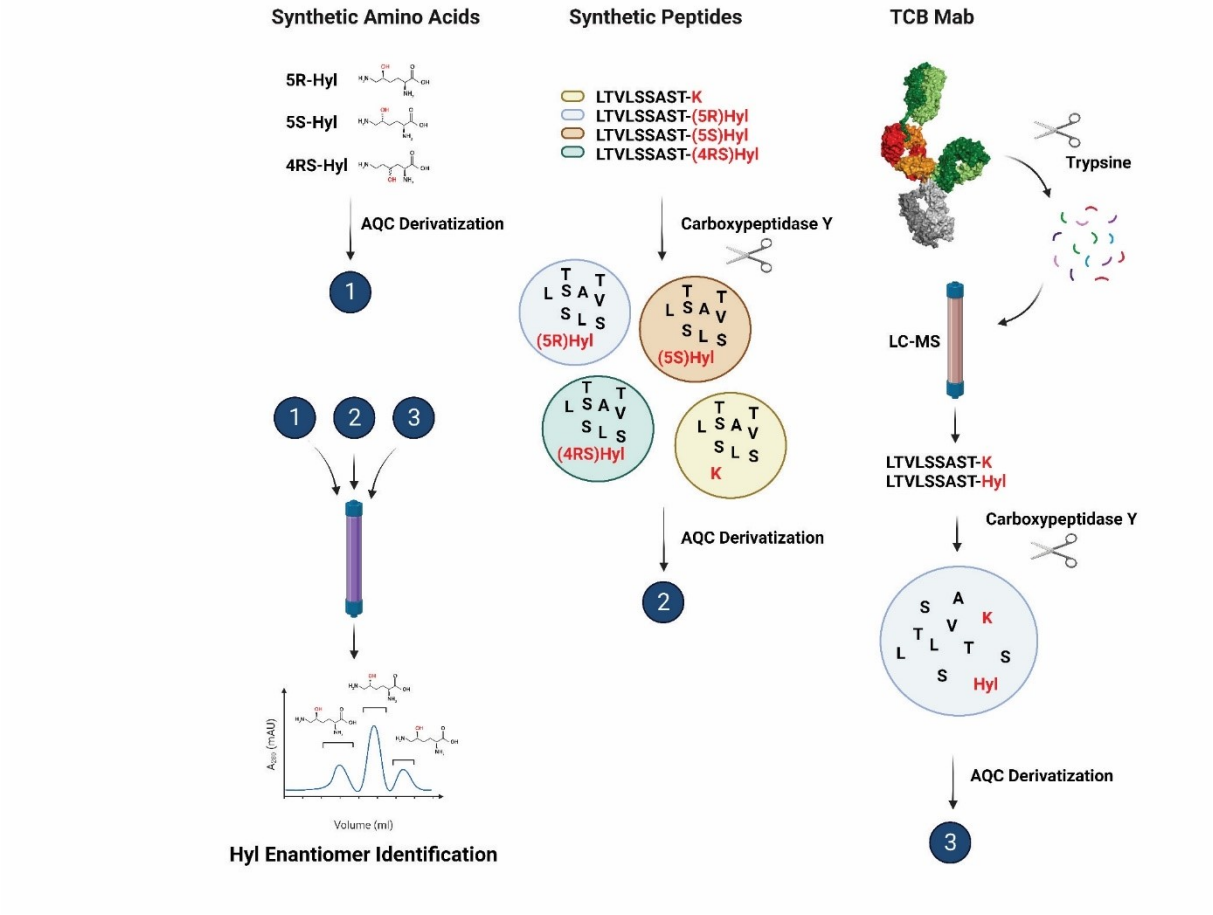

Supplementary Figure S5 Analytical approach to identify TCB mAb modifying 2OG-dependent hydroxylase.

Supplementary Figure S6 PLOD1 sequence alignment human and Chinese hamster

```
PLOD1_HUMAN  MRPLLLLALL GWLLLAEAKG DAKPEDNLLV LTVATKETEG FRRFKRSAQF FNYKIQALGL GEDWNVEKGT SAGGGQKVRL LKKALEKHAD KEDLVILFAD  100
PLOD1_CRIGR  MRPLLLLAPL AWLLLAQAKD DAKLEDNLLV LTVATKETEG FRRFKRSAQF FNYKIQALGL GEDWSVDSGP SAGGGQKVRL LKKALEKHAH KEDLVILFTD  100

PLOD1_HUMAN  SYDVLFASGP RELLKKFRQA RSQVVFSAEE LIYPDRRLET KYPVVSDGKR FLGSGGFIGY APNLSKLVAE WEGQDSDSDQ LFYTKIFLDP EKREQINITL  200
PLOD1_CRIGR  SYDVVFASGP RELLKKFQQA KSRVVFSAEE LIYPDRRLEA KYPTVSDGKR FLGSGGFIGY APNLNKLVAE WEGQDSDSDQ LFYTKIFLDP EKREQINISL  200

PLOD1_HUMAN  DHRCRIFQNL DGALDEVVLK FEMGHVRARN LAYDTLPVLI HGNGPTKLQL NYLGNYIPRF WTFETGCTVC DEGLRSLKGI GDEALPTVLV GVFIEQPTPF  300
PLOD1_CRIGR  DHRCRIFQNL DGALDEVVLK FEMGHVRARN LAYDTLPVVI HGNGPTKLQL NYLGNYIPRF WTFETGCTVC DEGLRSLKGI GDEALPTVLV GVFIEQPTPF  300

PLOD1_HUMAN  VSLFFQRLLR LHYPQKHMRL FIHNHEQHHK AQVEEFLAQH GSEYQSVKLV GPEVRMANAD ARNMGADLCR QDRSCTYYFS VDADVALTEP NSLRLLIQQN  400
PLOD1_CRIGR  LSLFFLRLLR LRYPQKRMRL FIHNHEQHHK LEVEKFLAEH GTEYQSVKLV GPEVRMANAD ARNMGADLCR QDQTCTYYFS VDADVALTEP DSLRLLIEQN  400

PLOD1_HUMAN  KNVIAPLMTR HGRLWSNFWG ALSADGYYAR SEDYVDIVQG RRVGVWNVPY ISNIYLIKGS ALRGELQSSD LFHHSKLDPD MAFCANIRQQ DVFMFLTNRH  500
PLOD1_CRIGR  KNVIAPLMTR HGRLWSNFWG ALSADGYYAR SEDYVDIVQG RRVGVWNVPY ISNIYLIKGS ALRAELQHVD LFHYSKLDAD MSFCANVRQQ EVFMFLTNRH  500

PLOD1_HUMAN  TLGHLLSLDS YRTTHLHNDL WEVFSNPEDW KEKYIHQNYT KALAGKLVET PCPDVYWFPI FTEVACDELV EEMEHFGQWS LGNNKDNRIQ GGYENVPTID  600
PLOD1_CRIGR  TFGHLLSLDN YQTTHLHNDL WEVFSNPEDW KEKYIHENYT KALEGKLVEM PCPDVYWFPI FTEAACDELV EEMEHYGQWS LGDNKDNRIQ GGYENVPTID  600

PLOD1_HUMAN  IHMNQIGFER EWHKFLLEYI APMTEKLYPG YYTRAQFDLA FVVRYKPDEQ PSLMPHHDAS TFTINIALNR VGVDYEGGGC RFLRYNCSIR APRKGWTLMH  700
PLOD1_CRIGR  IHMNQITFER EWHKFLVEYI APMTEKLYPG YYTRAQFDLA FVVRYKPDEQ PSLMPHHDAS TFTVNIALNR VGQDYEGGGC RFLRYNCSIR APRKGWALMH  700

PLOD1_HUMAN  PGRLTHYHEG LPTTRGTRYI AVSFVDP  727
PLOD1_CRIGR  PGRLTHYHEG LPTTKGTRYI AVSFVDP  727
```

Supplementary Figure S7 PLOD2a sequence alignment human and Chinese hamster

```
PLOD2_HUMAN_SV-A  MGGCTVKPQ. ....LLLLAL VLHPWNPCLG ADSEKPSSIP TDKLLVITVA TKESDGFHRF MQSAKYFNYT VKVLGQGEEW RGGDGINSIG GGQKVRLMKE   95
PLOD2_CRIGR_SV-A  MGGRRVRPGR LGLLLLLRGL ALLSWAPGLG AAEETPSRIP ADKLLVITVA TKENDGFHRF MNSAKYFNYT VKVLGQGQEW RGGDGINSIG GGQKVRLMKE  100

PLOD2_HUMAN_SV-A  VMEHYADQDD LVVMFTECFD VIFAGGPEEV LKKFQKANHK VVFAADGILW PDKRLADKYP VVHIGKRYLN SGGFIGYAPY VNRIVQQWNL QDNDDDQLFY  195
PLOD2_CRIGR_SV-A  AMAQYASQED LVILFTECFD VVFAGGPEEV LKKFQKTNHK IVFAADGILW PDKRLAEKYP VVHIGKRYLN SGGFIGYAPY ISHLVQEWNL QDNDDDQLFY  200

PLOD2_HUMAN_SV-A  TKVYIDPLKR EAINITLDHK CKIFQTLNGA VDEVVLKFEN GKARAKNTFY ETLPVAINGN GPTKILLNYF GNYVPNSWTQ DNGCTLCEFD TVDLSAVDVH  295
PLOD2_CRIGR_SV-A  TKVYIDPVKR EAFNITLDHK CKIFQALNGA TDEVVLKFEN GKSRVKNTFY ETLPVAINGN GPTKILLNYF GNYVPNSWTQ EHGCALCDFD TIDLSAVDVH  300

PLOD2_HUMAN_SV-A  PNVSIGVFIE QPTPFLPRFL DILLTLDYPK EALKLFIHNK EVYHEKDIKV FFDKAKHEIK TIKIVGPEEN LSQAEARNMG MDFCRQDEKC DYYFSVDADV  395
PLOD2_CRIGR_SV-A  PKVTIGVFIE QPTPFLPRFL NLLLSLDYPK EALKLFIHNK EVYHEKDIKV FFDKAKHEIS TIKIVGPEEN LSQAEARNMG MDFCRQDEKC DYYFSVDADV  400

PLOD2_HUMAN_SV-A  VLTNPRTLKI LIEQNRKIIA PLVTRHGKLW SNFWGALSPD GYYARSEDYV DIVQGNRVGV WNVPYMANVY LIKGKTLRSE MNERNYFVRD KLDPDMALCR  495
PLOD2_CRIGR_SV-A  VLTNPRTLKN LIEQNRKIIA PLVTRHGKLW SNFWGALSPD GYYARSEDYV DIVQGKRVGI WNVPYMANVY LIQGKTLRSE MSERNYFVRD KLDPDMALCR  500

PLOD2_HUMAN_SV-A  NAREMGVFMY ISNRHEFGRL LSTANYNTSH YNNDLWQIFE NPVDWKEKYI NRDYSKIFTE NIVEQPCPDV FWFPIFSEKA CDELVEEMEH YGKWSGGKHH  595
PLOD2_CRIGR_SV-A  NAREMGMFMY ISNRHEFGRL LSTANYNTSH LNNDLWQIFE NPVDWKEKYI NRDYSKIFTE SIVEQPCPDV FWFPIFSERA CDELVEEMEH YGKWSGGKHH  600

PLOD2_HUMAN_SV-A  DSRISGGYEN VPTDDIHMKQ VDLENVWLHF IREFIAPVTL KVFAGYYTKG FALLNFVVKY SPERQRSLRP HHDASTFTIN IALNNVGEDF QGGGCKFLRY  695
PLOD2_CRIGR_SV-A  DSRISGGYEN VPTDDIHMKQ IGLENVWLHF IREFIAPVTL KVFAGYYTKG FALLNFVVKY SPERQRSLRP HHDASTFTIN IALNNVGEDF QGGGCKFLRY  700

PLOD2_HUMAN_SV-A  NCSIESPRKG WSFMHPGRLT HLHEGLPVKN GTRYIAVSFI DP  737
PLOD2_CRIGR_SV-A  NCSIESPRKG WSFMHPGRLT HLHEGLPVKN GTRYIAVSFI DP  742
```

Supplementary Figure S8 PLOD2b sequence alignment human and Chinese hamster

```
PLOD2_HUMAN-SV-B  MGGCTVKPQ. ....LLLLAL VLHPWNPCLG ADSEKPSSIP TDKLLVITVA TKESDGFHRF MQSAKYFNYT VKVLGQGEEW RGGDGINSIG GGQKVRLMKE   95
PLOD2_CRIGR_SV-B  MGGRRVRPGR LGLLLLLRGL ALLSWAPGLG AAEETPSRIP ADKLLVITVA TKENDGFHRF MNSAKYFNYT VKVLGQGQEW RGGDGINSIG GGQKVRLMKE  100

PLOD2_HUMAN-SV-B  VMEHYADQDD LVVMFTECFD VIFAGGPEEV LKKFQKANHK VVFAADGILW PDKRLADKYP VVHIGKRYLN SGGFIGYAPY VNRIVQQWNL QDNDDDQLFY  195
PLOD2_CRIGR_SV-B  AMAQYASQED LVILFTECFD VVFAGGPEEV LKKFQKTNHK IVFAADGILW PDKRLAEKYP VVHIGKRYLN SGGFIGYAPY ISHLVQEWNL QDNDDDQLFY  200

PLOD2_HUMAN-SV-B  TKVYIDPLKR EAINITLDHK CKIFQTLNGA VDEVVLKFEN GKARAKNTFY ETLPVAINGN GPTKILLNYF GNYVPNSWTQ DNGCTLCEFD TVDLSAVDVH  295
PLOD2_CRIGR_SV-B  TKVYIDPVKR EAFNITLDHK CKIFQALNGA TDEVVLKFEN GKSRVKNTFY ETLPVAINGN GPTKILLNYF GNYVPNSWTQ EHGCALCDFD TIDLSAVDVH  300

PLOD2_HUMAN-SV-B  PNVSIGVFIE QPTPFLPRFL DILLTLDYPK EALKLFIHNK EVYHEKDIKV FFDKAKHEIK TIKIVGPEEN LSQAEARNMG MDFCRQDEKC DYYFSVDADV  395
PLOD2_CRIGR_SV-B  PKVTIGVFIE QPTPFLPRFL NLLLSLDYPK EALKLFIHNK EVYHEKDIKV FFDKAKHEIS TIKIVGPEEN LSQAEARNMG MDFCRQDEKC DYYFSVDADV  400

PLOD2_HUMAN-SV-B  VLTNPRTLKI LIEQNRKIIA PLVTRHGKLW SNFWGALSPD GYYARSEDYV DIVQGNRVGV WNVPYMANVY LIKGKTLRSE MNERNYFVRD KLDPDMALCR  495
PLOD2_CRIGR_SV-B  VLTNPRTLKN LIEQNRKIIA PLVTRHGKLW SNFWGALSPD GYYARSEDYV DIVQGKRVGI WNVPYMANVY LIQGKTLRSE MSERNYFVRD KLDPDMALCR  500

PLOD2_HUMAN-SV-B  NAREMTLQRE KDSPTPETFQ MLSPPKGVFM YISNRHEFGR LLSTANYNTS HYNNDLWQIF ENPVDWKEKY INRDYSKIFT ENIVEQPCPD VFWFPIFSEK  595
PLOD2_CRIGR_SV-B  NAREMTLQRE KDSPTPETIQ MLRPPKGMFM YISNRHEFGR LLSTANYNTS HLNNDLWQIF ENPVDWKEKY INRDYSKIFT ESIVEQPCPD VFWFPIFSER  600

PLOD2_HUMAN-SV-B  ACDELVEEME HYGKWSGGKH HDSRISGGYE NVPTDDIHMK QVDLENVWLH FIREFIAPVT LKVFAGYYTK GFALLNFVVK YSPERQRSLR PHHDASTFTI  695
PLOD2_CRIGR_SV-B  ACDELVEEME HYGKWSGGKH HDSRISGGYE NVPTDDIHMK QIGLENVWLH FIREFIAPVT LKVFAGYYTK GFALLNFVVK YSPERQRSLR PHHDASTFTI  700

PLOD2_HUMAN-SV-B  NIALNNVGED FQGGGCKFLR YNCSIESPRK GWSFMHPGRL THLHEGLPVK NGTRYIAVSF IDP  758
PLOD2_CRIGR_SV-B  NIALNNVGED FQGGGCKFLR YNCSIESPRK GWSFMHPGRL THLHEGLPVK NGTRYIAVSF IDP  763
```

Supplementary Figure S9 PLOD3 sequence alignment human and Chinese hamster

```
PLOD3_HUMAN      MTSSGPGPRF LLLLPLLLP. ...PAASASD RPRGRDPVNP EKLLVITVAT AETEGYLRFL RSAEFFNYTV RTLGLGEEWR GGDVARTVGG GQKVRWLKKE   96
PLOD3_CRIGR_ASS  MAASGPEPRL FLLLLLLLPP PLLPVASASD RSRGSSPVNP DKLLVITVAT AETEGYRRFL QSAEFFNYTV RTLGLGHEWR GGDVARTVGG GQKVRWLKKE  100

PLOD3_HUMAN      MEKYADREDM IIMFVDSYDV ILAGSPTELL KKFVQSGSRL LFSAESFCWP EWGLAEQYPE VGTGKRFLNS GGFIGFATTI HQIVRQWKYK DDDDDQLFYT  196
PLOD3_CRIGR_ASS  MEKYANREDM IIMFVDSYDV ILASSPAELL KKFVQSGSHL LFSAEGFCWP EWGLAEQYPE VGMGKRFLNS GGFIGFAPTI HQIVRQWKYK DDDDDQLFYT  200

PLOD3_HUMAN      RLYLDPGLRE KLSLNLDHKS RIFQNLNGAL DEVVLKFDRN RVRIRNVAYD TLPIVVHGNG PTKLQLNYLG NYVPNGWTPE GGCGFCNQDR RTLPGGQPPP  296
PLOD3_CRIGR_ASS  RLYLDPGLRE KLKLNLDHKS RIFQNLNGAL DEVVLKFDQN RVRIRNVAYD TLPVVVHGNG PTKLQLNYLG NYVPNGWTPQ GGCGFCNQNQ RTLPGGQPPP  300

PLOD3_HUMAN      RVFLAVFVEQ PTPFLPRFLQ RLLLLDYPPD RVTLFLHNNE VFHEPHIADS WPQLQDHFSA VKLVGPEEAL SPGEARDMAM DLCRQDPECE FYFSLDADAV  396
PLOD3_CRIGR_ASS  RVLLAVFVEQ PTPFLPRFLQ RLLFLDYPRD RVSLFLHNNE VYHEPHIADV WPQLQAHFSA AKLVGPEEAL SPGEARDMAM DSCRQDPKCE FYFSLDADAV  400

PLOD3_HUMAN      LTNLQTLRIL IEENRKVIAP MLSRHGKLWS NFWGALSPDE YYARSEDYVE LVQRKRVGVW NVPYISQAYV IRGDTLRMEL PQRDVFSGSD TDPDMAFCKS  496
PLOD3_CRIGR_ASS  LTNPETLRIL IEQNRKVIAP MLSRHGKLWS NFWGALSPDE YYARSEDYVE LVQRKRVGVW NVPYISQAYV IRGETLRTEL PQKEVFSGSD TDPDMAFCKS  500

PLOD3_HUMAN      FRDKGIFLHL SNQHEFGRLL ATSRYDTEHL HPDLWQIFDN PVDWKEQYIH ENYSRALEGE GIVEQPCPDV YWFPLLSEQM CDELVAEMEH YGQWSGGRHE  596
PLOD3_CRIGR_ASS  LRDKGIFLHL SNQHEFGRLL ATSRYDTDHL HPDLWQIFDN PVDWKEQYIH ENYSRALDGQ GLVEQPCPDV YWFPLLTEQM CDELVEEMEH YGQWSGGRHE  600

PLOD3_HUMAN      DSRLAGGYEN VPTVDIHMKQ VGYEDQWLQL LRTYVGPMTE SLFPGYHTKA RAVMNFVVRY RPDEQPSLRP HHDSSTFTLN VALNHKGLDY EGGGCRFLRY  696
PLOD3_CRIGR_ASS  DSRLAGGYEN VPTVDIHMKQ VGYEDQWLQL LRTYVGPMTE YLFPGYHTKT RAVMNFVVRY RPDEQPSLRP HHDSSTFTLN VALNHKGVDY EGGGCRFLRY  700

PLOD3_HUMAN      DCVISSPRKG WALLHPGRLT HYHEGLPTTW GTRYIMVSFV DP  738
PLOD3_CRIGR_ASS  DCRISSPRKG WALLHPGRLT HYHEGLPTTR GTRYIMVSFV DP  742
```

a

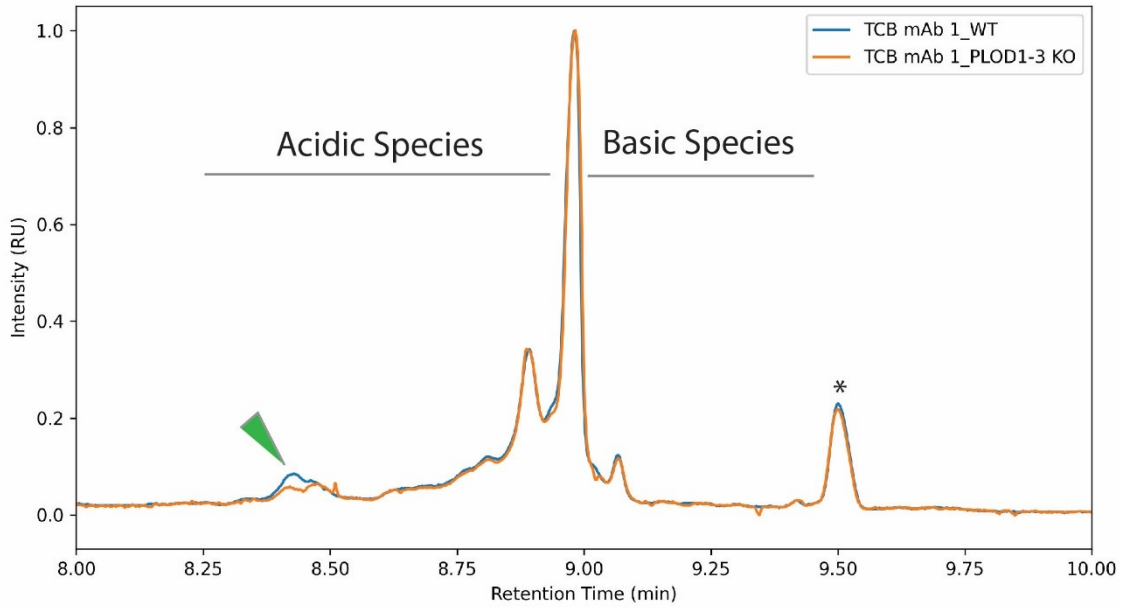

b

	Lysine	Hydroxylysine
pK´1	2.20	2.13
pK´2	8.90	8.62
pK´3	**10.28**	**9.67**

c

L-Lysyl **5R-Hydroxy-L-Lysyl**

more basic less basic

Supplementary Figure S10 TCB mAb 1 expressed by PLOD1-3 KO CHO cells show a minor shift in reduced acidic species. Cell culture supernatants of wild-type (wt) and CRISPR/Cas9 KO cultures for PLOD1-3 originating from TCB mAb 1 exprssing CHO cells were purified by ProtA and subsequently assessed by cIEF (capillary isoelectric focusing) for charge variant analysis. a) Removal of Hyl modification in TCB mAb 1 by PLOD1-3 KO (<1% Hyl, orange chromatogram) showed a decreased acidic species pattern (green arrow head) compared to the WT control (> 12% Hyl, blue chromatogram). The chromatograms were normalized to the intensity of the main peak species. Asterisk marks internal standard used in cIEF. b) Dissociation constants of Lysine and Hydroxylysine according Klemperer et al.[69] c) Schematic structure model of ionized L-Lysyl and 5R-Hydroxy-L-Lysyl in proteins with suggested basicity reduction of Hyl by interaction of the protonated epsilon amine and C5 hydroxyl group.

2.2 An arrayed CRISPR screen reveals Myc depletion to increase productivity of difficult-to-express complex antibodies in CHO cells

Niels Bauer, Benedikt Oswald, Maximilian Eiche, Lisa Schiller, Emma Langguth, Christian Schantz, Andrea Osterlehner, Amy Shen, Shahram Misaghi, Julian Stingele, Simon Ausländer, An arrayed CRISPR screen reveals Myc depletion to increase productivity of difficult-to-express complex antibodies in CHO cells, *Synthetic Biology*, Volume 7, Issue 1, 2022, ysac026, https://doi.org/10.1093/synbio/ysac026

Author contribution:
I established the experimental setup for the arrayed CRISPR screening. Further, I designed and analyzed all experiments. I performed all described experiments with exception of bioreactor handling and antibody purification. I wrote the manuscript.

SYNTHETIC BIOLOGY

Synthetic Biology, 2022, **7(1)**, 1–11
DOI: https://doi.org/10.1093/synbio/ysac026
Advance access publication date: 3 November 2022
Research Article

An arrayed CRISPR screen reveals Myc depletion to increase productivity of difficult-to-express complex antibodies in CHO cells

Niels Bauer[1,3], Benedikt Oswald[1], Maximilian Eiche[1], Lisa Schiller[1], Emma Langguth[1], Christian Schantz[1], Andrea Osterlehner[1], Amy Shen[2], Shahram Misaghi[2], Julian Stingele[3], and Simon Ausländer[1,*]

[1]Large Molecule Research, Roche Pharma Research and Early Development (pRED), Roche Innovation Center Munich, Penzberg, Germany
[2]Cell Culture and Bioprocess Operations Department, Genentech Inc., South San Francisco, CA, USA
[3]Gene Center and Department of Biochemistry, Ludwig-Maximilians-University Munich, Munich 81377, Germany
*Corresponding author: E-mail: simon.auslaender@roche.com

Abstract

Complex therapeutic antibody formats, such as bispecifics (bsAbs) or cytokine fusions, may provide new treatment options in diverse disease areas. However, the manufacturing yield of these complex antibody formats in Chinese Hamster Ovary (CHO) cells is lower than monoclonal antibodies due to challenges in expression levels and potential formation of side products. To overcome these limitations, we performed a clustered regularly interspaced short palindromic repeats (CRISPR)/CRISPR associated protein 9 (Cas9)-based knockout (KO) arrayed screening of 187 target genes in two CHO clones expressing two different complex antibody formats in a production-mimicking set-up. Our findings revealed that Myc depletion drastically increased product expression (>40%) by enhancing cell-specific productivity. The Myc-depleted cells displayed decreased cell densities together with substantially higher product titers in industrially-relevant bioprocesses using ambr15 and ambr250 bioreactors. Similar effects were observed across multiple different clones, each expressing a distinct complex antibody format. Our findings reinforce the mutually exclusive relationship between growth and production phenotypes and provide a targeted cell engineering approach to impact productivity without impairing product quality. We anticipate that CRISPR/Cas9-based CHO host cell engineering will transform our ability to increase manufacturing yield of high-value complex biotherapeutics.

Key words: CHO; CRISPR/Cas9; arrayed KO screening; antibody production

Graphical Abstract

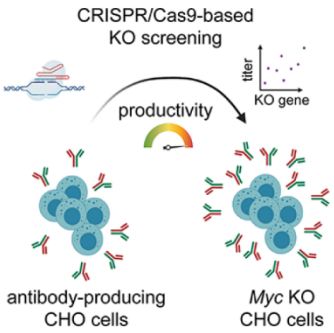

1. Introduction

The modular architecture of antibodies has been widely exploited to engineer a multitude of complex bispecific antibodies. This includes the number of antigen-binding sites, spatial relationship between different binding sites, molecule composition, size, flexibility, valency for each antigen and half-life (1). Bispecific heterodimeric antibody formats have been shown to extend the therapeutic target space with novel mechanisms of action through their dual specificity, e.g. delivery through biological barriers, effector cell recruitment or inactivation of receptors and ligands (2). To address these diverse mechanisms of action, bispecific antibodies (bsABs) can be rationally designed in many formats,

Submitted: 1 April 2022; **Received (in revised form):** 27 October 2022; **Accepted:** 2 November 2022

ranging from two small antigen-binding fragments to large multi-domain Immunoglobulin G (IgG)-like molecules. As of now, over 100 bsAbs are in clinical development with more than 30 different bsAb formats (3). This variety of bsAbs in clinical trials demonstrates that the field is utilizing a diverse panel of formats to fit the respective target product profile. Importantly, it has been recognized that the molecule format defines the functionality of the bsAbs (4). Identifying the most suitable format for a given mode of action requires novel *in vitro* assays during development, which enable screening of a large number of complex antibody formats for different antibody properties (5).

While the diversity of bsAb formats serves as a prerequisite to their extended therapeutic potential, the increasing complexity impairs a streamlined and reproducible production process. Their heterodimeric composition (3–4 different chains in contrast to two in IgG) poses inherent chain association problems, as 10–16 different antibody species can be formed with only one having the desired functionality (6). bsAb formats, therefore, require extensive optimization of the expression system with a focus on reducing the levels of undesired antibody species, besides yield and stability. Aiming to maximize the expression of individual chains of a bsAb is inadequate for reducing undesired antibody species, rather optimal subunit gene dosage of each chain is required to prevent the formation of unwanted product species (7). Specific molecule design strategies, e.g. knobs-into-holes technology combined with CrossMab technology greatly enhances correct chain association (8, 9). Additional progress was achieved by excluding position-specific effects by using targeted integration (TI) host(s), allowing for homogeneous gene expression via integrating predefined expression vectors in the TI landing pad (10, 11). Regardless, the manufacturing yields of complex antibody formats are lower than monoclonal antibodies, making them 'difficult-to-express' (DTE).

CHO cells serve as the preferred expression system for the commercial production of therapeutic proteins (12). During the development of stable recombinant CHO cell lines, high-producing clones are generated and tested extensively to identify lead clone(s) for commercial manufacturing use. Notably, clone performance early during the cell line development process and at small scales (shake flask, multiwells) is not necessarily predictive of industrial scale performance (13). Constant changes in CHO genome via rearrangements and DNA methylation patterns result in large diversity of genotypes spontaneously arising in CHO cell populations (14). This instability is a constant and unpredictable feature with no population being stable or uniform over an extended period of time (15, 16). However, the success of CHO cells in biomanufacturing is at least partly based on this flexibility to adapt to any given environment quickly (17). Importantly, once cells have physiologically adapted to their new environment, i.e. the bioreactor set-up, their phenotype remains stable, as long as this environment is kept (17). The field is, therefore, relying on miniaturized microbioreactor (MBR) systems as downscale models to closely mimic the production process of current good manufacturing practice in large-scale bioreactors (18). The MBR systems have been shown to reproduce the performance of CHO clones under conventional bioreactor production conditions (with regulated pH, dissolved oxygen, CO_2 and nutrition levels) (19).

The increasing demand of high-value DTE molecules is illustrated by more than 100 bsAbs currently in clinical trials, which underlines the need for developing high-yield expression systems. Clustered regularly interspaced short palindromic repeats (CRISPR) technology is a promising method to engineer multiple cellular features for improving the CHO expression system. Targeted engineering of host cells by CRISPR/CRISPR associated protein 9 (Cas9) has already been successfully utilized to improve cellular characteristics in downscale model systems, e.g. host cell protein contamination (20), improved productivity (21, 22) and product glycosylation patterns (23).

Typically, due to low single-gene knockout (KO) efficiency at the pool level, this involves isolation of KO subclones to study their individual phenotypes. However, KO subclones can show remarkable phenotypical heterogeneity (24). Consequently, it remains unclear whether any observed effect reflects a general phenotype of the introduced KO or is solely a feature of a particular clone (25, 26).

Here, we devised a pooled single-gene-KO-based approach to determine the average effect of any genetic perturbation in order to obtain more reliable screening results. We screened the depletion of 187 target genes for their effect on the expression of two different DTE antibody formats in two CHO clones. While several hits increased titer >10%, we demonstrate that *Myc* KO strongly increased product expression (>40%) by enhancing cell-specific productivity under bioreactor conditions. *Myc* KO cells displayed decreased cell densities together with substantially higher product titers in industrial-relevant bioprocesses using ambr15 and ambr250 bioreactors. These effects were consistent across multiple additional CHO clones each expressing a distinct complex antibody format.

2. Materials and Methods

2.1 Cell culture

All cell lines were created using a previously generated CHO Host Cell Line (International patent publication number WO 2019/126 634 A2). CHO cells were cultured in a proprietary Dulbecco's Modified Eagle's Medium/F12-based medium in 125–500-ml shake flask vessels at 150 rpm, 37°C, 80% rH and 5% CO_2. Cells were passaged at a seeding density of 3–6 × 10^5 cells/ml every 3–4 days. Pools of cells that stably express bsAb molecules were generated as described (10). Briefly, expression plasmids were transfected into CHO cells by MaxCyte STX electroporation (MaxCyte, Inc.). The transfected cells were then selected and the expression of mAb was confirmed by flow cytometry via human IgG staining (BD FACS Canto II flow cytometer, BD). CHO clones were selected after single cell cloning by limited dilution, titer and binder validation by enzyme-linked immunosorbent assay and evaluation of volumetric productivity in fed-batch production assays in ambr15 and ambr250 bioreactors (Sartorius AG).

2.2 Fed-batch production assay

Fed-batch production cultures were performed in shake flasks or ambr15 or ambr250 bioreactors (Sartorius AG) with proprietary chemically-defined production media. Cells were seeded as indicated between 2 and 15 × 10^6 cells/ml on Day 0 of the production stage after adaptation to production media during two passages. Cultures received daily proprietary feed medium after Day 3 and additional feed bolus on Days 3 and 7, with optional bolus at Day 10. Cells were cultivated for 14 days. Production in the ambr15 system was operated at set points of 36°C, dO 30%, pH 7.0 and an agitation rate of 1200 rpm. Production in the ambr250 system was operated at set points of 35°C, dO 30%, pH 7.0 and an agitation rate of 1300 rpm with shift to 1600 rpm on Day 3.5.

2.3 Offline sample analysis

Process parameters were analyzed with Osmomat Auto (Gonotec GmbH, Berlin, Germany) for the measurement of osmolality and a

Cedex Bio HT Analyzer (Roche Diagnostics GmbH) for the measurement of product and selected metabolite concentrations. Total cell count, viable cell concentration and average cell diameter were measured by Cedex HiRes Analyzer (Roche Diagnostics GmbH).

Integrated cell volume and specific productivity rates (SPRs) for each condition were calculated based on the relationship shown:

$$IVCV_n = IVCV_{n-1} + \frac{VCV_n + VCV_{n-1}}{2} * (t_n - t_{n-1})$$

$$\mathrm{SPR}_{\mathrm{delta}_{\mathrm{IVCVn}}} = \frac{\mathrm{dcPRD}}{\mathrm{dIVCV}} = \frac{\mathrm{cPRD_n} - \mathrm{cPRD}_{n-1}}{\mathrm{IVCV_n} - \mathrm{IVCV}_{n-1}} * 24$$

2.4 Generation of pooled single-gene KOs and KO confirmation

Targets were deliberately chosen and guides were designed using the Geneious Prime software (version 2020.2.4, Off-target Library: CHO Reference Genome GCA_003668045.1_CriGri-PICR_genomic). All single guide ribonucleic acid (sgRNA) sequences and verification primers are listed in Supplementary Table S1. For KO introduction, CHO producer clones were transfected with ribonucleoprotein (RNP) complexes comprising gene-targeting sgRNA and Cas9 protein using the MaxCyte STX electroporation system (MaxCyte, Inc.). Guide RNA-Cas9 RNP complexes were prepared by mixing sgRNA (total of 40 pmol for each nucleofection) with an equimolar amount of Cas9 protein (TrueCut Cas9 Protein v2, Thermo Fisher Scientific Inc.) followed by incubation at room temperature (RT) for 20 min. Cells were washed in phosphate-buffered saline (PBS) (300 g, 5 min) and resuspended in the respective electroporation buffer (MaxCyte EP Buffer, Maxcyte Inc.).

Genomic DNA was extracted using QuickExtract™ DNA Extraction Solution (Lucigen) according to the manufacturer's instruction after cells have recovered from transfection (6–8 days post transfection). Polymerase chain reaction (PCR) (98°C for 30 s; 35 times: 98°C for 5 s, 60°C for 20 s and 72°C for 90 s/72°C for 90 s) was performed with the Q5 Polymerase 2× Master Mix (New England Biolabs, Inc.). Amplicons were purified with QIAquick® 96 PCR Purification Kit (Qiagen). Sanger sequencing was performed by Microsynth AG (Belgach, Switzerland). The PCR products produced were analyzed via electrophoresis on 2% agarose.

KO scores were assessed by the offline version of the Inference of CRISPR Edits software for analyzing Sanger sequencing data (available at https://github.com/synthego-open/ice).

2.5 Arrayed CRISPR KO screening workflow

For KO introduction, two CHO clones producing Molecules 1 and 2 (Figure 2a) were transfected with RNP complexes comprising gene-targeting sgRNA and Cas9 protein using the Lonza 96-well shuttle system (Lonza Group Ltd). Guide RNA–Cas9 RNP complexes were prepared by mixing sgRNA (40 pmol/sgRNA) with an equimolar amount of Cas9 protein (TrueCut Cas9 Protein v2, Thermo Fisher Scientific Inc.) followed by incubation at RT for 20 min. Electroporation (program DS 167) was performed after cells were washed in PBS (300 g, 5 min) and resuspended in the respective electroporation buffer (SF Cell Line 4D-Nucleofector™ X Kit, Lonza Group Ltd). After KO introduction, cells were cultivated in 24-well plates (Thermo Fisher Scientific Inc.) for 5 days. Genomic DNA for KO confirmation was extracted on Day 7 as described in the previous section. Cells were subsequently cultivated and, therefore, transferred in 24 deep-well plates (Porvair Sciences Ltd). Batch production cultures were performed in 24 deep-well plates with proprietary chemically-defined production media after upscale to a total volume of 4.5 ml. Cells were seeded with 5×10^6 cells/ml on Day 0 of the production stage after adaptation to production media during two passages. The batch production supernatant was harvested after cultivation for 4 days without any additional feeds.

2.6 Antibody analytics in supernatant

Supernatants were clarified (1000 g, 30 min, 4°C centrifugation and 1.2-μm filtration, AcroPrep 96 Filter Plates, Pall Cooperation). Analytical protein A chromatography was performed by ultra high performance liquid chromatography with ultraviolet (UV) light detection (Dionex Ultimate 3000 UHPLC fitted with POROS™ A 20 μm Column, Thermo Fisher Scientific Inc.).

Antibody integrity was analyzed after protein A affinity chromatography (PreDictor RoboColumn MabSelect SuRe, Cytiva) and normalization with protein quantitation using UV measurement (Nanoquant Infinite M200, Tecan). Percentage of correctly assembled antibodies (Main-Peak) was assessed by capillary electrophoresis sodium dodecyl sulfate (CE-SDS; HT Antibody Analysis 200 assay on the LabChip GXII system, PerkinElmer) under non-reducing conditions by relative quantification of the expected protein size to total protein content.

Antibody quality was analyzed by liquid chromatography–mass spectrometry (LC-MS) as described by Haberger *et al.* (27). Poros A purified antibody material was denatured in 0.36 M Tris, 2 mM ethylenediaminetetraacetic acid and 6 M Gua, pH 7. For reduction, 4 μl of 1 M dithiothreitol (DTT, Roche) was added, followed by incubation at 37°C for 1 h. After alkylation of free cysteines by adding 10.4 μl of 1 M iodoacetic acid and incubation at RT in the dark for 15 min, the reaction was stopped by adding 2 μl of 1 M DTT. The buffer was exchanged to digestion buffer (50 mM Tris/HCl and 2 mM $CaCl_2$, pH 7.5) by application onto a NAP-5 gel filtration column (GE Healthcare). Subsequently, the NAP-5 eluate (500 μl) was mixed with 10 μl of a 0.25 mg/ml trypsin solution (Trypsin Proteomics grade, Roche) in 10 mM HCl and incubated at 37°C for 1 h. The digest was stopped by adding 10 μl of 54 mM Met in 80% formic acid in water. Ten microliters of the tryptic peptide mixture were injected for analysis.

Samples were separated on a RP C18 column (BEH C18 1.7 μm, 2.1 × 150 mm; Waters) using an UltiMate 3000 Rapid Separation LC (Thermo Fisher Scientific Inc.) and analyzed online with an Orbitrap Fusion Tribrid electrospray mass spectrometer (Thermo Fisher Scientific Inc.). The mobile phases consisted of 0.1% formic acid in water (Solvent A) and 0.1% formic acid in acetonitrile (Solvent B). The chromatography was carried out using a gradient from 1 to 35% Solvent B in 45 min and finally from 35 to 80% Solvent B in 3 min using a flow rate of 300 μl/min. UV absorption was measured at a wavelength of 220 nm. The Rapid Separation Liquid Chromatography system and mass spectrometer were connected by PEEK capillary tubing. Data acquisition was controlled by the Orbitrap Tribrid MS Series Instrument Control Software Version 3.4 (Thermo Fisher Scientific Inc.). Parameters for MS detection were adjusted according to existing knowledge gained from experience with peptide analysis of recombinant antibodies.

2.7 RNA sample preparation and analysis

Control and KO pool cells (10×10^6) sampled from the ambr15® bioreactor on Day 10 were washed twice in PBS and snap-frozen in liquid nitrogen. RNA extraction, Illumina stranded TruSeq RNA library preparation, poly(A) enrichment and sequencing (NextSeq, v2.5, high.output 1 × 75 bp) was performed by Microsynth AG

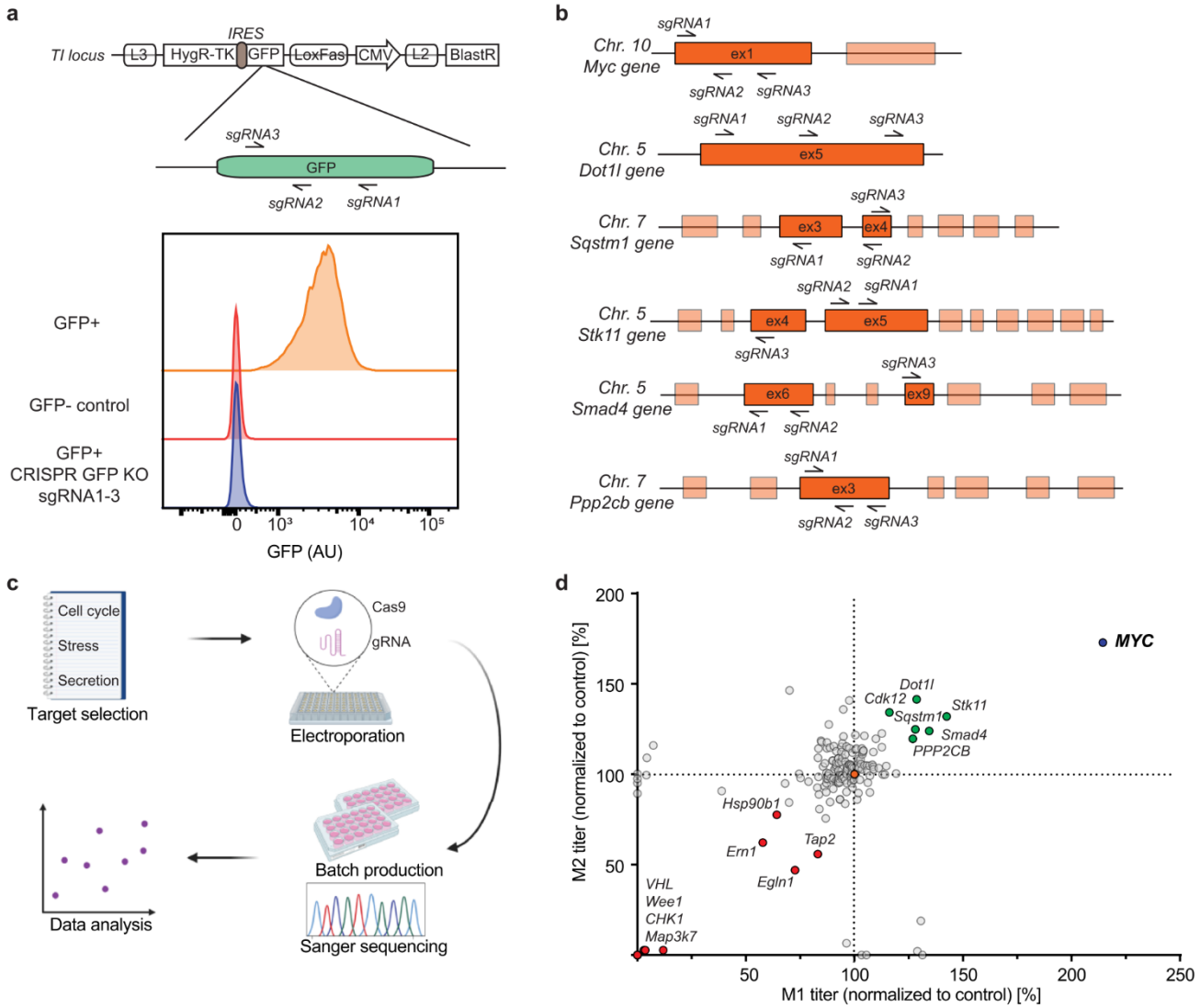

Figure 1. Arrayed CRISPR-screening-workflow identifies *Myc* KO as beneficial KO for productivity. (a) RNP-based pooled single-gene KO protocol, using three sgRNAs binding in close genomic proximity and targeting the landing pad-encoded GFP in the TI-CHO host cell line. After GFP KO, cells were grown for 6 days and analyzed using flow cytometry. (b) Experimental outline of the pooled single-gene KO strategy, exemplary shown for *Myc*, *Stk11*, *Dot1l*, *Smad4*, *Sqstm1* and *Ppp2cb* gene KO. (c) Experimental high-level outline of the arrayed CRISPR/Cas9 screening process. Key target key players of different cellular pathways including cell growth, protein secretion, stress responses and others were knocked-out using CRISPR/Cas9, and CHO cells were tested in a production-mimicking batch process. (d) Normalized bsAb titers after protein A purification from the arrayed CRISPR/Cas9 KO screening using a production-mimicking 4-day batch process.

(Belgach, Switzerland). Sequences for the transgene and the reference genome were analyzed separately. Reads were aligned using the HISAT2 package (version 2.2.1), and transcript abundance was calculated with featureCounts (version 2.0.1). The percentage of reads that mapped to either the transgene or the reference sequence ranged from 80.7 to 90.2%. Differential expression was calculated using edgeR by pooling untreated and *Myc* KO production clones as biological replicates. Significant changes in expression level were defined based on *P*-value ($P < 0.05$) and fold change ($|FC| > 1.25$) cut-offs. Over-representation analysis (ORA) was performed on all significantly changed genes by g:profiler (https://biit.cs.ut.ee/gprofiler/).

3. Results

3.1 An arrayed CRISPR/Cas9 KO screen reveals *Myc* KO to increase complex bsAB productivity

CRISPR/Cas9-based gene KOs are the preferred choice for simple, fast and efficient perturbation of target gene functions. To be able to evaluate the effect of any given KO in an efficient and unbiased manner, we established a highly-efficient RNP-based multi-guide pooled single-gene KO strategy for a TI-CHO cell line (10). Our optimized RNP-based KO protocol was established by targeting the landing pad encoding green fluorescent protein (GFP) in the TI-CHO host cell line using three sgRNAs binding in close genomic proximity and resulted in a complete loss of GFP fluorescence 6 days after RNP delivery (Figure 1a, Supplementary Figure S1a). Utilizing this pooled single-gene KO strategy (selected examples are shown in Figure 1b), we rationally chose 187 key players of different cellular pathways including cell growth, protein secretion, stress responses and others as target genes for KO (Figure 1c and Supplementary Table S1). To test the effect of each KO on productivity, we subjected all single-gene KO pools to a 4-day batch production process, which mimics the conditions used in state-of-the-art bioprocesses. We verified that variation of product titer within our screening system was limited to <3% of standard deviation (Supplementary Figure S1b).

KO of these target genes in two CHO clones revealed that pooled KO of *Dot1l, Stk11, Cdk12, Sqstm1, Smad4* and *Ppp2cb* improved productivity of both clones by >10% in a batch process (Figure 1d, M1: Cytokine Fusion, M2: 1 + 1 Ligand Binder). Interestingly, KO of the proto-oncogene *Myc* led to a substantial relative titer increase of 1.7–2.1× fold in the two cell clones (Figure 1d). KO of conditionally essential genes *Rbx1, Vhl, Wee1* and *Chk1* and KO of the essential gene *Map3k7* resulted in loss of the cell population after KO in one or both tested CHO clones, confirming the highly-efficient KO protocol (28) (Figure 1d). PCR amplification of our multi-guide target sites within the genes revealed substantial locus fragmentation compared to the unmodified locus, exemplarily showed for *Myc, Stk11, Dot1il, Smad4, Sqstm1* and *Ppp2cb* (Supplementary Figure S1d). We found no significant differences in main product quantities as measured by CE-SDS of protein-A-purified supernatants, indicating that the correct assembly of the antibody chains was not perturbed by the introduced KOs (Supplementary Figure S1c). Intrigued by the strong impact of *Myc* KO on productivity, we decided to focus on its validation across different cell lines and molecule formats.

3.2 *Myc* KO reduces cell proliferation and consistently improves SPRs in PSB clones

Next we wanted to exclude the option that the observed *Myc* KO phenotype is an artifact of the two tested CHO clones. We, therefore, tested *Myc* KO and respective control cells performance side-by-side on seven different CHO clones from a primary seed bank (PSB) of M1 for production performance under fed-batch conditions in ambr15 bioreactors, an important step for the selection of lead clones during cell line development (Figure 2a). All *Myc* KO pools showed a volumetric productivity increase between 7 and 29% compared to control cells (Figure 2b) and no loss in product quality, as assessed by CE-SDS analysis (Figure 2c). Simultaneously, we observed a substantial decrease in viable cell density (VCD) during the bioprocess, displayed by a 28% reduced peak VCD at Day 7 (Figure 2d). This is in line with previous findings where depletion of Myc resulted in the inhibited proliferation of tumor cells (29). Cell division ceased around Day 7 during the fed batch with peak VCD in general reached on Day 7. However, cells continued to grow in volume and increased their average diameter by 3 μm, which amounts to 2-fold between the start and end of the fed batch (Figure 2e). *Myc* KO pools showed an additional 15% increase in cell volume on average compared to control cells, indicating a partial shift from cell division toward cell growth by *Myc* KO (Figure 2e).

To rule out that the phenotype observed after *Myc* KO was the result of undesired locus fragmentation, we generated *Myc* KO with individual sgRNAs instead of the previous multiplexing approach. Using multiple sgRNAs simultaneously can lead to unintended on-target effects as for example rearrangements in the genome that affect protein production. We tested Myc ablation with three different sgRNA sequences independently using two different producer clones during fed-batch production (Figure 1b). Notably, all three sgRNAs target the coding sequence of *Myc*, but share no sequence similarity and have different predicted off-target sequences (Supplementary Table S4). All three used sgRNAs improved volumetric productivity in both CHO clones as well as decreased peak VCD during fed-batch production (Supplementary Figure S2c and d).

We conclude that *Myc* KO improved volumetric productivity consistently in CHO clones, potentially through a general switch from growth toward production phenotype.

3.3 *Myc* KO improves specific productivity regardless of the molecule format

Next, we evaluated whether *Myc* KO improves productivity of other CHO clones expressing various complex molecule formats in an MBR set-up. We selected eight antibody-producing PSB candidates each producing a distinct complex format (Figure 3a: M1: Cytokine Fusion, M3/M9: 1 + 1 CrossMab, mAB, M4: mAB, M5: DutaFab, M6: Brain Shuttle Fusion, M7: 2 + 1 T-Cell Bispecific, M8: Fc-Fragment). To enable KO quantification by Sanger trace decomposition, we reduced the amount of sgRNA to one and observe the predicted *Myc* KO efficiencies between 13 and 80% in the production clones (Supplementary Table S2). We, therefore, expected an intermediate impact on productivity phenotype; however, by conducting experiments in a pool format we could simultaneously exclude any potential impacts that would otherwise be introduced via sub-cloning process. We analyzed all *Myc* KO and respective control cells side-by-side for production performance using an industrial-relevant fed-batch process in ambr15 bioreactors. Of note, production clones display substantial clonal heterogeneity and therefore show increased variation in general cell characteristics (14).

Remarkably, all *Myc* KO pools showed improved volumetric productivity, in most cases immediately after the beginning of the production process (Figure 3b). On average, the *Myc* KO pools showed a 17% reduction in peak VCD, indicating that Myc supports cell division during fed-batch production (Figure 3c). In general, cell division ceased quickly during the fed batch with peak VCD reached on Day 3. However, cells continued to grow in size and increased their average diameter by 3–5 μm between the start and end of the fed batch in *Myc* KO conditions (Figure 3d). *Myc* KO pools showed an additional 8% increase in cell size compared to control cells throughout the fed batch, indicating a partial shift from cell division toward cell volume growth upon *Myc* KO. The increased overall product is based on higher SPRs of *Myc* KO pools during the whole process: on average SPR increased between 14 and 99% (Figure 3e).

To verify that *Myc* KO led to the accumulation of high-quality product we tested the overall protein composition as well as post-translational modifications (PTMs) of each molecule. Increased protein production puts additional load on the secretory pathway that, in turn, might affect folding and PTMs. CE-SDS analysis of *Myc* KO pools and controls demonstrate highly comparable overall molecule composition (Supplementary Figure S2a). Additionally, we analyzed Fc glycosylation, Asn deamidation, Met oxidation, Lys-loss, and N/C-terminal modifications at the peptide level by LC-MS. We did not find any significant alterations on the PTM pattern on molecules produced in *Myc* KO cells, as compared to the control (Supplementary Table S5).

To evaluate the molecular basis for increased SPR of *Myc* KO cells, we analyzed the CHO cell transcriptome by RNA-Seq at Day 10 of fed-batch production. Depending on the production clone, between 8 and 29% of the transcriptome was derived from the antibody transgenes (Figure 3f). This percentage increased on average by 3%, indicating that a generally higher portion of *Myc* KO cells' transcriptome contained the antibody transgenes. Upon transcript normalization, *Myc* KO cells

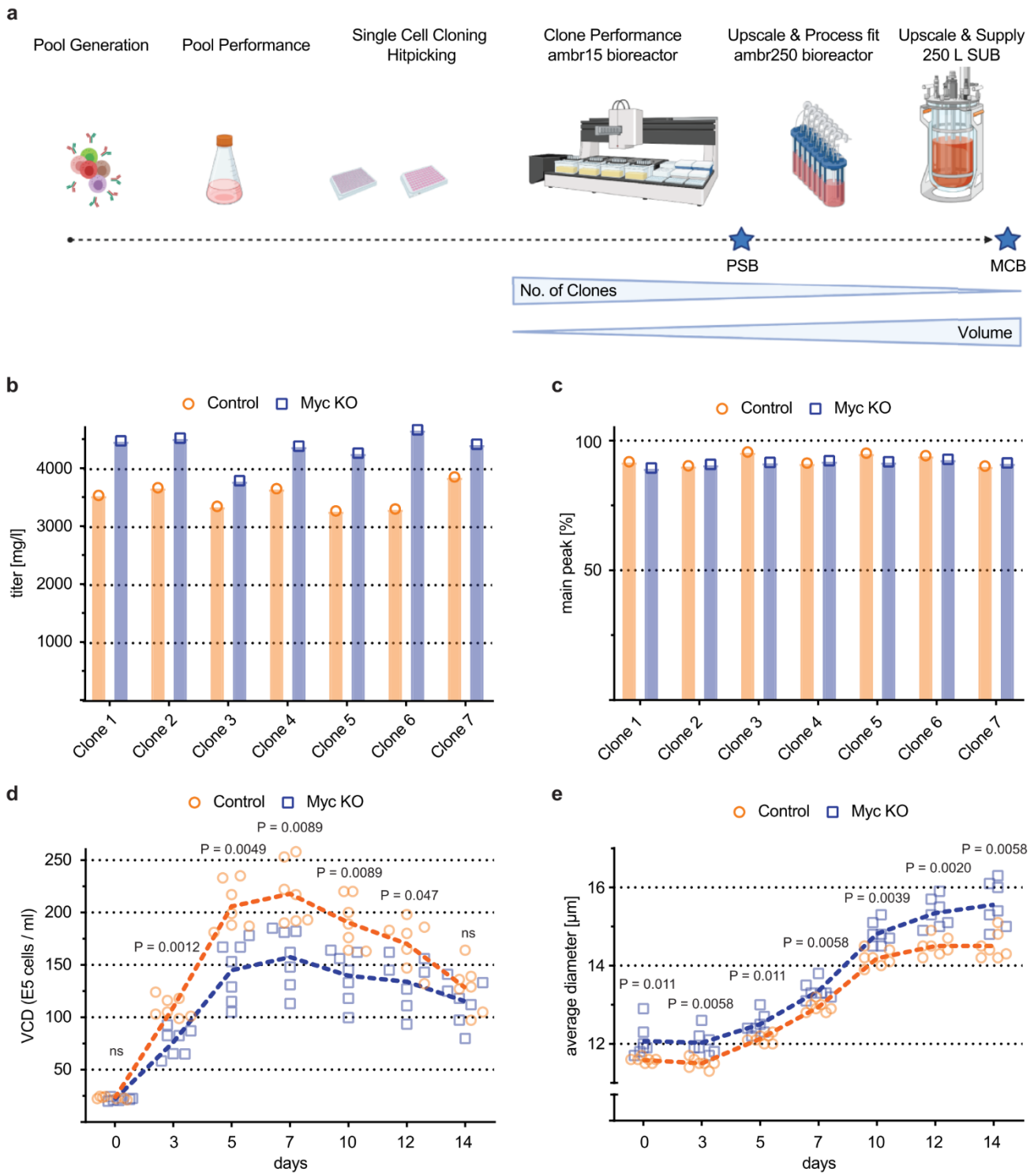

Figure 2. The beneficial effects of *Myc* KO are consistent among all tested clones of a bsAb PSB. (a) Schematic overview of an industrial cell line development process. Stable expression pools are tested for pool performance, and high-productivity pools undergo single cell cloning. Clones are expanded, banked (PSB) and tested for clone performance in ambr15 bioreactors. After upscale and validation using ambr250 bioreactors, the best-performing PSB clone will be expanded as the master cell bank. Illustration created with BioRender.com. (b) Day-14 titers of ambr15 fed-batch process after protein A purification. *Myc* KO pools and mock-treated control cells of seven high-productivity PSB clones expressing a cytokine-fusion bsAb (M1) are shown. (c) Day-14 product quality (main peak, CE-SDS) of ambr15 fed-batch process of *Myc* KO pools and mock-treated control cells of seven high-productivity PSB clones expressing a cytokine-fusion bsAb (M1) are shown. (d) VCD and (e) average diameter of individual cells during the 14-day ambr15 fed-batch process. All data are mean ± SEM. *P* = adjusted *P*-values. Statistical significance was determined using the Holm–Sidak method. Each row was analyzed individually, without assuming a consistent SD.

showed 22–32% increase in relative antibody transcript abundance (Figure 3g). This indicates that the enhanced productivity phenotype of *Myc* KO cells may result from increased expression levels of antibody chain-encoding transcripts. ORA further showed that Myc depletion resulted in the enrichment of kyoto encyclopedia of genes and genomes pathways' protein processing in the

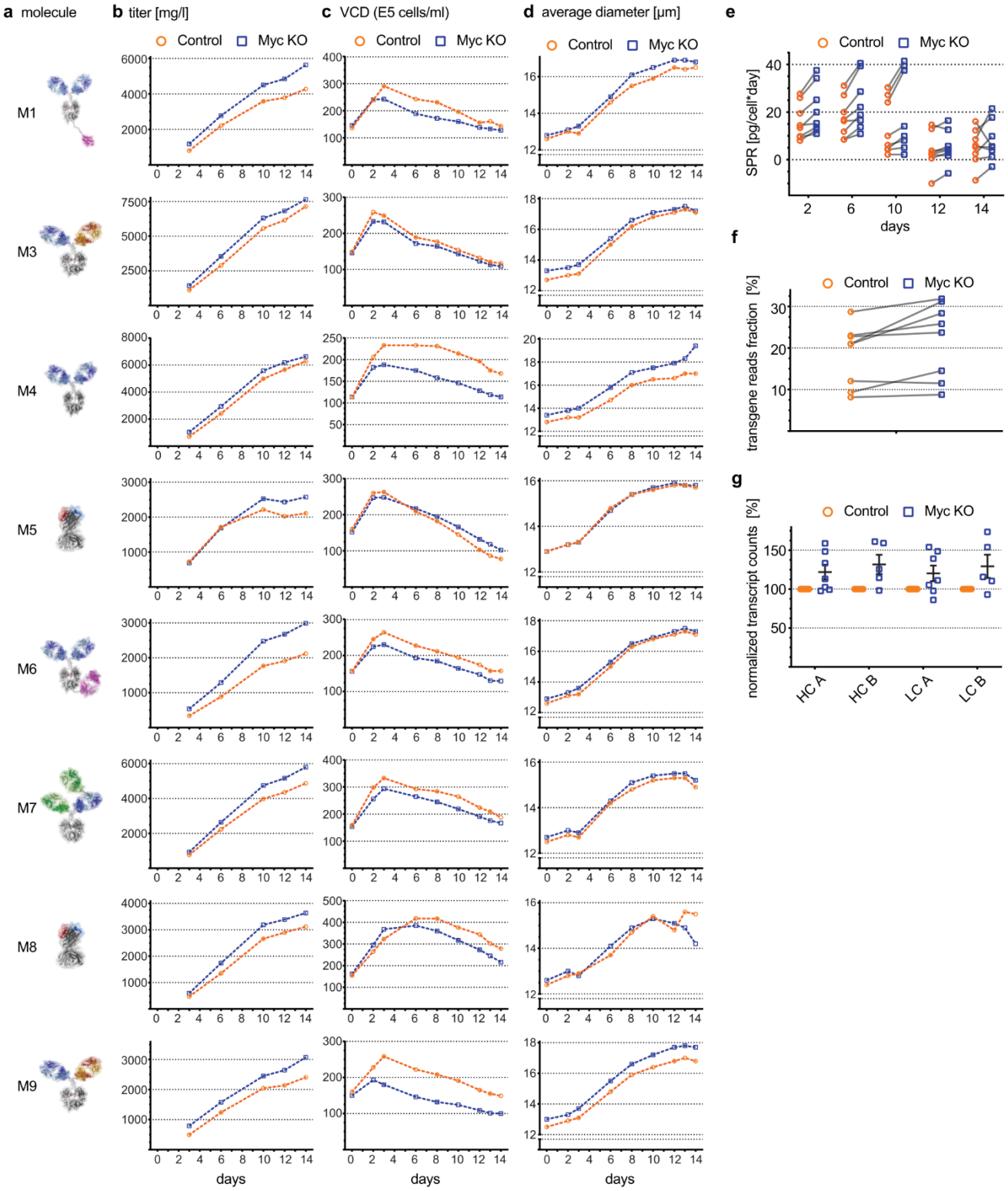

Figure 3. Myc depletion improves specific productivity of various CHO clones regardless of the expressed complex molecule format. (a) Schematic drawing of the individual molecule formats. All CHO clones resulted from individual industrial-relevant cell line developments. (b) Product titers of ambr15 fed-batch process after protein A purification. Simultaneous assessment of (c) VCD and (d) average cell diameter. Production clone performance of mock-treated control cells compared to *Myc* KO cells. (e) Specific production rates over the course of the ambr15 fed-batch process comparing mock-treated control cells with *Myc* KO cells. Specific production rates were calculated based on the product titers after protein A purification and the integrated cell volume over time. (f) Fraction of reads mapped to bsAb transgene sequences out of all reads that were successfully mapped to the Chinese Hamster RefSeq genes. All transgene chains were included in the analysis. Data from Day 10 of the ambr15 fed-batch process. (g) Normalized transcript counts from *Myc* KO cells mapping to one of the bsAB transgene chains relative to mock-treated control cells. Data from Day 10 of the ambr15 fed-batch process.

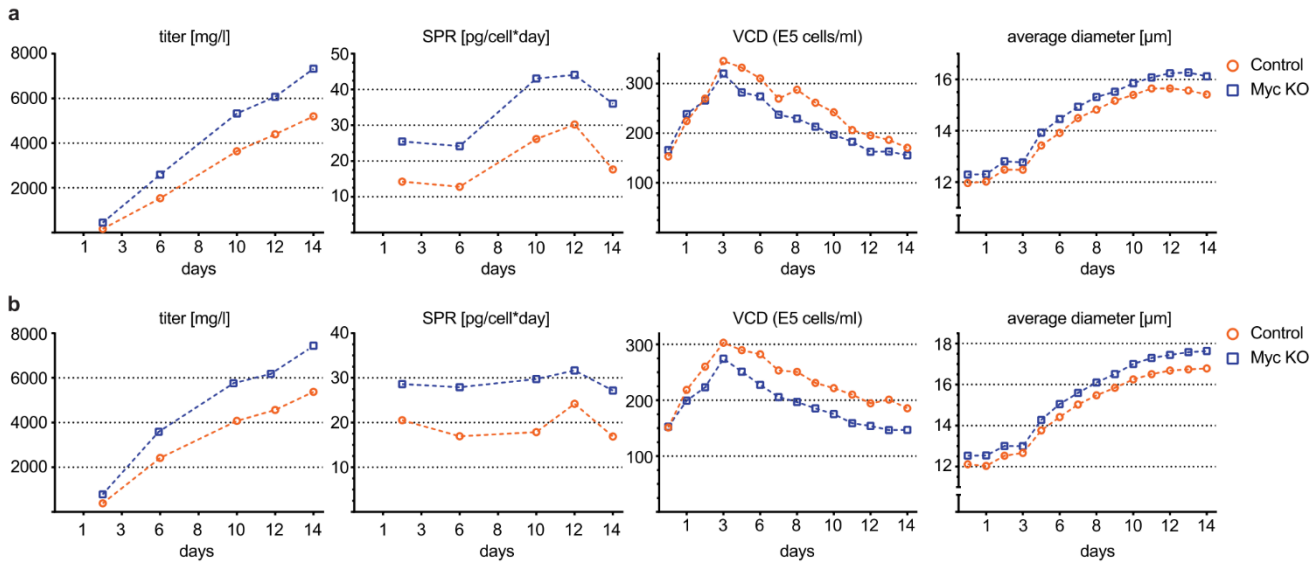

Figure 4. *Myc* KO cells reliably improve SPRs after upscale and bioprocess fit. CHO clones for Molecules 1 and 2 were cultivated in an industrially-relevant ambr250 fed-batch process. (a) Production-related data for Molecule 1 and (b) Molecule 2 with product titers after protein A purification, SPRs, VCD and average diameter (from left to right).

endoplasmic reticulum (ER) and protein export (Supplementary Table S3). Simultaneously, transcripts associated with the ER in general are significantly upregulated in Myc-depleted cells. This suggests that *Myc* KO further improved productivity of CHO clones by the increased expression of ER-related pathways.

These data indicate that *Myc* KO improved production performance of CHO cells in industrially-relevant production processes, regardless of the type of therapeutic protein and without impacting product quality.

3.4 Myc KO cells reliably improve production performance in scale-up ambr250 bioprocesses

The successful application of *Myc* KO cells in commercial scale processes requires the use of a reliable and qualified scale-down model (SDM). The ambr15 system is only suited as a SDM within bench scale (up to 200-l stirred bioreactors) (19, 30). To replicate the fermentation results within commercial scales, we next evaluated the performance of *Myc* KO in a scale-up fed-batch bioprocess using the ambr250 system (31). The higher cultivation volume (200–250 ml compared to 10–15 ml in the ambr15) allowed for increased sampling and product profiling, which otherwise would result in the substantial loss of production biomass in the ambr15 system. To verify the *Myc* KO in the ambr250 system, we generated *Myc* KOs in two lead industrial-relevant production cell lines (M1 and M2, Figure 4a and b).

Immediately after starting fed-batch production, *Myc* KO cells displayed increased volumetric productivity resulting in 38–41% increased titer on Day 14 of the fed-batch process. bsAb titers increased by 2067 and 2128 mg/l, respectively, with SPR of the *Myc* KO cells constantly higher throughout the process and in both cell lines by 8–23 pg/(cell × d). Peak VCD was reached on Day 3 and decreased steadily afterward, with *Myc* KO cells reaching lower VCD throughout the production process. After cells ceased to divide, cell growth continued in size with all conditions increasing their average diameter by 4–6 µm until the end of the fed-batch process. *Myc* KO cells showed an additional 14–16% increased size compared to control cells. The product profile from cell line molecule M1 (Cytokine Fusion) was assessed by CE-SDS and size-exclusion chromatography and showed comparable main product and aggregation rates in the supernatant after protein A purification (Supplementary Figure S2b, left panel). The product profile from cell line molecule M2 (1 + 1 ligand binder) displayed slightly reduced main product levels (Supplementary Figure S2b, right panel).

Together, our findings indicate that *Myc* KO cells displayed a superior phenotype during ambr250 fed-batch production by further boosting specific and volumetric productivity of clones in an industrially-relevant production process.

4. Discussion

Despite decades of improvements in CHO bioprocesses, high-value DTE bsABs still challenge current production capacities. To generate a high-yield expression system, genetic modifications of the expression system are increasingly used to improve their suboptimal secretory phenotype. Previous studies have shown that the productivity of DTE antibodies can be enhanced by decoupling growth and production phases (32–34). This results in the downregulation of cell proliferation and a redistribution of cellular resources toward increased recombinant protein production (35). Common strategies to halt proliferation and increase productivity included mild hypothermic cultivation (36), osmotic stress (37), addition of chemical agents (38) or genetic engineering (34).

However, not all cell lines with high productivity show an increase in productivity by lowering temperature or increasing osmolarity during production, suggesting that these strategies are product, cell line or even clone specific (39, 40). In this study, we therefore decided to apply an unbiased screening approach by introducing CRISPR-induced KOs into CHO clones expressing DTE complex antibody formats and measured productivity increase side-by-side to the non-engineered parent clone. We identified *Myc* KO to consistently increase productivity of multiple CHO clones expressing different DTE formats in industrially-relevant bioprocess applications. In addition to the superior production phenotype, *Myc* KO cells exhibit reduced cell growth, increased cell volume and substantially improved SPRs.

The transcriptomic analysis of *Myc* KO cells demonstrates a substantial increase of antibody-encoding transcripts in fed-batch production processes. Thus, the improved specific productivity upon Myc depletion appears to be, at least partly, related to the observed higher mRNA levels. Studies using a range of cell lines suggest that higher transgene mRNA levels contribute to improved specific production rates until a certain saturation level of mRNA, after which the control may shift to post-translational events (41). Here, we found that CHO clones devote up to 29% of their total mRNA to the transgene, which is increased by ∼4% on average by Myc depletion. Interestingly, the relative transcript count shifted to a much higher proportion toward the transgene, resulting in a relative increase in transgene transcript levels by ∼25%. Thus, Myc depletion redistributed transcriptional resources toward the transgene transcription. It is conceivable that the strong gene expression elements used in the transgene attract the freed transcriptional resources previously spent on cell division and thus increase the relative abundance of transgene mRNA. These transcriptional changes were associated with higher expression of ER-related proteins. Myc depletion seems to impact both transgene transcription and translational machinery of CHO clones and extends their overall production capacities. This observation was supported by the findings that while all the *Myc* KO clones expressing different molecules showed increased specific productivity, two did not increase their transgene mRNA levels.

A similar phenotypic change, i.e. the shift from reduced cell proliferation toward increased cell volume and higher specific production rates, was observed in a recent study in CHO production cells when overexpressing the BLIMP1 gene (42). The authors associate the effects of BLIMP1 overexpression with the repression of Myc levels, indicating a similar biological mechanism to direct Myc ablation. However, in contrast to our study, no increase in transgene mRNA levels was observed after BLIMP1 overexpression (42). Myc as a direct engineering target has been addressed in different contexts before, due to its general role in cell proliferation and apoptosis. For example, Myc overexpression in CHO cells was previously shown to result in increased cell densities and growth rates (43). In contrast, the suppression of Myc results in inhibited cell proliferation, together with G1/G0 cell cycle arrest and decreased apoptosis (44). Due to the strong effect of *Myc* KO on cell proliferation, cells with intact endogenous Myc will proliferate faster compared to their KO counterpart. This may explain the observed varying levels of *Myc* KO levels in the different CHO clones.

Utilizing multiple KOs could further amplify the beneficial effect observed with *Myc* KO. This could especially be the case if the productivity is increased by different mechanisms, e.g. increasing transgene transcript abundance while simultaneously alleviating secretory bottlenecks during folding or secretion. Kol *et al.* have shown that this multiplexed engineering approach can modify multiple cellular characteristics simultaneously, i.e. reducing unnecessary host cell proteins while simultaneously increasing productivity and cell growth (20). Future studies could combine the partially beneficial effects we observed after *Dot1l*, *Stk11*, *Cdk12*, *Sqstm1*, *Smad4* and *PPP2CB* KO in combination with *Myc* KO.

Finally, it is worth noting that the effects of Myc ablation on productivity might synergize well with high-cell density production processes, where the higher SPRs together with increased cell densities lead to substantially improved volumetric titers. In these production conditions, the inhibition of cell proliferation has lesser impact on volumetric titer, as these processes start with cell densities of 10–20 × 10^6 cells/ml or more. In summary, the data provided in this manuscript illustrate the potential of CRISPR/Cas9-based CHO host cell engineering and provide an avenue to increase manufacturing yields of high-value complex biotherapeutics.

Supplementary data

Supplementary data are available at SYNBIO online.

Data availability

The data supporting the findings of this study are available within the article and its supplementary materials. Nucleic acid sequences encoding for antibody sequences are proprietary to Roche.

Material availability

CRISPR/Cas9 gRNAs are available upon request. Nucleic acids and cell lines encoding for antibody sequences are proprietary to Roche.

Funding

Roche Diagnostics GmbH and Genentech funded all of this work; Inc. European Research Council under the European Union's Horizon 2020 research and innovation programme [801750 to J.S.]; Alfried Krupp Prize for Young University Teachers awarded by the Alfried-Krupp von Bohlen und Halbach-Stiftung [to J.S.]; European Molecular Biology Organization [YIP4644 to J.S.]; Vallee Foundation [to J.S.]; Deutsche Forschungsgemeinschaft (German Research Foundation) [Project-ID 213249687—SFB 1064 to J.S.].

Acknowledgments

The authors are grateful to Harald Duerr, Bianca Nussbaum, Korbinian Kneidl, Uta Werner and Stephanie Kappelsberger for bsAB purification and product quality analytics. Furthermore, they thank Jasmin Inzinger and Christian Schwald for ambr250 cultivation, Stefan Klostermann for bioinformatics support and Dominique Ostler for providing the Lonza 96-shuttle system. They are also grateful to Anke Marshall, Karen Dericks and Julia Bercher for cell culture support as well as Markus Haberger and Michaela Hook for LC-MS analysis.

Author contributions

N.B., B.O., M.E., L.S., E.L. and A.O. designed, performed and analyzed the experiments. S.A. conceived the project and obtained funding. S.A., C.S., A.S., S.M. and J.S. interpreted the results and helped in improving the manuscript. N.B. wrote the manuscript with input from all authors.

Conflict of interest statement. A patent based on this work has been filed with authors N.B, B.O. and S.A. as inventors. N.B., B.O., M.E., L.S., E.L., C.S., A.O., A.S., S.M. and S.A. were employees of Roche Diagnostics GmbH or Genentech, Inc., which developed and sold pharmaceuticals during the time when this research was carried out. All other authors declare no competing interests.

References

1. Spiess,C., Zhai,Q. and Carter,P.J. (2015) Alternative molecular formats and therapeutic applications for bispecific antibodies. *Mol. Immunol.*, **67**, 95–106.

2. Klein,C., Sustmann,C., Thomas,M., Stubenrauch,K., Croasdale,R., Schanzer,J., Brinkmann,U., Kettenberger,H., Regula,J.T. and Schaefer,W. (2012) Progress in overcoming the chain association issue in bispecific heterodimeric IgG antibodies. *MAbs*, **4**, 653–663.
3. Labrijn,A.F., Janmaat,M.L., Reichert,J.M. and Parren,P.W.H.I. (2019) Bispecific antibodies: a mechanistic review of the pipeline. *Nat. Rev. Drug Discov.*, **18**, 585–608.
4. Nie,S., Wang,Z., Moscoso-Castro,M., D'Souza,P., Lei,C., Xu,J. and Gu,J. (2020) Biology drives the discovery of bispecific antibodies as innovative therapeutics. *Antib. Ther.*, **3**, 18–62.
5. Dengl,S., Mayer,K., Bormann,F., Duerr,H., Hoffmann,E., Nussbaum,B., Tischler,M., Wagner,M., Kuglstatter,A., Leibrock,L. *et al.* (2020) Format chain exchange (FORCE) for high-throughput generation of bispecific antibodies in combinatorial binder-format matrices. *Nat. Commun.*, **11**, 4974.
6. Schaefer,W., Volger,H.R., Lorenz,S., Imhof-Jung,S., Regula,J.T., Klein,C. and Molhoj,M. (2016) Heavy and light chain pairing of bivalent quadroma and knobs-into-holes antibodies analyzed by UHR-ESI-QTOF mass spectrometry. *MAbs*, **8**, 49–55.
7. Wang,Q., Chen,Y., Park,J., Liu,X., Hu,Y., Wang,T., McFarland,K. and Betenbaugh,M.J. (2019) Design and production of bispecific antibodies. *Antibodies (Basel)*, **8**, 43.
8. Carter,P. (2001) Bispecific human IgG by design. *J. Immunol. Methods*, **248**, 7–15.
9. Schaefer,W., Regula,J.T., Bahner,M., Schanzer,J., Croasdale,R., Durr,H., Gassner,C., Georges,G., Kettenberger,H., Imhof-Jung,S. *et al.* (2011) Immunoglobulin domain crossover as a generic approach for the production of bispecific IgG antibodies. *Proc. Natl. Acad. Sci. USA*, **108**, 11187–11192.
10. Carver,J., Ng,D., Zhou,M., Ko,P., Zhan,D., Yim,M., Shaw,D., Snedecor,B., Laird,M.W., Lang,S. *et al.* (2020) Maximizing antibody production in a targeted integration host by optimization of subunit gene dosage and position. *Biotechnol. Prog.*, **36**, e2967.
11. Ng,D., Zhou,M.X., Zhan,D.J., Yip,S., Ko,P., Yim,M., Modrusan,Z., Joly,J., Snedecor,B., Laird,M.W. *et al.* (2021) Development of a targeted integration Chinese hamster ovary host directly targeting either one or two vectors simultaneously to a single locus using the Cre/Lox recombinase-mediated cassette exchange system. *Biotechnol. Progr.*, **37**, e3140.
12. Wurm,F.M. (2004) Production of recombinant protein therapeutics in cultivated mammalian cells. *Nat. Biotechnol.*, **22**, 1393–1398.
13. Porter,A.J., Dickson,A.J. and Racher,A.J. (2010) Strategies for selecting recombinant CHO cell lines for cGMP manufacturing: realizing the potential in bioreactors. *Biotechnol. Progr.*, **26**, 1446–1454.
14. Weinguny,M., Klanert,G., Eisenhut,P., Lee,I., Timp,W. and Borth,N. (2021) Subcloning induces changes in the DNA-methylation pattern of outgrowing Chinese hamster ovary cell colonies. *Biotechnol. J.*, **16**, e2000350.
15. Vcelar,S., Jadhav,V., Melcher,M., Auer,N., Hrdina,A., Sagmeister,R., Heffner,K., Puklowski,A., Betenbaugh,M., Wenger,T. *et al.* (2018) Karyotype variation of CHO host cell lines over time in culture characterized by chromosome counting and chromosome painting. *Biotechnol. Bioeng.*, **115**, 165–173.
16. Weinguny,M., Klanert,G., Eisenhut,P., Jonsson,A., Ivansson,D., Lovgren,A. and Borth,N. (2020) Directed evolution approach to enhance efficiency and speed of outgrowth during single cell subcloning of Chinese hamster ovary cells. *Comput. Struct. Biotec.*, **18**, 1320–1329.
17. Wurm,M. and Wurm,F. (2021) Naming CHO cells for biomanufacturing: genome plasticity and variant phenotypes of cell populations in bioreactors question the relevance of old names. *Biotechnol. J.*, **16**, e2100165.
18. Sandner,V., Pybus,L.P., McCreath,G. and Glassey,J. (2019) Scale-down model development in ambr systems: an industrial perspective. *Biotechnol. J.*, **14**, 1700766.
19. Rameez,S., Mostafa,S.S., Miller,C. and Shukla,A.A. (2014) High-throughput miniaturized bioreactors for cell culture process development: reproducibility, scalability, and control. *Biotechnol. Progr.*, **30**, 718–727.
20. Kol,S., Ley,D., Wulff,T., Decker,M., Arnsdorf,J., Schoffelen,S., Hansen,A.H., Jensen,T.L., Gutierrez,J.M., Chiang,A.W.T. *et al.* (2020) Multiplex secretome engineering enhances recombinant protein production and purity. *Nat. Commun.*, **11**, 1908.
21. Lin,P.C., Liu,R., Alvin,K., Wahyu,S., Murgolo,N., Ye,J., Du,Z. and Song,Z. (2021) Improving antibody production in stably transfected CHO cells by CRISPR-Cas9-mediated inactivation of genes identified in a large-scale screen with Chinese hamster-specific siRNAs. *Biotechnol. J.*, **16**, e2000267.
22. Raab,N., Mathias,S., Alt,K., Handrick,R., Fischer,S., Schmieder,V., Jadhav,V., Borth,N. and Otte,K. (2019) CRISPR/Cas9-mediated knockout of MicroRNA-744 improves antibody titer of CHO production cell lines. *Biotechnol. J.*, **14**, e1800477.
23. Louie,S., Haley,B., Marshall,B., Heidersbach,A., Yim,M., Brozynski,M., Tang,D., Lam,C., Petryniak,B., Shaw,D. *et al.* (2017) FX knockout CHO hosts can express desired ratios of fucosylated or afucosylated antibodies with high titers and comparable product quality. *Biotechnol. Bioeng.*, **114**, 632–644.
24. Ko,P., Misaghi,S., Hu,Z., Zhan,D., Tsukuda,J., Yim,M., Sanford,M., Shaw,D., Shiratori,M., Snedecor,B. *et al.* (2018) Probing the importance of clonality: single cell subcloning of clonally derived CHO cell lines yields widely diverse clones differing in growth, productivity, and product quality. *Biotechnol. Prog.*, **34**, 624–634.
25. Joberty,G., Falth-Savitski,M., Paulmann,M., Bosche,M., Doce,C., Cheng,A.T., Drewes,G. and Grandi,P. (2020) A tandem guide RNA-based strategy for efficient CRISPR gene editing of cell populations with low heterogeneity of edited alleles. *CRISPR J.*, **3**, 123–134.
26. Wurm,F.M. and Wurm,M.J. (2017) Cloning of CHO cells, productivity and genetic stability—a discussion. *Processes*, **5**, 20.
27. Haberger,M., Heidenreich,A.K., Hook,M., Fichtl,J., Lang,R., Cymer,F., Adibzadeh,M., Kuhne,F., Wegele,H., Reusch,D. *et al.* (2021) Multiattribute monitoring of antibody charge variants by cation-exchange chromatography coupled to native mass spectrometry. *J. Am. Soc. Mass Spectrom.*, **32**, 2062–2071.
28. Gurumayum,S., Jiang,P., Hao,X., Campos,T.L., Young,N.D., Korhonen,P.K., Gasser,R.B., Bork,P., Zhao,X.M., He,L.J. *et al.* (2021) OGEE v3: online GEne essentiality database with increased coverage of organisms and human cell lines. *Nucleic Acids Res.*, **49**, D998–D1003.
29. Wang,H., Mannava,S., Grachtchouk,V., Zhuang,D., Soengas,M.S., Gudkov,A.V., Prochownik,E.V. and Nikiforov,M.A. (2008) c-Myc depletion inhibits proliferation of human tumor cells at various stages of the cell cycle. *Oncogene*, **27**, 1905–1915.
30. Janakiraman,V., Kwiatkowski,C., Kshirsagar,R., Ryll,T. and Huang,Y.M. (2015) Application of high-throughput mini-bioreactor system for systematic scale-down modeling, process characterization, and control strategy development. *Biotechnol. Progr.*, **31**, 1623–1632.
31. Manahan,M., Nelson,M., Cacciatore,J.J., Weng,J., Xu,S. and Pollard,J. (2019) Scale-down model qualification of ambr® 250 high-throughput mini-bioreactor system for two commercial-scale mAb processes. *Biotechnol. Progr.*, **35**, e2870.
32. Misaghi,S., Chang,J. and Snedecor,B. (2014) It's time to regulate: coping with product-induced nongenetic clonal instability in CHO

cell lines via regulated protein expression. *Biotechnol. Progr.*, **30**, 1432–1440.
33. Poulain,A., Perret,S., Malenfant,F., Mullick,A., Massie,B. and Durocher,Y. (2017) Rapid protein production from stable CHO cell pools using plasmid vector and the cumate gene-switch. *J. Biotechnol.*, **255**, 16–27.
34. Fussenegger,M., Schlatter,S., Datwyler,D., Mazur,X. and Bailey,J.E. (1998) Controlled proliferation by multigene metabolic engineering enhances the productivity of Chinese hamster ovary cells. *Nat. Biotechnol.*, **16**, 468–472.
35. Donaldson,J.S., Dale,M.P. and Rosser,S.J. (2021) Decoupling growth and protein production in CHO cells: a targeted approach. *Front. Bioeng. Biotech.*, **9**, 658325.
36. Oguchi,S., Saito,H., Tsukahara,M. and Tsumura,H. (2006) pH condition in temperature shift cultivation enhances cell longevity and specific hMab productivity in CHO culture. *Cytotechnology*, **52**, 199–207.
37. Takagi,M., Moriyama,T. and Yoshida,T. (2001) Effects of shifts up and down in osmotic pressure on production of tissue plasminogen activator by Chinese hamster ovary cells in suspension. *J. Biosci. Bioeng.*, **91**, 509–514.
38. Park,J.H., Noh,S.M., Woo,J.R., Kim,J.W. and Lee,G.M. (2016) Valeric acid induces cell cycle arrest at G1 phase in CHO cell cultures and improves recombinant antibody productivity. *Biotechnol. J.*, **11**, 487–496.
39. Zou,W., Edros,R. and Al-Rubeai,M. (2018) The relationship of metabolic burden to productivity levels in CHO cell lines. *Biotechnol. Appl. Bioc.*, **65**, 173–180.
40. Yoon,S.K., Kim,S.H. and Lee,G.M. (2003) Effect of low culture temperature on specific productivity and transcription level of anti-4-1BB antibody in recombinant Chinese hamster ovary cells. *Biotechnol. Prog.*, **19**, 1383–1386.
41. Dinnis,D.M., Stansfield,S.H., Schlatter,S., Smales,C.M., Alete,D., Birch,J.R., Racher,A.J., Marshal,C.T., Nielsen,L.K. and James,D.C. (2006) Functional proteomic analysis of GS-NS0 murine myeloma cell lines with varying recombinant monoclonal antibody production rate. *Biotechnol. Bioeng.*, **94**, 830–841.
42. Torres,M. and Dickson,A.J. (2021) Overexpression of transcription factor BLIMP1/prdm1 leads to growth inhibition and enhanced secretory capacity in Chinese hamster ovary cells. *Metab. Eng.*, **67**, 237–249.
43. Ifandi,V. and Al-Rubeai,M. (2003) Stable transfection of CHO cells with the c-myc gene results in increased proliferation rates, reduces serum dependency, and induces anchorage independence. *Cytotechnology*, **41**, 1–10.
44. Zhang,X., Ge,Y.L. and Tian,R.H. (2009) The knockdown of c-myc expression by RNAi inhibits cell proliferation in human colon cancer HT-29 cells in vitro and in vivo. *Cell. Mol. Biol. Lett.*, **14**, 305–318.

Supplementary Information

An arrayed CRISPR screen reveals *Myc* depletion to increase productivity of difficult-to-express complex antibodies in CHO cells

Niels Bauer[1,3], Benedikt Oswald[1], Maximilian Eiche[1], Lisa Schiller[1], Emma Langguth[1], Christian Schantz[1], Andrea Osterlehner[1], Amy Shen[2], Shahram Misaghi[2], Julian Stingele[3] & Simon Ausländer[1]

[1]Large Molecule Research, Roche Pharma Research and Early Development (pRED), Roche Innovation Center Munich, Penzberg, Germany; [2]Cell Culture and Bioprocess Operations Department, Genentech Inc., South San Francisco, CA, USA; [3]Gene Center and Department of Biochemistry, Ludwig-Maximilians-University Munich, 81377 Munich, Germany.

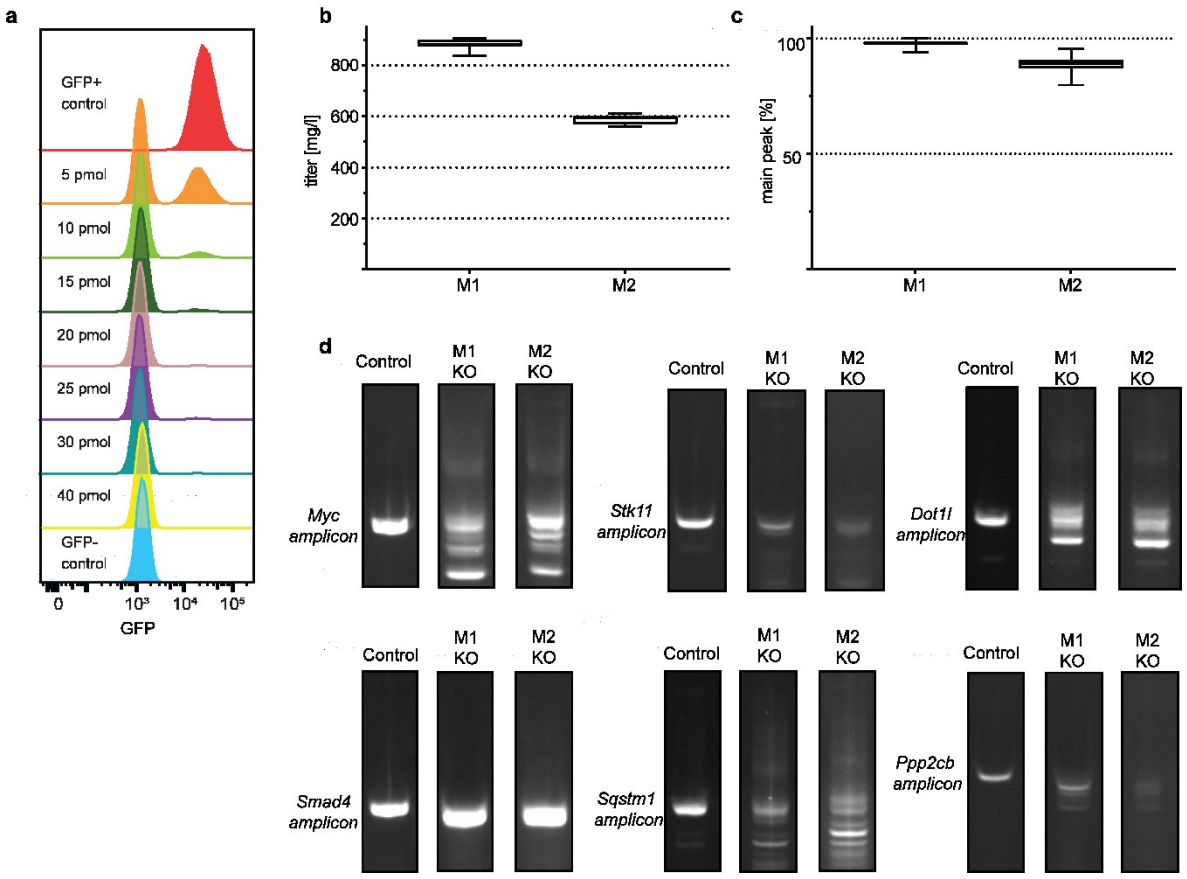

Supplementary Figure 1 | Quality control of the pooled CRISPR/Cas9 arrayed screening.

a) Ribonucleoprotein-based KO protocol, using three sgRNAs binding in close genomic proximity and targeting the landing pad-encoded GFP in the TI-CHO host cell line. After GFP KO, cells were grown for 6 days and analyzed using flow cytometry. Titration of RNP dosage (5-40 pmol) used for transfection. **b)** bsAb titer and **c)** product quality (main peak measured by CE-SDS) after protein A purification of untreated control cells (n = 23) of producer clones expressing molecule 1 or molecule 2. **d)** Agarose gel electrophoresis (2% agarose) of PCR-amplified products using PCR primers flanking the target regions of the used sgRNAs. Box plots illustrate median value and inter-quartile range. Whiskers represent minimum and maximum values.

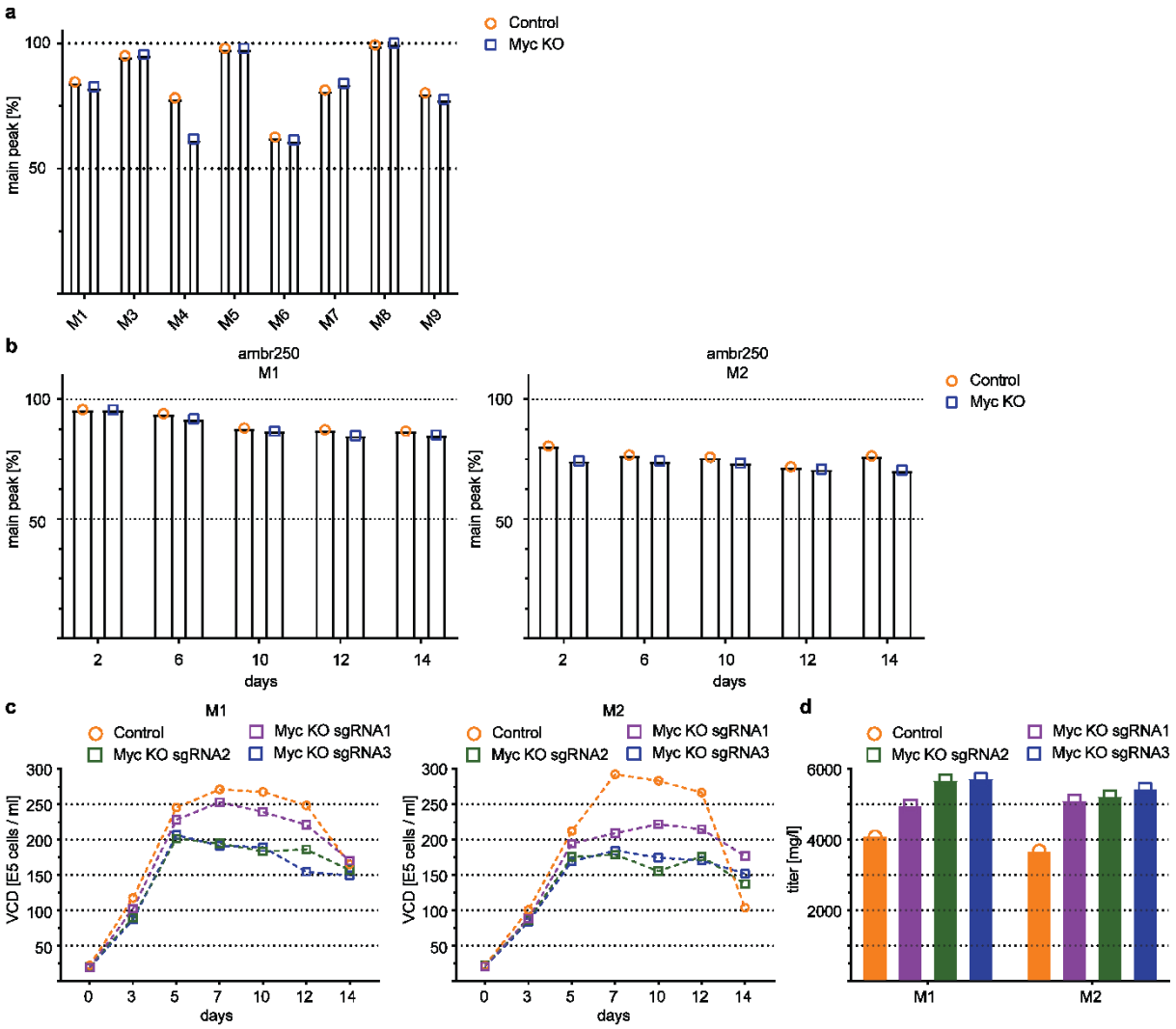

Supplementary Figure 2 | Quality control of the ambr fed batch processes and sgRNA validation

a) Product quality (main peak measured by CE-SDS) comparison after protein A purification of mock-treated cells and *Myc* KO pools. Purified supernatant taken on day 14 of cultivation in ambr15 fed batch process. **b)** Product quality (main peak measured by CE-SDS) comparison after protein A purification of mock-treated cells and *Myc* KO pools. Purified supernatant taken on day 10 of cultivation in ambr250 fed batch process. **c)** Viable cell density (VCD) of control and *Myc* KO cells during the 14-day ambr15 fed batch process. **d)** Harvest (day 14) product titers of ambr15 fed batch process after protein A purification.

2.3 Genomic barcoding for clonal diversity monitoring and control in cell-based complex antibody production

Niels Bauer, Christoph Oberist, Michaela Poth, Julian Stingele, Oliver Popp & Simon Ausländer, Genomic barcoding for clonal diversity monitoring and control in cell-based complex antibody production. *Scientific Reports*, Volume 14, Issue 1, 2024, Pages 14587, https://doi.org/10.1038/s41598-024-65323-7

Author contribution:
I established the experimental setup for the genomic barcoding method. Further, I designed and analyzed all experiments. I performed all described experiments with exception of limited dilution, bioreactor handling and antibody purification. I wrote the manuscript.

scientific reports

Check for updates

OPEN

Genomic barcoding for clonal diversity monitoring and control in cell-based complex antibody production

Niels Bauer[1,2], Christoph Oberist[1], Michaela Poth[1], Julian Stingele[2], Oliver Popp[1] & Simon Ausländer[1]✉

Engineered mammalian cells are key for biotechnology by enabling broad applications ranging from in vitro model systems to therapeutic biofactories. Engineered cell lines exist as a population containing sub-lineages of cell clones that exhibit substantial genetic and phenotypic heterogeneity. There is still a limited understanding of the source of this inter-clonal heterogeneity as well as its implications for biotechnological applications. Here, we developed a genomic barcoding strategy for a targeted integration (TI)-based CHO antibody producer cell line development process. This technology provided novel insights about clone diversity during stable cell line selection on pool level, enabled an imaging-independent monoclonality assessment after single cell cloning, and eventually improved hit-picking of antibody producer clones by monitoring of cellular lineages during the cell line development (CLD) process. Specifically, we observed that CHO producer pools generated by TI of two plasmids at a single genomic site displayed a low diversity (< 0.1% RMCE efficiency), which further depends on the expressed molecules, and underwent rapid population skewing towards dominant clones during routine cultivation. Clonal cell lines from one individual TI event demonstrated a significantly lower variance regarding production-relevant and phenotypic parameters as compared to cell lines from distinct TI events. This implies that the observed cellular diversity lies within pre-existing cell-intrinsic factors and that the majority of clonal variation did not develop during the CLD process, especially during single cell cloning. Using cellular barcodes as a proxy for cellular diversity, we improved our CLD screening workflow and enriched diversity of production-relevant parameters substantially. This work, by enabling clonal diversity monitoring and control, paves the way for an economically valuable and data-driven CLD process.

Keywords CHO, Barcoding, Lineage tracing, Antibody production

Recombinant antibodies continue to lead biopharmaceuticals in numbers of approvals (53.5% of US and EU approvals 2018–2022), sales (80.2% of total biopharmaceutical sales) and their impact on global health[1]. 67% of recombinant antibodies are produced by mammalian cell systems[1], dictated by the need of correctly folded and glycosylated protein with human-like post-translational modifications (PTMs).

All cells used in a mammalian expression system, including Chinese hamster ovary (CHO), mouse myeloma line (NS0), and HEK293 cells, have been initially isolated from living tissue[2]. During the immortalization process each of these cell lines have undergone undefined selective expansion of sub-lineages, exhibiting substantial genetic and phenotypic heterogeneity[3]. As such, mammalian expression systems demonstrate close resemblance to cancer cells, when comparing genetic and phenotypic instability observed within cancer patients or in bioreactors[3].

The majority of mammalian expression systems use random integration and/or gene amplification systems based on dihydrofolate (DHFR) reductase or glutamine synthetase (GS), resulting in further increased intrinsic heterogeneity of such expression cells[4]. Gene amplification procedures aim to boost transgene copy number dramatically (up to 1000 copies per cell) by using either DHFR, or GS-deficient CHO cell lines for the transfection,

[1]Large Molecule Research, Roche Pharma Research and Early Development (pRED), Roche Innovation Center Munich, Penzberg, Germany. [2]Gene Center and Department of Biochemistry, Ludwig-Maximilians-Universität München, 81377 Munich, Germany. ✉email: simon.auslaender@roche.com

followed by gene amplification in the presence of methotrexate (MTX) or methionine sulphoximine (MSX), respectively[5]. These procedures result in substantial heterogeneity due to copy number variation, rearrangement of transgene cassettes, and position effects of the integrated plasmids[6,7]. The final total variety in cellular behavior enables screening of genetic and phenotypically distinct cell lines with high likelihood to identify high producer cells.

The intrinsic cellular heterogeneity of expression systems is in stark contrast to regulatory quality control requirements (*i.e.* Quality by Design), which aim to reduce product heterogeneity to a minimum. To ensure a robust and reproducible production process, cellular heterogeneity needs to be limited after generation of a suitable expression pool. Current regulatory guidelines therefore require that the producing cell is being derived from a single cell origin, as clonal derivation is generally believed to increase the likelihood of stable product quality[8–10].

This regulatory view on the importance of clonal derivation was affirmed recently[11], despite increasing evidence that "clonality" itself is unsuitable to address process robustness or reproducibility during manufacturing[12]. Rather clonal steps display a "genetic bottleneck" in which genomic and phenotypic distinct populations are separated briefly until giving rise to emerging new populations[13–15]. Remarkably, even clonally derived cell banks can give rise to genetically distinct subpopulation within less than 2 months[16]. Thus, clonal cell lines still display a wide array of production-relevant phenotypes.

Despite many studies describing the types of genetic and phenotypic variability within mammalian expression systems, the underlying sources remain incompletely understood[14,17,18]. Previous studies hint towards an interplay between genomic plasticity, epigenetics, stochastic gene expression, changing environmental conditions, copy number and positions effects[19,20]. While most of these areas remain unsolved, the field has increasingly moved to site-specific integration technologies that enable exclusion of the copy number and position effects of transgenes. This has resulted in increased process stability and displays the most promising approach to compromise between clonal variability and process stability so far[21,22].

In the development of biopharmaceutical-producing cell lines, the lack of insight into cellular biology prevents an economic and data-driven cell line development (CLD) process. As variation within a given cellular population and their influencing factors remain elusive, excessive clone screening is required. Especially, it is unclear to which extent clonal variability is inherently occurring and which part is induced by changes in the environmental conditions defined by different CLD stages.

DNA-based barcoding of cells has emerged as a powerful technology with broad applications in basic biology and synthetic biology. Barcoding single cells in vivo allows for tracking their fate in diseases and reveals novel insights in genotypic and phenotypic profiles of *e.g.* cancer sub-lineages[23,24]. Pooled knock-in screenings of genetically-engineered barcoded libraries enable high-throughput testing of millions of genetic variants in an isogenic context. Consequently, massive parallel phenotypic perturbation screenings that are coupled to next-generation sequencing readouts in bulk or at single-cell level become feasible[25]. Recently, genetically-barcoded knock-in libraries have been used for deciphering optimal targeted integration loci in CHO antibody producer cells[26] as well as first genome-wide pooled CRISPR KO screenings to improve cellular bioproduction properties[27].

Here, we have further expanded the application area of genetic barcoding and developed a cellular single-copy targeted integration barcoding strategy based on dual-plasmid recombinase-mediates-cassette exchange (RMCE)[22] to monitor CHO producer cell lineages expressing three distinct complex bispecific antibodies. This enabled quantification of clonal diversity at pool level as well as clonal lineage tracing during selection, single cell cloning, expansion, and subsequent testing in scale-down bioreactors.

Using this system, we could quantify, for the first time, the absolute number of integration events generated by dual plasmid RMCE, which revealed stable pool composition pre-/ and post-selection. We demonstrate that very few cells (less than 0.1% of the original population) successfully undergo dual plasmid RMCE and simultaneously survive selection pressure, and discovered that dominant clones rapidly overgrow the population during routine cultivation. By discriminating between cell lineages within stable pools, we establish that the clonal origin largely determines phenotypic variability regarding production-relevant parameters, which further correlates with shared epigenetic profiles. In the context of targeted integration (TI), we introduce cellular diversity as a constant feature, largely independent of environmental influences during the CLD process. We demonstrate that cellular barcodes can be used as a proxy for cellular diversity, resulting in an improved CLD screening workflow and substantially enriched diversity of production-relevant parameters. Collectively, these data highlight the use of genomic barcoding as a key method to monitor and control cellular phenotypes during TI-based CLD workflows.

Results

Low transcriptome diversity within cell line development workflow

We were interested in the cellular population diversity at different stages of an isogenic TI CLD platform[22]. This platform is based on simultaneous dual-plasmid RMCE-mediated targeted integration into a single genomic locus thus generating isogenic cells, which theoretically excludes variability derived from position effects, copy number and epigenetic silencing (Fig. 1a).

We harvested cells at three different stages of the CLD process: the GFP-expressing host cell ("host"), a stable bispecific antibody expression pool with a distinct gene configuration in our TI platform ("stable pool"), and a final producer clone ("clone") that has been derived from the same stable pool. Each population was transcriptionally profiled on single-cell level using scRNAseq (Chromium Single Cell 3' solution) and, after merging and batch correction, we observed no relevant cell population substructures (Fig. 1b). We hypothesized that variability in the expression of genes encoding the recombinant protein is insufficient to contribute to significant global transcriptomic differences during the CLD process.

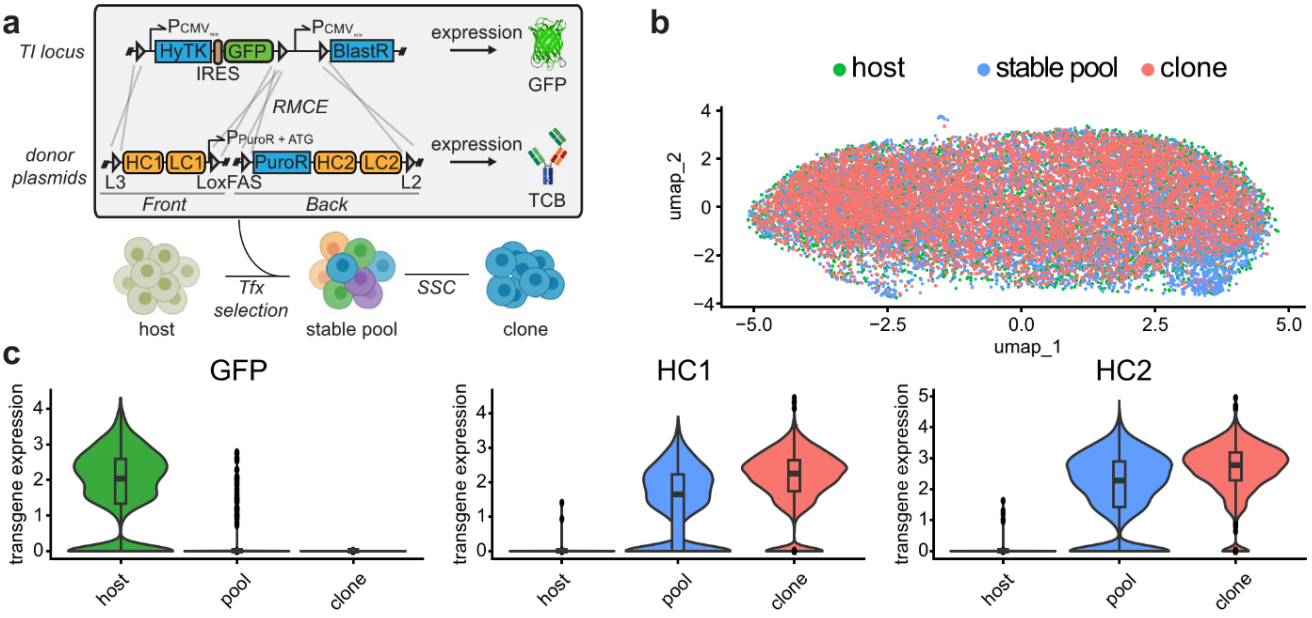

Figure 1. CHO cells are remarkably similar across the CLD process (**a**) Dual plasmid (front and back plasmid) integration strategy via recombinase-mediated-cassette-exchange (RMCE) into a CHO host cell line containing a landing pad (with lox acceptor sites: L3, LoxFAS, L2). Host cells express GFP and sensitive to FIAU due to thymidine kinase expression. Single copy targeted integration is enforced by negative selection (FIAU) and positive selection (puromycin). The start codon for the puromycin CDS is located on the front plasmid. (**b**) Overlay of single-cell transcriptome profiles from host cells containing the RMCE landing pad (expressing GFP), a stable expression pool, and clonal cell line originating from the expression pool. (**c**) Average levels of transgene expression in single-cell transcriptome profiles of host, stable pool, and clonal cells. UMAP, uniform manifold approximation and projection; HCL, host cell line; Pool, stable expression pool; Clone, stable expression clonal cell line.

We therefore specifically analyzed GFP expression within the host population and noticed some degree of variability with a fraction of cells showing no GFP expression (Fig. 1c, left panel). This variability was more pronounced in stable pools where a substantial fraction of cells showed no detectable expression of heavy chain 1 (HC1) and 2 (HC2, Fig. 1c, middle and right panel). In contrast, we observed a substantially smaller variability in HC1 and HC2 expression in a monoclonal cell population. This population had underwent recent single cell cloning and had been pre-selected based on high production performance.

The data indicate that while the overall cellular gene expression is remarkably similar across transfection, stable pool selection, and single cell cloning, transgene expression remains variable in host cells and stable expression pools.

Single-copy targeted barcode integration in stable CHO producer cells

To shed light on the source of transgene expression variety we aimed to implement a genetic lineage tracing method within our CLD workflow. To achieve this, we developed an exhaustive single-copy genetic barcode labeling method, implemented within a state-of-the-art CLD workflow applicable for therapeutic protein production. Most barcode delivery methods (retroviral-based) lead to an inhomogeneous labeling of the population with possibly no or multiple barcode integration per individual cell clone. In contrast, the implementation of a barcode within an isogenic dual-plasmid RMCE-mediated targeted integration into a single genomic locus, allows for the selective expansion of clones with mainly single-copy integration[22]. Notably, the start codon of the puromycin resistance gene is placed on the "Front" expression vector, ensuring that only cells with in-frame- and targeted-integration survive the selection procedure. Additionally, all cells with off-target integration of the expression plasmids do not lose the Thymidine kinase selection marker that is encoded in the landing pad of the host cell line. Overall, only clonal cells undergoing correct on-target recombination between the three LoxP sites become resistant to puromycin and survive in the presence of FIAU. This stringent selection process substantially increases the proportion of single-copy targeted integration survivors.

A N15 barcode region was included into one of two plasmids ("Back") adjacent to the lox site outside of the coding sequence (Fig. 2a). The N15 region is placed in close proximity to the genomic area outside the landing pad, allowing discrimination between on-target and off-target integration events by positioning of the primer binding sites during amplicon deep sequencing. To additionally incorporate cell line metadata, we added 10 fixed positions to the N15 region and devised a nucleotide representation of year, number of CLD (in the respective year), used host cell line and expressed biotherapeutic molecule (Fig. 2b). We validated the plasmid library by amplicon deep sequencing and observed a near uniform barcode representation with homogenous nucleotide

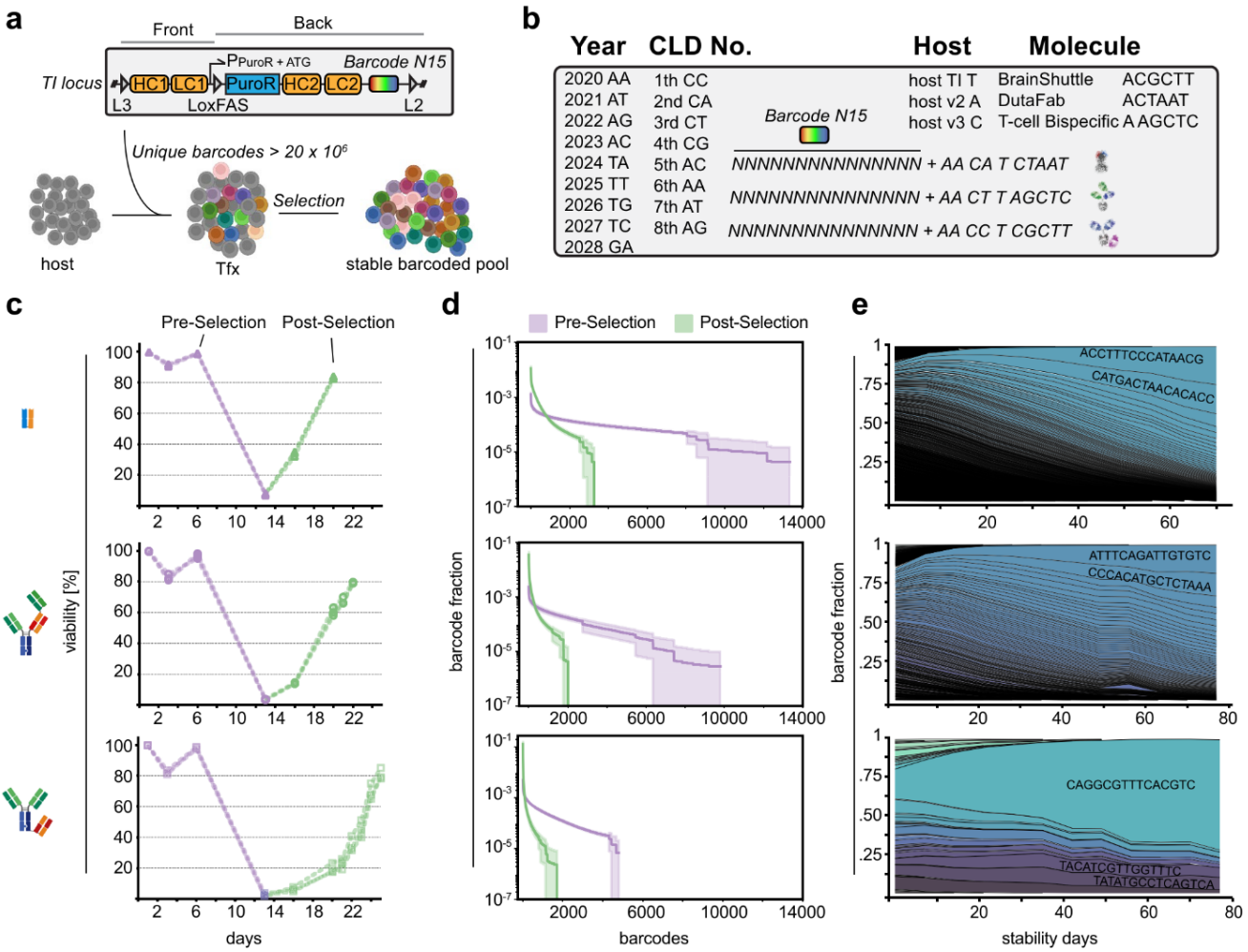

Figure 2. Single-copy targeted barcode integration in stable CHO producer pools (**a**) Notably, the barcode library (N15) is placed adjacent to the L2 lox site to discriminate on- and off-target integration events. (**b**) Barcode sequence design used in this project. Total barcodes combines a randomized N15 region with 10 fixed positions for cell line meta-data. (**c**) CHO host cells were transfected with Front and Back plasmid containing the barcode library at day 0. Selection started at day 6 and continued until cell pool recovery (cell viability > 80%). Note the different cell pool recovery kinetics. (n = 3) (**d**) Barcodes reflect the amount of successful RMCE events and thus the pool diversity. Note the substantially lower pool diversity at the post-selection time point (green) as compared to the pre-selection time point (purple). The error bands represent the standard deviations of biological replicates (n = 3) (**e**) Pool composition drifts during prolonged cultivation and diversity decreases substantially within 80 days. Notably, the effect is more pronounced in case the initial pool diversity is lower. Averaged fraction values of biological replicates (n = 3). (**f**) Retrospective analysis of barcode composition found after single cell cloning and random sampling for 96 clones (ambr15). Width of line indicates relative fraction of cells carrying a unique barcode in the cellular population.

composition at each position (Supplementary Fig. 1a,b). This provides a minimum diversity of $> 2 \times 10^7$, enough to label 10^5 cells with < 0.3% collision probability (Supplementary Fig. 1c,d).

To investigate a representative repertoire of therapeutic proteins produced in CHO cell lines, we selected three different molecules based on the observed viability loss of the cell population during stable pool selection: 5–10%: **M1** DutaFab, 1–5%: **M2** TCB, < 1%: **M3** BS-Fusion (Fig. 2c). We analyzed the clonal diversity of respective CHO cell pools expressing M1-M3 during stable pool selection at two time points: (i) pre-selection at day five post-transfection and (ii) post-selection at the day the cell population reached ~ 80%viability.

We transfected 4.5×10^6 cells of the host cell line with respective antibody-encoding TI and Cre recombinase-encoding plasmids by electroporation at day 0 followed by a recovery phase without selection pressure. Selection pressure (+ Puromycin & FIAU) was started subsequently at day 5 ("Pre-Selection") and lowest cell viability was reached at day 13 for all CHO pools. The recovery time until reaching ~ 80% cell viability differed dramatically depending on the complexity of the encoded molecule and associated gene configuration (M1: day 20, M2: day 22, M3: day 26) (Fig. 2c). This observation was consistent with our previous experience showing that the speed of CHO pool recovery during resistance marker-based stable cell pool selection is linked to the complexity of molecules encoded on the expression plasmids (unpublished observation). DutaFab (M1) expressing cell lines recover quickly, potentially because of their overall smaller size and corresponding smaller plasmid sizes. In

contrast, TCBs (M2) and BS-Fusion (M3) molecules are complex multi-domain fusion molecules, which makes them increasingly difficult-to-express for CHO biofactories[28]. Interestingly, pool composition was approximately 3.5–4.0 times higher at the pre-selection time point (M1: Ø 10060, M2: Ø 6355, M3: Ø 4560) as compared to post-selection across molecules, indicative of rapid clone loss during the stringent selection process (Fig. 2d). Recovered stable pools consisted of a low total amount of barcodes (M1: Ø 2884, M2: Ø 1691, M3: Ø 1158) with a skewed population distribution already at post-selection. Notably, in M3 the most abundant barcode encompassed 10% of the population at the post-selection time point.

Next, we analyzed population dynamics of the three M1-M3-expressing stable CHO pools for a total of 11 weeks with selection pressure. In all three biological replicates, the number of barcodes detected in each population decreased substantially with loss of 80–87% of barcode variants over the observed time course (Fig. 2e). This indicates that stable CHO pools display rapid clonal dynamics under standardized cell cultivation conditions.

Overall, these experiments demonstrate that CHO producer pools generated by TI display a low diversity, which further depends on the expressed molecules, and undergo rapid population skewing towards dominant clones.

Improving efficiency of limited dilution and alternative proof-of-monoclonality by genetic barcoding

Motivated by the success of using cellular barcoding for monitoring CHO producer pools, we next explored the use of barcoding for assurance of monoclonality. To limit heterogeneity of cell banks and ensure consistent product quality, proof of monoclonality has become an important measure of regulatory-approved antibody manufacturing processes. Genetic barcoding offers the inclusion of a cell-intrinsic nucleotide marker which can be repetitively used to validate monoclonality and identity at any given stage and time of a given antibody producer cell clone throughout the production process. Similar approaches based on NGS-analysis of single nucleotide variants or targeted locus amplification products have been published recently[29,30]. However, we speculated that the assessment of genetic barcodes at a pre-defined stable locus offers higher sensitivity, *i.e.* detection of minor subpopulations below 1%, and is not subject to change during cultivation of clonal cell lines.

We cross-validated two monoclonal cell lines by image detection at single cell cloning stage and subsequent Sanger sequencing of barcodes at day 18 (Supplementary Fig. 2a–c). To test the sensitivity of barcode detection within our workflow we mixed the two validated barcoded cell clones at different ratios and measured barcode occurrence via deep sequencing ($> 36 \times 10^6$ reads). To discriminate genuine barcodes from background introduced by sequencing errors, we included an unbiased knee-point filter method and detected clonal cross-contamination reliable in mixtures at ratios of 1:10–1:1000 (Supplementary Fig. 3a). In addition, we could detect 3, 5, and 17 different monoclonal cell lines in a defined pool (Supplementary Fig. 3b).

Monoclonality is traditionally validated by microscopy after limited dilution to achieve a single cell per well based on Poisson distribution[31]. However, limited dilution (LD) is inherently inefficient with most wells either empty or containing more than one cell. To determine if genetic barcoding can improve the single cell cloning process, we compared the number of clones detected with traditional image detection and manual inspection with the amount of clones detected by cellular barcoding. First, we mimicked a traditional single cell cloning process by limited dilution using a Poisson parameter $\lambda = 0.6$ (Fig. 3a). We found that for cells, which were classified as monoclonal by traditional image detection, barcoding confirmed the presence of a single barcode in all observed cases (Fig. 3b). Notably, image detection overestimated the number of clones per well by ~ 60% as compared to barcode detection (Fig. 3b). We hypothesized that the number of clones is overestimated by image detection because of poor outgrowth rates during limited dilution.

Therefore, for wells with 2 cells, we inspected consecutive images of wells on d2 after seeding. Notably, we frequently observed only 1 cell with distinct cell division events (Fig. 3c,d, top 3 panels). In one case, we observed cell divisions of both cells, and another case with a potential cell division event (Fig. 3c,d, bottom 2 panels). In case only a single cell survives and gives rise to a new clonal population we should observe a single genuine barcode. We analyzed the new potential clonal populations by deep sequencing at day 18 after seeding. Indeed, for clones where we previously identified only one cell survivor, only a single genuine barcode was detected in the population (Fig. 3e, top 3 panels). In contrast, we observed that for 2 cell survivors, 2 distinct barcodes were detected (Fig. 3e, bottom 2 panels). The barcode analyses also confirmed the presence of only 1 genuine barcode for the cell division event. Intrigued by the possibility to redefine assurance of clonal derivation by a cell intrinsic feature, we calculated the probability of clonality (PoC) when exchanging imaging evidence with barcode analysis. First, we assessed project-specific survival statistics, which represents the best approximation of PoC in the absence of imaging and method-validation studies ($\alpha = 0.372$, based on 1552 wells with confluence > 10% at day 18 out of a total of 7767 plated wells) Ref.[31]. Next, based on the known relative frequency of barcodes at the time of limited dilution (Table S2), we estimated a "worst-case" probability for barcode collisions in all cases of an amount of k cells > 1 per well. Finally, this calculated to a PoC of 99.63%, when multiplying the probabilities for an amount of $k > 1$ cells in one well with the probabilities that: (i) at least two barcodes collide and (ii) both cells survive and form colonies. Collectively, these data indicate that barcode detection not only confirmed results of monoclonality assessment via image detection during limited dilution, but outperforms imaging evidence for assessment of PoC. Notably, imaging evidence overestimates the number of clones because of non-proliferating and duplet cells, while barcoding only counts viable monoclonal populations. Thus, NGS-derived cellular barcode readouts represent an improved imaging-independent monoclonality assessment method for CHO producer cell lines, offering a very high PoC (> 99.5%) by analysis of a cell intrinsic feature and project-specific survival statistics[31]. In addition, our barcode methods enables the option to revisit cell line identity (i.e. exclude clone mix-ups) and integrity (i.e. clone cross-contamination) at any given stage and time during the CLD process.

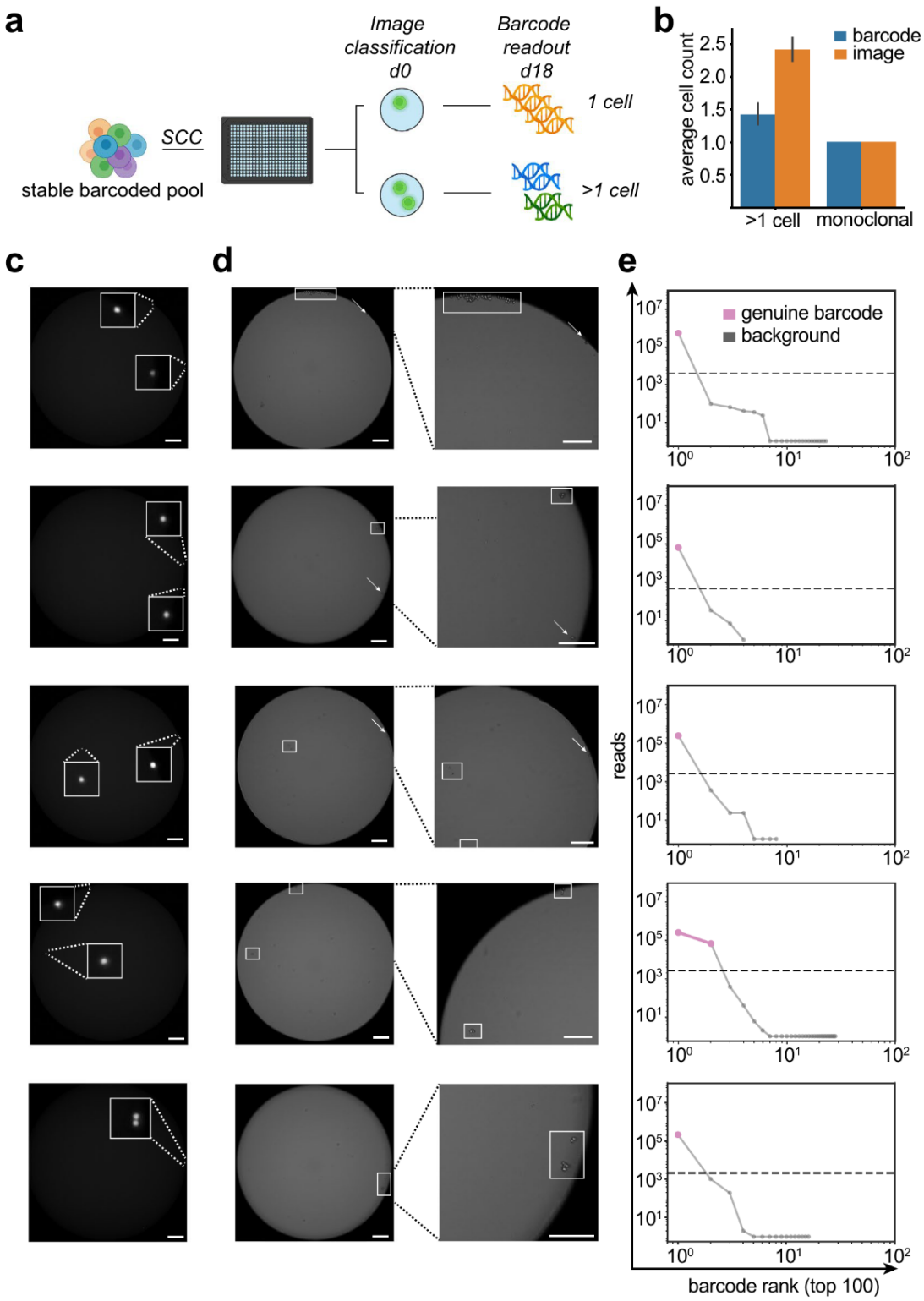

Figure 3. Cellular barcoding can reliably detect clonal status of cell lines during single-cell cloning (**a**) Stable barcoded expression pools were single cell cloned by limited dilution in 384 well plates. Monoclonality was assessed by fluorescent imaging directly after seeding at d0 and barcodes were detected via amplicon deep sequencing at day 18. Wells were grouped based on the initial image based classification in either wells with 1 cell or > 1 cell. (**b**) Bar graphs depicting average number of barcodes detected by the barcoding method as compared to an automated image analysis method. Samples are grouped according to initial image classification to wells containing only 1 cell and > 1 cell, n = 96. Error bars indicate SD. (**c**) Fluorescence imaging at d0 directly after seeding of barcoded stable pools in 384 well plates. This image was used for initial classification of wells. (**d**) Bright-field imaging at day 2 after single-cell cloning (left panel) and magnified view on the cell colonies (right panel). Cell colonies with visible division are marked with a rectangle, cells without visible division are marked by an arrow. Size bar indicates 200 µm. (**e**) The number of barcodes were detected via amplicon deep sequencing and unique top 100 barcodes are plotted. Dashed line indicates the minimum read count cutoff to discriminate erroneous barcodes from genuine barcodes using an unbiased knee point detection algorithm. (**c**) Initial fluorescent imaging directly after seeding cells into 384-well plates during single-cell cloning. Cells are marked by an arrow (**d**).

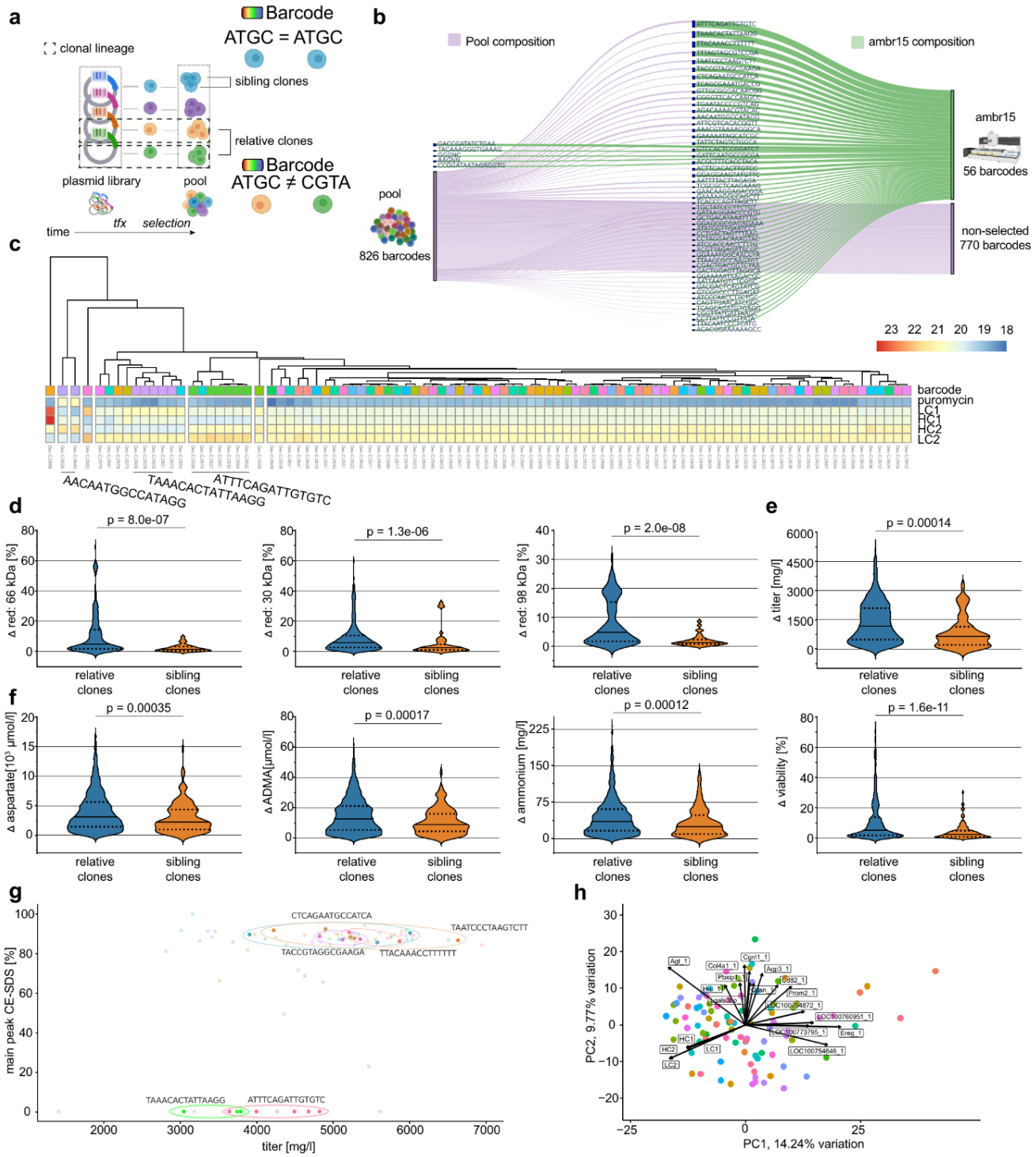

Figure 4. Clonal origin predicts similarity in bioprocess relevant features despite overall similarity (**a**) Experimental outline to evaluate the cellular production performance of clonal cells which originated from different RMCE events. Clones were randomly selected (confluence threshold) and expanded for testing in ambr15 microbioreactors. (**b**) Hierarchical clustering of individual producer clones by antibody chain expression in bulk transcriptome profiling. Note the distance of cells, which share the same barcode. Violin plot comparing (**c**) absolute differences in product quality parameters, (**d**) metabolite concentrations, and (**e**) cellular features between unique barcodes (relative clones) as compared to barcodes with ≥ 3 occurrences (sibling clones). Dotted line indicates the arithmetic mean. FDR-adjusted statistical significance was calculated by Wilcoxon rank-sum test. (**f**) Product quality (main peak measured by CE-SDS) and titer after protein A purification of clonal cells. Clonal cells with identical barcodes are color matched. Barcodes which occurred ≥ 3 times (sibling clones) are highlighted (circle). (**g**) Principal component analysis (PCA) of bulk transcriptome data from 94 randomly selected clonal cell lines. Cells were sampled at day 10 during a 14-day fed batch process in ambr15 bioreactors. Clonal cells with identical barcodes are color matched.

Cells originating from individual RMCE events share cellular phenotypes

Despite exclusion of position effects and copy number variation by using targeted integration technologies (*e.g.* RMCE-based), cell clones generated from stable expression pools display a relatively high variability of production-relevant readouts such as volumetric titer, metabolite profile and growth rates[15]. The described genetic barcoding method allows us to trace clonal CHO lineages from the time point of transfection onwards. Importantly, this allows discrimination between related cell clones originating from the same TI event but derived from different single cell cloning events ("sibling clones" that share the same barcode sequence and occurred from a cell duplication event in the CHO pool after transfection) and those from different TI events ("relative clones" with different barcodes) (Fig. 4a).

To test whether the phenotypic variability in cell clones is a stochastic event or whether it was predetermined, we generated cell clones from one barcoded CHO producer pool. Cell clones were selected randomly during limited dilution with a confluence threshold of 10% at day 12 in the 96-well plate. The composition of barcodes within all tested clones in the ambr15 stage was comparable to the barcode composition within the originating cell pool (Fig. 4b). Notably, frequent and rare barcode variants (from the original pool) were present in the final clonal populations. Cell clones were then tested for production-relevant markers using a downscale micro bioreactor system (ambr15).

Remarkably, cell clones clustered partially based on antibody chain transcript levels at day 10 of the ambr15 fed batch run (Fig. 4c). We speculated that cells originating from the same TI events ("sibling clones", same barcode) may show less phenotypic variance as compared to cells from distinct TI events ("relative clones", unique barcodes). To holistically compare phenotypic distance between clones we next compared pairs of absolute differences within all measured phenotypic data points. We selected 34 "sibling clones" (3 or more barcode occurrences) and 33 "relative clones" and observed a significantly lower variance in the group of "sibling clones" as compared to the group of "relative clones" for secreted antibody chain fragments (Fig. 4d), cellular features (Fig. 4e), and metabolite consumption (Fig. 4f). A list of all tested parameters which were statistically significant is provided (Table S1). The lower phenotypic distance was also apparent when we compared product titer with overall product quality (main peak CE-SDS), where we observed clusters of sibling clones(Fig. 4g)). In agreement with our previous results, bulk transcriptomic profiling during the ambr15 fed batch revealed little overall differences. PCA of gene expression between clones displayed low variation, PC1 explaining 14.24% and PC2 9.77% of variation (Fig. 4h). Notably, antibody chain expression was dominant in the component loading of PC1 and PC2.

The lower variance observed within clones sharing the same barcodes ("sibling clones") raises the question as to how phenotypic variance is generated within the cell line generation process. A recent study by Weinguny and colleagues hints toward the single cell cloning process, where a distinct DNA methylation pattern emerged in each clone[32]. We therefore asked whether the TI event could influence the epigenetic landscape in a similar way and analyzed the genome-wide methylation profile of 12 clones (6 "sibling clones" same barcode, 6 "relative clones"). Indeed, "sibling clones" cluster closely as compared to "relative clones" (Suppl. Fig. 4a–d). In the analyzed subset most of the differential methylation occurs in intergenic regions and in regions which could not be mapped to defined chromosomes (Suppl. Fig. 4b,c).

Collectively, the data indicate that the majority of observed phenotypic diversity is pre-existing and cell-intrinsic. While some diversity remains within cells sharing the same barcode ("sibling clones"), the majority of phenotypic diversity is explained by the common origin of cells occurring from the identical TI event.

Clonal diversity control

The increased diversity of cells from distinct TI events implies that we can utilize barcodes as a proxy for cellular diversity during the cell line development process. First, we integrated barcode assessment during hit-picking in the limited dilution process and could therefore monitor the cellular origin of clones during the CLD workflow. Second, we designed one group with enriched diversity, *i.e.* containing only unique barcodes ("relatives clones"), and a second group with decreased diversity, *i.e.* with many "sibling clones" sharing the identical barcode (Fig. 5a). We hypothesized that the group with enriched barcode diversity would show a higher degree of phenotypic variance as compared to the group with decreased barcode diversity.

We evaluated the cellular diversity of cell clones in ambr15 bioreactors during 14 day fed batch production. Intriguingly and in line with our previous results, key phenotypic parameters as volumetric titer values, glutamate consumption and viable cell density did demonstrate substantially increased variability (Fig. 5b). To identify the best performing clone in a population, the screening burden increases with the amount of diversity. Thus, we next simulated the maximum observed titer when systematically sampling different numbers of cell clones. Specifically, we randomly picked n previously measured titer values from cell clones three times independently and plotted the relationship between screening depth (increased amount of n clones) against the maximum titer achieved within each subset. This allowed us to estimate, whether the increased phenotypic diversity would increase or decrease the amount of clones necessary to include the top producer clones.

We observed that despite a lower average titer in the enriched diversity group, the maximum titer was reached when screening substantially lower number of clones and with higher confidence (lower SD) as compared to the decreased diversity arm (Fig. 5c).

Together, our data indicate that cellular barcodes can serve as a proxy for cellular diversity and can improve CLD screening workflows towards enriched diversity of production-relevant parameters substantially.

Discussion

In this study, we have developed a virus-free method for exhaustive single-copy genomic labeling to track cell populations. In establishing and validating this method, we have focused on a state-of-the-art targeted integration CLD workflow for CHO-cell biofactories producing a panel of three distinct complex antibodies.

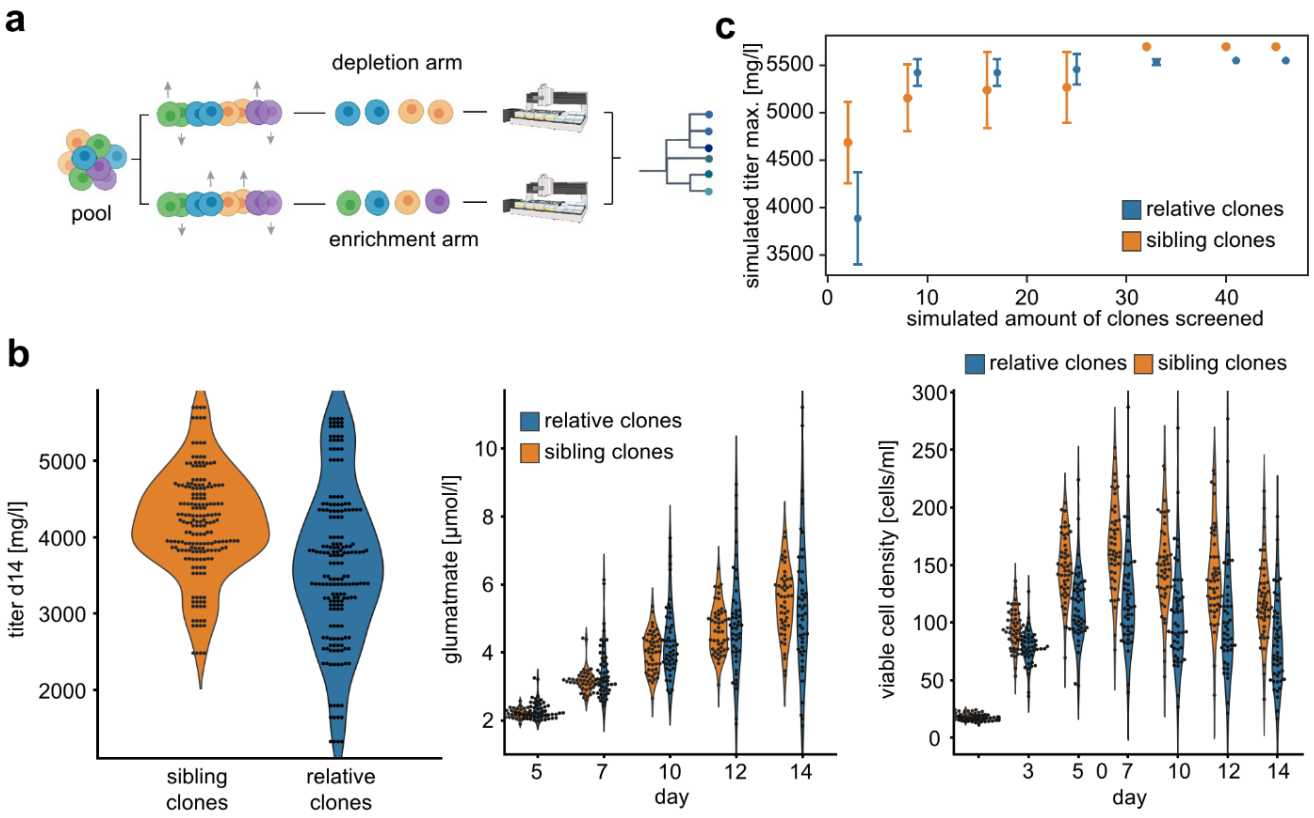

Figure 5. Clonal diversity controls results in leaner CLD process (**a**) Experimental outline of clonal diversity control during the cell line development (CLD) process. Cellular barcodes were used as proxy for cellular diversity and classified in two groups. The depletion arm contained 48 clones with 15 different barcodes, the enrichment arm 48 clones with 48 distinct barcodes. (**b**) Absolute values for antibody titer after protein A purification(left panel), glutamate levels (middle panel), and viable cell density (right panel) grouped by classification into depletion or enrichment arm of cellular diversity. (**c**) Average values for maximum titer simulation of three independent CLD processes when screening different amount of clones. The error bars represent the standard deviations of the simulated titer values.

Our results show that overall transcriptional diversity within the population is low with no distinct sub-population present at any time during the CLD process, as previously shown for CHO and HEK cells[33]. In contrast, transgene expression shows a high degree of variability within the host (originally clonal, but passaged over > 6 months) and a stable pool population despite the use of an isogenic, single-copy targeted integration method. Clonal cells, which have undergone recent (< 12 weeks) single cell cloning, display substantially lower intra-population variability in transgene expression. We speculate that the observed variability in transgene expression results from pre-existing and cell-intrinsic factors rather than environmental conditions, supporting the model that no immortalized cell population is uniform over a longer period of time[17]. To test which factors dominantly contribute to diversity in an isogenic targeted integration system, we utilized a genetic barcoding method to trace individual TI lineages after the TI event across stable pool generation, single cell cloning, and subsequent phenotypic characterization. Importantly, moving from previous random integration of transgene towards isogenic targeted integration methods excludes variation due to placement and copy number effects[21].

In line with previous work[13], we show that expression cell lines undergo dramatic clonal fluctuations during stable pool selection, with skewed populations already before full population recovery. Additionally, isogenic targeted integration was achieved at the cost of integration efficiency with surprisingly low amount of integration events. We link the low integration efficiency with use of a dual plasmid integration system, which is further reduced by increasing plasmid cargo size[34] and/or complexity of the expression molecules. While a homogenous population is a desired outcome of a typical engineering approach[21], remaining diversity enables flexibility and adaptability for efficient cell line development. Our method allows the preservation of remaining diversity for large cargo engineering approaches with inherently low efficiency rates.

Of note, cell lineages which contribute to the highest fraction of the stable pool (barcode ATTTCAGATTGT GTC, Figs. 2e and 4g), result in clones which do express reduced or misfolded protein. We speculate that protein expression utilizes a finite supply of cellular energy, and cells with lower expression burden can divert more resources to growth-supporting processes[35]. This is supported by our previous work where we showed that high producer cell clones devote a substantial proportion (up to 29%) of their global transcriptome towards antibody transgenes[36]. Hence, cells with reduced transgene expression burden quickly dominate the stable population. A simple way to mitigate enrichment of cells with growth advantages over time is the pool separation by single cell

cloning at the earliest time point, possibly even during stable pool selection. This will prevent the enrichment of cell clones which found ways to suppress transgene expression even in an isogenic context, possible by CMV promoter methylation[37].

Assurance of clonal origin, despite growing evidence that clonal origin alone does not guarantee homogeneity[12], remains a valuable tool to reduce cellular diversity. Direct imaging evidence of single cell origin combined with cell survival statistics displays the preferred option with the highest confidence[31]. The strong focus on the probability of clonality, does however underestimate whether a cell line is of clonal origin, as microtiter wells with more than one cell at the time point of seeding are excluded. We show that NGS-based barcode detection during the single cell cloning process confirms the results obtained by traditional image detection for wells with only 1 cell. Intriguingly, in microtiter wells with > 1 cell NGS-based barcoding can correct false negative wells (with only 1 cell surviving or duplet cells with ongoing cell division) as only surviving cells are evaluated with our method. NGS-based barcoding, by characterizing inherent biological features of the cell line itself, is independent of changes in the single cell cloning workflow that alter the single cell cloning error rate. While populations below 0.1% avoid detection in our project (Supplementary Fig. 3a), NGS-based barcoding exceeds image-based detection which commonly shows error rates between 1–2% (reviewed by Chen, et al.[31]). This technology therefore provides a substantial improved assurance of monoclonality.Further, the method offers the re-evaluation of identity and integrity of cell lines at any later time point as it displays an inherent genetic feature of the cell.

Our results also raise the possibility that drivers for diversity in previous random integration approaches are not necessarily consistent with such drivers in a TI context. Here we show that in a TI context, the clonal origin largely determines phenotypic variability, which in turn is heritable from the original host cell. This suggests cellular diversity as a constant feature, *i.e.* the result of long-term emergence of subpopulations possibly due to genetic and epigenetic adaptations. In contrast, previous studies in the context of random integration postulate that cellular phenotypic variability is linked to environmental influences during single cell cloning[32], or stochastic gene expression[20]. While we cannot exclude these effects completely in our study, the majority of diversity could be linked to the original cell lineage. The diversity seems however to be, at least partially, driven by pre-existing epigenetic modifications as cells with common origin share genome-wide methylation profiles. The heritage of clonal diversity implies that pre-existing epi-/genetic factors are the main drivers for clonal phenotypic diversity in our setting.

We demonstrated that tracking this diversity allows the increase of phenotypic diversity, which in turn leads to a more efficient screening in simulated CLD rounds. Reduced sampling during clone screening reliably reveals cell clones with high productivity, as titer values quickly plateau with increased screening depth. Consequently, future CLD campaigns may utilize barcode analysis to exclude sibling clones in a revised hitpicking strategy (i.e. expansion of selected cell clones from 384 to 96 well plates). Thus, the freed-up capacity can be utilized by parallel screening of 2–4 CLD campaigns with 48–24 cell clones, respectively. While this will reduce invested resources and screening timelines due to 2–fourfold higher throughput compared to current clone screening protocols (with regard to ambr15 capacity), we further envision very lean screening campaigns, which skip small-scale (ambr15) clone evaluation and directly proceed to scale-up evaluation in ambr250 devices. In summary, genomic barcoding will aid lean CLD screening strategies by providing a novel tool to enrich pre-existing diversity while preserving the benefits of TI, which will ultimately reduce drug manufacturing costs for complex recombinant therapeutic products.

Conclusions

During the development of a novel engineered cell line various sub-lineages of cell clones occur that exhibit substantial genetic and phenotypic heterogeneity. In the context of TI, we developed a barcoding technology, which allowed us to identify of clonal heritage as the major source of phenotypic variability. Therefore, clonal lineage tracing during cell line engineering displays a new source of inter-clonal heterogeneity monitoring and control with broad implications for biotechnological applications.

Methods

Cell culture and single cell cloning

All cell lines were created using a previously generated CHO Host Cell Line (international patent publication number WO 2019/126,634 A2). CHO cells were cultivated in a proprietary chemically-defined medium in 125–500 mL shake flask vessels at 150 rpm, 37 °C, 80% rH, and 5% CO_2. Cells can be cultivated in any other chemically defined media after adaptation. Cells were passaged at a seeding density of $3–6 \times 10^5$ cells/mL every 3–4 days. Pools of cells that stably express bsAb molecules were generated as previously described by Carver and colleagues[38]. Briefly, expression plasmids were transfected into CHO cells by MaxCyte STX electroporation (MaxCyte, Inc). Transfected cells were then selected and expression of mAb was confirmed by flow cytometry via human IgG staining (BD FACS Canto II flow cytometer, BD). Stable CHO pools were seeded into 384 well plates (seeding density 0.6 cells/well) and expanded randomly to 96 well plates using a confluence threshold of 10%. To generate clonal cell lines, the presence of an individual cell was confirmed by fluorescent and bright field imaging and manual inspectionat day 0 and day 2 after fluorescent staining (NYONE Scientific: SYNENTEC GmbH, Elmshorn, Germany). Cells which showed at least 50% were further expanded and cryoconserved.

Fed batch production assay

Fed batch production cultures were performed in ambr15 bioreactors (Sartorius AG, Goettingen, Germany) with proprietary chemically defined production media. Cells were seeded at 2×10^6 cells/ml on day 0 of the production stage after adaptation to production media during 2 passages. Cultures received proprietary feed bolus on day

3, 6, 9, and 12. Cells were cultivated for 14 days. Production in the ambr15 system were operated at set points of 37 ℃, dO 40%, pH 7.2, and an agitation rate of 1300 rpm.

Off-line sample analysis

Process parameters were analyzed with Osmomat auto (Gonotec GmbH, Berlin, Germany) for the measurement of osmolality and a Cedex Bio HT Analyzer (Roche Diagnostics GmbH) for the measurement of product and selected metabolite concentrations. Total cell count, viable cell concentration, and average cell diameter was measured by Cedex HiRes Analyzer (Roche Diagnostics GmbH, Mannheim, Germany). Amino acid and metabolite analysis was performed using an in-house LC–MS (Ultivo Triple Quadrupole LC/MS System, Agilent Technologies Inc., Santa Clara, CA, USA) procedure with stable isotope-labeled internal standards for calibration.

Generation of barcoded libraries

Constructs used in this study were generated by standard cloning procedures, with sequences synthesized by Twist Biosciences and restriction digest cloning of the final plasmids. The randomized region N15 was introduced into the final plasmid by Genewiz. For genomic DNA, DNA of 10^8 cells was extracted using the Blood & Cell Culture DNA Maxi Kit (Qiagen) according to manufacturer's instructions. Amplicons for deep sequencing were generated with primers flanking the barcode region, 100 ng plasmid DNA as input, and 30 cycles of amplification by PCR. For detection of cellular barcodes, 2 µg of gDNA was used as input, with 30 cycles of amplification by PCR with primers flanking the barcode and one primer located outside of the RMCE integration site (to discriminate between off- and on-target integration events). Sequencing libraries were prepared using the KAPA HyperPlus Kit (Roche) using 50–100 ng (fix 20 µl purified PCR) of amplicon DNA as input, no fragmentation step, and between 20 and 24 cycles of amplification of PCR (post-ligation library amplification) to reach 1 µg of total DNA library per sample. Libraries were sequenced by Genewiz using the NovaSeq 6000 platform (Illumina) with 30 M paired-end 150 bp reads per sample.

Antibody analytics in supernatant

Supernatants were clarified (1000 g, 30 min, 4 ℃ centrifugation and 1.2 µm filtration, AcroPrep 96 Filter Plates, Pall Cooperation). Analytical protein A chromatography was performed by UHPLC with UV detection (Dionex Ultimate 3000 UHPLC fitted with POROS™ A 20 µm Column, Thermo Fisher Scientific Inc.).

Antibody integrity was analyzed after protein A affinity chromatography (PreDictor RoboColumn MabSelect SuRe, Cytiva) and normalization with protein quantitation using UV measurement (Nanoquant Infinite M200, Tecan). Percentage of correctly assembled antibodies (main peak) was assessed by CE-SDS (HT Antibody Analysis 200 assay on the LabChip GXII system, PerkinElmer) under non-reducing conditions by relative quantification of the expected protein size to total protein content.

Bulk RNA-seq sample preparation and data analysis

Barcoded cells (1×10^6) sampled from the ambr15 bioreactor on day 10 were washed twice in PBS and snap-frozen in liquid nitrogen. RNA extraction, Illumina stranded TruSeq RNA library preparation, poly(A) enrichment, and sequencing (NextSeq, v2.5, high.output 1*75 bp) was performed by Microsynth AG (Belgach, Switzerland). Sequences for the transgene and mitochondrial DNA were included manually into the reference genome (GCF_003668045.3, PICRH1.0). Reads were aligned using the hisat2 package (version 2.2.1)[39] and transcript abundance was calculated with featureCounts (version 2.0.1)[40]. For downstream analysis we used PCAtools (v2.2.0)[41] and for differential expression edgeR (v3.32.1)[42].

Barcode analysis

To characterize the diversity of the barcode libraries, forward and reverse paired-end raw reads (2×150 bp) were trimmed for universal Illumina adapters using cutadapt (v4.1)[43] and subsequently merged with flash (v1.2.11)[44]. Barcodes were extracted with detection of the flanking region (**M1**: GCTTAGCCGCTTAAT AACATCTAA TGCGTA, **M2**: CTTAGCCGCTTAAT AACTTAGCTCGCGTA, **M3**: GCTTAGCCGCTTAAT AACCTCGCT TGCGTA) and all reads which did not match the expected barcode length of 15 discarded. Reverse complement reads were reversed with FASTX toolkit (v0.0.14). Final barcode diversity was estimated using the Chao1 capture-recapture estimator[45] based on barcodes observed in replicate resampling at varying depths. Collision probability (defined as the fraction of cells at start of experiment which share a barcode due to coincidence of independent barcoding events, rather than common clonal origin) was analyzed as previously described by Horns and colleagues[46]. Quickly, for a given number of cells N, we sampled N barcodes without replacement from the observed barcode pool (with sampling probability proportional to the barcode's abundance). We calculated the fraction of the sampled barcodes that were unique within the sample, designated p, then the collision probability was 1–p.

Sensitivity of barcodes as clone cross-contamination reporter

Previously characterized barcoded CHO cell lines (verified as monoclonal by fluorescent microscopy followed by barcode Sanger sequencing) were cultivated and 10^6 cells were mixed in predetermined ratios. Sequencing libraries were prepared from genomic DNA as described above. Reads were preprocessed as described above with an additional step of barcode clustering using a Levenshtein distance of 1 with Starcode (v1.4)[47]. The number of clone barcodes was detected with an $N = 2$ for cross-contamination, or N as indicated in Figure S2, using an unbiased knee point threshold based on the read count distribution[46].

Single-cell RNA-seq and data analysis

Cells were thawed simultaneously to prevent bias based on different cell age. Cryopreserved cells frozen in exponential growth phase were subjected to sequencing. Single-cell library preparation and sequencing was performed on the 10 × Genomics platform by GENEWIZ Germany GmbH (Leipzig, Germany). Sequences for the transgene and mitochondrial DNA were included manually into the reference genome (GCF_003668045.3, PICRH1.0). Reads were aligned to this custom reference genome and quantified using CellRanger (v6.0.1)[48]. For downstream analysis we used Seurat (v5.0.0)[49]. Cells which contained less than 4000 features or displayed mitochondrial DNA content of more than 5% were discarded. Cell cycle phase was predicted using homologous genes between Mus musculus and Cricetulus griseus for regressing out cell cycle effects[50]. After pre-processing, the 3 datasets were merged into a single Seurat object (FastMNNIntegration method, consistent good performance across datasets)[51]. 5.10 Probability of clonality including cell population distributions.

To estimate the probability of at least two identical clones occurring in a single well, we utilized a Poisson distribution model.

$$P_{\lambda}(k) = \frac{\lambda^k}{k!}e^{-\lambda}$$

The parameter λ represents the average number of cells per well and k represents the specific number of cells in a well. Clone probabilities P_i were derived from the relative barcode distributions at the time of limited dilution and normalized such that the sum of all $P_i = 1$. The probability $P(K = k)$ that k cells are in a well follows a Poisson distribution:

$$P(K = k) = \frac{\lambda^k}{k!}e^{-\lambda}$$

where K is the random variable for the number of cells in a well. The probability that all k cells are different clones is given by:

$$P(alldifferent|k) = \prod_{i=0}^{k-1}(1-P_0),$$

where n is the number of different clones and P_0 is the normalized probability of the clone with the highest appearance. It assumes that each cell has the highest probability of being the same clone. Using the highest clone probability for all cells represents the worst-case scenario because it maximizes the likelihood of having at least two identical clones in a well. This approach provides a conservative estimate, ensuring robustness in the analysis. The probability that at least two identical clones are present among k cells is:

$$P(atleasttwoidentical|k) = 1 - P\left(alldifferent\middle|k\right)$$

The probability that a well with k cells shows cell growth is used as described in "Method 3" by Chen and colleagues[31] and given by:

$$G_k = \begin{cases} aifk = 1 \\ k * a * (1-a)^{k-1} ifk > 1 \end{cases}$$

where a is the single cell recovery rate, calculated by solving for a in the equation

$$N * \sum_{k=1}^{100} P_{\mu}(k) * \left(1 - (1-a)^k\right) = W$$

where N is the total number of wells, W is the number of wells with cell growth (defined here by > 10% confluence on day 18 after limited dilution), and μ is the average number of cells per well. a represents the probability that a single cell will recover and grow into a colony. For wells with more than one cell, the probability of growth is adjusted to account for the possibility that only one cell recovers while the others do not. The overall probability that at least two identical clones occur in a well is calculated by summing over all possible k (from 2 to a maximum k, here 10, as more than 10 cells per well are sufficiently unlikely):

$$P(atleasttwoidentical) = \sum_{k=2}^{10}\left(\frac{\lambda^k e^{-\lambda}}{k!} * \left(1 - \prod_{i=0}^{k-1}(1-P_0)\right) * G_k\right)$$

This formula describes the probability that at least two identical clones occur in a well, based on the Poisson distribution of cell counts, the normalized clone probabilities, and the cell recovery rate.

Material availability

Nucleic acids and cell lines encoding for antibody sequences are proprietary to Roche.

Data availability

The data supporting the findings of this study are available within the article and its supplementary materials. Nucleic acid sequences encoding for antibody sequences are proprietary to Roche.

Received: 25 March 2024; Accepted: 19 June 2024
Published online: 25 June 2024

References

1. Walsh, G. & Walsh, E. Biopharmaceutical benchmarks 2022. *Nat. Biotechnol.* **40**, 1722–1760. https://doi.org/10.1038/s41587-022-01582-x (2022).
2. Knight, K. L. The evolution of tissue culture. *Nat. Med.* **14**, 710–710. https://doi.org/10.1038/nm0708-710 (2008).
3. Wurm, M. J. & Wurm, F. M. Naming CHO cells for bio-manufacturing: Genome plasticity and variant phenotypes of cell populations in bioreactors question the relevance of old names. *Biotechnol. J.* https://doi.org/10.1002/biot.202100165 (2021).
4. Cacciatore, J. J., Chasin, L. A. & Leonard, E. F. Gene amplification and vector engineering to achieve rapid and high-level therapeutic protein production using the Dhfr-based CHO cell selection system. *Biotechnol. Adv.* **28**, 673–681. https://doi.org/10.1016/j.biotechadv.2010.04.003 (2010).
5. Noh, S. M., Sathyamurthy, M. & Lee, G. M. Development of recombinant Chinese hamster ovary cell lines for therapeutic protein production. *Curr. Opin. Chem. Eng.* **2**, 391–397. https://doi.org/10.1016/j.coche.2013.08.002 (2013).
6. Kim, N. S., Byun, T. H. & Lee, G. M. Key determinants in the occurrence of clonal variation in humanized antibody expression of cho cells during dihydrofolate reductase mediated gene amplification. *Biotechnol. Prog.* **17**, 69–75. https://doi.org/10.1021/bp000144h (2001).
7. Kim, N. S., Kim, S. J. & Lee, G. M. Clonal variability within dihydrofolate reductase-mediated gene amplified Chinese hamster ovary cells: Stability in the absence of selective pressure. *Biotechnol. Bioeng.* **60**, 679–688 (1998).
8. Food, U. & Administration, D. *Points to Consider in the Manufacture and Testing of Monoclonal Antibody Products for Human Use* (US Department of Health and Human Services, 1997).
9. Plavsic, M. Q5D derivation and characterization of cell substrates used for production of biotechnological/biological products. In *ICH Quality Guidelines: An Implementation Guide* (eds Teasdale, A. *et al.*) 375–393 (Wiley, 2017).
10. Organization, W. H. & Organization, W. H. Recommendations for the evaluation of animal cell cultures as substrates for the manufacture of biological medicinal products and for the characterization of cell banks. *WHO Technical Report Series* **978** (2010).
11. Welch, J. T. & Arden, N. S. Considering, "clonality": A regulatory perspective on the importance of the clonal derivation of mammalian cell banks in biopharmaceutical development. *Biologicals* **62**, 16–21. https://doi.org/10.1016/j.biologicals.2019.09.006 (2019).
12. Frye, C. *et al.* Industry view on the relative importance of "clonality" of biopharmaceutical-producing cell lines. *Biologicals* **44**, 117–122. https://doi.org/10.1016/j.biologicals.2016.01.001 (2016).
13. Porter, S. N., Baker, L. C., Mittelman, D. & Porteus, M. H. Lentiviral and targeted cellular barcoding reveals ongoing clonal dynamics of cell lines in vitro and in vivo. *Genome Biol.* https://doi.org/10.1186/gb-2014-15-5-r75 (2014).
14. Tharmalingam, T. *et al.* Characterization of phenotypic and genotypic diversity in subclones derived from a clonal cell line. *Biotechnol. Prog.* **34**, 613–623. https://doi.org/10.1002/btpr.2666 (2018).
15. Ko, P. *et al.* Probing the importance of clonality: Single cell subcloning of clonally derived CHO cell lines yields widely diverse clones differing in growth, productivity, and product quality. *Biotechnol. Prog.* **34**, 624–634. https://doi.org/10.1002/btpr.2594 (2018).
16. Rouiller, Y. *et al.* Reciprocal translocation observed in end-of-production cells of a commercial CHO-based process. *PDA J. Pharm. Sci. Technol.* **69**, 540–552. https://doi.org/10.5731/pdajpst.2015.01063 (2015).
17. Vcelar, S. *et al.* Karyotype variation of CHO host cell lines over time in culture characterized by chromosome counting and chromosome painting. *Biotechnol. Bioeng.* **115**, 165–173. https://doi.org/10.1002/bit.26453 (2018).
18. He, L., Winterrowd, C., Kadura, I. & Frye, C. Transgene copy number distribution profiles in recombinant CHO cell lines revealed by single cell analyses. *Biotechnol. Bioeng.* **109**, 1713–1722. https://doi.org/10.1002/bit.24428 (2012).
19. Vcelar, S. *et al.* Changes in chromosome counts and patterns in CHO cell lines upon generation of recombinant cell lines and subcloning. *Biotechnol. J.* https://doi.org/10.1002/biot.201700495 (2018).
20. Pilbrough, W., Munro, T. P. & Gray, P. Intraclonal protein expression heterogeneity in recombinant CHO cells. *PLoS One* **4**, e8432. https://doi.org/10.1371/journal.pone.0008432 (2009).
21. Grav, L. M. *et al.* Minimizing clonal variation during mammalian cell line engineering for improved systems biology data generation. *ACS Synth. Biol.* **7**, 2148–2159. https://doi.org/10.1021/acssynbio.8b00140 (2018).
22. Ng, D. *et al.* Development of a targeted integration Chinese hamster ovary host directly targeting either one or two vectors simultaneously to a single locus using the Cre/Lox recombinase-mediated cassette exchange system. *Biotechnol. Prog.* **37**, e3140. https://doi.org/10.1002/btpr.3140 (2021).
23. Sankaran, V. G., Weissman, J. S. & Zon, L. I. Cellular barcoding to decipher clonal dynamics in disease. *Science* https://doi.org/10.1126/science.abm5874 (2022).
24. Serrano, A., Berthelet, J., Naik, S. H. & Merino, D. Mastering the use of cellular barcoding to explore cancer heterogeneity. *Nat. Rev. Cancer* **22**, 609–624. https://doi.org/10.1038/s41568-022-00500-2 (2022).
25. Cheng, J. Y. *et al.* Massively parallel CRISPR-based genetic perturbation screening at single-cell resolution. *Adv. Sci.* https://doi.org/10.1002/advs.202204484 (2023).
26. Hilliard, W. & Lee, K. H. A compendium of stable hotspots in the CHO genome. *Biotechnol. Bioeng.* **120**, 2133–2143. https://doi.org/10.1002/bit.28390 (2023).
27. Xiong, K. *et al.* An optimized genome-wide, virus-free CRISPR screen for mammalian cells. *Cell Rep. Methods* https://doi.org/10.1016/j.crmeth.2021.100062 (2021).
28. Li, Z. M., Fan, Z. L., Wang, X. Y. & Wang, T. Y. Factors affecting the expression of recombinant protein and improvement strategies in Chinese hamster ovary cells. *Front. Bioeng. Biotech.* https://doi.org/10.3389/fbioe.2022.880155 (2022).
29. Kuhn, A., Le Fourn, V., Fisch, I. & Mermod, N. Genome-wide analysis of single nucleotide variants allows for robust and accurate assessment of clonal derivation in cell lines used to produce biologics. *Biotechnol. Bioeng.* **117**, 3628–3638. https://doi.org/10.1002/bit.27534 (2020).
30. Aebischer-Gumy, C., Moretti, P., Little, T. A. & Bertschinger, M. Analytical assessment of clonal derivation of eukaryotic/CHO cell populations. *J. Biotechnol.* **286**, 17–26. https://doi.org/10.1016/j.jbiotec.2018.08.020 (2018).
31. Chen, C. *et al.* Methods for estimating the probability of clonality in cell line development. *Biotechnol. J.* **15**, e1900289. https://doi.org/10.1002/biot.201900289 (2020).
32. Weinguny, M. *et al.* Subcloning induces changes in the DNA-methylation pattern of outgrowing Chinese hamster ovary cell colonies. *Biotechnol. J.* **16**, e2000350. https://doi.org/10.1002/biot.202000350 (2021).
33. Borsi, G. *et al.* Single-cell RNA sequencing reveals homogeneous transcriptome patterns and low variance in a suspension CHO-K1 and an adherent HEK293FT cell line in culture conditions. *J. Biotechnol.* **364**, 13–22. https://doi.org/10.1016/j.jbiotec.2023.01.006 (2023).
34. Troyanovsky, B., Bitko, V., Pastukh, V., Fouty, B. & Solodushko, V. The functionality of minimal piggybac transposons in mammalian cells. *Mol. Ther. Nucl. Acids* https://doi.org/10.1038/mtna.2016.76 (2016).
35. Ingram, D. & Stan, G. B. Modelling genetic stability in engineered cell populations. *Nat. Commun.* **14**, 3471. https://doi.org/10.1038/s41467-023-38850-6 (2023).

36. Bauer, N. *et al.* An arrayed CRISPR screen reveals Myc depletion to increase productivity of difficult-to-express complex antibodies in CHO cells. *Syn. Biol.* https://doi.org/10.1093/synbio/ysac026 (2022).
37. Osterlehner, A., Simmeth, S. & Göpfert, U. Promoter methylation and transgene copy numbers predict unstable protein production in recombinant Chinese hamster ovary cell lines. *Biotechnol. Bioeng.* **108**, 2670–2681. https://doi.org/10.1002/bit.23216 (2011).
38. Carver, J. *et al.* Maximizing antibody production in a targeted integration host by optimization of subunit gene dosage and position. *Biotechnol. Prog.* **36**, e2967. https://doi.org/10.1002/btpr.2967 (2020).
39. Kim, D., Paggi, J. M., Park, C., Bennett, C. & Salzberg, S. L. Graph-based genome alignment and genotyping with HISAT2 and HISAT-genotype. *Nat. Biotechnol.* https://doi.org/10.1038/s41587-019-0201-4 (2019).
40. Liao, Y., Smyth, G. K. & Shi, W. featureCounts: An efficient general purpose program for assigning sequence reads to genomic features. *Bioinformatics* **30**, 923–930. https://doi.org/10.1093/bioinformatics/btt656 (2014).
41. Blighe, K. & Lun, A. PCAtools: everything Principal Components Analysis. (2019).
42. Robinson, M. D., McCarthy, D. J. & Smyth, G. K. edgeR: A bioconductor package for differential expression analysis of digital gene expression data. *Bioinformatics* **26**, 139–140. https://doi.org/10.1093/bioinformatics/btp616 (2010).
43. Marcel, M. Cutadapt removes adapter sequences from high-throughput sequencing reads. *EMBnet. J.* https://doi.org/10.14806/ej.17.1.200 (2011).
44. Magoc, T. & Salzberg, S. L. FLASH: Fast length adjustment of short reads to improve genome assemblies. *Bioinformatics* **27**, 2957–2963. https://doi.org/10.1093/bioinformatics/btr507 (2011).
45. Chao, A. Estimating the population size for capture-recapture data with unequal catchability. *Biometrics* **43**, 783–791 (1987).
46. Horns, F. *et al.* Engineering RNA export for measurement and manipulation of living cells. *Cell* https://doi.org/10.1016/j.cell.2023.06.013 (2023).
47. Zorita, E., Cusco, P. & Filion, G. J. Starcode: Sequence clustering based on all-pairs search. *Bioinformatics* **31**, 1913–1919. https://doi.org/10.1093/bioinformatics/btv053 (2015).
48. Zheng, G. X. Y. *et al.* Massively parallel digital transcriptional profiling of single cells. *Nat. Commun.* https://doi.org/10.1038/ncomms14049 (2017).
49. Hao, Y. H. *et al.* Dictionary learning for integrative, multimodal and scalable single-cell analysis. *Nat. Biotechnol.* https://doi.org/10.1038/s41587-023-01767-y (2023).
50. Kowalczyk, M. S. *et al.* Single-cell RNA-seq reveals changes in cell cycle and differentiation programs upon aging of hematopoietic stem cells. *Genome Res.* **25**, 1860–1872. https://doi.org/10.1101/gr.192237.115 (2015).
51. Chazarra-Gil, R., van Dongen, S., Kiselev, V. Y. & Hemberg, M. Flexible comparison of batch correction methods for single-cell RNA-seq using BatchBench. *Nucleic Acids Res.* https://doi.org/10.1093/nar/gkab004 (2021).

Acknowledgements

The authors are grateful to Harald Duerr, Ursula Bernoecker, Holger Kropp, Bianca Nussbaum, Korbinian Kneidl, Uta Werner, and Stephanie Kappelsberger for bsAB purification and product quality analytics. Furthermore, we thank, Frederik Schroeter, Ulrike Vollertsen, and Katja Montan for HT-MS analysis. We are also grateful to Viktoria Kroenauer, Thorsten Dzidowski, Karen Dericks, Andrea Osterlehner, Laura Woltering, Katharine Mueller, Tzu-Chia Wang, Annett Kaeske, Marie Pfautsch, Francesco Masperi, Benedikt Oswald, Anne-Marie Lavoie, Maximilian Eiche, and Paul Waetzig for single cell cloning, ambr15 cultivation and general support. Finally, we also thank Ulrich Göpfert for helpful discussions. Schematic drawings were partially created with Biorender.com.

Author contributions

N.B & C.O designed, performed, and analyzed the experiments. M.P provided statistical analysis. S.A & O.P conceived the project and obtained funding. S.A, J.S. and O.P interpreted the results and helped in improving the manuscript. N.B wrote the manuscript with input from all the authors. All authors read and approved the final manuscript.

Funding

Roche Diagnostics GmbH funded all of this research. Research in the lab of Julian Stingele is funded by European Research Council (ERC Starting Grant 801750 DNAProteinCrosslinks), the Alfried Krupp Prize for Young University Teachers awarded by the Alfried-Krupp von Bohlen und Halbach-Stiftung, European Molecular Biology Organization (YIP4644), a Vallee Foundation Scholarship, and Deutsche Forschungsgemeinschaft (DFG, German Research Foundation) (Project ID 213249687—SFB 1064, Project-ID 393547839—SFB 1361).

Competing interests

A patent based on this work (Application No. EP 23214270.3) has been filed with authors N. Bauer, O. Popp and S. Auslaender as inventors. N. Bauer, C. Oberist, M. Poth, O. Popp, and S. Auslaender are employees of Roche Diagnostics GmbH, which develops and sells pharmaceuticals. All other authors declare no competing interests.

Additional information

Supplementary Information The online version contains supplementary material available at https://doi.org/10.1038/s41598-024-65323-7.

Correspondence and requests for materials should be addressed to S.A.

Supplementary Information

Genomic barcoding for clonal diversity monitoring and control in cell-based complex antibody production

Niels Bauer[1,2], Christoph Oberist[1], Michaela Poth[1], Julian Stingele[2], Oliver Popp[1] & Simon Ausländer[1,*]

[1]Large Molecule Research, Roche Pharma Research and Early Development (pRED), Roche Innovation Center Munich, Penzberg, Germany;

[2]Gene Center and Department of Biochemistry, Ludwig-Maximilians-Universität München, 81377 Munich.

**Corresponding author: E-Mail: simon.auslaender@roche.com*

Supplementary Figure 1 | Plasmid barcode libraries

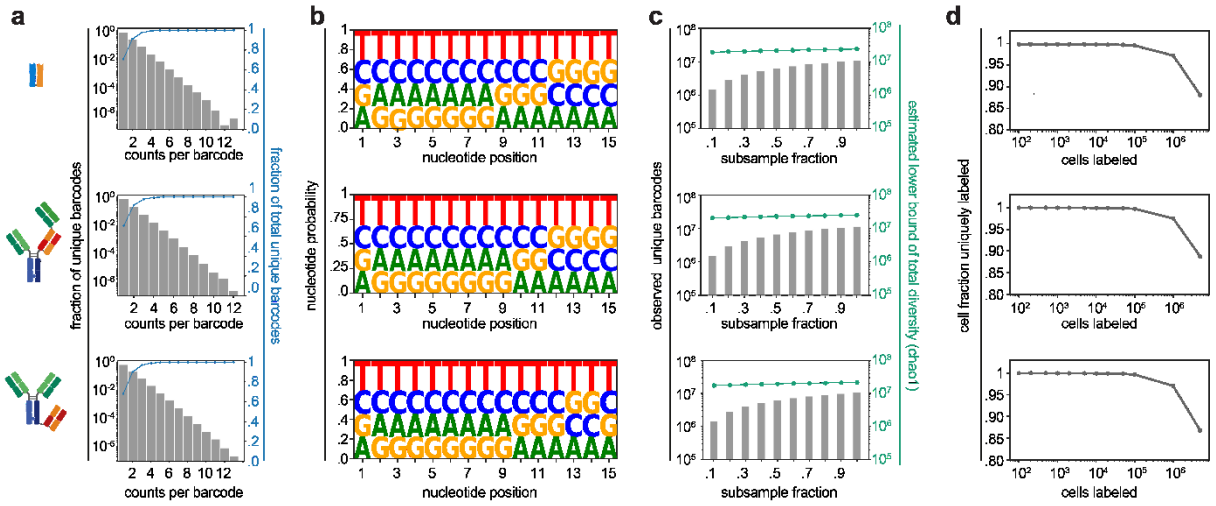

a) Diversity of Back plasmid barcode libraries was assessed by amplicon deep sequencing. **b)** Nucleotide probability at each position of the N15 barcode region. **c)** Lower bound of total barcode diversity within each library was estimated based on observed counts using the Chao1 capture-recapture estimator. **d)** Estimation of labeling capacity for each library was estimated by coincidental barcode collisions. Mean values for 100 replicate simulations (resampling).

Supplementary Figure 2 | Verification of monoclonality for two cell lines used for cross-contamination experiments

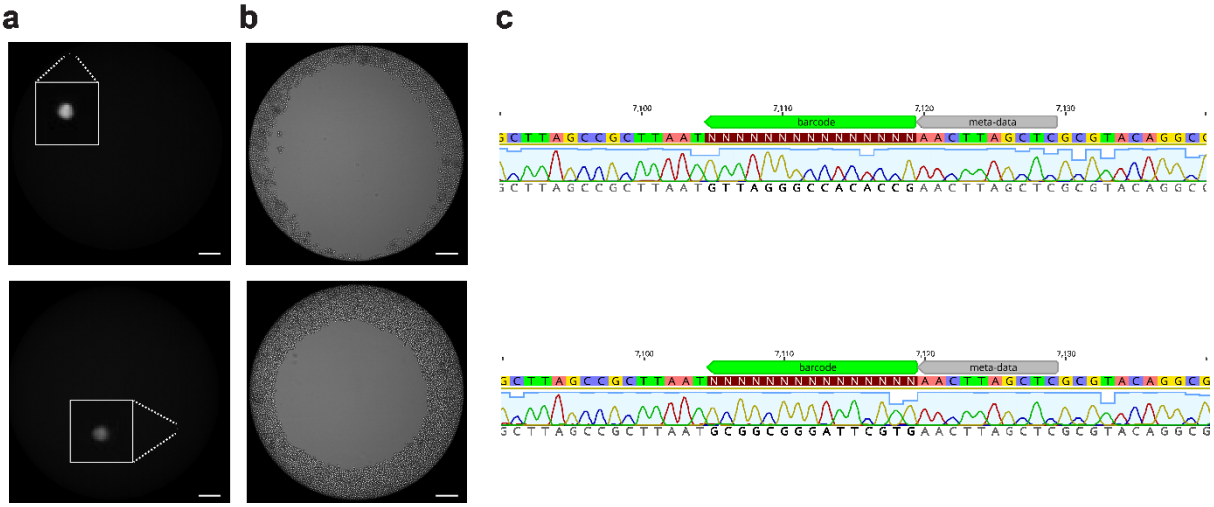

a) Fluorescence imaging at d0 directly after seeding of barcoded stable pools in 384 well plates. Image was used for proof-of-monoclonality. **b)** Bright-field imaging at day 12 after single-cell cloning. Scale bars indicate 200 µm. **c)** Sanger sequence trace aligned to the TI locus reference. Generated with Geneious version 2023.1 created by Biomatters.

Supplementary Figure 3 | Detection of clone cross-contamination

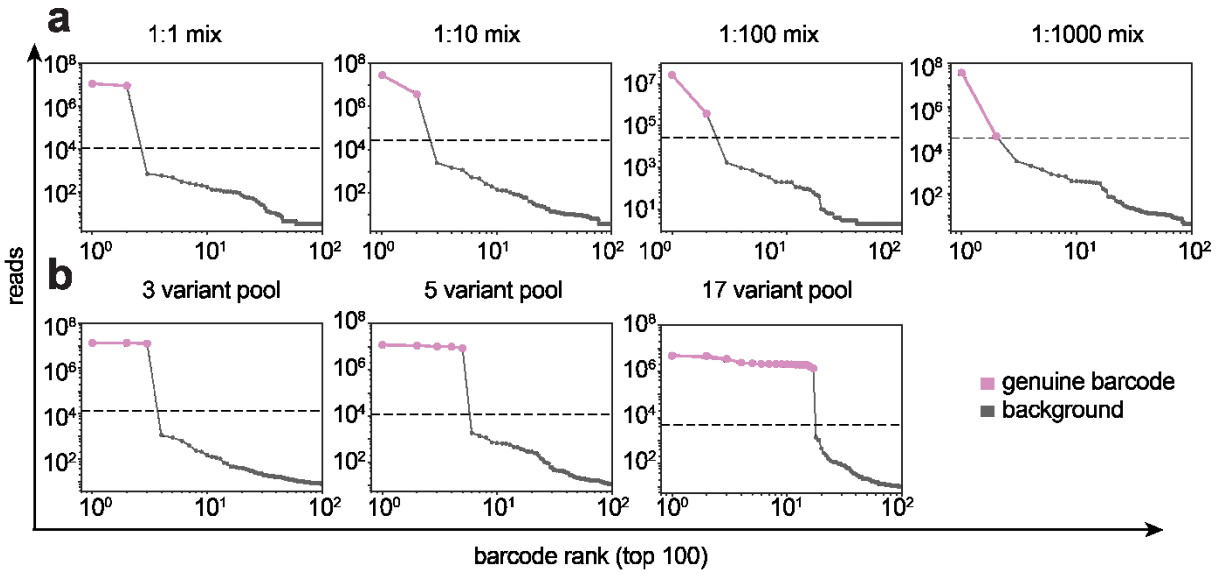

a) Two barcoded clones were mixed and barcodes detected via amplicon deep sequencing. **b)** 3, 5, and 17 distinct barcodes were mixed prior to amplicon deep sequencing. Unique top 100 barcodes detected are plotted. Dashed line indicates the minimum read count cutoff to discriminate erroneous barcodes from genuine barcodes using an unbiased knee point detection algorithm.

Supplementary Figure 4 | Epigenetic profiling shows differential methylation in clones from distinct RMCE events.

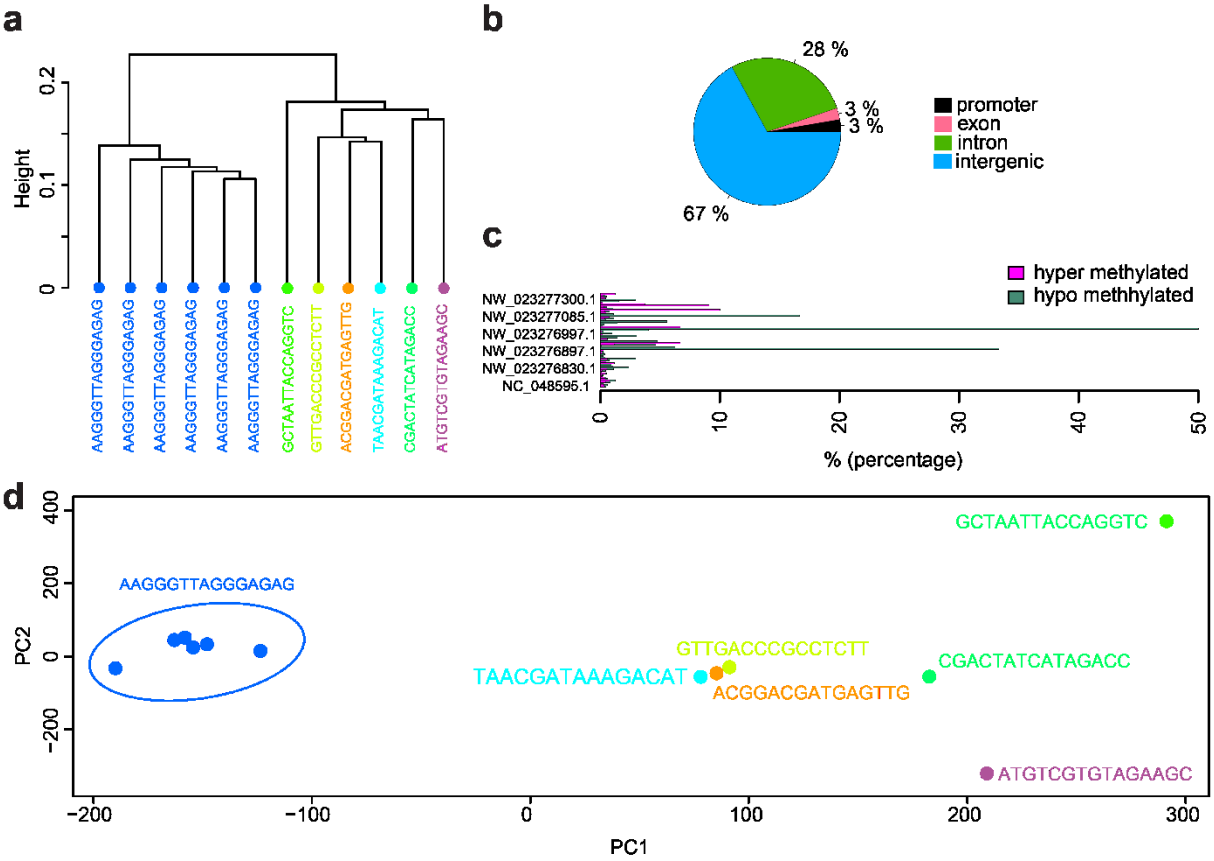

a) Hierarchical clustering of whole-genome methylation analysis for 12 clones, with 6 sharing an identical barcode (blue) and 6 with a unique barcode. **b)** The gene region of significant differential methylation events. **c)** Significant (p-value ≤ 0.05) hyper- and hypomethylation events per chromosome between min and max values observed within the 12 clones. **d)** Principal Component Analysis of all 12 methylation profiles showing principal component 1 and principal component 2 for each sample.

3 General discussion

3.1 Rational cell engineering in CHO biofactories

Synthetic biology, inspired by forward-engineering principles to program desired cellular behavior, allows reconstruction of cellular behavior using existing or new biological building blocks. In case the function of biological modules is known, i.e. characterized gene-phenotype relationships, conventional genetic engineering approaches (overexpression and KOs) effectively fine-tunes bioprocess fit, transgene expression or quality attributes of CHO biofactories. While such approaches are straightforward, cell lines frequently exhibit mixed phenotypes combining stochastic phenotype variation with programmed cellular behavior impeding rational cell engineering approaches. Further, the apparent and partially unpredictable interdependency of specific products with the host system, dose-dependent effects, and CHO strain variation, create the need for custom cell engineering on a case-by-case basis. This is exemplified by the conflicting results of overexpressing the ER-resident molecular chaperon PDI, when comparing reports in different CHO strains, overexpression methods, and different recombinant model proteins (Borth et al., 2005; Davis et al., 2000; Johari et al., 2015; Mohan et al., 2007; Pybus et al., 2014; X. Zhang et al., 2024). The function of overexpressed genes can deviate substantially as compared to their physiological function, where individual genes are rarely expressed at such high rates and in isolation. Thus, empirical cell engineering by modifying expression of individual genes within complex biological systems continues to be long and arduous. From a holistic perspective, our inability to accurately predict the outcomes of genetic designs from a set of known inputs remains a significant challenge.

5R-Hyl formation in mammalian cells is catalyzed by either PLOD1/2/3 or JMJD4/JMJD6/7 (Markolovic et al., 2015). Given the high degree of sequence conservation between these enzymes in human and CHO cells, conserved iron as well as 2-oxoglutarate cofactor and substrate binding sites, identical enzymatic functions in CHO cells as compared to their human counterpart were likely (Bauer et al., 2024a). End-point enzymatic reactions display much less complex biological network topology, as compared to gene regulatory networks with higher-order functional redundancy (Sorrells & Johnson, 2015). Here, PLOD1-3 isoenzymes showed functional redundancy to generate 5R-Hyl micro heterogeneities and simultaneous ablation of all three proteins resulted in removal of 5R-Hyl levels during bioprocess production. However, the removal of 5R-Hyl as micro heterogeneities in therapeutic pharmaceuticals was accompanied by unintended effects during bioproduction,

such as increased cell growth, mild improvement of cellular productivity, and decrease of acidic species in the antibody product. Further, the study did not investigate the mechanistic explanation for the observed phenotype and the option remains that other indirect effects and pathways result in 5R-Hyl elimination or the observed change in bioproduction behavior. Comparative investigations on the systems level (i.e. transcriptomic or proteomic profiling) between KO and unmodified CHO cells can potentially hint towards the underlying mechanisms and cellular objectives driving the observed phenotype. Differential gene expression and knowledge base-driven pathway analysis can then identify which biological pathways change in response to PLOD ablation. Notably, PLOD1 has been described to markedly induce transcriptional activity of E2F1 (B. J. Li et al., 2021), which in turn regulates activity of SIRT-1, a histone deacetylase that inhibits p53 in response to DNA damage and restricts apoptosis (C. G. Wang et al., 2006). SIRT-1 gene KO has been recently demonstrated to improve cellular productivity and higher cell viability at the end of fed batch fermentation (WO 2020/260327A1). Measuring activity of SIRT-1 and E2F1 in PLOD1 KO and WT background using biochemical assays or immunoprecipitation can identify candidates and pathways responsible for increased bioproduction. Alternatively, hydroxylation of lysyl residues is critical for collagen biosynthesis, especially for conversion of fibril-forming collagens into stable supramolecular structures (Knott & Bailey, 1998; Qi & Xu, 2018). While the role of supramolecular collagen for tissue formation is well described, studies on the role of extracellular matrix (ECM) formation for suspension cells are currently lacking. Interestingly, PLODs have previously been associated with ECM remodeling either intra- or extracellularly (Salo et al., 2006). It can be hypothesized, that deposition and crosslinking of collagen displays a legacy feature of suspension-adapted cells with no functional value during bioproduction. Supportive to this hypothesis, a recent study identified several proteins associated with the extracellular matrix expressed by CHO cells, which impaired cellular productivity and cell growth due to occupation of cellular resources (i.e. SPARC, GPR56, NID1, LGALS3BP, BGN) (Kol et al., 2020). Alternatively, studies have identified various distinct interaction partner for PLOD1 (ER complex together with P3H3 and CYPB, and SC65) (Heard et al., 2016), PLOD2 (forming a chaperone complex with FKBP65, HSP47, and BiP) (Duran et al., 2017), and PLOD3 (colocalizing with GLT25D1/2) (Liefhebber et al., 2010), indicative for involvement in different biological pathways and functions. Especially PLOD3, responsible for approximately half of 5R-Hyl modifications in our study, has three domains encompassing catalytic sites for glycosyltransferase, accessory, and lysyl hydroxylase activity (Scietti et al., 2018). It remains unclear which of these functions are conserved in the context of CHO biofactories and contribute to elevated

cell growth and productivity observed in the presented study. To test the involved biological functions, KO cell lines which re-express either WT or mutant versions of the individual genes can be examined for their capability to express 5R-Hyl and cell growth during bioproduction. In summary, ablation of PLODs is associated with removal of 5R-Hyl micro heterogeneities, elevated cell growth, and mild improvement of cellular productivity. The precise mechanisms remain unknown and open to investigation. Nonetheless, KO of PLODs offers reliable removal of 5R-Hyl micro heterogeneities, circumventing detailed characterization to determine their impact on drug efficacy, safety, and the establishment of analytical control strategies to maintain consistent product quality.

Scenarios with similarly manageable design options are prone to rational testing of genetic ablations to optimize CHO bioprocess fit. The described approach can likely be transferred to various process-induced micro heterogeneities as a consequence of post-translational modifications, such as N- and O-type glycosylations, cysteine modifications, galactosylations, carbonylations, oxidations, glycation, aspartate isomerizations, and C-terminal lysine variations (Geist et al., 2013; Gramer, 2014; Raju & Jordan, 2012). Empirical optimizations are frequently performed in design-build-test-learn (DBTL) cycles, where generated data from the test phase is used to learn important cellular characteristics for the next iteration. Such DBTL cycles thrive in more defined contexts with *a priori* mechanistic understanding, demonstrated by reliable CHO engineering results in modification of apoptosis (Cost et al., 2010; Macaraeg et al., 2013; Tang et al., 2022) and terminal N-glycosylation reactions (Chai et al., 2020; Haryadi et al., 2013; Son et al., 2011). Guided by increasingly sophisticated computational predictions, DBTL cycles can continue to tackle more complex pathways such as core protein secretion (261 gene products, organized in 12 subsystems) (Kol et al., 2020) and general N-glycosylation (Stach et al., 2019). By choosing the best fitted constraints to the biological task, these algorithms support and refine mechanistic understanding of cellular processes at play. For example, while flux-balance analysis performs well in predicting metabolic shifts in response to changed bioreactor conditions (Gopalakrishnan et al., 2024) they fail to predict glycosylation patterns of knock-out profiles (i.e. the outcome of perturbing specific glycosylation enzymes) (Spahn et al., 2016). Instead, the biological task “glycosylation” can be accurately predicted using Markov chains, which simulates a “memoryless” chain of events instead of optimal flux through a network (Liang et al., 2020; Rubino & Sericola, 2014; Spahn et al., 2016). Notably, this model predicted the outcome of experimental KO of B4galt1/3 and St3gal3/4 of four different glycosylated therapeutics precisely (i.e. Rituximab, erythropoietin, Enbrel, and alpha-1

antitrypsin) (Liang et al., 2020). Similarly, the tasks involve in general secretion of proteins can be more accurately described by combining context-specific gene expression data with genome scale models of the secretion pathway (Masson et al., 2024). This essentially quantifies “secretory tasks” (e.g. disulfide bond formation, N-glycan processing, recognition of misfolded protein) from omics data in the respective cellular situation, which might enable the description of underlying molecular mechanisms based on simple omics data in the future.

3.2 CRISPR screenings for CHO biofactories

CRISPR screens are well suited to uncover genes involved in production-relevant biological processes on a genome-wide scale, partly closing the gap in understanding the underlying molecular mechanisms of high-producer phenotypes in CHO cells. Pooled CRISPR screens depend on validated and specific reporter assays for each phenotype of interest (Bock et al., 2022). In the absence of such reporter assays, initial studies have focused dominantly on drug-induced survival-associated phenotypes with limited translations for bioprocessing (S. H. Kim et al., 2023; Kretzmer et al., 2022; Xiong et al., 2021b). In contrast, productivity readouts are more difficult to achieve as recombinant antibodies are secreted into supernatant. This displays a major caveat in the field: the information about high-productivity (i.e. the secreted antibody) cannot be used to enrich the responsible cell fraction if both are physically separated. Reporter cell lines express fluorescence proteins for efficient flow cytometry sorting, however, the recombinant product differs substantially in their requirement towards the host secretion machinery, e.g. protein sequence, ER-folding, and post-translational modifications. While reporter proteins are usually sufficient to indicate simple transcriptional activity, such as the identification of transcriptionally active genomic hotspots (Crawford et al., 2013), they do not reliably mimic the complex post-translational cellular burden which can lead to biased screening results. Measuring surface labeling of secreted proteins transiently associated with the cell surface may provide an acceptable compromise between readout quality and throughput (S. H. Kim et al., 2024). However, results of this screening approach have not been validated in a controlled bioprocess platform (fed-batch or intensified fed-batch in scale-down bioreactors, representative of large-scale production). Moreover, control cells have been harvested at different time points (after day 9 compared to day 10/12 for KO samples), cell viability drops early (reaching <80% viability at day 7), and titers reach a maximum of 0.8 g/l (S. H. Kim et al., 2024), indicative of nutrient limitations in the absence of feeding (Sellick et al., 2011). Finally, any perturbation that reduce cell fitness drops out of such positive selection screening. Essentially this type of screening does not allow to discriminate fitness impairing variants from perturbations which show improved productivity associated with impaired fitness. Importantly, screens which target improved productivity of cells should expect simultaneous fitness defects due to the well described inverse correlation between growth and transgene expression (Frei et al., 2020; G. W. Li et al., 2014; Scott et al., 2010).

Given the complexity of creating representative reporter assays for evaluation of cellular secretion capacity, the second study of this thesis employed an arrayed CRISPR screening

format using a batch production mode in 24-deep well plates. Arrayed CRISPR screenings allow characterization of complex phenotypes due to the physical separation of each perturbation in individual compartments (Bock et al., 2022). 24-deep well plate formats have been previously demonstrated to reflect cellular productivity ranks reasonably well during CLD screening (Mora et al., 2018). As a result of the screening, Myc depletion was identified to improve productivity 1.7-2.1x fold and in turn impair cell growth (Bauer et al., 2022). The initial results were subsequently confirmed across clones, various antibody-formats, and after scale-up (ambr15 and ambr250 scale-down bioreactor systems), confirming Myc KO as a robust strategy to improve productivity of CHO biofactories. The increased cellular productivity was associated with a higher invest of transcriptional resources towards to transgene when comparing Myc KO to WT cells. Multiple studies have observed increased transcript abundance of the transgene for elevated productivity, however the methods to achieve such transcription boosts are context-specific and incompletely understood (Lattenmayer et al., 2006; Z. Lee et al., 2024; S. M. Noh et al., 2018). Especially, elevated HC transcript levels correlate well with cellular productivity when accompanied by LC excess (C. J. Lee et al., 2009). To achieve higher transcript levels, increased transgene copy numbers (regardless of random or targeted integration of transgenes) results in varying results with generally low correlation and fast plateauing of productivity and transcript levels with higher copy numbers (Z. Lee et al., 2024; S. M. Noh et al., 2018). This suggests, that productivity is limited transcriptionally until reaching stoichiometric imbalance with the downstream post-transcriptional secretory machinery (Schlatter et al., 2005). In the presented study, Myc KO was accompanied by increased transgene levels as well as elevated ER-related proteins indicative of a more general cellular reprogramming towards bioproduction. While increased transgene levels could result from higher activity of CMV promoters in S phase (Brightwell et al., 1997) or freed cellular resources due to impaired proliferation (Xia et al., 2006), the precise mechanism of cellular reprogramming by Myc KO in CHO biofactories remain elusive. Recent studies suggest that ectopic expression of transcription factors or master regulators, such as BLIMP1 or Myc, potentially mimics the high secretory phenotype of plasma cells in nature (Raab et al., 2024; Shaffer et al., 2002; Torres & Dickson, 2021). Notably, repression of Myc transcription is necessary for terminal differentiation of B lymphocytes and ceases in IgG-secreting plasma cells (Larsson et al., 1991; K.-I. Lin et al., 2000). Due to the pleiotropic effects of Myc on almost every cellular process a more comprehensive model is currently lacking and hypothetical mechanisms of action are rather vague in nature. However, Myc is central for cell growth regulation with many growth-promoting signals converging on Myc (Chou et al., 2010; Palomero et al.,

2006; Roussel et al., 1991). Given that the results of the presented study are conflicting to multiple studies which describe beneficial effects on bioproduction for ectopic overexpression of Myc (Ifandi & Al-Rubeai, 2003; Kuystermans & Al-Rubeai, 2009; Latorre et al., 2023), two settings seem plausible: one, slow biomass accumulation penalizes final volumetric productivity and increased cell growth consequently results in increased product yield (Mahé et al., 2022); two, biomass is maximized using high seeding density processes and/or perfusion processes where productivity is restricted by nutrients, peak osmolarity, or accumulation of waste metabolites (J. L. Xu et al., 2020; W. J. Xu et al., 2023; Yongkya et al., 2019). Notably, only the first case is likely profiting from additional mitogenic stimuli by ectopic overexpression of Myc. The presented study suggests, that Myc KO can further enhance high cell density production processes which accumulated sufficient biomass by other means (e.g. N-1 perfusion, volume concentration, and long seed train cultivation). This is supported by the rescue of specific productivity rates by Myc KO, which are frequently reduced in high cell density processes, indicative of a mutually exclusive cell fate decision for either growth or production. Further studies need to explore the link between Myc KO, elevated transgene and ER-protein transcript levels, and attenuated proliferation to identify the precise role of Myc for bioproduction. However, the role of Myc is further supported by a recent study describing BLIMP1 overexpression, a transcription factor which is highly expressed in all natural antibody-secreting cells and associated with Myc repression, resulted in decreased cell proliferation and improved productivity of CHO cells (Torres & Dickson, 2021). Due to their potency in regulating productivity and cell proliferation, pleiotropic effectors such as BLIMP1 and Myc represent promising candidates for proliferation control strategies. Such studies could additionally investigate the involved biological functions by generating Myc KO cell lines which re-express Myc under control of inducible promoters for fine-tuned ectopic expression control. Titration of Myc levels, potentially using mutant versions, will enable not only system level investigations of Myc effects, but also proliferation control during bioproduction without the need for small-molecule treatment, elevated osmolarity or temperature shifts. Of note, the effects of Myc ablation were complementary to proliferation control strategies already implemented in the bioprocess and amplified each other, i.e. increased osmolarity combined with mild hypothermia, growth-inhibiting small molecules, and Myc ablation (Oguchi et al., 2006; J. H. Park et al., 2016; Takagi et al., 2001). Presumably, initial studies which focused on less potent CDKs as effector genes can be revisited using BLIMP1 and Myc to drive and control cell proliferation (Fussenegger et al., 1998).

To enable genome-wide interrogation of complex productivity phenotypes, peptide barcoding (flycodes) may provide the necessary link between responsible genotype (knockout or sgRNA) and readout (secreted antibody in the supernatant) (Egloff et al., 2019; Matsuzaki et al., 2021). While such libraries are currently limited to few thousands variants, the matching of NGS and LC-MS/MS data would allow backtracking of high expressing flycode-tagged antibodies to their respective producer cell. Combined with *a priori* sgRNA library nesting and sequencing, all flycode-sgRNA pairs are unambiguously assignable. As a result, overrepresentation of flycode variants indicate higher productivity of the respective sgRNA and thus a specific KO in a pooled screening approach. Without the need for high sample throughput, this screen can utilize bench-top bioreactors, effectively screening a wide array of genetic variants in a controlled system with reliable bioprocessing conditions.

3.2 Clone-to-clone diversity during cell line development

Similar to cancer or immortalized cell lines, CHO cells exhibit extensive genetic and phenotypic instability (M. J. Wurm & Wurm, 2021). Consequently, subpopulation of CHO cells, i.e. subclones, arise constantly and exhibit substantial genetic and phenotypic heterogeneity. This instability manifests as a double-edged sword in bioproduction: while instability guarantees a wide array of functional competence (i.e. adapt to a given environment or produce recombinant proteins), it simultaneously contributes to unpredictable long term outcomes for CLD (i.e. sustained product expression, homogenous post-translational modifications). This variance can be distinguished based on a variety of features, e.g. accumulating single-nucleotide variants (SNVs) (Kuhn et al., 2020), chromosomal instability (Baik & Lee, 2018; Vcelar et al., 2018a), or by tracking clonal populations (Moeller et al., 2020; Porter et al., 2014). Genomic plasticity in turn results in clonal evolution caused by biological mechanisms such as heritable variation, genetic drift, selection and environmental changes (Turajlic et al., 2019). During CLD, CHO cells therefore exhibit remarkable clone-to-clone variability (even within isogenic and clonal populations) and strong phenotypical drift during long-term cultivation. While the general mechanisms at play are characterized, their individual contribution and implications in the context of generating CHO biofactories are insufficiently understood. Especially the extent and quality of heritable phenotypic features is conflicting, with studies describing epi-/genetic mutations during long-term cultivation (i.e. the constant accumulation of mutations by erroneous DNA replication) and epi-/genetic drift (i.e. random changes in the genetic makeup by bottleneck or founder effects) over the course of subcloning and cryopreservation as dominant effects for causing phenotypic heterogeneity (Baik & Lee, 2018; S. L. Davies et al., 2013; Feichtinger et al., 2016; Ko et al., 2018).

Therefore, the third study of this thesis aimed to dissect the factors predominantly contributing to phenotypic diversity in an isogenic TI expression system during CLD. By using unique genetic labels individual TI lineages can be traced back after the TI event across stable pool generation, single cell cloning, and subsequent phenotypic characterization (Bauer et al., 2024b). Presumably and based on studies investigating the source of clonal heterogeneity in context of random integration of expression plasmids, subcloning generates quasi-species by founder effects and consecutive micro-evolution until accumulation of sufficient biomass for productivity tests and cryopreservation (S. L. Davies et al., 2013; Eigen & Schuster, 1977; Vcelar et al., 2018a; F. M. Wurm, 2013). Random integration clones show a wide panel of copy number variations and variable integration

sites, suffering from a unique and genomic context-dependent set of homologous recombination, gene silencing, expression plasmid fragmentation, and occurrence of tandem repeats, all contributing to volatile productivity of clonal populations (Du et al., 2013; Huhn et al., 2022; Osterlehner et al., 2011). Additionally, subcloning potentially alters the DNA methylation pattern of cells randomly, resulting in escalated diversification of production relevant phenotypes (Weinguny et al., 2020; Weinguny et al., 2021). In line with this model, induction of random changes in the DNA methylation pattern by KD or inhibition of DNA methyltransferases mimics cellular stress during subcloning and significantly enriches outliers with regard to cellular productivity (N. Marx et al., 2022). However, the beneficial effect was limited to cell populations with low productivity, suggesting that only cells with low transcription rates of transgenes can experience stochastic upregulation and consequently increased transgene mRNA levels. The observed findings could not be transferred to cells with already high productivity, which likely demonstrate high transgene transcription rates. In the presented study, we re-visited the major sources of diversification after targeted integration into a pre-defined transcriptionally active genetic hotspot. Speculatively, cells generated by TI show a substantially higher fraction of high productivity phenotypes and thus allow identification of sources contributing to clonal diversity beyond random DNA methylation, copy number, placement, and rearrangement influences. Strikingly, DNA methylation patterns from TI-generated clones clustered closely in clones from identical TI lineages (sibling clones), despite undergoing individual subcloning procedures, media adaptation and clone screening. Moreover, sibling clones (different clones but originating from the identical TI event) showed significantly similar phenotypic behavior with regard to metabolism, cell growth, and product characteristics. This suggests, that the majority of phenotypic heterogeneity is determined *a priori*, heritable, and established at the time of the TI event (or earlier). Instead, the study suggest the model that most functional heterogeneity is “stored” in aged (host-) cell lines with increased genomic diversification and linearly increases over cellular generations. This increased genomic diversification influences transgene expression likely *in trans* by factors which were not investigated in the presented study. However, given the remarkable variation in productivity despite shared global transcriptome and methylation profiles, it can be conceived that subtle and mild changes in cellular networks have dramatic consequences for cellular productivity. This is also supported by the inability to accurately predict CHO biofactory performance based on early clonal biomarkers as of now (Desmurget et al., 2024). To identify early biomarkers of high productivity phenotypes, future studies can utilize barcode lineage tracing to substantially mitigate experimental noise introduced by clonal drift effects from the time point of

transfection onwards. Comparing high and low producing biological replicates (i.e. identical barcodes but different clones) will allow higher sensitivity and detection of minor changes associated with higher productivity phenotypes, with less influence of the stochastic gene expression changes observed by unrelated clonal variation. Notably, previous studies were unable to correct for such clonal variation, as clonal lineages could not be detected and backtracked so far.

The results in the presented study are incompatible with the quasi-species concept, instead asserting that TI CLD essentially mitigates epi-/genetic drift effects. Instead, actively transcribed regions of the genome were effectively shilded from DNA methylation changes during subcloning (Weinguny et al., 2021), which would include the genomic hotspot used during TI. Random integration cell clones generated by gene amplification methods are likely more prone to DNA methylation changes, as their productivity depends on consistent expression of up to 1000 copies in individual genomic contexts. Utilization of an individual genetic hotspot with single-copy integration thus increases robustness of expression and, at least partly, protects transgene productivity from epigenetic changes.

Long-term genomic diversification exists as a constant feature, resulting in increased heterogeneity of aged cell lines depending on environmental contexts. Routine cultivation of isogenic TI cell lines imposes comparably mild environmental selection pressure, which is not averting phenotypic homogeneity (Sergeeva et al., 2020). Genomic barcoding allows control over the amount of variants (i.e. TI events) selected to undergo phenotypic characterization during clone screening and alleviates the screening burden of CHO biofactories during CLD. The study thus contributes to understanding of the underlying dynamics of CHO cell evolution resulting in improved CLD strategies. Ultimately, this paves the way for controlling cellular diversity to fine tune phenotypic behavior and enables future studies to investigate the cellular mechanisms at play which are associated with high productivity phenotypes.

4 List of Abbreviations

6-TG	6-thioguanine
AD	Actuator domain
ADCC	Antibody-dependent cellular cytotoxicity
AGE	advanced glycation end products
ATF	Activating transcription factor
ATM	Ataxia telangiectasia mutated
ATR	Ataxia telangiectasia and Rad3-related protein
Bak	Bcl-2 homologous antagonist/killer
Bax	Bcl-2-associated X protein
Bcl-2	B-cell lymphoma 2
BCL-xL	B-cell lymphoma-extra large
BHK	Baby hamster kidney
BiP	Binding immunoglobulin protein
BLIMP1	B lymphocyte-induced maturation protein-1
BS	Brainshuttle
bsAb	Bispecific antibody
C/EBP-α	CCAAT/Enhancer binding protein alpha
CAR	Chimeric antigen receptor
Cas9	CRISPR-associated protein 9
CEF1α	Chinese hamster elongation factor-1 alpha
CERT	Ceramide transfer protein
CFL1	Cofilin-1
CH1	Constant heavy 1
CHO	Chinese Hamster Ovary
CLD	Cell line development
CMP-SAT	cytidine monophosphate-sialic acid-sialic acid transporter
COBRA	Constraint-based reconstruction and analysis
CQA	Critical quality attributes
Cre	Causes recombination
CRISPR	Clustered regularly interspaced short palindromic repeats
DBD	DNA binding domain
dCas9	dead Cas9
DHFR	Dihydrofolate reductase
DNA	Deoxyribonucleic acid
DO	Dissolved oxygen
DSB	Double-strand break
DTE	Difficult to express
DTT	Dithiothreitol
E2F	E2 promoter-binding factor
eIF3	Eukaryotic translation initiation factor 3
ELISA	Enzyme-linked immunosorbent assay
EMEA	European medicines agency
ER	Endoplasmatic reticulum
FA	Formic acid
FAIM	Fas apoptosis inhibitory molecule
FasL	Fas cell surface death receptor ligand
FBA	Fluc balance analysis
FDA	Food and drug administration
Flp	Flippase
FRT	FLP recognition target
FUT	Fucosyltransferase
FX	Fucosyltransferase 10
GADD34	Growth arrest and DNA damage-inducible Protein 34
GADD45	Growth arrest and DNA damage-inducible 45
GalT	Galactosyltransferase
GEM	Genome-scale metabolic models
GMD	GDP-mannose 4,6-dehydratase
GNE	Glucosamine (UDP-N-acetyl)-2-epimerase/N-acetylmannosamine kinase
GnT	N-acetylglucosaminyltransferase

GOI	Gene of interest
GPCR	G protein-coupled receptor
gRNA	guide RNA
GS	Glutamine synthetase
HC	Heavy chain
hCMV-IE1	Human cytomegalovirus immediate early 1
HCP	Host cell proteins
HDR	Homology directed repair
HEK	Human embryonic kidney
HMW	High moleculare weight
HPLC	High pressure liquid chromatography
HPRT1	Guanine phosphoribosyltransferase 1
HSP	Heat shock protein
Hyl	5R-hydroxylysine
ICE	Inference of CRISPR edits
IgG	Immunoglobulin G
IVCD	Integrated viable cell density
JMJC	Jumonji domain-containing
kbp	kilo-base pair
KD	Knockdown
KDEL	Lysine (K), Aspartic acid (D), Glutamic acid (E), and Leucine (L)
KO	Knockout
KRAB	Krüppel-associated box
LacI	Lactose operon repressor
LC	Light chain
LDH	Lactate dehydrogenase
loxP	locus of crossover in P1
mAB	Monoclonal antibody
MCAF	MBD1-containing chromatin-associated factor
MCP1	Mitochondrial pyruvate carrier 1
MCP2	Mitochondrial pyruvate carrier 2
miR	microRNA
mRNA	Messenger ribonucleic acid
MS	Mass spectrometry
mTOR	Mechanistic target of rapamycin
MTX	Methotrexate
NF-κB	Nuclear Factor kappa-light-chain-enhancer of activated B cells
NGNA	N-glycolylneuraminic acid
NHEJ	Non-homologous end-joining
NS0	Non secreting murine myeloma
nt	nucleotide
p21CIP1	Cyclin-dependent kinase inhibitor 1
p27	Cyclin-dependent kinase inhibitor 1B
p65	RelA
PBS	Phosphate-buffered saline
PCA	Principle component analysis
PCR	Polymerase chain reaction
PDHK	Pyruvate dehydrogenase kinase
PERK	Protein kinase RNA-like endoplasmic reticulum kinase
pg	Picogram
pH	Potential of hydrogen
PLOD	Procollagen-lysine 2-oxoglutarate 5-dioxygenases
PNP	Purine nucleoside phosphorylase
pO2	Partial pressure of oxygen
pRED	Pharma Research and Early Development
PTEN	Phosphatase and tensin homolog
PTM	Post-translational modification
RMCE	Recombinase-mediates cassette exchange
RMD	Rudimentary
RNA	Ribonucleic acid
RNAi	RNA interference
RNP	Ribonucleoprotein

rpm	revolutions per minute
rTetR	reversed TetR
RTK	Receptor tyrosine kinase
scFv	Single-chain variable fragment
SEAP	Secreted alkaline phosphatase
SEC	Size eclusion chromatography
SERPINB1	Serine Protease Inhibitor, Clade B (Ovalbumin), Member 1
SETDB1	SET domain, bifurcated 1
sgRNA	single guide RNA
siRNA	small interfering RNA
SNARE	Soluble NSF attachment protein receptor
STB	Stirred tank bioreactor
SV-40	Simian vacuolating virus 40
TALE	Transcription activator-like effector
TCA	Trichloroacetic acid
TCB	T-cell bispecific
TCB mAbs	T-cell bispecific monoclonal antibodies
TetR	Tetracycline repressor
TEV	Tobacco etch virus protease
TI	Targeted integration
TMM	Trimmed mean of M value method
TNF	Tumor necrosis factor
TRAIL	TNF-related apoptosis-inducing ligand
TRIS	Tris(hydroxymethyl)aminomethane
UPLC	Ultra-performance liquid chromatography
UTR	Untranslated region
UV	Ultraviolet
VCD	Viable cell density
VCP	Valosin-containing protein
VH	Variable heavy
VL	Variable light
VP16	Viral protein 16
WHO	World health organization
WI-38	Wistar Institute-38
WT	Wildtype
XBP1S	X-box binding protein 1, spliced form
XIAP	X-linked inhibitor of apoptosis protein
XIC	Extracted ion chromatogram
XKG	Xaa-Lys-Gly
YY1	Ying yang 1
ZFP	Zinc finger protein
ZFR	Zing finger RNA-binding protein

5 Acknowledgements

During the PhD celebration event held on October 25 2024, the opening of the event was marked by a speech delivered by *Dr. CHO*. At around 3:00 PM, he took the stage and addressed the audience with the following remarks:

„Greetings and welcome. Ich bin Niels. This text has not been written using a large language model.

I am very happy. Happy that you are all here. Happy that my PhD journey has ended. Happy that we celebrate this milestone together.

If you start reading my thesis you will stumble upon a weird quotation from Thích, a Zen master: “for things to reveal themselves to us, we need to be ready to abandon our views about them”. Gaining revelations, by letting go of something? I do not understand. The mysteries of life are a problem to solve. Solving by gaining insights and revelations! Dissecting bigger problems into smaller sub problems and using scientific rigor until you know it all.

And I started my PhD not understanding.

This journey started more than 5 years ago. Years I spent on asking questions about one cell line which is as much characterized as it is not (if you want to know more, all details are written in the thesis). One answer is followed by two questions: something which can be seen as having a long lasting struggle, or being on an interesting journey (Erich Fromm would approve). Typically we emphasize the downs, while missing the ups, sometimes so much that our light loses brightness for a while.

When I ask another master for advice he says:
“To be Jedi is to face the truth and choose. Give off light, or darkness, Padawan. Be a candle, or the night. “

The struggle for insight is as tiring as it is rewarding. The swings, these ups and downs, the beginning and the end, are all part of the same one journey. Each local peak required, each one welcome.

5 Acknowledgements

“Patience you must have, my young Padawan” Yoda keeps saying and “This is the way” the Mandalorian answers.

I am very grateful for these 5 years, a fact which I see much clearer now towards the end, as compared to within. While we walk our path in life we keep looking forward, but we understand things backwards.

We struggle and keep stumbling, gaining stability with each step. “A master has failed more times, than a beginner has ever tried” (this was the last Yoda quote). And I learned that
A equals B, is true as well as, A does not equal B, is true. If I am capable of abandoning my view about things, I start to understand. A, B, maybe.

The mystery of life is not a problem to solve, but a reality to experience. And I want to thank you for being part of this experience. Today is a celebration of what we achieved together, the journey which we shared, the ups and downs (hopefully today will be an up). This is something I could not have done alone.

I want to take the time to emphasize this fact. Emphasizing by introducing my PhD awards!

These rewards reflect the most exceptional contributions to my journey, paving my path and helping me walk on it.

I start with shared first place: Simon & Julian. Simon and Julian not only share their studies at the University of Konstanz, but also their most exceptional leadership and mentoring style. Usually people I meet have individual strengths: either scientific rigor or aptitude, a lot of empathy and inter-people skills, an analytical mind or a lot of creativity. It is rare that supervisors combine a multitude of skills. And even more rare to combine all of them. This journey would have been impossible for me without their unwavering support. A huge round of applause for the World’s Best Doctoral Supervisors: Simon and Julian!!!

Next first place goes to the most amazing Labs in the world!
These labs excel not only by their astonishing output and performance, their kindness, or their scientific expertise. But importantly by the amount of care and help they provide for each other. One for all and all for one! Normally one can only become a member of one of them. But as part of both worlds all I can say is: a huge round of applause for the world’s

best research laboratories!!!! It’s hard to say which one is better, so it’s easier to distribute one to be the best academic and one the best industrial research lab of the world.

Next first place goes to the hidden champions. Their contribution cannot be mentioned in text or speech, as no words exist which could possible describe the amount nor quality of meaning for me. I mean except for the things I said right now. Please meet family Bauer (including future members) and friends!!! A huge amount of applause!

And the final first place goes to our amazing sponsor of beer, the benefactor of brews, and the purveyor of pints. His brewing mastery is only matched by his CHO fermentation skills. This sponsor is the grand guarding of golden ales, the champion of chilled chalices. The maestro of malts, the wizard of wheat, and the virtuoso of vibrant vintages. He proudly presents the legacy of luscious lagers, our today’s repertoire of robust refreshments. The connoisseur of craft and sultan of sips: Oli!!!

The buffet is opened!”

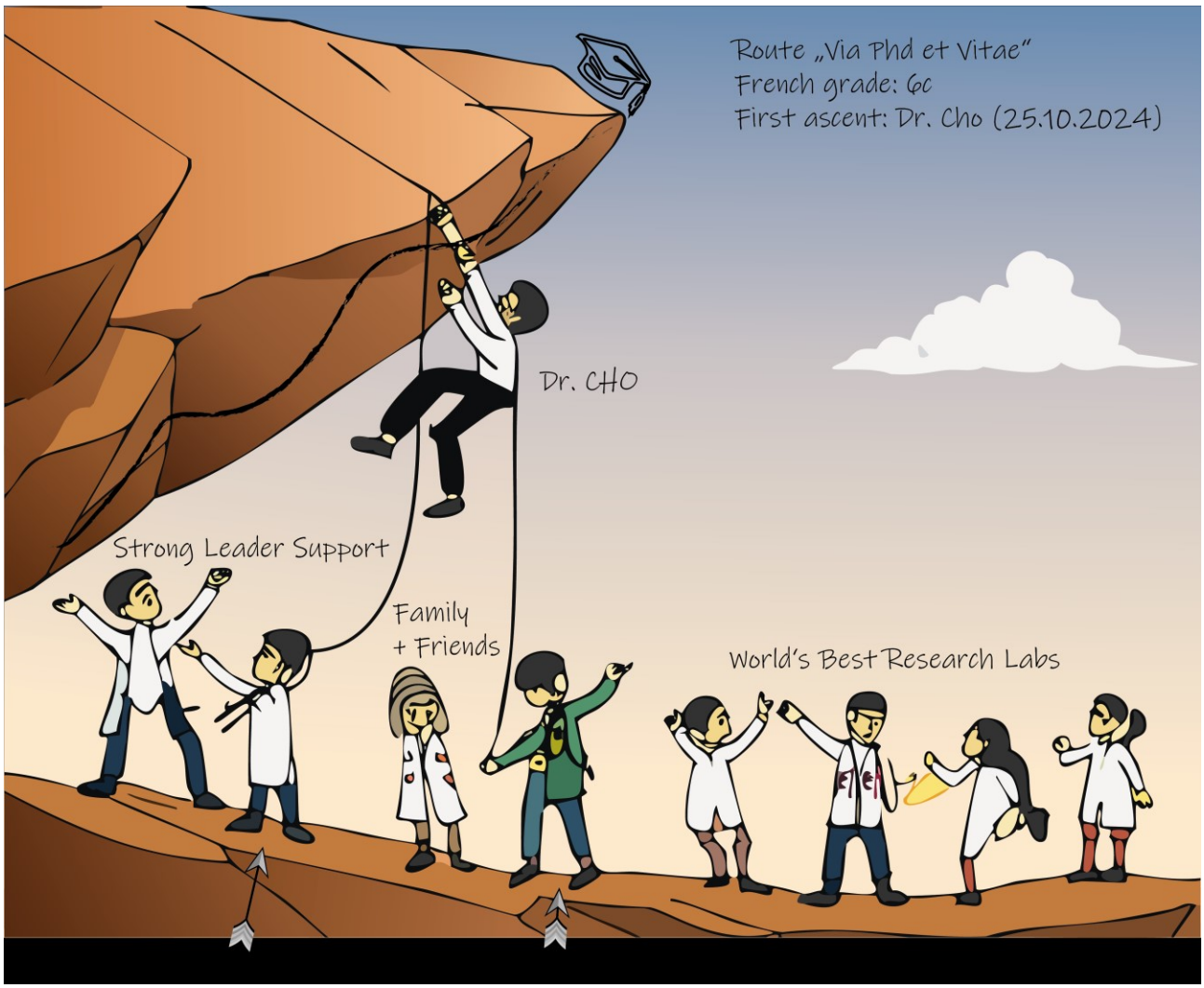

Figure 14 Via PhD et vitae. Climber on an overhanging rock. He is having troubles holding himself to the rock. People on the ground look up and are preparing to catch him if he falls. The people on the ground open their hands so that the climber would fall directly into their arms. The people on the ground look like a team working in biotechnology laboratories wearing lab coats. The rope belaying the climber looks like a DNA double helix

6 References

Alerasool, N., Segal, D., Lee, H., & Taipale, M. (2020). An efficient KRAB domain for CRISPRi applications in human cells. *Nature Methods, 17*(11), 1093-+. doi:10.1038/s41592-020-0966-x

Altamura, R., Doshi, J., & Benenson, Y. (2022). Rational design and construction of multi-copy biomanufacturing islands in mammalian cells. *Nucleic Acids Research, 50*(1), 561-578. doi:10.1093/nar/gkab1214

Altenschmidt, U., Kahl, R., Moritz, D., Schnierle, B. S., Gerstmayer, B., Wels, W., & Groner, B. (1996). Cytolysis of tumor cells expressing the Neu/erbB-2, erbB-3, and erbB-4 receptors by genetically targeted naive T lymphocytes. *Clinical Cancer Research, 2*(6), 1001-1008.

Arden, N., & Betenbaugh, M. J. (2004). Life and death in mammalian cell culture: strategies for apoptosis inhibition. *Trends in Biotechnology, 22*(4), 174-180. doi:10.1016/j.tibtech.2004.02.004

Astley, K., Naciri, M., Racher, A., & Al-Rubeai, M. (2007). The role of p21^{cip1} in adaptation of CHO cells to suspension and protein-free culture. *Journal of Biotechnology, 130*(3), 282-290. doi:10.1016/j.jbiotec.2007.04.012

Ausländer, S., Ausländer, D., Müller, M., Wieland, M., & Fussenegger, M. (2012). Programmable single-cell mammalian biocomputers. *Nature, 487*(7405), 123-+. doi:10.1038/nature11149

Ausländer, S., & Fussenegger, M. (2013). From gene switches to mammalian designer cells: present and future prospects. *Trends in Biotechnology, 31*(3), 155-168. doi:10.1016/j.tibtech.2012.11.006

Ausländer, S., & Fussenegger, M. (2017). Synthetic RNA-based switches for mammalian gene expression control. *Current Opinion in Biotechnology, 48*, 54-60. doi:10.1016/j.copbio.2017.03.011

Ausländer, S., Ketzer, P., & Hartig, J. S. (2010). A ligand-dependent hammerhead ribozyme switch for controlling mammalian gene expression. *Molecular Biosystems, 6*(5), 807-814. doi:10.1039/b923076a

Ausländer, S., Stücheli, P., Rehm, C., Ausländer, D., Hartig, J. S., & Fussenegger, M. (2014). A general design strategy for protein-responsive riboswitches in mammalian cells. *Nature Methods, 11*(11), 1154-1160. doi:10.1038/Nmeth.3136

Bacchus, W., Weber, W., & Fussenegger, M. (2013). Increasing the dynamic control space of mammalian transcription devices by combinatorial assembly of homologous regulatory elements from different bacterial species. *Metabolic Engineering, 15*, 144-150. doi:10.1016/j.ymben.2012.11.003

Baer, G. M., Shaddock, J. H., Houff, S. A., Harrison, A. K., & Gardner, J. J. (1982). Human Rabies Transmitted by Corneal Transplant. *Archives of Neurology, 39*(2), 103-107. doi:DOI 10.1001/archneur.1982.00510140037010

Baik, J. Y., & Lee, K. H. (2018). Growth Rate Changes in CHO Host Cells Are Associated with Karyotypic Heterogeneity. *Biotechnol J, 13*(3), e1700230. doi:10.1002/biot.201700230

Baker, K. N., Rendall, M. H., Hills, A. E., Hoare, M., Freedman, R. B., & James, D. C. (2001). Metabolic control of recombinant protein glycan processing in NS0 and CHO cells. *Biotechnology and Bioengineering, 73*(3), 188-202. doi:DOI 10.1002/bit.1051

Baker, O., Tsurkan, S., Fu, J., Klink, B., Rump, A., Obst, M., . . . Stewart, A. F. (2017). The contribution of homology arms to nuclease-assisted genome engineering. *Nucleic Acids Research, 45*(13), 8105-8115. doi:10.1093/nar/gkx497

Bandyopadhyay, A. A., O'Brien, S. A., Zhao, L., Fu, H. Y., Vishwanathan, N., & Hu, W. S. (2019). Recurring genomic structural variation leads to clonal instability and loss of productivity. *Biotechnol Bioeng, 116*(1), 41-53. doi:10.1002/bit.26823

Bareither, R., Bargh, N., Oakeshott, R., Watts, K., & Pollard, D. (2013). Automated disposable small scale reactor for high throughput bioprocess development: a proof of concept study. *Biotechnol Bioeng, 110*(12), 3126-3138. doi:10.1002/bit.24978

Barnes, L. M., Bentley, C. M., & Dickson, A. J. (2001). Characterization of the stability of recombinant protein production in the GS-NS0 expression system. *Biotechnol Bioeng, 73*(4), 261-270. doi:10.1002/bit.1059

Barnes, L. M., Bentley, C. M., & Dickson, A. J. (2003). Stability of protein production from recombinant mammalian cells. *Biotechnology and Bioengineering, 81*(6), 631-639. doi:10.1002/bit.10517

Barnes, L. M., Moy, N., & Dickson, A. J. (2006). Phenotypic variation during cloning procedures: analysis of the growth behavior of clonal cell lines. *Biotechnol Bioeng, 94*(3), 530-537. doi:10.1002/bit.20856

Barron, N., Kumar, N., Sanchez, N., Doolan, P., Clarke, C., Meleady, P., . . . Clynes, M. (2011). Engineering CHO cell growth and recombinant protein productivity by overexpression of miR-7. *Journal of Biotechnology, 151*(2), 204-211. doi:10.1016/j.jbiotec.2010.12.005

Bateman, E., & Paule, M. R. (1988). Promoter Occlusion during Ribosomal-Rna Transcription. *Cell, 54*(7), 985-992. doi:Doi 10.1016/0092-8674(88)90113-4

Bauer, N., Boettger, M., Papadaki, S., Leitner, T., Klostermann, S., Kettenberger, H., . . . Popp, O. (2024a). Procollagen-Lysine 2-Oxoglutarate 5-Dioxygenases are Responsible for 5R-Hydroxylysine Modification of Therapeutic T-Cell Bispecific Monoclonal Antibodies Produced by Chinese Hamster Ovary Cells. *Manuscript submitted for publication*.

Bauer, N., Oberist, C., Poth, M., Stingele, J., Popp, O., & Ausländer, S. (2024b). Genomic barcoding for clonal diversity monitoring and control in cell-based complex antibody production. *Scientific Reports, 14*(1), 14587. doi:10.1038/s41598-024-65323-7

Bauer, N., Oswald, B., Eiche, M., Schiller, L., Langguth, E., Schantz, C., . . . Ausländer, S. (2022). An arrayed CRISPR screen reveals Myc depletion to increase productivity of difficult-to-express complex antiboaies in CHO cells. *Synthetic Biology, 7*(1). doi:10.1093/synbio/ysac026

Beal, K. M., Bandara, K. R., Ali, S. R., Sonak, R. G., Barnes, M. R., Scarcelli, J. J., & Zhang, L. (2023). The impact of expression vector position on transgene transcription allows for rational expression vector design in a targeted integration system. *Biotechnology Journal, 18*(9). doi:10.1002/biot.202300038

Beale, A. J. (1979). Choice of cell substrate for biological products. *Microbial Pathogenesis: Infection and Immunity, 2nd Edition, 118*, 83-97. doi:10.1007/978-1-4684-0997-0_9

Benveniste, R. E., Callahan, R., Sherr, C. J., Chapman, V., & Todaro, G. J. (1977). Two distinct endogenous type C viruses isolated from the asian rodent Mus cervicolor: conservation of virogene sequences in related rodent species. *Journal of Virology, 21*(3), 849-862. doi:doi:10.1128/jvi.21.3.849-862.1977

Berting, A., Farcet, M. R., & Kreil, T. R. (2010). Virus susceptibility of Chinese hamster ovary (CHO) cells and detection of viral contaminations by adventitious agent testing. *Biotechnol Bioeng, 106*(4), 598-607. doi:10.1002/bit.22723

Bertolotti, A., Zhang, Y. H., Hendershot, L. M., Harding, H. P., & Ron, D. (2000). Dynamic interaction of BiP and ER stress transducers in the unfolded-protein response. *Nature Cell Biology, 2*(6), 326-332. doi:Doi 10.1038/35014014

Beuger, V., Künkele, K. P., Koll, H., Gärtner, A., Bähner, M., Burtscher, H., & Klein, C. (2009). Short-hairpin-RNA-mediated silencing of fucosyltransferase 8 in Chinese-hamster ovary cells for the production of antibodies with enhanced antibody immune effector function. *Biotechnology and Applied Biochemistry, 53*, 31-37. doi:10.1042/Ba20080220

Bi, J. X., Shuttleworth, J., & Ai-Rubeai, M. (2004). Uncoupling of cell growth and proliferation results in enhancement of productivity in p21-arrested CHO cells. *Biotechnology and Bioengineering, 85*(7), 741-749. doi:10.1002/bit.20025

Bibila, T. A., & Flickinger, M. C. (1992). Use of a Structured Kinetic-Model of Antibody-Synthesis and Secretion for Optimization of Antibody-Production Systems .1. Steady-State Analysis. *Biotechnology and Bioengineering, 39*(3), 251-261. doi:DOI 10.1002/bit.260390302

Bock, C., Datlinger, P., Chardon, F., Coelho, M. A., Dong, M. B., Lawson, K. A., . . . Zhuang, X. (2022). High-content CRISPR screening. *Nat Rev Methods Primers, 2*(1). doi:10.1038/s43586-022-00098-7

Borsi, G., Motheramgari, K., Dhiman, H., Baumann, M., Sinkala, E., Sauerland, M., . . . Borth, N. (2023). Single-cell RNA sequencing reveals homogeneous transcriptome patterns and low variance in a suspension CHO-K1 and an adherent HEK293FT cell line in culture conditions. *Journal of Biotechnology, 364*, 13-22. doi:10.1016/j.jbiotec.2023.01.006

Borth, N., Mattanovich, D., Kunert, R., & Katinger, H. (2005). Effect of increased expression of protein disulfide isomerase and heavy chain binding protein on antibody secretion in a recombinant CHO cell line. *Biotechnol Prog, 21*(1), 106-111. doi:10.1021/bp0498241

Borth, N., Zeyda, M., Kunert, R., & Katinger, H. (2002). Efficient selection of high-producing subclones during gene amplification of recombinant Chinese hamster ovary cells by flow cytometry and cell sorting (vol 71, pg 266, 2001). *Biotechnology and Bioengineering, 77*(1), 118-118. doi:10.1002/bit.10186

Bosshard, S., Duroy, P. O., & Mermod, N. (2019). A role for alternative end-joining factors in homologous recombination and genome editing in Chinese hamster ovary cells. *DNA Repair, 82*. doi:ARTN 102691, 10.1016/j.dnarep.2019.102691

Brewster, R. C., Weinert, F. M., Garcia, H. G., Song, D., Rydenfelt, M., & Phillips, R. (2014). The Transcription Factor Titration Effect Dictates Level of Gene Expression. *Cell, 156*(6), 1312-1323. doi:10.1016/j.cell.2014.02.022

Brezinsky, S. C., Chiang, G. G., Szilvasi, A., Mohan, S., Shapiro, R. I., MacLean, A., . . . Thill, G. (2003). A simple method for enriching populations of transfected CHO cells for cells of higher specific productivity. *Journal of Immunological Methods, 277*(1-2), 141-155. doi:10.1016/s0022-1759(03)00108-x

Brightwell, G., Poirier, V., Cole, E., Ivins, S., & Brown, K. W. (1997). Serum-dependent and cell cycle-dependent expression from a cytomegalovirus-based mammalian expression vector. *Gene, 194*(1), 115-123. doi:Doi 10.1016/S0378-1119(97)00178-9

Brinkmann, U., & Kontermann, R. E. (2017). The making of bispecific antibodies. *MAbs, 9*(2), 182-212. doi:10.1080/19420862.2016.1268307

Brown, A. J., & James, D. C. (2016). Precision control of recombinant gene transcription for CHO cell synthetic biology. *Biotechnology Advances, 34*(5), 492-503. doi:10.1016/j.biotechadv.2015.12.012

Brown, A. J., Sweeney, B., Mainwaring, D. O., & James, D. C. (2015). NF-κB, CRE and YY1 elements are key functional regulators of CMV promoter-driven transient gene expression in CHO cells. *Biotechnology Journal, 10*(7), 1019-1028. doi:10.1002/biot.201400744

Bryan, L., Henry, M., Barron, N., Gallagher, C., Kelly, R. M., Frye, C. C., . . . Meleady, P. (2021). Differential expression of miRNAs and functional role of mir-200a in high and low productivity CHO cells expressing an Fc fusion protein. *Biotechnology Letters, 43*(8), 1551-1563. doi:10.1007/s10529-021-03153-7

Buchs, J. (2001). Introduction to advantages and problems of shaken cultures. *Biochem Eng J, 7*(2), 91-98. doi:10.1016/s1369-703x(00)00106-6

Bulté, D. B., Palomares, L. A., Parra, C. G., Martínez, J. A., Contreras, M. A., Noriega, L. G., & Ramírez, O. T. (2020). Overexpression of the mitochondrial pyruvate carrier reduces lactate production and increases recombinant protein productivity in CHO cells. *Biotechnology and Bioengineering, 117*(9), 2633-2647. doi:10.1002/bit.27439

Butler, M. (2005). Animal cell cultures: recent achievements and perspectives in the production of biopharmaceuticals. *Appl Microbiol Biotechnol, 68*(3), 283-291. doi:10.1007/s00253-005-1980-8

Cain, K., Peters, S., Hailu, H., Sweeney, B., Stephens, P., Heads, J., . . . Dickson, A. (2013). A CHO cell line engineered to express XBP1 and ERO1-L has increased levels of transient protein expression. *Biotechnology Progress, 29*(3), 697-706. doi:10.1002/btpr.1693

Carroll, D. (2014). Genome engineering with targetable nucleases. *Faseb Journal, 28*(1).

Carvalhal, A. V., Marcelino, I., & Carrondo, M. J. T. (2003). Metabolic changes during cell growth inhibition by p27 overexpression. *Applied Microbiology and Biotechnology, 63*(2), 164-173. doi:10.1007/s00253-003-1385-5

Carver, J., Ng, D., Zhou, M., Ko, P., Zhan, D. J., Yim, M., . . . Hu, Z. L. (2020). Maximizing antibody production in a targeted integration host by optimization of subunit gene dosage and position. *Biotechnology Progress, 36*(4). doi:ARTN, 2967, 10.1002/btpr.2967

Castellano, B. M., Tang, D. M., Marsters, S., Lam, C., Liu, P. T., Rose, C. M., . . . Misaghi, S. (2023). Activation of the PERK branch of the unfolded protein response during production reduces specific productivity in CHO cells via downregulation of PDGFRa and IRE1a signaling. *Biotechnology Progress, 39*(5). doi:10.1002/btpr.3354

Castro, N. G., Bjelic, J., Malhotra, G., Huang, C., & Alsaffar, S. H. (2021). Comparison of the Feasibility, Efficiency, and Safety of Genome Editing Technologies. *International Journal of Molecular Sciences, 22*(19). doi:ARTN 10355, 10.3390/ijms221910355

Chai, Y. R., Cao, X. X., Ge, M. M., Mi, C. L., Guo, X., & Wang, T. Y. (2020). Knockout of cytidine monophosphate-N-acetylneuraminic acid hydroxylase in Chinese hamster ovary cells by CRISPR/Cas9-based gene-editing technology. *Biochemical Engineering Journal, 161*. doi:ARTN 107663, 10.1016/j.bej.2020.107663

Chang, M., Kumar, A., Kumar, S., Huhn, S., Timp, W., Betenbaugh, M., & Du, Z. (2022). Epigenetic comparison of CHO hosts and clones reveals divergent methylation and transcription patterns across lineages. *Biotechnol Bioeng, 119*(4), 1062-1076. doi:10.1002/bit.28036

Cheng, J. K., Lewis, A. M., Kim, D. S., Dyess, T., & Alper, H. S. (2016). Identifying and retargeting transcriptional hot spots in the human genome. *Biotechnology Journal, 11*(8), 1100-1109. doi:10.1002/biot.201600015

Chin, C. L., Chin, H. K., Chin, C. S. H., Lai, E. T., & Ng, S. K. (2015). Engineering selection stringency on expression vector for the production of recombinant human alpha1-antitrypsin using Chinese Hamster ovary cells. *Bmc Biotechnology, 15*. doi:ARTN 44, 10.1186/s12896-015-0145-9

Chiu, J., Valente, K. N., Levy, N. E., Min, L., Lenhoff, A. M., & Lee, K. H. (2017). Knockout of a difficult-to-remove CHO host cell protein, lipoprotein lipase, for improved polysorbate stability in monoclonal antibody formulations. *Biotechnology and Bioengineering, 114*(5), 1006-1015. doi:10.1002/bit.26237

Chou, Y. T., Lin, H. H., Lien, Y. C., Wang, Y. H., Hong, C. F., Kao, Y. R., . . . Wu, C. W. (2010). EGFR Promotes Lung Tumorigenesis by Activating miR-7 through a Ras/ERK/Myc Pathway That Targets the Ets2 Transcriptional Repressor ERF. *Cancer Research, 70*(21), 8822-8831. doi:10.1158/0008-5472.Can-10-0638

Cong, L., Ran, F. A., Cox, D., Lin, S. L., Barretto, R., Habib, N., . . . Zhang, F. (2013). Multiplex Genome Engineering Using CRISPR/Cas Systems. *Science, 339*(6121), 819-823. doi:10.1126/science.1231143

Conte, C., Dastugue, B., & Vaury, C. (2002). Promoter competition as a mechanism of transcriptional interference mediated by retrotransposons. *Embo Journal, 21*(14), 3908-3916. doi:DOI 10.1093/emboj/cdf367

Cost, G. J., Freyvert, Y., Vafiadis, A., Santiago, Y., Miller, J. C., Rebar, E., . . . Gregory, P. D. (2010). BAK and BAX Deletion Using Zinc-Finger Nucleases Yields Apoptosis-Resistant CHO Cells. *Biotechnology and Bioengineering, 105*(2), 330-340. doi:10.1002/bit.22541

Crawford, Y., Zhou, M., Hu, Z. L., Joly, J., Snedecor, B., Shen, A., & Gao, A. (2013). Fast Identification of Reliable Hosts for Targeted Cell Line Development from a Limited-Genome Screening Using Combined φC31 Integrase and CRE-Lox Technologies. *Biotechnology Progress, 29*(5), 1307-1315. doi:10.1002/btpr.1783

Cristea, S., Freyvert, Y., Santiago, Y., Holmes, M. C., Urnov, F. D., Gregory, P. D., & Cost, G. J. (2013). In vivo cleavage of transgene donors promotes nuclease-mediated targeted integration. *Biotechnology and Bioengineering, 110*(3), 871-880. doi:10.1002/bit.24733

Dahodwala, H., & Lee, K. H. (2019). The fickle CHO: a review of the causes, implications, and potential alleviation of the CHO cell line instability problem. *Current Opinion in Biotechnology, 60*, 128-137. doi:10.1016/j.copbio.2019.01.011

Davies, J., Jiang, L. Y., Pan, L. Z., LaBarre, M. J., Anderson, D., & Reff, M. (2001). Expression of GnTIII in a recombinant anti-CD20 CHO production cell line:: Expression of antibodies with altered glycoforms leads to an increase in ADCC through higher affinity for FcγRIII. *Biotechnology and Bioengineering, 74*(4), 288-294. doi:DOI 10.1002/bit.1119.abs

Davies, S. L., Lovelady, C. S., Grainger, R. K., Racher, A. J., Young, R. J., & James, D. C. (2013). Functional heterogeneity and heritability in CHO cell populations. *Biotechnology and Bioengineering, 110*(1), 260-274. doi:10.1002/bit.24621

Davis, R., Schooley, K., Rasmussen, B., Thomas, J., & Reddy, P. (2000). Effect of PDI overexpression on recombinant protein secretion in CHO cells. *Biotechnology Progress, 16*(5), 736-743. doi:DOI 10.1021/bp000107q

Deans, T. L., Cantor, C. R., & Collins, J. J. (2007). A tunable genetic switch based on RNAi and repressor proteins for regulating gene expression in mammalian cells. *Cell, 130*(2), 363-372. doi:10.1016/j.cell.2007.05.045

DeBerardinis, R. J., Lum, J. J., Hatzivassiliou, G., & Thompson, C. B. (2008). The biology of cancer: Metabolic reprogramming fuels cell growth and proliferation. *Cell Metabolism, 7*(1), 11-20. doi:10.1016/j.cmet.2007.10.002

Deer, J. R., & Allison, D. S. (2004). High-level expression of proteins in mammalian cells using transcription regulatory sequences from the Chinese hamster EF-1α gene. *Biotechnology Progress, 20*(3), 880-889. doi:10.1021/bp034383r

Demain, A. L., & Vaishnav, P. (2009). Production of recombinant proteins by microbes and higher organisms. *Biotechnology Advances, 27*(3), 297-306. doi:10.1016/j.biotechadv.2009.01.008

Derouazi, M., Martinet, D., Schmutz, N. B., Flaction, R., Wicht, M., Bertschinger, M., . . . Wurm, F. M. (2006). Genetic characterization of CHO production host DG44 and derivative recombinant cell lines. *Biochemical and Biophysical Research Communications, 340*(4), 1069-1077. doi:10.1016/j.bbrc.2005.12.111

Desmurget, C., Perilleux, A., Souquet, J., Borth, N., & Douet, J. (2024). Molecular biomarkers identification and applications in CHO bioprocessing. *Journal of Biotechnology, 392*, 11-24. doi:10.1016/j.jbiotec.2024.06.005

Din, M. O., Danino, T., Prindle, A., Skalak, M., Selimkhanov, J., Allen, K., . . . Hasty, J. (2016). Synchronized cycles of bacterial lysis for delivery. *Nature, 536*(7614), 81-+. doi:10.1038/nature18930

Dixon, T. A., Williams, T. C., & Pretorius, I. S. (2021). Sensing the future of bio-informational engineering. *Nature Communications, 12*(1). doi:ARTN 388, 10.1038/s41467-020-20764-2

Doig, S. D., Baganz, F., & Lye, G. J. (2006). High throughput screening and process optimisation. *Basic biotechnology, 3*.

Donaldson, J., Kleinjan, D. J., & Rosser, S. (2022). Synthetic biology approaches for dynamic CHO cell engineering. *Curr Opin Biotechnol, 78*, 102806. doi:10.1016/j.copbio.2022.102806

Doolan, P., Meleady, P., Barron, N., Henry, M., Gallagher, R., Gammell, P., . . . Clynes, M. (2010). Microarray and Proteomics Expression Profiling Identifies Several Candidates, Including the Valosin-Containing Protein (VCP), Involved in Regulating High Cellular Growth Rate in Production CHO Cell Lines. *Biotechnology and Bioengineering, 106*(1), 42-56. doi:10.1002/bit.22670

Doudna, J. A., & Charpentier, E. (2014). The new frontier of genome engineering with CRISPR-Cas9. *Science, 346*(6213), 1077-+. doi:ARTN 1258096, 10.1126/science.1258096

Dreesen, I. A., & Fussenegger, M. (2011). Ectopic expression of human mTOR increases viability, robustness, cell size, proliferation, and antibody production of chinese hamster ovary cells. *Biotechnol Bioeng, 108*(4), 853-866. doi:10.1002/bit.22990

Du, Z. M., Mujacic, M., Le, K., Caspary, G., Nunn, H., Heath, C., & Reddy, P. (2013). Analysis of heterogeneity and instability of stable mAb-expressing CHO cells. *Biotechnology and Bioprocess Engineering, 18*(2), 419-429. doi:10.1007/s12257-012-0577-1

Duran, I., Martin, J. H., Weis, M. A., Krejci, P., Konik, P., Li, B., . . . Krakow, D. (2017). A Chaperone Complex Formed by HSP47, FKBP65, and BiP Modulates Telopeptide Lysyl Hydroxylation of Type I Procollagen. *Journal of Bone and Mineral Research, 32*(6), 1309-1319. doi:10.1002/jbmr.3095

Egloff, P., Zimmermann, I., Arnold, F. M., Hutter, C. A. J., Morger, D., Opitz, L., . . . Seeger, M. A. (2019). Engineered peptide barcodes for in-depth analyses of binding protein libraries. *Nature Methods, 16*(5), 421-+. doi:10.1038/s41592-019-0389-8

Egrie, J. C., & Browne, J. K. (2001). Development and characterization of novel erythropoiesis stimulating protein (NESP). *British Journal of Cancer, 84*, 3-10. doi:DOI 10.1054/bjoc.2001.1746

Eigen, M., & Schuster, P. (1977). Hypercycle - Principle of Natural Self-Organization .A. Emergence of Hypercycle. *Naturwissenschaften, 64*(11), 541-565. doi:Doi 10.1007/Bf00450633

Eisenhut, P., Marx, N., Borsi, G., Papez, M., Ruggeri, C., Baumann, M., & Borth, N. (2024). Manipulating gene expression levels in mammalian cell factories: An outline of synthetic molecular toolboxes to achieve multiplexed control. *New Biotechnology, 79*, 1-19. doi:10.1016/j.nbt.2023.11.003

Eisenhut, P., Mebrahtu, A., Barzadd, M. M., Thalén, N., Klanert, G., Weinguny, M., . . . Rockberg, J. (2020). Systematic use of synthetic 5′-UTR RNA structures to tune protein translation improves yield and quality of complex proteins in mammalian cell factories. *Nucleic Acids Research, 48*(20). doi:ARTN e119, 10.1093/nar/gkaa847

Elliott, S., Lorenzini, T., Asher, S., Aoki, K., Brankow, D., Buck, L., . . . Egrie, J. (2003). Enhancement of therapeutic protein , activities through glycoengineering. *Nature Biotechnology, 21*(4), 414-421. doi:10.1038/nbt799

EMEA. (2014a). EMEA guideline on similar biological medicinal products containing biotechnology-derived proteins as active substance: Quality issues. Retrieved from http://www.ebe-biopharma.eu/uploads/Modules/Newsroom/ema:chmp:bwp:247713:2012.pdf

EMEA. (2014b). Guideline on similar biological medicinal products containing biotechnology-derived proteins as active substance: Non-clinical and clinical issues. Retrieved from http://www.ema.europa.eu/docs/en_GB/document_library/Scientific_guideline/2015/01/WC500180219.pdf

Emmerling, V. V., Fischer, S., Stiefel, F., Holzmann, K., Handrick, R., Hesse, F., . . . Otte, K. (2016). Temperature-sensitive miR-483 is a conserved regulator of recombinant protein and viral vector production in mammalian cells. *Biotechnology and Bioengineering, 113*(4), 830-841. doi:10.1002/bit.25853

Eon-Duval, A., Broly, H., & Gleixner, R. (2012). Quality attributes of recombinant therapeutic proteins: An assessment of impact on safety and efficacy as part of a quality by design development approach. *Biotechnology Progress, 28*(3), 608-622. doi:10.1002/btpr.1548

Eshhar, Z., Waks, T., Gross, G., & Schindler, D. G. (1993). Specific Activation and Targeting of Cytotoxic Lymphocytes through Chimeric Single Chains Consisting of Antibody-Binding Domains and the Gamma-Subunit or Zeta-Subunit of the Immunoglobulin and T-Cell Receptors. *Proceedings of the National Academy of Sciences of the United States of America, 90*(2), 720-724. doi:DOI 10.1073/pnas.90.2.720

Eszterhas, S. K., Bouhassira, E. E., Martin, D. I. K., & Fiering, S. (2002). Transcriptional interference by independently regulated genes occurs in any relative arrangement of the genes and is influenced by chromosomal integration position. *Molecular and Cellular Biology, 22*(2), 469-479. doi:Doi 10.1128/Mcb.22.2.469-479.2002

FDA. (2012a). Guidance for industry quality considerations in demonstrating biosimilarity to a reference protein product. Retrieved from http://www.fda.gov/downloads/drugs/guidancecomplianceregulatoryinformation/guidances/ucm291134.pdf

FDA. (2012b). Guidance for industry scientific considerations in demonstrating biosimilarity to a reference product. Retrieved from http://www.fda.gov/downloads/drugs/guidancecomplianceregulatoryinformation/guidances/ucm291128.pdf

Feichtinger, J., Hernandez, I., Fischer, C., Hanscho, M., Auer, N., Hackl, M., . . . Borth, N. (2016). Comprehensive genome and epigenome characterization of CHO cells in response to evolutionary pressures and over time. *Biotechnol Bioeng, 113*(10), 2241-2253. doi:10.1002/bit.25990

Feist, A. M., & Palsson, B. O. (2010). The biomass objective function. *Curr Opin Microbiol, 13*(3), 344-349. doi:10.1016/j.mib.2010.03.003

Ferreira, J. P., Overton, K. W., & Wang, C. L. (2013). Tuning gene expression with synthetic upstream open reading frames. *Proceedings of the National Academy of Sciences of the United States of America, 110*(28), 11284-11289. doi:10.1073/pnas.1305590110

Figueroa, B., Chen, S. L., Oyler, G. A., Hardwick, J. M., & Betenbaugh, M. J. (2004). Aven and Bcl-X enhance protection against apoptosis for mammalian cells exposed to various culture conditions. *Biotechnology and Bioengineering, 85*(6), 589-600. doi:10.1002/bit.10913

Fire, A., Xu, S. Q., Montgomery, M. K., Kostas, S. A., Driver, S. E., & Mello, C. C. (1998). Potent and specific genetic interference by double-stranded RNA in. *Nature, 391*(6669), 806-811. doi:Doi 10.1038/35888

Fischer, S., Buck, T., Wagner, A., Ehrhart, C., Giancaterino, J., Mang, S., . . . Otte, K. (2014). A functional high-content miRNA screen identifies miR-30 family to boost recombinant protein production in CHO cells. *Biotechnology Journal, 9*(10), 1279-1292. doi:10.1002/biot.201400306

Fischer, S., Handrick, R., Aschrafi, A., & Otte, K. (2015a). Unveiling the principle of microRNA-mediated redundancy in cellular pathway regulation. *Rna Biology, 12*(3), 238-247. doi:10.1080/15476286.2015.1017238

Fischer, S., Handrick, R., & Otte, K. (2015b). The art of CHO cell engineering: A comprehensive retrospect and future perspectives. *Biotechnology Advances, 33*(8), 1878-1896. doi:10.1016/j.biotechadv.2015.10.015

Fischer, S., Paul, A. J., Wagner, A., Mathias, S., Geiss, M., Schandock, F., . . . Otte, K. (2015c). miR-2861 as novel HDAC5 inhibitor in CHO cells enhances productivity while maintaining product quality. *Biotechnology and Bioengineering, 112*(10), 2142-2153. doi:10.1002/bit.25626

Flickinger, M. C. (2010). *Encyclopedia of industrial biotechnology : bioprocess, bioseparation and cell technology*. Hoboken, N.J.: Wiley.

Florin, L., Pegel, A., Becker, E., Hausser, A., Olayioye, M. A., & Kaufmann, H. (2009). Heterologous expression of the lipid transfer protein CERT increases therapeutic protein productivity of mammalian cells. *Journal of Biotechnology, 141*(1-2), 84-90. doi:10.1016/j.jbiotec.2009.02.014

Foecking, M. K., & Hofstetter, H. (1986). Powerful and Versatile Enhancer-Promoter Unit for Mammalian Expression Vectors. *Gene, 45*(1), 101-105. doi:Doi 10.1016/0378-1119(86)90137-X

Fox, S. R., Patel, U. A., Yap, M. G. S., & Wang, D. I. C. (2004). Maximizing interferon-γ production by Chinese hamster ovary cells through temperature shift optimization:: Experimental and modeling. *Biotechnology and Bioengineering, 85*(2), 177-184. doi:10.1002/bit.10861

Frei, T., Cella, F., Tedeschi, F., Gutiérrez, J., Stan, G. B., Khammash, M., & Siciliano, V. (2020). Characterization and mitigation of gene expression burden in mammalian cells. *Nature Communications, 11*(1). doi:ARTN 4641, 10.1038/s41467-020-18392-x

Frye, C., Deshpande, R., Estes, S., Francissen, K., Joly, J., Lubiniecki, A., . . . Anderson, K. (2016). Industry view on the relative importance of "clonality" of biopharmaceutical-producing cell lines. *Biologicals, 44*(2), 117-122. doi:10.1016/j.biologicals.2016.01.001

Fujita, N., Watanabe, S., Ichimura, T., Ohkuma, Y., Chiba, T., Saya, H., & Nakao, M. (2003). MCAF mediates MBD1-dependent transcriptional repression. *Molecular and Cellular Biology, 23*(8), 2834-2843. doi:10.1128/MCB.23.8.2834-2843.2003

Fukuda, N., Senga, Y., & Honda, S. (2019). and knockout CHO cell lines to diminish the risk of contamination with host cell proteins. *Biotechnology Progress, 35*(4). doi:ARTN e2820, 10.1002/btpr.2820

Fukuta, K., Abe, R., Yokomatsu, T., Kono, N., Asanagi, M., Omae, F., . . . Makino, T. (2000). Remodeling of sugar chain structures of human interferon-γ. *Glycobiology, 10*(4), 421-430. doi:DOI 10.1093/glycob/10.4.421

Fussenegger, M., Mazur, X., & Bailey, J. E. (1997). A novel cytostatic process enhances the productivity of Chinese hamster ovary cells. *Biotechnology and Bioengineering, 55*(6), 927-939. doi:Doi 10.1002/(Sici)1097-0290(19970920)55:6<927::Aid-Bit10>3.0.Co;2-4

Fussenegger, M., Schlatter, S., Datwyler, D., Mazur, X., & Bailey, J. E. (1998). Controlled proliferation by multigene metabolic engineering enhances the productivity of Chinese hamster ovary cells. *Nature Biotechnology, 16*(5), 468-472. doi:DOI 10.1038/nbt0598-468

Gaidukov, L., Wroblewska, L., Teague, B., Nelson, T., Zhang, X., Liu, Y., . . . Weiss, R. (2018). A multi-landing pad DNA integration platform for mammalian cell engineering. *Nucleic Acids Research, 46*(8), 4072-4086. doi:10.1093/nar/gky216

Galili, U. (2004). Immune response, accommodation, and tolerance to transplantation carbohydrate antigens. *Transplantation, 78*(8), 1093-1098. doi:10.1097/01.tp.0000142673.32394.95

Geist, B. J., Davis, D., McIntosh, T., Yang, T. Y., Goldberg, K., Han, C., . . . Davis, H. M. (2013). A novel approach for the simultaneous quantification of a therapeutic monoclonal antibody in serum produced from two distinct host cell lines. *MAbs, 5*(1), 150-161. doi:10.4161/mabs.22773

Gerety, R. J., & Aronson, D. L. (1982). Plasma Derivatives and Viral-Hepatitis. *Transfusion, 22*(5), 347-351. doi:DOI 10.1046/j.1537-2995.1982.22583017454.x

Gerngross, T. U. (2004). Advances in the production of human therapeutic proteins in yeasts and filamentous fungi. *Nat Biotechnol, 22*(11), 1409-1414. doi:10.1038/nbt1028

Ghaderi, D., Taylor, R. E., Padler-Karavani, V., Diaz, S., & Varki, A. (2010). Implications of the presence of N-glycolylneuraminic acid in recombinant therapeutic glycoproteins. *Nat Biotechnol, 28*(8), 863-867. doi:10.1038/nbt.1651

Ghaderi, D., Zhang, M., Hurtado-Ziola, N., & Varki, A. (2012). Production platforms for biotherapeutic glycoproteins. Occurrence, impact, and challenges of non-human sialylation. *Biotechnology and Genetic Engineering Reviews Vol 28, Issue 1, 28*(1), 147-175. doi:10.5661/bger-28-147

Gibson, D. G., Benders, G. A., Andrews-Pfannkoch, C., Denisova, E. A., Baden-Tillson, H., Zaveri, J., . . . Smith, H. O. (2008). Complete chemical synthesis, assembly, and cloning of a genome. *Science, 319*(5867), 1215-1220. doi:10.1126/science.1151721

Gitzinger, M., Kemmer, C., El-Baba, M. D., Weber, W., & Fussenegger, M. (2009). Controlling transgene expression in subcutaneous implants using a skin lotion containing the apple metabolite phloretin. *Proceedings of the National Academy of Sciences of the United States of America, 106*(26), 10638-10643. doi:10.1073/pnas.0901501106

Gitzinger, M., Kemmer, C., Fluri, D. A., El-Baba, M. D., Weber, W., & Fussenegger, M. (2012). The food additive vanillic acid controls transgene expression in mammalian cells and mice. *Nucleic Acids Research, 40*(5). doi:ARTN e37, 10.1093/nar/gkr1251

Gödecke, N., Herrmann, S., Hauser, H., Mayer-Bartschmid, A., Trautwein, M., & Wirth, D. (2021). Rational Design of Single Copy Expression Cassettes in Defined Chromosomal Sites Overcomes Intraclonal Cell-to-Cell Expression Heterogeneity and Ensures Robust Antibody Production. *Acs Synthetic Biology, 10*(1), 145-157. doi:10.1021/acssynbio.0c00519

Gopalakrishnan, S., Johnson, W., Valderrama-Gomez, M. A., Icten, E., Tat, J., Ingram, M., . . . Lewis, N. E. (2024). COSMIC-dFBA: A novel multi-scale hybrid framework for bioprocess modeling. *Metab Eng, 82*, 183-192. doi:10.1016/j.ymben.2024.02.012

Gossen, M., Freundlieb, S., Bender, G., Muller, G., Hillen, W., & Bujard, H. (1995). Transcriptional Activation by Tetracyclines in Mammalian-Cells. *Science, 268*(5218), 1766-1769. doi:DOI 10.1126/science.7792603

Gramer, M. J. (2014). Product Quality Considerations for Mammalian Cell Culture Process Development and Manufacturing. *Mammalian Cell Cultures for Biologics Manufacturing, 139*, 123-166. doi:10.1007/10_2013_214

Graumann, K., & Premstaller, A. (2006). Manufacturing of recombinant therapeutic proteins in microbial systems. *Biotechnol J, 1*(2), 164-186. doi:10.1002/biot.200500051

Grav, L. M., Sergeeva, D., Lee, J. S., Marin de Mas, I., Lewis, N. E., Andersen, M. R., . . . Kildegaard, H. F. (2018). Minimizing Clonal Variation during Mammalian Cell Line Engineering for Improved Systems Biology Data Generation. *ACS Synth Biol, 7*(9), 2148-2159. doi:10.1021/acssynbio.8b00140

Gronemeyer, P., Ditz, R., & Strube, J. (2014). Trends in Upstream and Downstream Process Development for Antibody Manufacturing. *Bioengineering (Basel), 1*(4), 188-212. doi:10.3390/bioengineering1040188

Guo, Q., Mintier, G., Ma-Edmonds, M., Storton, D., Wang, X., Xiao, X., . . . Feder, J. N. (2018). 'Cold shock' increases the frequency of homology directed repair gene editing in induced pluripotent stem cells. *Scientific Reports, 8*. doi:ARTN 2080, 10.1038/s41598-018-20358-5

Gutierrez, J. M., Feizi, A., Li, S., Kallehauge, T. B., Hefzi, H., Grav, L. M., . . . Lewis, N. E. (2020). Genome-scale reconstructions of the mammalian secretory pathway predict metabolic costs and limitations of protein secretion. *Nat Commun, 11*(1), 68. doi:10.1038/s41467-019-13867-y

Gutierrez, J. M., & Lewis, N. E. (2015). Optimizing eukaryotic cell hosts for protein production through systems biotechnology and genome-scale modeling. *Biotechnol J, 10*(7), 939-949. doi:10.1002/biot.201400647

Hackl, M., Borth, N., & Grillari, J. (2012). miRNAs - pathway engineering of CHO cell factories that avoids translational burdening. *Trends in Biotechnology, 30*(8), 405-406. doi:DOI 10.1016/j.tibtech.2012.05.002

Hafeez, U., Gan, H. K., & Scott, A. M. (2018). Monoclonal antibodies as immunomodulatory therapy against cancer and autoimmune diseases. *Current Opinion in Pharmacology, 41*, 114-121. doi:10.1016/j.coph.2018.05.010

Hammond, S., & Lee, K. H. (2012). RNA interference of cofilin in Chinese hamster ovary cells improves recombinant protein productivity. *Biotechnology and Bioengineering, 109*(2), 528-535. doi:10.1002/bit.23322

Hansen, H. G., Pristovsek, N., Kildegaard, H. F., & Lee, G. M. (2017). Improving the secretory capacity of Chinese hamster ovary cells by ectopic expression of effector genes: Lessons learned and future directions. *Biotechnology Advances, 35*(1), 64-76. doi:10.1016/j.biotechadv.2016.11.008

Haredy, A. M., Nishizawa, A., Honda, K., Ohya, T., Ohtake, H., & Omasa, T. (2013). Improved antibody production in Chinese hamster ovary cells by overexpression. *Cytotechnology, 65*(6), 993-1002. doi:10.1007/s10616-013-9631-x

Haryadi, R., Zhang, P. Q., Chan, K. F., & Song, Z. W. (2013). CHO-gmt5, a novel CHO glycosylation mutant for producing afucosylated and asialylated recombinant antibodies. *Bioengineered, 4*(2), 90-94. doi:10.4161/bioe.22262

Heard, M. E., Besio, R., Weis, M., Rai, J., Hudson, D. M., Dimori, M., . . . Morello, R. (2016). -Null Mice Provide Evidence for a Novel Endoplasmic Reticulum Complex Regulating Collagen Lysyl Hydroxylation. *Plos Genetics, 12*(4). doi:ARTN e1006002, 10.1371/journal.pgen.1006002

Hefzi, H., Ang, K. S., Hanscho, M., Bordbar, A., Ruckerbauer, D., Lakshmanan, M., . . . Lewis, N. E. (2016). A Consensus Genome-scale Reconstruction of Chinese Hamster Ovary Cell Metabolism. *Cell Syst, 3*(5), 434-443 e438. doi:10.1016/j.cels.2016.10.020

Heiden, M. G. V., Cantley, L. C., & Thompson, C. B. (2009). Understanding the Warburg Effect: The Metabolic Requirements of Cell Proliferation. *Science, 324*(5930), 1029-1033. doi:10.1126/science.1160809

Hilleman, M. R. (1968). Cells, vaccines and the pursuit of precedent. In (Vol. 29, pp. 463-470): Nat. Cancer Inst. Monogr.

Ho, S. C. L., & Yang, Y. S. (2014). Identifying and engineering promoters for high level and sustainable therapeutic recombinant protein production in cultured mammalian cells. *Biotechnology Letters, 36*(8), 1569-1579. doi:10.1007/s10529-014-1523-4

Hornstein, B. D., Roman, D., Arévalo-Soliz, L. M., Engevik, M. A., & Zechiedrich, L. (2016). Effects of Circular DNA Length on Transfection Efficiency by Electroporation into HeLa Cells. *PLoS One, 11*(12). doi:ARTN e0167537, 10.1371/journal.pone.0167537

Hsu, P. D., Lander, E. S., & Zhang, F. (2014). Development and Applications of CRISPR-Cas9 for Genome Engineering. *Cell, 157*(6), 1262-1278. doi:10.1016/j.cell.2014.05.010

Huang, C. J., Lin, H., & Yang, X. M. (2012). Industrial production of recombinant therapeutics in Escherichia coli and its recent advancements. *Journal of Industrial Microbiology & Biotechnology, 39*(3), 383-399. doi:10.1007/s10295-011-1082-9

Huang, X., Guo, H., Tammana, S., Jung, Y. C., Mellgren, E., Bassi, P., . . . Zhou, X. (2010). Gene transfer efficiency and genome-wide integration profiling of Sleeping Beauty, Tol2, and piggyBac transposons in human primary T cells. *Mol Ther, 18*(10), 1803-1813. doi:10.1038/mt.2010.141

Hughes, M., Thomson, R. O., Knight, P., & Stephen, J. (1974). The immunopurification of tetanus toxoid. *J Appl Bacteriol, 37*(4), 603-621. doi:10.1111/j.1365-2672.1974.tb00485.x

Huhn, S., Chang, M. P., Kumar, A., Liu, R., Jiang, B., Betenbaugh, M., . . . Du, Z. M. (2022). Chromosomal instability drives convergent and divergent evolution toward advantageous inherited traits in mammalian CHO bioproduction lineages. *Iscience, 25*(4). doi:ARTN 10407410.1016/j.isci.2022.104074

Ifandi, V., & Al-Rubeai, M. (2003). Stable transfection of CHO cells with the c-myc gene results in increased proliferation rates, reduces serum dependency, and induces anchorage independence. *Cytotechnology, 41*(1), 1-10. doi:Doi 10.1023/A:1024203518501

Ifandi, V., & Al-Rubeai, M. (2005). Regulation of cell proliferation and apoptosis in CHO-K1 cells by the coexpression of c-Myc and Bcl-2. *Biotechnology Progress, 21*(3), 671-677. doi:10.1021/bp049594q

Inao, T., Kawabe, Y., Yamashiro, T., Kameyama, Y., Wang, X., Ito, A., & Kamihira, M. (2015). Improved transgene integration into the Chinese hamster ovary cell genome using the Cre- system. *Journal of Bioscience and Bioengineering, 120*(1), 99-106. doi:10.1016/j.jbiosc.2014.11.019

Ishida, M., Haga, R., Nishimura, N., Matuzaki, H., & Nakano, R. (1990). High Cell-Density Suspension-Culture of Mammalian Anchorage Independent Cells - Oxygen-Transfer by Gas Sparging and Defoaming with a Hydrophobic Net. *Cytotechnology, 4*(3), 215-225. doi:Doi 10.1007/Bf00563782

Itakura, K., Hirose, T., Crea, R., Riggs, A. D., Heyneker, H. L., Bolivar, F., & Boyer, H. W. (1977). Expression in Escherichia-Coli of a Chemically Synthesized Gene for Hormone Somatostatin. *Science, 198*(4321), 1056-1063. doi:DOI 10.1126/science.412251

Ivarsson, M., Villiger, T. K., Morbidelli, M., & Soos, M. (2014). Evaluating the impact of cell culture process parameters on monoclonal antibody -glycosylation. *Journal of Biotechnology, 188*, 88-96. doi:10.1016/j.jbiotec.2014.08.026

Jadhav, V., Hackl, M., Bort, J. A. H., Wieser, M., Harreither, E., Kunert, R., . . . Grillari, J. (2012). A screening method to assess biological effects of microRNA overexpression in Chinese hamster ovary cells. *Biotechnology and Bioengineering, 109*(6), 1376-1385. doi:10.1002/bit.24490

Jadhav, V., Hackl, M., Druz, A., Shridhar, S., Chung, C. Y., Heffner, K. M., . . . Borth, N. (2013). CHO microRNA engineering is growing up: Recent successes and future challenges. *Biotechnology Advances, 31*(8), 1501-1513. doi:10.1016/j.biotechadv.2013.07.007

Jari, M., Abdoli, S., Bazi, Z., Shamsabadi, F. T., Roshanmehr, F., & Shahbazi, M. (2024). Enhancing protein production and growth in chinese hamster ovary cells through miR-107 overexpression. *Amb Express, 14*(1). doi:ARTN 16, 10.1186/s13568-024-01670-y

Jayapal, K. R., Wlaschin, K. F., Hu, W. S., & Yap, M. G. S. (2007). Recombinant protein therapeutics from CHO cells - 20 years and counting. *Chemical Engineering Progress, 103*(10), 40-47.

Jenkins, N., Parekh, R. B., & James, D. C. (1996). Getting the glycosylation right: Implications for the biotechnology industry. *Nature Biotechnology, 14*(8), 975-981. doi:DOI 10.1038/nbt0896-975

Jeon, M. K., Yu, D. Y., & Lee, G. M. (2011). Combinatorial engineering of and for reducing lactate production and improving cell growth in dihydrofolate reductase-deficient Chinese hamster ovary cells. *Applied Microbiology and Biotechnology, 92*(4), 779-790. doi:10.1007/s00253-011-3475-0

Jeong, Y. T., Choi, O., Lim, H. R., Son, Y. D., Kim, H. J., & Kim, J. H. (2008). Enhanced Sialylation of Recombinant Erythropoietin in CHO Cells by Human Glycosyltransferase Expression. *Journal of Microbiology and Biotechnology, 18*(12), 1945-1952. doi:10.4014/jmb.0800.546

Jinek, M., Chylinski, K., Fonfara, I., Hauer, M., Doudna, J. A., & Charpentier, E. (2012). A programmable dual-RNA-guided DNA endonuclease in adaptive bacterial immunity. *Science, 337*(6096), 816-821. doi:10.1126/science.1225829

Johari, Y. B., Estes, S. D., Alves, C. S., Sinacore, M. S., & James, D. C. (2015). Integrated cell and process engineering for improved transient production of a "difficult-to-express" fusion protein by CHO cells. *Biotechnology and Bioengineering, 112*(12), 2527-2542. doi:10.1002/bit.25687

Jones, R. D., Qian, Y. L., Siciliano, V., DiAndreth, B., Huh, J., Weiss, R., & Del Vecchio, D. (2020). An endoribonuclease-based feedforward controller for decoupling resource-limited genetic modules in mammalian cells. *Nature Communications, 11*(1). doi:ARTN 5690, 10.1038/s41467-020-19126-9

Kanda, Y., Imai-Nishiya, H., Kuni-Kamochi, R., Mori, K., Inoue, M., Kitajima-Miyama, K., . . . Satoh, M. (2007). Establishment of a GDP-mannose 4,6-dehydratase (GMD) knockout host cell line: A new strategy for generating completely non-fucosylated recombinant therapeutics. *Journal of Biotechnology, 130*(3), 300-310. doi:10.1016/j.jbiotec.2007.04.025

Kaneko, Y., Sato, R., & Aoyagi, H. (2010). Changes in the quality of antibodies produced by Chinese hamster ovary cells during the death phase of cell culture. *Journal of Bioscience and Bioengineering, 109*(3), 281-287. doi:10.1016/j.jbiosc.2009.09.043

Kaneyoshi, K., Kuroda, K., Uchiyama, K., Onitsuka, M., Yamano-Adachi, N., Koga, Y., & Omasa, T. (2019). Secretion analysis of intracellular "difficult-to-express" immunoglobulin G (IgG) in Chinese hamster ovary (CHO) cells. *Cytotechnology, 71*(1), 305-316. doi:10.1007/s10616-018-0286-5

Karst, D. J., Steinebach, F., & Morbidelli, M. (2018). Continuous integrated manufacturing of therapeutic proteins. *Current Opinion in Biotechnology, 53*, 76-84. doi:10.1016/j.copbio.2017.12.015

Kaufman, R. J., & Sharp, P. A. (1982). Amplification and Expression of Sequences Cotransfected with a Modular Dihydrofolate-Reductase Complementary-DNA Gene. *Journal of Molecular Biology, 159*(4), 601-621. doi:Doi 10.1016/0022-2836(82)90103-6

Kaufmann, H., Mazur, X., Marone, R., Bailey, J. E., & Fussenegger, M. (2001). Comparative analysis of two controlled proliferation strategies regarding product quality, influence on tetracycline-regulated gene expression, and productivity. *Biotechnology and Bioengineering, 72*(6), 592-602. doi:Doi 10.1002/1097-0290(20010320)72:6<592::Aid-Bit1024>3.3.Co;2-A

Kemmer, C., Gitzinger, M., Daoud-El Baba, M., Djonov, V., Stelling, J., & Fussenegger, M. (2010). Self-sufficient control of urate homeostasis in mice by a synthetic circuit. *Nat Biotechnol, 28*(4), 355-360. doi:10.1038/nbt.1617

Ketzer, P., Kaufmann, J. K., Engelhardt, S., Bossow, S., von Kalle, C., Hartig, J. S., . . . Nettelbeck, D. M. (2014). Artificial riboswitches for gene expression and replication control of DNA and RNA viruses. *Proceedings of the National Academy of Sciences of the United States of America, 111*(5), E554-E562. doi:10.1073/pnas.1318563111

Khosla, C., Curtis, J. E., Demodena, J., Rinas, U., & Bailey, J. E. (1990). Expression of Intracellular Hemoglobin Improves Protein-Synthesis in Oxygen-Limited Escherichia-Coli. *Bio-Technology, 8*(9), 849-853. doi:DOI 10.1038/nbt0990-849

Kildegaard, H. F., Baycin-Hizal, D., Lewis, N. E., & Betenbaugh, M. J. (2013). The emerging CHO systems biology era: harnessing the 'omics revolution for biotechnology. *Current Opinion in Biotechnology, 24*(6), 1102-1107. doi:10.1016/j.copbio.2013.02.007

Kim, J. Y., Kim, Y. G., & Lee, G. M. (2012). CHO cells in biotechnology for production of recombinant proteins: current state and further potential. *Applied Microbiology and Biotechnology, 93*(3), 917-930. doi:10.1007/s00253-011-3758-5

Kim, N. S., & Lee, G. M. (2002). Inhibition of sodium butyrate-induced apoptosis in recombinant Chinese hamster ovary cells by constitutively expressing antisense RNA of caspase-3. *Biotechnology and Bioengineering, 78*(2), 217-228. doi:10.1002/bit.10191

Kim, S. H., Park, J. H., Shin, S., Shin, S., Chun, D., Kim, Y. G., . . . Lee, G. M. (2024). Genome-Wide CRISPR/Cas9 Screening Unveils a Novel Target ATF7IP-SETDB1 Complex for Enhancing Difficult-to-Express Protein Production. *Acs Synthetic Biology, 13*(2), 634-647. doi:10.1021/acssynbio.3c00646

Kim, S. H., Shin, S., Baek, M., Xiong, K., Karottki, K. J. L., Hefzi, H., . . . Lee, G. M. (2023). Identification of hyperosmotic stress-responsive genes in Chinese hamster ovary cells via genome-wide virus-free CRISPR/Cas9 screening. *Metabolic Engineering, 80*, 66-77. doi:10.1016/j.ymben.2023.09.006

Kim, W., Kim, Y., & Lee, G. (2014). Gadd45-induced cell cycle G2/M arrest for improved transient gene expression in Chinese hamster ovary cells. *Biotechnology and Bioprocess Engineering, 19*(3), 386-393. doi:10.1007/s12257-014-0151-0

King, Z. A., Lloyd, C. J., Feist, A. M., & Palsson, B. O. (2015). Next-generation genome-scale models for metabolic engineering. *Curr Opin Biotechnol, 35*, 23-29. doi:10.1016/j.copbio.2014.12.016

King, Z. A., Lu, J., Dräger, A., Miller, P., Federowicz, S., Lerman, J. A., . . . Lewis, N. E. (2016). BiGG Models: A platform for integrating, standardizing and sharing genome-scale models. *Nucleic Acids Research, 44*(D1), D515-D522. doi:10.1093/nar/gkv1049

Kito, M., Itami, S., Fukano, Y., Yamana, K., & Shibui, T. (2002). Construction of engineered CHO strains for high-level production of recombinant proteins. *Appl Microbiol Biotechnol, 60*(4), 442-448. doi:10.1007/s00253-002-1134-1

Klein, C., Sustmann, C., Thomas, M., Stubenrauch, K., Croasdale, R., Schanzer, J., . . . Schaefer, W. (2012). Progress in overcoming the chain association issue in bispecific heterodimeric IgG antibodies. *MAbs, 4*(6), 653-663. doi:10.4161/mabs.21379

Knott, L., & Bailey, A. J. (1998). Collagen cross-links in mineralizing tissues: A review of their chemistry, function, and clinical relevance. *Bone, 22*(3), 181-187. doi:Doi 10.1016/S8756-3282(97)00279-2

Ko, P., Misaghi, S., Hu, Z. L., Zhan, D. J., Tsukuda, J., Yim, M., . . . Shen, A. (2018). Probing the importance of clonality: Single cell subcloning of clonally derived CHO cell lines yields widely diverse clones differing in growth, productivity, and product quality. *Biotechnology Progress, 34*(3), 624-634. doi:10.1002/btpr.2594

Kol, S., Ley, D., Wulff, T., Decker, M., Arnsdorf, J., Schoffelen, S., . . . Lewis, N. E. (2020). Multiplex secretome engineering enhances recombinant protein production and purity. *Nat Commun, 11*(1), 1908. doi:10.1038/s41467-020-15866-w

Konermann, S., Brigham, M. D., Trevino, A. E., Joung, J., Abudayyeh, O. O., Barcena, C., . . . Zhang, F. (2015). Genome-scale transcriptional activation by an engineered CRISPR-Cas9 complex. *Nature, 517*(7536), 583-U332. doi:10.1038/nature14136

Krawczyk, K., Xue, S., Buchmann, P., Charpin-El-Hamri, G., Saxena, P., Hussherr, M. D., . . . Fussenegger, M. (2020). Electrogenetic cellular insulin release for real-time glycemic control in type 1 diabetic mice. *Science, 368*(6494), 993-+. doi:10.1126/science.aau7187

Krenitsky, T. A., Rideout, J. L., Chao, E. Y., Koszalka, G. W., Gurney, F., Crouch, R. C., . . . Vinegar, R. (1986). Imidazo[4,5-C]Pyridines (3-Deazapurines) and Their Nucleosides as Immunosuppressive and Antiinflammatory Agents. *Journal of Medicinal Chemistry, 29*(1), 138-143. doi:DOI 10.1021/jm00151a022

Kretzmer, C., Narasimhan, R. L., Lal, R. D., Balassi, V., Ravellette, J., Manjunath, A. K. K., . . . Razafsky, D. (2022). De novo assembly and annotation of the CHOZN® GS genome supports high-throughput genome-scale screening. *Biotechnology and Bioengineering, 119*(12), 3632-3646. doi:10.1002/bit.28226

Ku, S. C. Y., Ng, D. T. W., Yap, M. G. S., & Chao, S. H. (2008). Effects of overexpression of X-box binding protein 1 on recombinant protein production in Chinese hamster ovary and NS0 myeloma cells. *Biotechnology and Bioengineering, 99*(1), 155-164. doi:10.1002/bit.21562

Kuhn, A., Le Fourn, V., Fisch, I., & Mermod, N. (2020). Genome-wide analysis of single nucleotide variants allows for robust and accurate assessment of clonal derivation in cell lines used to produce biologics. *Biotechnology and Bioengineering, 117*(12), 3628-3638. doi:10.1002/bit.27534

Kuystermans, D., & Al-Rubeai, M. (2009). cMyc increases cell number through uncoupling of cell division from cell size in CHO cells. *Bmc Biotechnology, 9*. doi:Artn 76, 10.1186/1472-6750-9-76

Labrijn, A. F., Janmaat, M. L., Reichert, J. M., & Parren, P. W. H. I. (2019). Bispecific antibodies: a mechanistic review of the pipeline. *Nature Reviews Drug Discovery, 18*(8), 585-608. doi:10.1038/s41573-019-0028-1

Lai, T., Yang, Y., & Ng, S. K. (2013). Advances in Mammalian cell line development technologies for recombinant protein production. *Pharmaceuticals (Basel), 6*(5), 579-603. doi:10.3390/ph6050579

Lam, C., Carver, J., Ng, D., Zhan, D. J., Tang, D. M., Kandamkalam, T., . . . Misaghi, S. (2023). Combining regulated and constitutive protein expression significantly boosts protein expression by increasing productivity without affecting CHO cell growth. *Biotechnology Progress, 39*(3). doi:10.1002/btpr.3337

Lam, C., Santell, L., Wilson, B., Yim, M., Louie, S., Tang, D. M., . . . Misaghi, S. (2017). Taming hyperactive hDNase I: Stable inducible expression of a hyperactive salt- and actin-resistant variant of human deoxyribonuclease I in CHO cells. *Biotechnology Progress, 33*(2), 523-533. doi:10.1002/btpr.2439

Lara, A. R., Galindo, E., Ramírez, O. T., & Palomares, L. A. (2006). Living with heterogeneities in bioreactors. *Molecular Biotechnology, 34*(3), 355-381. doi:Doi 10.1385/Mb:34:3:355

Larsson, L. G., Schena, M., Carlsson, M., Sallstrom, J., & Nilsson, K. (1991). Expression of the C-Myc Protein Is down-Regulated at the Terminal Stages during Invitro Differentiation of B-Type Chronic Lymphocytic-Leukemia Cells. *Blood, 77*(5), 1025-1032.

Latorre, Y., Torres, M., Vergara, M., Berrios, J., Sampayo, M. M., Gödecke, N., . . . Altamirano, C. (2023). Engineering of Chinese hamster ovary cells for co-overexpressing MYC and XBP1s increased cell proliferation and recombinant EPO production. *Scientific Reports, 13*(1). doi:10.1038/s41598-023-28622-z

Lattenmayer, C., Loeschel, M., Steinfellner, W., Trummer, E., Mueller, D., Schriebl, K., . . . Kunert, R. (2006). Identification of transgene integration loci of different highly expressing recombinant CHO cell lines by FISH. *Cytotechnology, 51*(3), 171-182. doi:10.1007/s10616-006-9029-0

Laux, H., Romand, S., Nuciforo, S., Farady, C. J., Tapparel, J., Buechmann-Moeller, S., . . . Bodendorf, U. (2018). Degradation of recombinant proteins by Chinese hamster ovary host cell proteases is prevented by matriptase-1 knockout. *Biotechnology and Bioengineering, 115*(10), 2530-2540. doi:10.1002/bit.26731

Lee, A. H., Iwakoshi, N. N., & Glimcher, L. H. (2003). XBP-1 regulates a subset of endoplasmic reticulum resident chaperone genes in the unfolded protein response. *Molecular and Cellular Biology, 23*(21), 7448-7459. doi:10.1128/Mcb.23.21.7448-7459.2003

Lee, C. J., Seth, G., Tsukuda, J., & Hamilton, R. W. (2009). A Clone Screening Method Using mRNA Levels to Determine Specific Productivity and Product Quality for Monoclonal Antibodies. *Biotechnology and Bioengineering, 102*(4), 1107-1118. doi:10.1002/bit.22126

Lee, E. U., Roth, J., & Paulson, J. C. (1989). Alteration of Terminal Glycosylation Sequences on N-Linked Oligosaccharides of Chinese-Hamster Ovary Cells by Expression of Beta-Galactoside Alpha-2,6-Sialyltransferase. *Journal of Biological Chemistry, 264*(23), 13848-13855.

Lee, H. Y., Contreras, E., Register, A. C., Wu, Q., Abadie, K., Garcia, K., . . . Jiang, G. Y. (2019). Development of a bioassay to detect T-cell-activating impurities for T-cell-dependent bispecific antibodies. *Scientific Reports, 9*. doi:ARTN 3900, 10.1038/s41598-019-40689-1

Lee, J. S., Grav, L. M., Pedersen, L. E., Lee, G. M., & Kildegaard, H. F. (2016). Accelerated Homology-Directed Targeted Integration of Transgenes in Chinese Hamster Ovary Cells Via CRISPR/Cas9 and Fluorescent Enrichment. *Biotechnology and Bioengineering, 113*(11), 2518-2523. doi:10.1002/bit.26002

Lee, J. S., Ha, T. K., Park, J. H., & Lee, G. M. (2013). Anti-cell death engineering of CHO cells: Co-overexpression of Bcl-2 for apoptosis inhibition, Beclin-1 for autophagy induction. *Biotechnology and Bioengineering, 110*(8), 2195-2207. doi:10.1002/bit.24879

Lee, J. S., Kallehauge, T. B., Pedersen, L. E., & Kildegaard, H. F. (2015). Site-specific integration in CHO cells mediated by CRISPR/Cas9 and homology-directed DNA repair pathway. *Scientific Reports, 5*. doi:ARTN 8572, 10.1038/srep08572

Lee, J. S., Kildegaard, H. F., Lewis, N. E., & Lee, G. M. (2019). Mitigating Clonal Variation in Recombinant Mammalian Cell Lines. *Trends in Biotechnology, 37*(9), 931-942. doi:10.1016/j.tibtech.2019.02.007

Lee, J. S., Park, J. H., Ha, T. K., Samoudi, M., Lewis, N. E., Palsson, B. O., . . . Lee, G. M. (2018). Revealing Key Determinants of Clonal Variation in Transgene Expression in Recombinant CHO Cells Using Targeted Genome Editing. *ACS Synth Biol, 7*(12), 2867-2878. doi:10.1021/acssynbio.8b00290

Lee, K. H., Onitsuka, M., Honda, K., Ohtake, H., & Omasa, T. (2013). Rapid construction of transgene-amplified CHO cell lines by cell cycle checkpoint engineering. *Applied Microbiology and Biotechnology, 97*(13), 5731-5741. doi:10.1007/s00253-013-4923-9

Lee, Y. K., Brewer, J. W., Hellman, R., & Hendershot, L. M. (1999). BiP and immunoglobulin light chain cooperate to control the folding of heavy chain and ensure the fidelity of immunoglobulin assembly. *Molecular Biology of the Cell, 10*(7), 2209-2219. doi:DOI 10.1091/mbc.10.7.2209

Lee, Y. Y., Wong, K. T. K., Tan, J., Toh, P. C., Mao, Y. Y., Brusic, V., & Yap, M. G. S. (2009). Overexpression of heat shock proteins (HSPs) in CHO cells for extended culture viability and improved recombinant protein production. *Journal of Biotechnology, 143*(1), 34-43. doi:10.1016/j.jbiotec.2009.05.013

Lee, Z., Wan, J., Shen, A. M. Y., & Barnard, G. (2024). Gene copy number, gene configuration and LC/HC mRNA ratio impact on antibody productivity and product quality in targeted integration CHO cell lines. *Biotechnology Progress*. doi:10.1002/btpr.3433

Leitzgen, K., Knittler, M. R., & Haas, I. G. (1997). Assembly of immunoglobulin light chains as a prerequisite for secretion - A model for oligomerization-dependent subunit folding. *Journal of Biological Chemistry, 272*(5), 3117-3123. doi:DOI 10.1074/jbc.272.5.3117

Lenhard, B., Sandelin, A., & Carninci, P. (2012). REGULATORY ELEMENTS Metazoan promoters: emerging characteristics and insights into transcriptional regulation. *Nature Reviews Genetics, 13*(4), 233-245. doi:10.1038/nrg3163

Lewis, N. E., Liu, X., Li, Y. X., Nagarajan, H., Yerganian, G., O'Brien, E., . . . Palsson, B. O. (2013). Genomic landscapes of Chinese hamster ovary cell lines as revealed by the , draft genome. *Nature Biotechnology, 31*(8), 759-+. doi:10.1038/nbt.2624

Li, B. J., Yang, H., Shen, B., Huang, J. W., & Qin, Z. Q. (2021). Procollagen-lysine, 2-oxoglutarate 5-dioxygenase 1 increases cellular proliferation and colony formation capacity in lung cancer via activation of E2F transcription factor 1. *Oncology Letters, 22*(6). doi:ARTN 851, 10.3892/ol.2021.13112

Li, G. W., Burkhardt, D., Gross, C., & Weissman, J. S. (2014). Quantifying Absolute Protein Synthesis Rates Reveals Principles Underlying Allocation of Cellular Resources. *Cell, 157*(3), 624-635. doi:10.1016/j.cell.2014.02.033

Li, H. S., Wong, N. M., Tague, E., Ngo, J. T., Khalil, A. S., & Wong, W. W. (2022). High-performance multiplex drug-gated CAR circuits. *Cancer Cell, 40*(11), 1294-+. doi:10.1016/j.ccell.2022.08.008

Li, Y. F. (2019). A brief introduction of IgG-like bispecific antibody purification: Methods for removing product-related impurities. *Protein Expression and Purification, 155*, 112-119. doi:10.1016/j.pep.2018.11.011

Liang, C., Chiang, A. W. T., Hansen, A. H., Arnsdorf, J., Schoffelen, S., Sorrentino, J. T., . . . Lewis, N. E. (2020). A Markov model of glycosylation elucidates isozyme specificity and glycosyltransferase interactions for glycoengineering. *Curr Res Biotechnol, 2*, 22-36. doi:10.1016/j.crbiot.2020.01.001

Liefhebber, J. M. P., Punt, S., Spaan, W. J. M., & van Leeuwen, H. C. (2010). The human collagen beta(1-O)galactosyltransferase, GLT25D1, is a soluble endoplasmic reticulum localized protein. *Bmc Cell Biology, 11*. doi:Artn 33, 10.1186/1471-2121-11-33

Lim, S. F., Chuan, K. H., Liu, S., Loh, S. O. H., Chung, B. Y. F., Ong, C. C., & Song, Z. W. (2006). RNAi suppression of Bax and Bak enhances viability in fed-batch cultures of CHO cells. *Metabolic Engineering, 8*(6), 509-522. doi:10.1016/j.ymben.2006.05.005

Lin, K.-I., Lin, Y., & Calame, K. (2000). Repression of c-myc Is Necessary but Not Sufficient for Terminal Differentiation of B Lymphocytes In Vitro. *Molecular and Cellular Biology, 20*(23), 8684-8695. doi:10.1128/MCB.20.23.8684-8695.2000

Lin, N., Brooks, J., Sealover, N., George, H. J., & Kayser, K. J. (2015). Overexpression of in Chinese hamster ovary cells increases recombinant IgG productivity. *Journal of Biotechnology, 193*, 91-99. doi:10.1016/j.jbiotec.2014.10.040

Lin, P. C., Liu, R., Alvin, K., Wahyu, S., Murgolo, N., Ye, J., . . . Song, Z. (2021). Improving Antibody Production in Stably Transfected CHO Cells by CRISPR-Cas9-Mediated Inactivation of Genes Identified in a Large-Scale Screen with Chinese Hamster-Specific siRNAs. *Biotechnol J, 16*(3), e2000267. doi:10.1002/biot.202000267

Loh, W. P., Loo, B., Zhou, L. H., Zhang, P. Q., Lee, D. Y., Yang, Y. S., & Lam, K. P. (2014). Overexpression of microRNAs enhances recombinant protein production in Chinese hamster ovary cells. *Biotechnology Journal, 9*(9), 1140-1151. doi:10.1002/biot.201400050

Louie, S., Haley, B., Marshall, B., Heidersbach, A., Yim, M., Brozynski, M., . . . Misaghi, S. (2017). FX knockout CHO hosts can express desired ratios of fucosylated or afucosylated antibodies with high titers and comparable product quality. *Biotechnology and Bioengineering, 114*(3), 632-644. doi:10.1002/bit.26188

Lu, R. M., Hwang, Y. C., Liu, I. J., Lee, C. C., Tsai, H. Z., Li, H. J., & Wu, H. C. (2020). Development of therapeutic antibodies for the treatment of diseases. *Journal of Biomedical Science, 27*(1). doi:ARTN 1, 10.1186/s12929-019-0592-z

Ma, Y. T., Budde, M. W., Mayalu, M. N., Zhu, J. Q., Lu, A. C., Murray, R. M., & Elowitz, M. B. (2022). Synthetic mammalian signaling circuits for robust cell population control. *Cell, 185*(6), 967-+. doi:10.1016/j.cell.2022.01.026

Macaraeg, N. F., Reilly, D. E., & Wong, A. W. (2013). Use of an anti-apoptotic CHO cell line for transient gene expression. *Biotechnology Progress, 29*(4), 1050-1058. doi:10.1002/btpr.1763

Mahé, A., Martiné, A., Fagète, S., & Girod, P. A. (2022). Exploring the limits of conventional small-scale CHO fed-batch for accelerated on demand monoclonal antibody production. *Bioprocess and Biosystems Engineering, 45*(2), 297-307. doi:10.1007/s00449-021-02657-w

Maltais, J. S., Lord-Dufour, S., Morasse, A., Stuible, M., Loignon, M., & Durocher, Y. (2023). Repressing expression of difficult-to-express recombinant proteins during the selection process increases productivity of CHO stable pools. *Biotechnology and Bioengineering, 120*(10), 2840-2852. doi:10.1002/bit.28435

Manahan, M., Nelson, M., Cacciatore, J. J., Weng, J., Xu, S., & Pollard, J. (2019). Scale-down model qualification of ambr (R) 250 high-throughput mini-bioreactor system for two commercial-scale mAb processes. *Biotechnology Progress, 35*(6). doi:ARTN e2870, 10.1002/btpr.2870

Mariati, Yeo, J. H. M., Koh, E. Y. C., Ho, S. C. L., & Yang, Y. S. (2014). Insertion of core CpG island element into human CMV promoter for enhancing recombinant protein expression stability in CHO cells. *Biotechnology Progress, 30*(3), 523-534. doi:10.1002/btpr.1919

Markolovic, S., Wilkins, S. E., & Schofield, C. J. (2015). Protein Hydroxylation Catalyzed by 2-Oxoglutarate-dependent Oxygenases. *Journal of Biological Chemistry, 290*(34), 20712-20722. doi:10.1074/jbc.R115.662627

Martinez-Lopez, J. E., Coleman, O., Meleady, P., & Clynes, M. (2021). Transfection of miR-31*boosts oxidative phosphorylation metabolism in the mitochondria and enhances recombinant protein production in Chinese hamster ovary cells. *Journal of Biotechnology, 333*, 86-96. doi:10.1016/j.jbiotec.2021.04.012

Marx, N., Eisenhut, P., Weinguny, M., Klanert, G., & Borth, N. (2022). How to train your cell - Towards controlling phenotypes by harnessing the epigenome of Chinese hamster ovary production cell lines. *Biotechnology Advances, 56*. doi:ARTN 107924, 10.1016/j.biotechadv.2022.107924

Marx, V. (2016). Cell biology: delivering tough cargo into cells. *Nature Methods, 13*(1), 37-40. doi:10.1038/nmeth.3693

Masson, H. O., Samoudi, M., Robinson, C. M., Kuo, C. C., Weiss, L., Shams Ud Doha, K., . . . Lewis, N. E. (2024). Inferring secretory and metabolic pathway activity from omic data with secCellFie. *Metab Eng, 81*, 273-285. doi:10.1016/j.ymben.2023.12.006

Mathias, S., Wippermann, A., Raab, N., Zeh, N., Handrick, R., Gorr, I., . . . Otte, K. (2020). Unraveling what makes a monoclonal antibody difficult-to-express: From intracellular accumulation to incomplete folding and degradation via ERAD. *Biotechnology and Bioengineering, 117*(1), 5-16. doi:10.1002/bit.27196

Matsuzaki, Y., Aoki, W., Miyazaki, T., Aburaya, S., Ohtani, Y., Kajiwara, K., . . . Ueda, M. (2021). Peptide barcoding for one-pot evaluation of sequence-function relationships of nanobodies. *Scientific Reports, 11*(1). doi:ARTN 21516, 10.1038/s41598-021-01019-6

Mazur, X., Fussenegger, M., Renner, W. A., & Bailey, J. E. (1998). Higher productivity of growth-arrested Chinese hamster ovary cells expressing the cyclin-dependent kinase inhibitor p27. *Biotechnology Progress, 14*(5), 705-713. doi:DOI 10.1021/bp980062h

McClune, C. J., Alvarez-Buylla, A., Voigt, C. A., & Laub, M. T. (2019). Engineering orthogonal signalling pathways reveals the sparse occupancy of sequence space. *Nature, 574*(7780), 702-+. doi:10.1038/s41586-019-1639-8

Meents, H., Enenkel, B., Eppenberger, H. M., Werner, R. G., & Fussenegger, M. (2002). Impact of coexpression and coamplification of sICAM and antiapoptosis determinants , on productivity, cell survival, and mitochondria number in CHO-DG44 grown in suspension and serum-free media. *Biotechnology and Bioengineering, 80*(6), 706-716. doi:10.1002/bit.10449

Miller, I. C., Castro, M. G., Maenza, J., Weis, J. P., & Kwong, G. A. (2018). Remote Control of Mammalian Cells with Heat-Triggered Gene Switches and Photothermal Pulse Trains. *Acs Synthetic Biology, 7*(4), 1167-1173. doi:10.1021/acssynbio.7b00455

Minch, S. L., Kallio, P. T., & Bailey, J. E. (1995). Tissue-Plasminogen Activator Coexpressed in Chinese-Hamster Ovary Cells with Alpha(2,6)-Sialyltransferase Contains Neuac-Alpha(2,6)Gal-Beta(1,4)Glc-N-Acr Linkages. *Biotechnology Progress, 11*(3), 348-351. doi:DOI 10.1021/bp00033a015

Misaghi, S., Chang, J., & Snedecor, B. (2014). It's Time to Regulate: Coping With Product-Induced Nongenetic Clonal Instability in CHO Cell Lines Via Regulated Protein Expression. *Biotechnology Progress, 30*(6), 1432-1440. doi:10.1002/btpr.1970

Moeller, J., Rosenberg, M., Riecken, K., Poertner, R., Zeng, A. P., & Jandt, U. (2020). Quantification of the dynamics of population heterogeneities in CHO cultures with stably integrated fluorescent markers. *Analytical and Bioanalytical Chemistry, 412*(9), 2065-2080. doi:10.1007/s00216-020-02401-5

Mohan, C., Park, S. H., Chung, J. Y., & Lee, G. M. (2007). Effect of doxycycline-regulated protein disulfide isomerase expression on the specific productivity of recombinant CHO cells: Thrombopoietin and antibody. *Biotechnology and Bioengineering, 98*(3), 611-615. doi:10.1002/bit.21453

Moore, C. B., Guthrie, E. H., Huang, M. T., & Taxman, D. J. (2010). Short hairpin RNA (shRNA): design, delivery, and assessment of gene knockdown. *Methods Mol Biol, 629*, 141-158. doi:10.1007/978-1-60761-657-3_10

Moorhead, P. S., Nicholls, W. W., Perkins, F. T., & Hayflick, L. (1974). Standards of karyology for human diploid cells. *J Biol Stand, 2*(2), 95-101. doi:10.1016/0092-1157(74)90023-7

Mora, A., Zhang, S., Carson, G., Nabiswa, B., Hossler, P., & Yoon, S. (2018). Sustaining an efficient and effective CHO cell line development platform by incorporation of 24-deep well plate screening and multivariate analysis. *Biotechnology Progress, 34*(1), 175-186. doi:10.1002/btpr.2584

Morgens, D. W., Wainberg, M., Boyle, E. A., Ursu, O., Araya, C. L., Tsui, C. K., . . . Bassik, M. C. (2017). Genome-scale measurement of off-target activity using Cas9 toxicity in high-throughput screens. *Nature Communications, 8*. doi:ARTN 15178, 10.1038/ncomms15178

Morsut, L., Roybal, K. T., Xiong, X., Gordley, R. M., Coyle, S. M., Thomson, M., & Lim, W. A. (2016). Engineering Customized Cell Sensing and Response Behaviors Using Synthetic Notch Receptors. *Cell, 164*(4), 780-791. doi:10.1016/j.cell.2016.01.012

Müller, D., Katinger, H., & Grillari, J. (2008). MicroRNAs as targets for engineering of CHO cell factories. *Trends in Biotechnology, 26*(7), 359-365. doi:10.1016/j.tibtech.2008.03.010

Nehlsen, K., Schucht, R., da Gama-Norton, L., Krömer, W., Baer, A., Cayli, A., . . . Wirth, D. (2009). Recombinant protein expression by targeting pre-selected chromosomal loci. *Bmc Biotechnology, 9*. doi:Artn 100, 10.1186/1472-6750-9-100

Ng, D., Zhou, M. X., Zhan, D. J., Yip, S., Ko, P., Yim, M., . . . Shen, A. (2021). Development of a targeted integration Chinese hamster ovary host directly targeting either one or two vectors simultaneously to a single locus using the Cre/Lox recombinase-mediated cassette exchange system. *Biotechnology Progress, 37*(4). doi:ARTN e3140, 10.1002/btpr.3140, Ngantung, F. A., Miller, P. G., Brushett, F. R., Tang, G. L., & Wang, D. I. C. (2006). RNA interference of sialidase improves glycoprotein sialic acid content consistency. *Biotechnology and Bioengineering, 95*(1), 106-119. doi:10.1002/bit.20997

Nissim, L., & Bar-Ziv, R. H. (2010). A tunable dual-promoter integrator for targeting of cancer cells. *Molecular Systems Biology, 6*. doi:ARTN 444, 10.1038/msb.2010.99

Noh, S. M., Shin, S., & Lee, G. M. (2018). Comprehensive characterization of glutamine synthetase-mediated selection for the establishment of recombinant CHO cells producing monoclonal antibodies. *Sci Rep, 8*(1), 5361. doi:10.1038/s41598-018-23720-9

Noh, S. M., Shin, S., & Lee, G. M. (2019). Cell Line Development for Therapeutic Protein Production. In *Cell Culture Engineering* (pp. 23-47).

Nov, D., Gama-Norton, L., Riemer, P., Sandhu, U., Schucht, R., & Hauser, H. (2007). Road to precision: recombinase-based targeting technologies for genome engineering. *Current Opinion in Biotechnology, 18*(5), 411-419. doi:10.1016/j.copbio.2007.07.013

Nunberg, J. H., Kaufman, R. J., Schimke, R. T., Urlaub, G., & Chasin, L. A. (1978). Amplified Dihydrofolate-Reductase Genes Are Localized to a Homogeneously Staining Region of a Single Chromosome in a Methotrexate-Resistant Chinese-Hamster Ovary Cell Line. *Proceedings of the National Academy of Sciences of the United States of America, 75*(11), 5553-5556. doi:DOI 10.1073/pnas.75.11.5553

O'Callaghan, P. M., McLeod, J., Pybus, L. P., Lovelady, C. S., Wilkinson, S. J., Racher, A. J., . . . James, D. C. (2010). Cell Line-Specific Control of Recombinant Monoclonal Antibody Production by CHO Cells. *Biotechnology and Bioengineering, 106*(6), 938-951. doi:10.1002/bit.22769

Oguchi, S., Saito, H., Tsukahara, M., & Tsumura, H. (2006). pH Condition in temperature shift cultivation enhances cell longevity and specific hMab productivity in CHO culture. *Cytotechnology, 52*(3), 199-207. doi:10.1007/s10616-007-9059-2

Ong, E. C., Smidt, P., & McGrew, J. T. (2019). Limiting the metabolic burden of recombinant protein expression during selection yields pools with higher expression levels. *Biotechnology Progress, 35*(5). doi:ARTN e2839, 10.1002/btpr.2839

Osterlehner, A., Simmeth, S., & Göpfert, U. (2011). Promoter Methylation and Transgene Copy Numbers Predict Unstable Protein Production in Recombinant Chinese Hamster Ovary Cell Lines. *Biotechnology and Bioengineering, 108*(11), 2670-2681. doi:10.1002/bit.23216

Otsuka, R., Harada, N., Aoki, S., Shirai, K., Nishitsuji, K., Nozaki, A., . . . Sakaue, H. (2016). C-terminal region of GADD34 regulates eIF2α dephosphorylation and cell proliferation in CHO-K1 cells. *Cell Stress & Chaperones, 21*(1), 29-40. doi:10.1007/s12192-015-0633-9

Pacis, E., Yu, M., Autsen, J., Bayer, R., & Li, F. (2011). Effects of Cell Culture Conditions on Antibody , -linked Glycosylation-What Affects High Mannose 5 Glycoform. *Biotechnology and Bioengineering, 108*(10), 2348-2358. doi:10.1002/bit.23200

Palomero, T., Lim, W. K., Odom, D. T., Sulis, M. L., Real, P. J., Margolin, A., . . . Ferrando, A. A. (2006). NOTCH1 directly regulates - and activates a feed-forward-loop transcriptional network promoting leukemic cell growth. *Proceedings of the National Academy of Sciences of the United States of America, 103*(48), 18261-18266. doi:10.1073/pnas.0606108103

Park, J. H., Noh, S. M., Woo, J. R., Kim, J. W., & Lee, G. M. (2016). Valeric acid induces cell cycle arrest at G1 phase in CHO cell cultures and improves recombinant antibody productivity. *Biotechnology Journal, 11*(4), 487-496. doi:10.1002/biot.201500327

Park, S. Y., Choi, D. H., Song, J., Lakshmanan, M., Richelle, A., Yoon, S., . . . Lee, D. Y. (2024). Driving towards digital biomanufacturing by CHO genome-scale models. *Trends Biotechnol*. doi:10.1016/j.tibtech.2024.03.001

Pasquinelli, A. E. (2012). NON-CODING RNA MicroRNAs and their targets: recognition, regulation and an emerging reciprocal relationship. *Nature Reviews Genetics, 13*(4), 271-282. doi:10.1038/nrg3162

Pasquinelli, A. E., Reinhart, B. J., Slack, F., Martindale, M. Q., Kuroda, M. I., Maller, B., . . . Ruvkun, G. (2000). Conservation of the sequence and temporal expression of , -7 heterochronic regulatory RNA. *Nature, 408*(6808), 86-89. doi:Doi 10.1038/35040556

Patel, Y. D., Brown, A. J., Zhu, J., Rosignoli, G., Gibson, S. J., Hatton, D., & James, D. C. (2021). Control of Multigene Expression Stoichiometry in Mammalian Cells Using Synthetic Promoters. *ACS synthetic biology, 10*(5), 1155-1165.

Peng, R. W., Abellan, E., & Fussenegger, M. (2011). Differential Effect of Exocytic SNAREs on the Production of Recombinant Proteins in Mammalian Cells. *Biotechnology and Bioengineering, 108*(3), 611-620. doi:10.1002/bit.22986

Petricciani, J., & Sheets, R. (2008). An overview of animal cell substrates for biological products. *Biologicals, 36*(6), 359-362. doi:10.1016/j.biologicals.2008.06.004

Pham, P. L., Kamen, A., & Durocher, Y. (2006). Large-scale Transfection of mammalian cells for the fast production of recombinant protein. *Molecular Biotechnology, 34*(2), 225-237. doi:Doi 10.1385/Mb:34:2:225

Phan, Q. V., Contzen, J., Seemann, P., & Gossen, M. (2017). Site-specific chromosomal gene insertion: Flp recombinase versus Cas9 nuclease. *Sci Rep, 7*(1), 17771. doi:10.1038/s41598-017-17651-0

Pilbrough, W., Munro, T. P., & Gray, P. (2009). Intraclonal protein expression heterogeneity in recombinant CHO cells. *PLoS One, 4*(12), e8432. doi:10.1371/journal.pone.0008432

Pollock, J., Ho, S. V., & Farid, S. S. (2013). Fed-batch and perfusion culture processes: economic, environmental, and operational feasibility under uncertainty. *Biotechnol Bioeng, 110*(1), 206-219. doi:10.1002/bit.24608

Porter, S. N., Baker, L. C., Mittelman, D., & Porteus, M. H. (2014). Lentiviral and targeted cellular barcoding reveals ongoing clonal dynamics of cell lines in vitro and in vivo. *Genome Biology, 15*(5). doi:ARTN R75, 10.1186/gb-2014-15-5-r75

Posner, J., Barrington, P., Brier, T., & Datta-Mannan, A. (2019). Monoclonal Antibodies: Past, Present and Future. *Handb Exp Pharmacol, 260*, 81-141. doi:10.1007/164_2019_323

Poulain, A., Mullick, A., Massie, B., & Durocher, Y. (2019). Reducing recombinant protein expression during CHO pool selection enhances frequency of high-producing cells. *Journal of Biotechnology, 296*, 32-41. doi:10.1016/j.jbiotec.2019.03.009

Poulain, A., Perret, S., Malenfant, F., Mullick, A., Massie, B., & Durocher, Y. (2017). Rapid protein production from stable CHO cell pools using plasmid vector and the cumate gene-switch. *Journal of Biotechnology, 255*, 16-27. doi:10.1016/j.jbiotec.2017.06.009

Pristovsek, N., Nallapareddy, S., Grav, L. M., Hefzi, H., Lewis, N. E., Rugbjerg, P., . . . Kildegaard, H. F. (2019). Systematic Evaluation of Site-Specific Recombinant Gene Expression for Programmable Mammalian Cell Engineering. *Acs Synthetic Biology, 8*(4), 758-774. doi:10.1021/acssynbio.8b00453

Proudfoot, N. J. (1986). Transcriptional Interference and Termination between Duplicated Alpha-Globin Gene Constructs Suggests a Novel Mechanism for Gene-Regulation. *Nature, 322*(6079), 562-565. doi:DOI 10.1038/322562a0

Puck, T. T., Cieciura, S. J., & Robinson, A. (1958). Genetics of somatic mammalian cells. III. Long-term cultivation of euploid cells from human and animal subjects. *J Exp Med, 108*(6), 945-956. doi:10.1084/jem.108.6.945

Puck, T. T., & Kao, F. T. (1967). Genetics of somatic mammalian cells. V. Treatment with 5-bromodeoxyuridine and visible light for isolation of nutritionally deficient mutants. *Proc Natl Acad Sci U S A, 58*(3), 1227-1234. doi:10.1073/pnas.58.3.1227

Pybus, L. P., Dean, G., West, N. R., Smith, A., Daramola, O., Field, R., . . . James, D. C. (2014). Model-Directed Engineering of "Difficult-to-Express" Monoclonal Antibody Production by Chinese Hamster Ovary Cells. *Biotechnology and Bioengineering, 111*(2), 372-385. doi:10.1002/bit.25116

Qi, Y. F., & Xu, R. (2018). Roles of PLODs in Collagen Synthesis and Cancer Progression. *Frontiers in Cell and Developmental Biology, 6*. doi:ARTN 66, 10.3389/fcell.2018.00066

Qian, Y., Huang, H. H., Jimenez, J. I., & Del Vecchio, D. (2017). Resource Competition Shapes the Response of Genetic Circuits. *ACS Synth Biol, 6*(7), 1263-1272. doi:10.1021/acssynbio.6b00361

Quax, T. E. F., Claassens, N. J., Söll, D., & van der Oost, J. (2015). Codon Bias as a Means to Fine-Tune Gene Expression. *Molecular Cell, 59*(2), 149-161. doi:10.1016/j.molcel.2015.05.035

Raab, N., Zeh, N., Kretz, R., Weiss, L., Stadermann, A., Lindner, B., . . . Otte, K. (2024). Nature as blueprint: Global phenotype engineering of CHO production cells based on a multi-omics comparison with plasma cells. *Metabolic Engineering, 83*, 110-122. doi:10.1016/j.ymben.2024.03.007

Raab, N., Zeh, N., Schlossbauer, P., Mathias, S., Lindner, B., Stadermann, A., . . . Otte, K. (2022). A blueprint from nature: miRNome comparison of plasma cells and CHO cells to optimize therapeutic antibody production. *N Biotechnol, 66*, 79-88. doi:10.1016/j.nbt.2021.10.005

Raju, T. S., & Jordan, R. E. (2012). Galactosylation variations in marketed therapeutic antibodies. *MAbs, 4*(3), 385-391. doi:10.4161/mabs.19868

Randall, T. D., Parkhouse, R. M. E., & Corley, R. B. (1992). J-Chain Synthesis and Secretion of Hexameric Igm Is Differentially Regulated by Lipopolysaccharide and Interleukin-5. *Proceedings of the National Academy of Sciences of the United States of America, 89*(3), 962-966. doi:DOI 10.1073/pnas.89.3.962

Rapp, U. R., & Todaro, G. J. (1978). Generation of oncogenic type C viruses: rapidly leukemogenic viruses derived from C3H mouse cells in vivo and in vitro. *Proc Natl Acad Sci U S A, 75*(5), 2468-2472. doi:10.1073/pnas.75.5.2468

Reinhart, D., Damjanovic, L., Kaisermayer, C., & Kunert, R. (2015). Benchmarking of commercially available CHO cell culture media for antibody production. *Applied Microbiology and Biotechnology, 99*(11), 4645-4657. doi:10.1007/s00253-015-6514-4

Richelle, A., David, B., Demaegd, D., Dewerchin, M., Kinet, R., Morreale, A., . . . von Stosch, M. (2020). Towards a widespread adoption of metabolic modeling tools in biopharmaceutical industry: a process systems biology engineering perspective. *Npj Systems Biology and Applications, 6*(1). doi:ARTN 6, 10.1038/s41540-020-0127-y

Ridgway, J. B. B., Presta, L. G., & Carter, P. (1996). 'Knobs-into-holes' engineering of antibody C(H)3 domains for heavy chain heterodimerization. *Protein Engineering, 9*(7), 617-621. doi:DOI 10.1093/protein/9.7.617

Riglar, D. T., Giessen, T. W., Baym, M., Kerns, S. J., Niederhuber, M. J., Bronson, R. T., . . . Silver, P. A. (2017). Engineered bacteria can function in the mammalian gut long-term as live diagnostics of inflammation. *Nature Biotechnology, 35*(7), 653-+. doi:10.1038/nbt.3879

Rish, A. J., Drennen, J. K., & Anderson, C. A. (2022). Metabolic trends of Chinese hamster ovary cells in biopharmaceutical production under batch and fed-batch conditions. *Biotechnology Progress, 38*(1). doi:ARTN e3220, 10.1002/btpr.3220

Robinson, J. L., Kocabas, P., Wang, H., Cholley, P. E., Cook, D., Nilsson, A., . . . Nielsen, J. (2020). An atlas of human metabolism. *Science Signaling, 13*(624). doi:ARTN eaaz1482, 10.1126/scisignal.aaz1482

Roobol, A., Roobol, J., Smith, M. E., Carden, M. J., Hershey, J. W. B., Willis, A. E., & Smales, C. M. (2020). Engineered transient and stable overexpression of translation factors eIF3i and eIF3c in CHOK1 and HEK293 cells gives enhanced cell growth associated with increased c-Myc expression and increased recombinant protein synthesis. *Metabolic Engineering, 59*, 98-105. doi:10.1016/j.ymben.2020.02.001

Rossger, K., Charpin-El Hamri, G., & Fussenegger, M. (2013). Reward-based hypertension control by a synthetic brain-dopamine interface. *Proc Natl Acad Sci U S A, 110*(45), 18150-18155. doi:10.1073/pnas.1312414110

Roussel, M. F., Cleveland, J. L., Shurtleff, S. A., & Sherr, C. J. (1991). Myc Rescue of a Mutant Csf-1 Receptor Impaired in Mitogenic Signaling. *Nature, 353*(6342), 361-363. doi:DOI 10.1038/353361a0

Rubino, G., & Sericola, B. (2014). *Markov Chains and Dependability Theory*. Cambridge: Cambridge University Press.

Ruiz-Vela, A., Opferman, J. T., Cheng, E. H. Y., & Korsmeyer, S. J. (2005). Proapoptotic BAX and BAK control multiple initiator caspases. *Embo Reports, 6*(4), 379-385. doi:10.1038/sj.embor.7400375

Rydenfelt, M., Cox, R. S., Garcia, H., & Phillips, R. (2014). Statistical mechanical model of coupled transcription from multiple promoters due to transcription factor titration. *Physical Review E, 89*(1). doi:ARTN 012702, 10.1103/PhysRevE.89.012702

Salo, A. M., Wang, C. G., Sipilä, L., Sormunen, R., Vapola, M., Kervinen, P., . . . Myllylä, R. (2006). Lysyl hydroxylase 3 (LH3) modifies proteins in the extracellular space, a novel mechanism for matrix remodeling. *Journal of Cellular Physiology, 207*(3), 644-653. doi:10.1002/jcp.20596

Samy, A., Kaneyoshi, K., & Omasa, T. (2020). Improvement of Intracellular Traffic System by Overexpression of KDEL Receptor 1 in Antibody-Producing CHO Cells. *Biotechnology Journal, 15*(6). doi:ARTN 1900352, 10.1002/biot.201900352

Sauerwald, T. M., Betenbaugh, M. J., & Oyler, G. A. (2002). Inhibiting apoptosis in mammalian cell culture using the caspase inhibitor XIAP and deletion mutants. *Biotechnology and Bioengineering, 77*(6), 704-716. doi:10.1002/bit.10154

Scahill, S. J., Devos, R., Vanderheyden, J., & Fiers, W. (1983). Expression and Characterization of the Product of a Human Immune Interferon Cdna Gene in Chinese-Hamster Ovary Cells. *Proceedings of the National Academy of Sciences of the United States of America-Biological Sciences, 80*(15), 4654-4658. doi:DOI 10.1073/pnas.80.15.4654

Scarcelli, J. J., Hone, M., Beal, K., Ortega, A., Figueroa, B., Starkey, J. A., & Anderson, K. (2018). Analytical subcloning of a clonal cell line demonstrates cellular heterogeneity that does not impact process consistency or robustness. *Biotechnology Progress, 34*(3), 602-612. doi:10.1002/btpr.2646

Schaefer, W., Regula, J. T., Bahner, M., Schanzer, J., Croasdale, R., Durr, H., . . . Klein, C. (2011). Immunoglobulin domain crossover as a generic approach for the production of bispecific IgG antibodies. *Proceedings of the National Academy of Sciences of the United States of America, 108*(27), 11187-11192. doi:10.1073/pnas.1019002108

Schlatter, S., Stansfield, S. H., Dinnis, D. M., Racher, A. J., Birch, J. R., & James, D. C. (2005). On the optimal ratio of heavy to light chain genes for efficient recombinant antibody production by CHO cells. *Biotechnology Progress, 21*(1), 122-133. doi:10.1021/bp049780w

Scietti, L., Chiapparino, A., De Giorgi, F., Fumagalli, M., Khoriauli, L., Nergadze, S., . . . Forneris, F. (2018). Molecular architecture of the multifunctional collagen lysyl hydroxylase and glycosyltransferase LH3 (vol 9, 3163, 2018). *Nature Communications, 9*. doi:ARTN 3912, 10.1038/s41467-018-06481-x

Scott, M., Gunderson, C. W., Mateescu, E. M., Zhang, Z. G., & Hwa, T. (2010). Interdependence of Cell Growth and Gene Expression: Origins and Consequences. *Science, 330*(6007), 1099-1102. doi:10.1126/science.1192588

Sellick, C. A., Croxford, A. S., Maqsood, A. R., Stephens, G., Westerhoff, H. V., Goodacre, R., & Dickson, A. J. (2011). Metabolite Profiling of Recombinant CHO Cells: Designing Tailored Feeding Regimes That Enhance Recombinant Antibody Production. *Biotechnology and Bioengineering, 108*(12), 3025-3031. doi:10.1002/bit.23269

Sergeeva, D., Lee, G. M., Nielsen, L. K., & Grav, L. M. (2020). Multicopy Targeted Integration for Accelerated Development of High-Producing Chinese Hamster Ovary Cells. *ACS Synth Biol, 9*(9), 2546-2561. doi:10.1021/acssynbio.0c00322

Shaffer, A. L., Lin, K. I., Kuo, T. C., Yu, X., Hurt, E. M., Rosenwald, A., . . . Staudt, L. M. (2002). Blimp-1 orchestrates plasma cell differentiation by extinguishing the mature B cell gene expression program. *Immunity, 17*(1), 51-62. doi:Doi 10.1016/S1074-7613(02)00335-7

Shearwin, K. E., Callen, B. P., & Egan, J. B. (2005). Transcriptional interference - a crash course. *Trends in Genetics, 21*(6), 339-345. doi:10.1016/j.tig.2005.04.009

Shimizu, S., Kanaseki, T., Mizushima, N., Mizuta, T., Arakawa-Kobayashi, S., Thompson, C. B., & Tsujimoto, Y. (2004). Role of Bcl-2 family proteins in a non-apoptotic programmed cell death dependent on autophagy genes. *Nature Cell Biology, 6*(12), 1221-1228. doi:10.1038/ncb1192

Shin, S. W., & Lee, J. S. (2020). CHO Cell Line Development and Engineering via Site-specific Integration: Challenges and Opportunities. *Biotechnology and Bioprocess Engineering, 25*(5), 633-645. doi:10.1007/s12257-020-0093-7

Shukla, A. A., Hubbard, B., Tressel, T., Guhan, S., & Low, D. (2007). Downstream processing of monoclonal antibodies - Application of platform approaches. *Journal of Chromatography B-Analytical Technologies in the Biomedical and Life Sciences, 848*(1), 28-39. doi:10.1016/j.jchromb.2006.09.026

Siciliano, M., Stallings, R., & Adair, G. (1985). The genetic map of the Chinese hamster and the genetic consequences of chromosomal rearrangements in CHO cells. *Molecular cell genetics, 40*.

Son, Y. D., Jeong, Y. T., Park, S. Y., & Kim, J. H. (2011). Enhanced sialylation of recombinant human erythropoietin in Chinese hamster ovary cells by combinatorial engineering of selected genes. *Glycobiology, 21*(8), 1019-1028. doi:10.1093/glycob/cwr034

Sorrells, T. R., & Johnson, A. D. (2015). Making Sense of Transcription Networks. *Cell, 161*(4), 714-723. doi:10.1016/j.cell.2015.04.014

Spahn, P. N., Hansen, A. H., Hansen, H. G., Arnsdorf, J., Kildegaard, H. F., & Lewis, N. E. (2016). A Markov chain model for N-linked protein glycosylation - towards a low-parameter tool for model-driven glycoengineering. *Metabolic Engineering, 33*, 52-66. doi:10.1016/j.ymben.2015.10.007

Spiess, C., Zhai, Q., & Carter, P. J. (2015). Alternative molecular formats and therapeutic applications for bispecific antibodies. *Mol Immunol, 67*(2 Pt A), 95-106. doi:10.1016/j.molimm.2015.01.003

Srirangan, K., Loignon, M., & Durocher, Y. (2020). The use of site-specific recombination and cassette exchange technologies for monoclonal antibody production in Chinese Hamster ovary cells: retrospective analysis and future directions. *Critical Reviews in Biotechnology, 40*(6), 833-851. doi:10.1080/07388551.2020.1768043

Stach, C. S., McCann, M. G., O'Brien, C. M., Le, T. S., Somia, N., Chen, X., . . . Smanski, M. (2019). Model-Driven Engineering of N-Linked Glycosylation in Chinese Hamster Ovary Cells. *ACS Synth Biol, 8*(11), 2524-2535. doi:10.1021/acssynbio.9b00215

Stinski, M. F., & Isomura, H. (2008). Role of the cytomegalovirus major immediate early enhancer in acute infection and reactivation from latency. *Medical Microbiology and Immunology, 197*(2), 223-231. doi:10.1007/s00430-007-0069-7

Strain, B., Morrissey, J., Antonakoudis, A., & Kontoravdi, C. (2023). How reliable are Chinese hamster ovary (CHO) cell genome-scale metabolic models? *Biotechnology and Bioengineering, 120*(9), 2460-2478. doi:10.1002/bit.28366

Strotbek, M., Florin, L., Koenitzer, J., Tolstrup, A., Kaufmann, H., Hausser, A., & Olayioye, M. A. (2013). Stable microRNA expression enhances therapeutic antibody productivity of Chinese hamster ovary cells. *Metabolic Engineering, 20*, 157-166. doi:10.1016/j.ymben.2013.10.005

Sung, Y. H., Lee, J. S., Park, S. H., Koo, J., & Lee, G. M. (2007). Influence of co-down-regulation of caspase-3 and caspase-7 by siRNAs on sodium butyrate-induced apoptotic cell death of Chinese hamster ovary cells producing thrombopoietin. *Metabolic Engineering, 9*(5-6), 452-464. doi:10.1016/j.ymben.2007.08.001

Svab, Z., Braga, L., Guarnaccia, C., Labik, I., Herzog, J., Baralle, M., . . . Skoko, N. (2021). High Throughput miRNA Screening Identifies miR-574-3p Hyperproductive Effect in CHO Cells. *Biomolecules, 11*(8). doi:ARTN 1125, 10.3390/biom11081125

Sweet, B. H., & Hilleman, M. R. (1960). The vacuolating virus, S.V. 40. *Proc Soc Exp Biol Med, 105*, 420-427. doi:10.3181/00379727-105-26128

Swim, H. E., & Parker, R. F. (1957). Culture characteristics of human fibroblasts propagated serially. *Am J Hyg, 66*(2), 235-243. doi:10.1093/oxfordjournals.aje.a119897

Takagi, M., Moriyama, T., & Yoshida, T. (2001). Effects of shifts up and down in osmotic pressure on production of tissue plasminogen activator by Chinese hamster ovary cells in suspension. *Journal of Bioscience and Bioengineering, 91*(5), 509-514. doi:DOI 10.1263/jbb.91.509

Tan, J. G. L., Lee, Y. Y., Wang, T. H., Yap, M. G. S., Tan, T. W., & Ng, S. K. (2015). Heat shock protein 27 overexpression in CHO cells modulates apoptosis pathways and delays activation of caspases to improve recombinant monoclonal antibody titre in fed-batch bioreactors. *Biotechnology Journal, 10*(5), 790-U173. doi:10.1002/biot.201400764

Tang, D. M., Lam, C., Bauer, N., Auslaender, S., Snedecor, B., Laird, M. W., & Misaghi, S. (2022). Bax and Bak knockout apoptosis-resistant Chinese hamster ovary cell lines significantly improve culture viability and titer in intensified fed-batch culture process. *Biotechnology Progress, 38*(2). doi:ARTN e3228, 10.1002/btpr.3228

Tharmalingam, T., Barkhordarian, H., Tejeda, N., Daris, K., Yaghmour, S., Yam, P., . . . Stevens, J. (2018). Characterization of phenotypic and genotypic diversity in subclones derived from a clonal cell line. *Biotechnol Prog, 34*(3), 613-623. doi:10.1002/btpr.2666

Thompson, L. H., & Baker, R. M. (1973). Isolation of mutants of cultured mammalian cells. *Methods Cell Biol, 6*, 209-281. doi:10.1016/s0091-679x(08)60052-7

Tian, J., & Andreadis, S. T. (2009). Independent and high-level dual-gene expression in adult stem-progenitor cells from a single lentiviral vector. *Gene Therapy, 16*(7), 874-884. doi:10.1038/gt.2009.46

Todaro, G. J., Benveniste, R. E., Sherwin, S. A., & Sherr, C. J. (1978). MAC-1, a new genetically transmitted type C virus of primates: “low frequency” activation from stumptail monkey cell cultures. *Cell, 13*(4), 775-782. doi:https://doi.org/10.1016/0092-8674(78)90227-1

Todaro, G. J., Sherr, C. J., & Benveniste, R. E. (1976). Baboons and their close relatives are unusual among primates in their ability to release nondefective endogenous type C viruses. *Virology, 72*(1), 278-282. doi:10.1016/0042-6822(76)90331-7

Torres, M., & Dickson, A. J. (2021). Overexpression of transcription factor BLIMP1/prdm1 leads to growth inhibition and enhanced secretory capacity in Chinese hamster ovary cells. *Metabolic Engineering, 67*, 237-249. doi:10.1016/j.ymben.2021.07.004

Tsherniak, A., Vazquez, F., Montgomery, P. G., Weir, B. A., Kryukov, G., Cowley, G. S., . . . Hahn, W. C. (2017). Defining a Cancer Dependency Map. *Cell, 170*(3), 564-576 e516. doi:10.1016/j.cell.2017.06.010

Turajlic, S., Sottoriva, A., Graham, T., & Swanton, C. (2019). Resolving genetic heterogeneity in cancer. *Nature Reviews Genetics, 20*(7), 404-416. doi:10.1038/s41576-019-0114-6

Tycko, J., Wainberg, M., Marinov, G. K., Ursu, O., Hess, G. T., Ego, B. K., . . . Bassik, M. C. (2019). Mitigation of off-target toxicity in CRISPR-Cas9 screens for essential non-coding elements. *Nature Communications, 10*. doi:ARTN 4063, 10.1038/s41467-019-11955-7

Tzelepis, K., Koike-Yusa, H., De Braekeleer, E., Li, Y., Metzakopian, E., Dovey, O. M., . . . Yusa, K. (2016). A CRISPR Dropout Screen Identifies Genetic Vulnerabilities and Therapeutic Targets in Acute Myeloid Leukemia. *Cell Rep, 17*(4), 1193-1205. doi:10.1016/j.celrep.2016.09.079

Uchida, N., Hanawa, H., Yamamoto, M., & Shimada, T. (2013). The Chicken Hypersensitivity Site 4 Core Insulator Blocks Promoter Interference in Lentiviral Vectors. *Human Gene Therapy Methods, 24*(2), 117-124. doi:10.1089/hgtb.2012.152

Urlaub, G., & Chasin, L. A. (1980). Isolation of Chinese hamster cell mutants deficient in dihydrofolate reductase activity. *Proc Natl Acad Sci U S A, 77*(7), 4216-4220. doi:10.1073/pnas.77.7.4216

Vaccines, C. o. T. C. V. a. (1963). Continuously Cultured Tissue Cells and Viral Vaccines: Potential advantages may be realized and potential hazards obviated by careful planning and monitoring. *Science, 139*(3549), 15-20. doi:10.1126/science.139.3549.15

van Beers, M. M. C., & Bardor, M. (2012). Minimizing immunogenicity of biopharmaceuticals by controlling critical quality attributes of proteins. *Biotechnology Journal, 7*(12), 1473-1484. doi:10.1002/biot.201200065

Varki, A. (2007). Glycan-based interactions involving vertebrate sialic-acid-recognizing proteins. *Nature, 446*(7139), 1023-1029. doi:10.1038/nature05816

Vasquez, K. M., Marburger, K., Intody, Z., & Wilson, J. H. (2001). Manipulating the mammalian genome by homologous recombination. *Proceedings of the National Academy of Sciences of the United States of America, 98*(15), 8403-8410. doi:DOI 10.1073/pnas.111009698

Vcelar, S., Jadhav, V., Melcher, M., Auer, N., Hrdina, A., Sagmeister, R., . . . Borth, N. (2018a). Karyotype variation of CHO host cell lines over time in culture characterized by chromosome counting and chromosome painting. *Biotechnol Bioeng, 115*(1), 165-173. doi:10.1002/bit.26453

Vcelar, S., Melcher, M., Auer, N., Hrdina, A., Puklowski, A., Leisch, F., . . . Borth, N. (2018b). Changes in Chromosome Counts and Patterns in CHO Cell Lines upon Generation of Recombinant Cell Lines and Subcloning. *Biotechnology Journal, 13*(3). doi:ARTN 1700495, 10.1002/biot.201700495

von Horsten, H. H., Ogorek, C., Blanchard, V., Demmler, C., Giese, C., Winkler, K., . . . Sandig, V. (2010). Production of non-fucosylated antibodies by co-expression of heterologous GDP-6-deoxy-D-lyxo-4-hexulose reductase. *Glycobiology, 20*(12), 1607-1618. doi:10.1093/glycob/cwq109

Walsh, G., & Walsh, E. (2022). Biopharmaceutical benchmarks 2022. *Nature Biotechnology, 40*(12), 1722-1760. doi:10.1038/s41587-022-01582-x

Wang, C. G., Chen, L. H., Hou, X. H., Li, Z. Y., Kabra, N., Ma, Y. H., . . . Chen, J. D. (2006). Interactions between E2F1 and SirT1 regulate apoptotic response to DNA damage. *Nature Cell Biology, 8*(9), 1025-U1109. doi:10.1038/ncb1468

Wang, H., An, W., Cao, R., Xia, L., Erdjument-Bromage, H., Chatton, B., . . . Zhang, Y. (2003). mAM facilitates conversion by ESET of dimethyl to trimethyl lysine 9 of histone H3 to cause transcriptional repression. *Molecular Cell, 12*(2), 475-487. doi:10.1016/j.molcel.2003.08.007

Wang, Q., Chen, Y., Park, J., Liu, X., Hu, Y., Wang, T., . . . Betenbaugh, M. J. (2019). Design and Production of Bispecific Antibodies. *Antibodies (Basel), 8*(3). doi:10.3390/antib8030043

Wang, T., Yu, H. Y., Hughes, N. W., Liu, B. X., Kendirli, A., Klein, K., . . . Sabatini, D. M. (2017). Gene Essentiality Profiling Reveals Gene Networks and Synthetic Lethal Interactions with Oncogenic Ras. *Cell, 168*(5), 890-+. doi:10.1016/j.cell.2017.01.013

Wang, T. Y., & Guo, X. (2020). Expression vector cassette engineering for recombinant therapeutic production in mammalian cell systems. *Applied Microbiology and Biotechnology, 104*(13), 5673-5688. doi:10.1007/s00253-020-10640-w

Wang, X., Hunter, A. K., & Mozier, N. M. (2009). Host Cell Proteins in Biologics Development: Identification, Quantitation and Risk Assessment. *Biotechnology and Bioengineering, 103*(3), 446-458. doi:10.1002/bit.22304

Wang, X. Y., Zhang, J. H., Zhang, X., Sun, Q. L., Zhao, C. P., & Wang, T. Y. (2016). Impact of Different Promoters on Episomal Vectors Harbouring Characteristic Motifs of Matrix Attachment Regions. *Scientific Reports, 6*. doi:ARTN 26446, 10.1038/srep26446

Weber, W., Baba, M., & Fussenegger, M. (2007). Synthetic ecosystems based on airborne inter- and intrakingdom communication. *Proceedings of the National Academy of Sciences of the United States of America, 104*(25), 10435-10440. doi:10.1073/pnas.0701382104

Weber, W., & Fussenegger, M. T. (2007). Inducible product gene expression technology tailored to bioprocess engineering. *Current Opinion in Biotechnology, 18*(5), 399-410. doi:10.1016/j.copbio.2007.09.002

Weber, W., Rimann, M., Spielmann, M., Keller, B., Daoud-El Baba, M., Aubel, D., . . . Fussenegger, M. (2004). Gas-inducible transgene expression in mammalian cells and mice. *Nature Biotechnology, 22*(11), 1440-1444. doi:10.1038/nbt1021

Weinguny, M., Klanert, G., Eisenhut, P., Jonsson, A., Ivansson, D., Lovgren, A., & Borth, N. (2020). Directed evolution approach to enhance efficiency and speed of outgrowth during single cell subcloning of Chinese Hamster Ovary cells. *Computational and Structural Biotechnology Journal, 18*, 1320-1329. doi:10.1016/j.csbj.2020.05.020

Weinguny, M., Klanert, G., Eisenhut, P., Lee, I., Timp, W., & Borth, N. (2021). Subcloning induces changes in the DNA-methylation pattern of outgrowing Chinese hamster ovary cell colonies. *Biotechnol J, 16*(6), e2000350. doi:10.1002/biot.202000350

Weis, B. L., Guth, N., Fischer, S., Wissing, S., Fradin, S., Holzmann, K. H., . . . Otte, K. (2018). Stable miRNA overexpression in human CAP cells: Engineering alternative production systems for advanced manufacturing of biologics using miR-136 and miR-3074. *Biotechnology and Bioengineering, 115*(8), 2027-2038. doi:10.1002/bit.26715

Weisse, A. Y., Oyarzún, D. A., Danos, V., & Swain, P. S. (2015). Mechanistic links between cellular trade-offs, gene expression, and growth. *Proceedings of the National Academy of Sciences of the United States of America, 112*(9), E1038-E1047. doi:10.1073/pnas.1416533112

Welch, J. T., & Arden, N. S. (2019). Considering "clonality": A regulatory perspective on the importance of the clonal derivation of mammalian cell banks in biopharmaceutical development. *Biologicals, 62*, 16-21. doi:10.1016/j.biologicals.2019.09.006

White, E., Kamieniarz-Gdula, K., Dye, M. J., & Proudfoot, N. J. (2013). AT-rich sequence elements promote nascent transcript cleavage leading to RNA polymerase II termination. *Nucleic Acids Research, 41*(3), 1797-1806. doi:10.1093/nar/gks1335

WHO. (1978). Interferon and other antiviral agents, with special reference to influenza: a memorandum. *Bull World Health Organ, 56*(2), 229-240.
WHO. (1987). *Acceptability of cell substrates for production of biologicals*.
WHO. (2023). WHO Model List of Essential Medicines - 23rd list, 2023. Retrieved from https://www.who.int/publications/i/item/WHO-MHP-HPS-EML-2023.02
Wieland, M., & Fussenegger, M. (2010). Ligand-dependent regulatory RNA parts for Synthetic Biology in eukaryotes. *Current Opinion in Biotechnology, 21*(6), 760-765. doi:10.1016/j.copbio.2010.06.010
Wolf, B., Piksa, M., Beley, I., Patoux, A., Besson, T., Cordier, V., . . . Kammüller, M. (2022). Therapeutic antibody glycosylation impacts antigen recognition and immunogenicity. *Immunology, 166*(3), 380-407. doi:10.1111/imm.13481
Wong, D. C. F., Wong, K. T. K., Nissom, P. M., Heng, C. K., & Yap, M. G. S. (2006). Targeting early apoptotic genes in batch and fed-batch CHO cell cultures. *Biotechnology and Bioengineering, 95*(3), 350-361. doi:10.1002/bit.20871
Wong, N. S. C., Yap, M. G. S., & Wang, D. I. C. (2006). Enhancing recombinant glycoprotein sialylation through CMP-sialic acid transporter over expression in chinese hamster ovary cells. *Biotechnology and Bioengineering, 93*(5), 1005-1016. doi:10.1002/bit.20815
Wu, S. C. Y., Meir, Y. J. J., Coates, C. J., Handler, A. M., Pelczar, P., Moisyadi, S., & Kaminski, J. M. (2006). is a flexible and highly active transposon as compared to, and in mammalian cells. *Proceedings of the National Academy of Sciences of the United States of America, 103*(41), 15008-15013. doi:10.1073/pnas.0606979103
Wurm, F. M. (2004). Production of recombinant protein therapeutics in cultivated mammalian cells. *Nature Biotechnology, 22*(11), 1393-1398. doi:10.1038/nbt1026
Wurm, F. M. (2013). CHO Quasispecies—Implications for Manufacturing Processes. *Processes, 1*(3), 296-311.
Wurm, F. M., & Hacker, D. (2011). First CHO genome. *Nature Biotechnology, 29*(8), 718-720. doi:10.1038/nbt.1943
Wurm, F. M., & Wurm, M. J. (2017). Cloning of CHO Cells, Productivity and Genetic Stability-A Discussion. *Processes, 5*(2). doi:ARTN 20, 10.3390/pr5020020
Wurm, M. J., & Wurm, F. M. (2021). Naming CHO cells for bio-manufacturing: Genome plasticity and variant phenotypes of cell populations in bioreactors question the relevance of old names. *Biotechnology Journal, 16*(7). doi:ARTN e2100165, 10.1002/biot.202100165
Xia, W., Bringmann, P., McClary, J., Jones, P. P., Manzana, W., Zhu, Y., . . . Cobb, R. R. (2006). High levels of protein expression using different mammalian CMV promoters in several cell lines. *Protein Expression and Purification, 45*(1), 115-124. doi:10.1016/j.pep.2005.07.008
Xie, L. Z., & Wang, D. I. C. (1997). Integrated approaches to the design of media and feeding strategies for fed-batch cultures of animal cells. *Trends in Biotechnology, 15*(3), 109-113. doi:Doi 10.1016/S0167-7799(97)01014-7
Xie, M., Ye, H., Wang, H., Charpin-El Hamri, G., Lormeau, C., Saxena, P., . . . Fussenegger, M. (2016). beta-cell-mimetic designer cells provide closed-loop glycemic control. *Science, 354*(6317), 1296-1301. doi:10.1126/science.aaf4006
Xie, M. Q., & Fussenegger, M. (2018). Designing cell function: assembly of synthetic gene circuits for cell biology applications. *Nature Reviews Molecular Cell Biology, 19*(8), 507-525. doi:10.1038/s41580-018-0024-z
Xing, Z., Kenty, B. M., Li, Z. J., & Lee, S. S. (2009). Scale-up analysis for a CHO cell culture process in large-scale bioreactors. *Biotechnol Bioeng, 103*(4), 733-746. doi:10.1002/bit.22287
Xiong, K., Karottki, K. J. C., Hefzi, H., Li, S., Grav, L. M., Li, S., . . . Pedersen, L. E. (2021a). Erratum: An optimized genome-wide, virus-free CRISPR screen for mammalian cells. *Cell Rep Methods, 1*(7), 100115. doi:10.1016/j.crmeth.2021.100115
Xiong, K., Karottki, K. J. C., Hefzi, H., Li, S., Grav, L. M., Li, S., . . . Pedersen, L. E. (2021b). An optimized genome-wide, virus-free CRISPR screen for mammalian cells. *Cell Rep Methods, 1*(4). doi:10.1016/j.crmeth.2021.100062
Xu, J. L., Rehmann, M. S., Xu, M. M., Zheng, S., Hill, C., He, Q., . . . Li, Z. J. (2020). Development of an intensified fed-batch production platform with doubled titers using N-1 perfusion seed for cell culture manufacturing. *Bioresources and Bioprocessing, 7*(1). doi:ARTN 17, 10.1186/s40643-020-00304-y
Xu, W. J., Lin, Y., Mi, C. L., Pang, J. Y., & Wang, T. Y. (2023). Progress in fed-batch culture for recombinant protein production in CHO cells. *Applied Microbiology and Biotechnology, 107*(4), 1063-1075. doi:10.1007/s00253-022-12342-x
Xu, X., Nagarajan, H., Lewis, N. E., Pan, S. K., Cai, Z. M., Liu, X., . . . Wang, J. (2011). The genomic sequence of the Chinese hamster ovary (CHO)-K1 cell line. *Nature Biotechnology, 29*(8), 735-U131. doi:10.1038/nbt.1932
Yamane-Ohnuki, N., Kinoshita, S., Inoue-Urakubo, M., Kusunoki, M., Iida, S., Nakano, R., . . . Satoh, M. (2004). Establishment of FUT8 knockout Chinese hamster ovary cells: an ideal host cell line for producing completely defucosylated antibodies with enhanced antibody-dependent cellular cytotoxicity. *Biotechnol Bioeng, 87*(5), 614-622. doi:10.1002/bit.20151
Yang, W. C., Lu, J., Kwiatkowski, C., Yuan, H., Kshirsagar, R., Ryll, T., & Huang, Y. M. (2014). Perfusion seed cultures improve biopharmaceutical fed-batch production capacity and product quality. *Biotechnol Prog, 30*(3), 616-625. doi:10.1002/btpr.1884
Yang, W. W., Zhang, J. H., Xiao, Y. X., Li, W. Q., & Wang, T. Y. (2022). Screening Strategies for High-Yield Chinese Hamster Ovary Cell Clones. *Frontiers in Bioengineering and Biotechnology, 10*. doi:ARTN 858478
10.3389/fbioe.2022.858478
Yang, Z., Wang, S., Halim, A., Schulz, M. A., Frodin, M., Rahman, S. H., . . . Clausen, H. (2015). Engineered CHO cells for production of diverse, homogeneous glycoproteins. *Nat Biotechnol, 33*(8), 842-844. doi:10.1038/nbt.3280
Ye, H. F., Daoud-El Baba, M., Peng, R. W., & Fussenegger, M. (2011). A Synthetic Optogenetic Transcription Device Enhances Blood-Glucose Homeostasis in Mice. *Science, 332*(6037), 1565-1568. doi:10.1126/science.1203535
Ye, H. F., & Fussenegger, M. (2014). Synthetic therapeutic gene circuits in mammalian cells. *Febs Letters, 588*(15), 2537-2544. doi:10.1016/j.febslet.2014.05.003
Yeo, H. C., Hong, J., Lakshmanan, M., & Lee, D. Y. (2020). Enzyme capacity-based genome scale modelling of CHO cells. *Metab Eng, 60*, 138-147. doi:10.1016/j.ymben.2020.04.005

Yin, J., Ren, W. K., Huang, X. G., Deng, J. P., Li, T. J., & Yin, Y. L. (2018). Potential Mechanisms Connecting Purine Metabolism and Cancer Therapy. *Frontiers in Immunology, 9*. doi:ARTN 1697
10.3389/fimmu.2018.01697

Yongkya, A., Xu, J. L., Tian, J., Oliveira, C., Zhao, J., McFarland, K., . . . Li, Z. J. (2019). Process intensification in fed-batch production bioreactors using non-perfusion seed cultures. *MAbs, 11*(8), 1502-1514. doi:10.1080/19420862.2019.1652075

Yun, C. Y., Liu, S., Lim, S. F., Wang, T. H., Chung, B. Y. F., Teo, J. J., . . . Song, Z. W. (2007). Specific inhibition of caspase-8 and-9 in CHO cells enhances cell viability in batch and fed-batch cultures. *Metabolic Engineering, 9*(5-6), 406-418. doi:10.1016/j.ymben.2007.06.001

Zambrowicz, B. P., Imamoto, A., Fiering, S., Herzenberg, L. A., Kerr, W. G., & Soriano, P. (1997). Disruption of overlapping transcripts in the ROSA beta geo 26 gene trap strain leads to widespread expression of beta-galactosidase in mouse embryos and hematopoietic cells. *Proceedings of the National Academy of Sciences of the United States of America, 94*(8), 3789-3794. doi:DOI 10.1073/pnas.94.8.3789

Zhang, B. H., Pan, X. P., Cobb, G. P., & Anderson, T. A. (2007). microRNAs as oncogenes and tumor suppressors. *Developmental Biology, 302*(1), 1-12. doi:10.1016/j.ydbio.2006.08.028

Zhang, J. P., Li, X. L., Li, G. H., Chen, W. Q., Arakaki, C., Botimer, G. D., . . . Zhang, X. B. (2017). Efficient precise knockin with a double cut HDR donor after CRISPR/Cas9-mediated double-stranded DNA cleavage. *Genome Biology, 18*. doi:ARTN 35, 10.1186/s13059-017-1164-8

Zhang, L., Inniss, M. C., Han, S., Moffat, M., Jones, H., Zhang, B. H., . . . Young, R. J. (2015). Recombinase-Mediated Cassette Exchange (RMCE) for Monoclonal Antibody Expression in the Commercially Relevant CHOK1SV Cell Line. *Biotechnology Progress, 31*(6), 1645-1656. doi:10.1002/btpr.2175

Zhang, M., Koskie, K., Ross, J. S., Kayser, K. J., & Caple, M. V. (2010). Enhancing Glycoprotein Sialylation by Targeted Gene Silencing in Mammalian Cells. *Biotechnology and Bioengineering, 105*(6), 1094-1105. doi:10.1002/bit.22633

Zhang, X., Wang, Y. K., Yi, D. D., Zhang, C., Ning, B. H., Fu, Y. S., . . . Wang, X. Y. (2024). Synergistic promotion of transient transgene expression in CHO cells by PDI/XBP-1s co-transfection and mild hypothermia. *Bioprocess and Biosystems Engineering, 47*(4), 557-565. doi:10.1007/s00449-024-02987-5

Zhao, M. L., Wang, J. X., Luo, M. Y., Luo, H., Zhao, M. Q., Han, L., . . . Zhu, J. W. (2018). Rapid development of stable transgene CHO cell lines by CRISPR/Cas9-mediated site-specific integration into C12orf35. *Applied Microbiology and Biotechnology, 102*(14), 6105-6117. doi:10.1007/s00253-018-9021-6

Zhou, M. X., Crawford, Y., Ng, D., Tung, J., Pynn, A. F. J., Meier, A., . . . Shen, A. (2011). Decreasing lactate level and increasing antibody production in Chinese Hamster Ovary cells (CHO) by reducing the expression of lactate dehydrogenase and pyruvate dehydrogenase kinases. *Journal of Biotechnology, 153*(1-2), 27-34. doi:10.1016/j.jbiotec.2011.03.003

Zhou, Q., Zhang, Y. J., Lu, X. X., Wang, C., Pei, X. X., Lu, Y. F., . . . Zhang, B. C. (2021). Stable overexpression of mutated PTEN in Chinese hamster ovary cells enhances their performance and therapeutic antibody production. *Biotechnology Journal, 16*(9). doi:ARTN e2000623, 10.1002/biot.202000623

Zoon, K. C., Buckler, C. E., Bridgen, P. J., & Gurari-Rotman, D. (1978). Production of human lymphoblastoid interferon by Namalva cells. *J Clin Microbiol, 7*(1), 44-51. doi:10.1128/jcm.7.1.44-51.1978

Zou, W., Edros, R., & Al-Rubeai, M. (2018). The relationship of metabolic burden to productivity levels in CHO cell lines. *Biotechnology and Applied Biochemistry, 65*(2), 173-180. doi:10.1002/bab.1574